(12) INTERNATIONAL APPLICATION PUBLISHED UNDER THE PATENT COOPERATION TREATY (PCT)

(19) World Intellectual Property Organization
International Bureau

(43) International Publication Date
29 November 2012 (29.11.2012)

WIPO | PCT

(10) International Publication Number
WO 2012/159215 A1

(51) International Patent Classification:
A61K 47/36 (2006.01) *A61P 35/00* (2006.01)
A61K 31/713 (2006.01) *A61P 9/10* (2006.01)
A61P 3/10 (2006.01)

(21) International Application Number:
PCT/CA2012/050342

(22) International Filing Date:
24 May 2012 (24.05.2012)

(25) Filing Language: English

(26) Publication Language: English

(30) Priority Data:
61/489,306 24 May 2011 (24.05.2011) US
61/489,302 24 May 2011 (24.05.2011) US

(71) Applicant *(for all designated States except US)*: **POLYVALOR S.E.C.** [CA/CA]; Office 220, 3535 Queen-Mary Road, Montréal, Québec H3V 1H8 (CA).

(72) Inventors; and
(75) Inventors/Applicants *(for US only)*: **MERZOUKI, Abderrazzak** [CA/CA]; 731 Place de l'eau Vive, Laval, Québec H2Y 2E1 (CA). **BUSCHMANN, Michael D.** [CA/CA]; 4329, King Edward Avenue, Montréal, Québec H4B 2H4 (CA).

(74) Agent: **NORTON ROSE CANADA LLP/S.E.N.C.R.L., S.R.L.**; Suite 2500, 1 place Ville-Marie, Montréal, Québec H3B 1R1 (CA).

(81) Designated States *(unless otherwise indicated, for every kind of national protection available)*: AE, AG, AL, AM, AO, AT, AU, AZ, BA, BB, BG, BH, BR, BW, BY, BZ, CA, CH, CL, CN, CO, CR, CU, CZ, DE, DK, DM, DO, DZ, EC, EE, EG, ES, FI, GB, GD, GE, GH, GM, GT, HN, HR, HU, ID, IL, IN, IS, JP, KE, KG, KM, KN, KP, KR, KZ, LA, LC, LK, LR, LS, LT, LU, LY, MA, MD, ME, MG, MK, MN, MW, MX, MY, MZ, NA, NG, NI, NO, NZ, OM, PE, PG, PH, PL, PT, QA, RO, RS, RU, RW, SC, SD, SE, SG, SK, SL, SM, ST, SV, SY, TH, TJ, TM, TN, TR, TT, TZ, UA, UG, US, UZ, VC, VN, ZA, ZM, ZW.

(84) Designated States *(unless otherwise indicated, for every kind of regional protection available)*: ARIPO (BW, GH, GM, KE, LR, LS, MW, MZ, NA, RW, SD, SL, SZ, TZ, UG, ZM, ZW), Eurasian (AM, AZ, BY, KG, KZ, RU, TJ, TM), European (AL, AT, BE, BG, CH, CY, CZ, DE, DK, EE, ES, FI, FR, GB, GR, HR, HU, IE, IS, IT, LT, LU, LV, MC, MK, MT, NL, NO, PL, PT, RO, RS, SE, SI, SK, SM, TR), OAPI (BF, BJ, CF, CG, CI, CM, GA, GN, GQ, GW, ML, MR, NE, SN, TD, TG).

Published:
— *with international search report (Art. 21(3))*
— *with sequence listing part of description (Rule 5.2(a))*

(54) **Title**: COMPOSITIONS AND METHODS FOR EFFICACIOUS AND SAFE DELIVERY OF SIRNA USING SPECIFIC CHITOSAN-BASED NANOCOMPLEXES

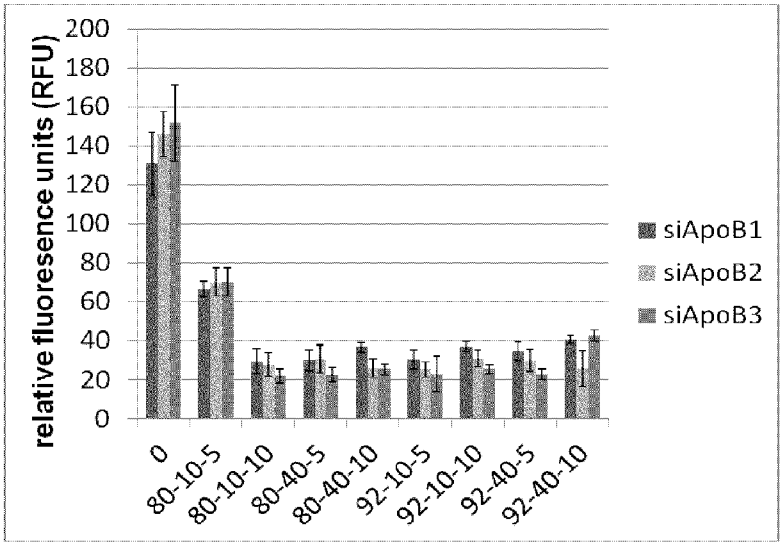

Fig. 4A

(57) **Abstract**: There is disclosed a composition and a method for the efficient delivery of a therapeutic RNAi-inducing nucleic acid to cells both *in vitro* and *in vivo* through specific formulations of a non viral delivery system using chitosans. Particularly, the composition contains a nucleic acid and a specific chitosan that has the following physico-chemical properties: a number-average molecular weight between 5 kDa and 200 kDa, a degree of deacetylation between 80% and 95% and a chitosan amine to nucleic acid phosphate ratio below 20.

WO 2012/159215 A1

COMPOSITIONS AND METHODS FOR EFFICACIOUS AND SAFE DELIVERY OF siRNA USING SPECIFIC CHITOSAN-BASED NANOCOMPLEXES

CROSS-REFERENCE TO RELATED APPLICATIONS

[0001] This application claims priority from U.S. provisional patent application 61/489,306 filed on May 24, 2011 and from U.S. provisional patent application 61/489,302 filed on May 24, 2011, herewith incorporated in their entirety.

TECHNICAL FIELD

[0002] The present description relates to a composition and a method for the efficient delivery of a therapeutic RNAi-inducing nucleic acid using specific chitosan based nanocomplexes.

BACKGROUND

[0003] Gene silencing by siRNA (short interfering RNA) is a developing field in biology and has evolved as a novel post-transcriptional gene silencing strategy with therapeutic potential. Based on the sequencing of the human genome and the understanding of the molecular causes of diseases, the possibility of turning off pathogenic genes at will is an appealing approach for treatment of a wide variety of clinical pathologies, such as diabetes, atherosclerosis and cancer. With siRNAs, virtually every gene in the human genome contributing to a disease becomes amenable to regulation, thus opening opportunities for drug discovery. Whereas locally administered siRNAs have already entered the first clinical trials, strategies for successful systemic delivery of siRNA are still in a preclinical stage of development.

Type II diabetes mellitus

[0004] Type II diabetes mellitus (T2DM) is a progressive metabolic disorder with diverse pathologic manifestations and is often associated with lipid metabolism and glycometabolic disorders (Bell et al., 2001, Nature, 414:788-791). Type II diabetes is characterized by a resistance to insulin action in peripheral tissues such as muscle, adipose tissue and liver. It is also characterized by a progressive failure in the ability of the islet β-cell to secrete

insulin. The long term effects of diabetes result from its vascular complications; micro vascular complications, retinopathy, neuropathy and nephropathy. Macro vascular complications are associated with type II diabetes as well, and include cardiovascular and cerebrovascular complications.

[0005] The main classes of anti-diabetic drugs known today are the following. Biguanides are a class of drugs that help control blood glucose by inhibiting hepatic glucose production, reducing intestinal absorption and enhancing peripheral glucose uptake. This class includes metformin, a drug that lowers both glucose and blood triglycerides level. Sulfonylurea is a class of drugs that helps in controlling or managing type II diabetes by stimulating the release of endogenous insulin from the β-cells of the pancreas. This class includes: tolbutamide, tolazamide, glisoxepide, glimipeide and glibomuride among others. Glycosidase inhibitors stimulate the release of insulin from pancreatic cells thus lowering blood sugar level and include repaglinide and nateglinide.

[0006] Unfortunately, these treatment modalities, even when combined, are frequently constrained by safety, tolerability, weight gain, oedema and gastrointestinal intolerance (Drucker et al., 2010, Nat Rev Drug Discov, 9:267-268; Nauck et al., 2009, Diabetes Care, 32:84-90; Ng et al., 2010, Prim Care Diabetes, 4:61-63; Truitt et al., 2010, Curr Med Res Opin, 26:1321-1331; and Wajcberg and Tavaria, 2009, Expert Opin Pharmacother, 10:135-142). In addition, as the disease progresses and β-cell function declines, efficacies of current treatments diminish (Turner et al., 1999, JAMA, 281:2005-2012).

[0007] The discovery of the incretin effect has provided a new avenue of treatment using a class of therapeutics capable of controlling T2DM with minimal adverse effects. The incretin effect is mainly mediated by glucagon like peptide 1 (GLP-1) which regulates postprandial blood glucose level via the stimulation of insulin secretion. GLP-1 has also indirect effects such as delay of gastric emptying, promoting satiety through its effect on the central nervous system, promoting β-cell growth and inhibiting β-cell apoptosis as demonstrated in animal models (Nauck et al., 2002, J Clin Endocrinol Metab, 87:1239-1246;

and Creutzfeldt et al., 1996, Diabetes Care, 19:580-586). However, the potential of GLP-1 in the clinic was hindered due to its rapid degradation by the ubiquitous serine protease dipeptidyl peptidase IV (DPP-IV). The discovery that DPP-IV cleaves the His:Ala:Glu sequence at the N-terminal region of GLP-1 permitted the development of DPP-IV resistant GLP-1 analogues and the development of DPP-IV inhibitors.

[0008] DPP-IV inhibitors are a new class of drugs that inhibit the proteolytic activity of dipeptidyl peptidase IV. The proteolytic activity of DPP-IV decreases blood level of glucoregulatory peptides, known as incretins. Inhibition of dipeptidyl peptidase IV thereby potentiates the action of these incretin, notably glucagon like peptide 1 (GLP-1). These inhibitors include Sitagliptin, Vildagliptin and Saxagliptin and are orally administrated once daily.

Atherosclerosis

[0009] Atherosclerosis is a chronic disease caused by the formation of atherosclerotic plaque in arteries. Atherosclerosis represents a multitude of cardiovascular diseases such as coronary heart disease, acute coronary syndrome and angina pectoris (Lloyd-Jones et al., 2010, Circulation, 121:e46-e215). In the United-States, the predicted economic cost of atherosclerosis for 2010 was US$503 billion, mainly due to direct medical and indirect productivity costs (Lloyd-Jones et al., 2010, Circulation, 121:948-954). Although causal factors for atherosclerosis remain unknown, increasing evidence suggest a high role of dyslipidemia, hyperlipidemia and inflammation in the pathogenesis of this disease (Hanson et al., 2006, Nat Rev Immunol, 6:508-519; Montecucco and Mach, 2008, Clin Interv Aging, 3:341-349). Currently, the reduction of morbidity and mortality due to atherosclerosis and related pathologies - Cardiovascular Diseases (CVD) - are mainly attributable to the aggressive clinical use of 3-hydroxy-3-methylglutaryl coenzyme A (HMG-CoA) reducatase inhibitors commonly named statin-based therapies (Vermissen et al., 2008, BMJ, 337:a2423). These therapies reduce low density lipoprotein cholesterol (LDL-C). Intervention studies have demonstrated reduced risk of CVD morbidity and mortality when lipid lowering therapies were administered. Additionally, the

decreased morbidity/mortality and LDL-C lowering demonstrate a log-linear association (Law et al., 1994, BMJ, 308:367-372).

[0010] An alternative approach to lowering LDL-C, and thus reducing atherosclerosis, is the inhibition or blocking of very low density lipoprotein (VLDL) secretion from the liver. This inhibition can be achieved through apolipoprotein B (ApoB) targeting since ApoB is necessary for VLDL secretion (Rutledge et al., 2010, Cell Biol, 88:251-267). ApoB is mainly expressed by hepatocytes and entherocytes in humans.

[0011] In humans, the ApoB gene is located on chromosome 2 (2q) and spans over 43kb. ApoB mRNA consists of 28 introns and 29 exons and is characterized by a 16 hour half life (Ludwig et al., 1987, DNA, 6:363-372; Scott, 1989, Curr Opin Cell Biol, 1:1141-1147). The translation of ApoB mRNA yields a protein with 4,536 amino acids and an apparent molecular weight of 517-550kDa thus representing one of the largest monomeric proteins. The importance of ApoB inhibition as an alternative therapy for atherosclerosis and its associated CVDs resides in the ability of ApoB to physically interact through its β-sheet domains with lipids such as phospholipids, cholesterol and cholesteryl esters to form large lipoproteins particles, namely VLDL, in the liver and cholymicrons in the intestine (reviewed in Rutledge et al., 2010, Biochem Cell Biol, 88:251-267).

Cancer

[0012] Classical cancer therapy includes the use of one or several chemotherapeutic drugs. These treatment modalities are associated with toxicity and severe side effects due to their non-specificity. Another major problem associated with chemotherapy is the development of chemoresistance with time. For example, resistance to chemotherapy is one of the major problems associated with the management of breast cancer.

[0013] Cancer cells employ a plethora of mechanisms to acquire resistance to one or more chemotherapeutic agent. Major mechanisms of drug resistance include (1) decreased intracellular uptake of soluble drugs, (2) genetic and

phenotypic changes in cells that change the capacity of drugs to cause the desired cell damage and (3) increased efflux of drugs by cell-surface transporters, leading to multidrug resistance (MDR). In all these cases resistance to a single chemotherapeutic entity is always associated with a wide-range drug resistance pattern against other chemotherapeutics.

[0014] One of the most common and studied resistance mechanisms is the reduction of intracellular drug concentration by transporter proteins that pump drugs out of cells before they reach the site of action, so that the cells adapt to low drug concentration without undergoing drug-induced cell death. Most of these transporters are in the ATP-binding cassette transmembrane protein super-family.

[0015] In humans, 48 ABC genes (genes in the ATP-binding cassette family) have been identified to date. In breast cancer, practically all MDR resistance reported to date were closely related to one of the following: p-glycoprotein (P-gp), multidrug resistance-related protein (MRP), and breast cancer resistance protein (BCRP).

[0016] The P-gp is the most common protein involved in ATP-dependent efflux of drugs in various cancer tissues. The over expression P-gp was believed for some time to be the only protein capable of conferring MDR in mammalian tumor cells. In breast cancer, 52% of chemotherapy-treated patients had their P-gp up regulated due to therapy. The gene encoding P-gp is termed ABCB1 (mdr1) and is located on chromosome 7 at the position q21.12. ABCB1 is composed of 28 exons whose product yield a 1.2 kb mRNA. Protein sequence analysis of P-gp revealed the presence of two extracytoplasmic domains, each containing 6 putative transmembrane segments, and an ATP-binding consensus motif.

[0017] Furthermore, one class of interesting enzymes involved in maintenance of genomic integrity and stability are DNA helicases. These proteins play important roles in DNA replication, repair, recombination and

transcription by an ATP dependant mechanism that unwinds duplex genomic strands allowing the repair machinery access to damaged or mispaired DNA.

[0018] For example, the RecQ family of helicases has been shown to play an important role in recombination, repair and Holliday junction formation. More recently, these helicases have been implicated in the process of posttranscriptional gene silencing (Cogoni and Macino, 1999, Science, 286:2342-2344). In this process, the helicase is required to separate the double stranded DNA before any hybridization and silencing mechanism could be initiated. Other roles have been put forward for proteins of this family. For example, RecQL1 is believed to play a role in nuclear protein transport since it interacts with both QIP1 and QIP2 proteins which function as nuclear localization signals as demonstrated in a two hybrid screening (Seki et al., 1997, 234:48-53).

[0019] The RecQ family consists of five members and can be divided into two groups according to whether they contain an additional carboxy- or amino-terminus group. Mutations in these genes lead to increased incidence of cancer as well as other physiologic abnormalities (Karow et al., 2000, Curr Opin Genet Dev, 10:32-38; Kawabe et al., 2000, Oncogene, 19:4767-4772). Such abnormalities include Blooms syndrome (BLM), Werner's syndrome (WRN) and the Rothmund-Thompson syndrome (RecQ4). The human RecQL1 gene was the first human member of this family to be identified and was shown to have extensive homology with the *E.coli* DNA helicase, RecQ, and is located on chromosome 12p11 (Puranam and Blackshear, 1994, J Biol Chem, 269:29838-29845; Puranam et al., 1995, Genomics, 26:595-598).

[0020] RecQL1 over expression in cancerous cell lines such as AsPC1, A549 and LS174T among others is believed to be driven in order to compensate the high recombination rate in these cancerous cells, thus preventing apoptosis (Futami et al., 2008, Cancer Sci, 99:71-80). RecQL1 gene silencing using specific siRNA in these cell lines or in a murine Xenograft model lead to an increased cancerous cell death and tumor mass reduction (Futami et al., 2008, Cancer Sci, 99:71-80).

[0021] Another class of enzymes involved in maintenance of homeostatic stability and functional integrity are RNA helicases. These enzymes are characterized by the presence of a centrally located "helicase domain", consisting of eight conserved motifs. Based on these motifs, RNA helicases are classified into families. These conserved motifs are required to perform the NTP hydrolysis and RNA unwinding functions (Linder et al., 2001, Trends Biochem Sci., 26:339-341; Tanner and Linder, 2001, Mol Cell, 8:251-262). Another function that has been associated with RNA helicases is disruption of RNA-protein interactions (Jankowsky et al., 2001, Science, 291:121-125). These enzymes are members of molecular complexes that can regulate both their NTPase and helicase activities (Silverman et al., 2003, Gene, 312:1-16). The intrinsic characteristics of these helicases play an important role in post transcriptional events since the modulation of RNA secondary structure regulates steps such as splicing (Balvay et al., 1993, Bioessays, 15:165-169) and translation (van der Velden and Thomas, 1999, Int J Biochem Cell Biol, 31:87-106).

[0022] Dysregulation of RNA processing molecules such as RNA helicase have been implicated in human pathologies and cancer development. Examples of these helicases implicated in human pathologies include DDX1/5/6/9/10 and DHX32 among others (Abdelhaleem, 2004, Anticancer Res, 2004, 24:3951-3953; Abdelhaleem, 2004, Biocim Biophys Acta, 1704:37-46). These helicases contain a characteristic DEAD box domain and are up-regulated in most cancers (Abdelhaleem, 2004, Anticancer Res, 2004, 24:3951-3953; Abdelhaleem, 2004, Biocim Biophys Acta, 1704:37-46).

[0023] There is still a need today to be provided with alternative therapies by sustaining siRNA delivery *in vivo*. Particularly, it would be highly desirable to be provided with an alternative means for treating type II diabetes mellitus, atherosclerosis and cancer.

SUMMARY

[0024] One aim of the present description is to provide a composition comprising chitosan and an RNA-inducing nucleic acid sequence wherein the

chitosan has a molecular weight (Mn) of 5 kDa to 200kDa, a degree of deacetylation (DDA) of 80% to 95%, and wherein the chitosan amine to nucleic acid phosphate ratio (N:P) is below 20.

[0025] Another aim of the present description is to provide a composition as described herein for the treatment of diabetes mellitus, atherosclerosis or cancer and/or related conditions in a patient.

[0026] In accordance with the present description there is provided a method of producing a composition for treating diabetes mellitus, atherosclerosis or or cancer and/or related conditions comprising admixing chitosan and an RNA-inducing nucleic acid sequence in an acidic medium, wherein the chitosan has a molecular weight (Mn) of 5 kDa to 200kDa, a degree of deacetylation (DDA) of 80% to 95%, and wherein the chitosan amine to nucleic acid phosphate ratio (N:P) is below 20.

[0027] In accordance with the present description, it is also provided the use of a composition as defined herein for the treatment of diabetes mellitus, atherosclerosis or cancer and/or related conditions in a patient; or in the manufacture of a medicament for the treatment of diabetes mellitus, atherosclerosis or cancer and/or related conditions in a patient.

[0028] One aim of the present description is to provide a composition as described herein for the treatment of cancer in a patient or the reversal of chemoresistance or a combination of both. In accordance with the present description there is provided a method of producing a composition for treating cancer or sensitizing chemoresistant cancer to classical chemotherapy or both.

[0029] Another aim of the present description is to provide a method of treating diabetes mellitus, atherosclerosis or cancer and/or related conditions in a patient comprising administering to the patient an effective amount of a composition as defined herein, more particularly a compostion comprsing chitosan and an RNA-inducing nucleic acid sequence, wherein the chitosan has a molecular weight (Mn) of 5 kDa to 200kDa, a degree of deacetylation (DDA) of

80% to 95%, and wherein the chitosan amine to nucleic acid phosphate ratio (N:P) is below 20.

[0030] It is also provided a method for delivering a nucleic acid sequence into a cell comprising the step of contacting the compositon as described herein with the cell.

[0031] In an embodiment, the molecular weight of chitosan is 5 to 15 kDa, the DDA from 90 to 95% and the N:P ratio is from 2 to 10; preferably the molecular weight of chitosan is 10 kDa, the DDA is 92% and the N:P ratio is 5.

[0032] In a further embodiment, the molecular weight of chitosan is 10 kDa, 40 kDa, 80 kDa, 150 kDa or 200 kDa.

[0033] In another embodiment, the chitosan comprises block distribution of acetyl groups or a chemical modification.

[0034] In a further embodiment, chitosan has a polydispersity between 1.0 and 7.0.

[0035] In a further embodiment, the RNA-inducing nucleic acid sequence is a double stranded linear deoxyribonucleic acid sequence between 10 to 50 nucleotides; the RNA-inducing nucleic acid sequence is a double stranded linear ribonucleic acid sequence between 10 to 50 nucleotides; the RNA-inducing nucleic acid sequence is a hairpin structure of deoxyribonucleic or ribonucleic acid sequence; and/or the RNA-inducing nucleic acid sequence is a short interfering RNA, a short hairpin RNA or an RNAi-inducing vector.

[0036] In another embodiment, the RNAi-inducing nucleic acid sequence is chemically modified either on the sugar backbone, phosphate backbone and/or the nucleotide base ring.

[0037] Preferably, the RNA-inducing nucleic acid sequence targets a gene involved in the pathogenesis of type II diabetes, atherosclerosis or cancer; such as for example a gene involved in tumor development, metastasis or the induction or acquisition of chemoresistance, a glycoregulating protein or an

atherogenic protein; such as for example an incretin degrading enzyme; such as for example dipeptydilpeptidase-IV (DPP-IV); such as for example Apolipoprotein B (ApoB), Apolipoprotein E (ApoE), Apolipoprotein B 100 (ApoB 100), Apolipoprotein B 48 (ApoB 48), Neutrophil gelatinase-associated lipocalin (NGAL), Matrix metalloproteinase-9 (MMP-9), or Cholesteryl ester transfer protein (CETP).

[0038] In another embodiment, the RNAi-inducing nucleic acid sequence targets a helicase protein, an RNA helicase, P68, DDX5, DDX32, DDX1, Akt, PKB, a member of the ABC transporters, MDR1, MRP, a member of the RAS family of proteins, SRC, HER2, EGFR, Abl, or Raf.

[0039] In another emdodiment, the helicase protein is a member of the RecQ family of helicases, such as for example RecQL1 DNA helicase. Additionally, the RNAi-inducing nucleic acid sequence targets MDR1.

[0040] In another embodiment, the diabetes mellitus related conditions are insulin-dependent diabetes mellitus (type I diabetes), noninsulin-dependent diabetes mellitus (type II diabetes), insulin resistance, hyperinsulinemia, diabetes-induced hypertension, obesity, damage to blood vessels, damage to eyes, damage to kidneys, damage to nerves, damage to autonomic nervous system, damage to skin, damage to connective tissue, and damage to immune system.

[0041] In a further embodiment, the atherosclerosis related conditions are cardiovascular diseases, such as for example coronary heart diseases, acute coronary syndromes or angina pectori.

[0042] In another embodiment, the composition reduces ApoB plasma levels; increases GLP-1 bioavailability; increases the control of glucose metabolism in the patient; reduces the blood glucose level in the patient; reduces the cholesterol level in the patient; reduces the low-density lipoprotein level in the patient; and/or reduces the weight gain in the patient.

[0043] In a further embodiment, the composition reduces ApoB plasma levels of at least 35% and LDL/VLDL cholesterol level of at least 20%.

[0044] In another embodiment, the composition is formulated for a subcutaneous administration, an intramuscular administration, an intravenous administration, an intradermal administration, intramammary administration, an intraperitoneal administration, an oral administration or a gastrointestinal administration.

[0045] In a particular embodiment, the composition is formulated for an injection at a dose of 1mg/kg.

[0046] In another embodiment, the composition described herein can comprise insulin, a glucosidase inhibitor, a sulfonylurea, a DPP-IV inhibitor or a hypoglycemic compound.

[0047] The composition described herein can also be formulated for concurrent administration with a suitable delivery reagent, insulin or a hypoglycemic compound; such as a delivery agent being Mirus Transit TKO® lipophilic reagent, lipofectin®, lipofectamine™, cellfectin®, polycations or liposomes; or such as an hypoglycemic compound being metformin, acarbose, acetohexamide, glimepiride, tolazamide, glipizide, glyburide, tolbutamide, chlorpropamide, thiazolidinediones, alpha glucosidase inhibitors, biguanindine derivatives, troglitazone, or a mixture thereof; such an sulfonylurea being tolbutanide, tolazamide, glisoxepide, glimipeide or glibomuride; such as a DPP-IV inhibitor being sitagliptin, vildagliptin or saxagliptin.

[0048] In an embodiment, the cancer is breast cancer, glioma, large intestinal cancer, lung cancer, small cell lung cancer, stomach cancer, liver cancer, blood cancer, bone cancer, pancreatic cancer, skin cancer, head or neck cancer, cutaneous or intraocular melanoma, uterine sarcoma, ovarian cancer, rectal or colorectal cancer, anal cancer, colon cancer, fallopian tube carcinoma, endometrial carcinoma, cervical cancer, vulval cancer, squamous cell carcinoma, vaginal carcinoma, Hodgkin's disease, non-Hodgkin's lymphoma, esophageal cancer, small intestine cancer, endocrine cancer,

thyroid cancer, parathyroid cancer, adrenal cancer, soft tissue tumor, urethral cancer, penile cancer, prostate cancer, chronic or acute leukemia, lymphocytic lymphoma, bladder cancer, kidney cancer, ureter cancer, renal cell carcinoma, renal pelvic carcinoma, CNS tumor, glioma, astrocytoma, glioblastoma multiforme, primary CNS lymphoma, bone marrow tumor, brain stem nerve gliomas, pituitary adenoma, uveal melanoma, testicular cancer, oral cancer, pharyngeal cancer, pediatric neoplasms, leukemia, neuroblastoma, retinoblastoma, glioma, rhabdomyoblastoma or sarcoma.

[0049] In another embodiment, the composition is formulated for concurrent administration with at least one of a suitable delivery reagent and an anti-cancer compound.

[0050] The suitable delivery agent can be Mirus Transit TKO® lipophilic reagent, Lipofectin®, Lipofectamine™, Cellfectin®, polycations or liposomes.

[0051] It is also described that the compositon is formulated for concurrent administration during a suitable anti-cancer therapy, such as an anti-cancer therapy being at least one of a surgical procedure, chemotherapy, hormonal therapy and localization radiation.

[0052] In a preferred embodiment, the composition does not induce liver toxicity and inflammation when administered.

[0053] The composition described herein can further comprise a transfection media having a pH varying from 5 to 7.1; can be formulated as a dried powder; and/or is a particulate suspension in aqueous media.

[0054] In another embodiment, the chitosan is dissolved in hydrochloric acid prior to admixing with the RNA-inducing nucleic acid sequence.

[0055] Preferably, the chitosan is dissolved in a glucosamine:HCl at a ratio of 1:1.

[0056] In another embodiment, the admixing of chitosan with the RNA-inducing nucleic acid sequence produces nanoparticles of spherical shape of sizes below 200nm, preferably the size of 45 to 156 nm.

[0057] In an embodiment, the cell is a primary cell, a transformed cell or an immortalized cell.

[0058] In another embodiment, the chitosan is dissolved in hydrochloric acid prior to admixing with the RNAi-inducing nucleic acid sequence.

[0059] In another embodiment, the Mn of chitosan is 10 kDa, the DDA is of 80% or 92%, and wherein the chitosan amine to nucleic acid phosphate ratio (N:P) is of 5 or 10.

BRIEF DESCRIPTION OF THE DRAWINGS

[0060] Reference will now be made to the accompanying drawings.

[0061] Fig. 1A illustrates environmental scanning electron microscopy (ESEM) images of spherical chitosan/ dsODN nanoparticles and population size distribution of **(A)** 92-10-5 chitosan/dsODN-DPP-IV nanoparticles, **(B)** 80-80-5 chitosan/dsODN-DPP-IV nanoparticles, **(C)** 80-10-10 chitosan/dsODN-DPP-IV nanoparticles, **(D)** 92-10-5 chitosan/dsODN-ApoB nanoparticles, **(E)** 80-80-5 chitosan/dsODN-ApoB nanoparticles and **(F)** 80-10-10 chitosan/dsODN-ApoB nanoparticles; and Fig. 1B illustrates environmental scanning electron micrograph (ESEM) images of spherical chitosan/dsODN nanoparticles and population size distribution: **(A)** 92-10-5 chitosan/dsODN-RecQL1 nanoparticles, **(B)** 80-40-5 chitosan/dsODN-RecQL1 nanoparticles, and **(C)** 80-10-10 chitosan/dsODN-RecQL1 nanoparticles.

[0062] Fig. 2A illustrates environmental scanning electron microscopy (ESEM) images of spherical chitosan/siRNA nanoparticles and population size distribution of **(A)** 80-10-5 chitosan/siRNA-ApoB nanoparticles, **(B)** 80-40-5 chitosan/siRNA-ApoB nanoparticles, **(C)** 92-10-5 chitosan/siRNA-ApoB nanoparticles and **(D)** 92-40-5 chitosan/siRNA-ApoB nanoparticles; and Fig. 2B illustrates environmental scanning electron micrograph (ESEM) images of

spherical chitosan/siRNA nanoparticles and population size distribution: **(A)** 80-10-5 chitosan/siRNA-MDR1 nanoparticles, **(B)** 80-200-5 chitosan/siRNA-MDR1 nanoparticles, **(C)** 92-10-5 chitosan/siRNA-MDR1 nanoparticles and **(D)** 92-150-5 chitosan/siRNA-MDR1 nanoparticles.

[0063] Fig. 3A illustrates a photographic representation of a polyacrylamide gel electrophoresis of chitosan/dsODN nanoparticles possessing various N:P ratios incubated at different pH values and during different time periods. Chitosan 92-10 complexed with **(A)** dsODN-DPP-IV and **(B)** dsODN-ApoB and incubated for 0.5h, 4h and 20h in pH6.5 (MES) and pH 8 (TAE) is shown; and Fig. 3B illustrates a polyacrylamide gel electrophoresis of chitosan/dsODN nanoparticles possessing various N:P ratios incubated at different pH and during different time periods. Chitosan 92-10 complexed with dsODN-RecQL1 and incubated for 0.5h, 4h and 20h in pH6.5 (MES) and pH 8 (TAE). If nanoparticles are not stable in the above-mentioned conditions, siRNA mimicking dsODN are released and migrate in the gel.

[0064] Fig. 4A illustrates histograms of chitosan/siRNA nanoparticle stability at a pH of 6.5, chitosan formulations at different DDA and MW were complexed to three different anti-ApoB siRNA sequences (siApoB1, siApoB2 and siApoB3) at N:P ratios of 5 and 10 and incubated for 20 hours, and following nanoparticle formation Ribogreen™, an RNA intercalating dye used for nucleic acid quantitation, was added to each sample to measure the uncomplexed RNA fraction so that high fluorescence values represent particle disassembly and instability; Fig. 4B illustrates a histogram demonstrating the influence of MW on nanoparticle size, chitosan at a DDA of 92% and different MW was complexed to anti-RecQL1 siRNA at different N:P ratio; Fig. 4C illustrates a histogram demonstrating the influence of MW on nanoparticle size, chitosan at a DDA of 80% and different MW was complexed to anti-RecQL1 siRNA at different N:P ratio; Fig .4D illustrates a histogram demonstrating the influence of MW on nanoparticle size. Chitosan at a DDA of 72% and different MW was complexed to anti-RecQL1 siRNA at different N:P ratio; and Fig. 4E illustrates a histogram demonstrating the effect of RecQL1 siRNA concentration on nanoparticle size, and the effect of salt on nanoparticle size as measured by dynamic light

scattering, chitosan with a DDA of 92%, a Molecular weight of 10 at an N:P ratio of 5 was complexed to increasing concentrations of anti-RecQL1 siRNA.

[0065] Fig. 5 illustrates the effect of DDA, MW and N:P ratio on nanoparticle stability at different pH where low fluorescence indicates particle stability. Chitosan with various DDA, MW was complexed to anti-MDR1 siRNA at different N:P ratio to form nanoparticles. The latter were incubated at different pH and siRNA release was measured using the Ribogreen ™ assay.

[0066] Fig. 6A illustrates results of nuclease protection assays of chitosan/dsODN nanoparticles, **(A)** chitosan (92-10-5 or 80-10-10) complexed with dsODN-DPP-IV, **(B)** dsODN-DPP-IV remaining after the DNAse I digestion, **(C)** chitosan (92-10-5 or 80-10-10) complexed with dsODN-ApoB, **(D)** dsODN-ApoB remaining after the DNAse I digestion, all digestions were assessed using the signal intensity of the treated samples with the control. (i.e. 0U DNAse I = 100% intensity); and Fig. 6B illustrates nuclease protection assays results of chitosan/dsODN nanoparticles: **(A)** chitosan (92-10-5, 80-40-5 or 80-10-10) complexed with dsODN-RecQL1, and **(B)** dsODN-RecQL1 remaining after the DNAse I digestion, all digestions were assessed using the signal intensity of the treated samples with the control. (i.e. 0U DNAse I = 100% intensity).

[0067] Fig. 7A illustrates histogram representations of the cellular uptake of dsODN /nanoparticles 24 hours post-transfection in several cell lines: **(A)** Chitosan (92-10-5, 80-80-5 or 80-10-10)/5'-6FAM labeled dsODN DPP-IV uptake in HepG2 cell lines; and **(B)** Chitosan (92-10-5, 80-80-5 or 80-10-10)/5'-6FAM labeled dsODN-ApoB uptake in HepG2, HEK293 and RAW264.7 cells, DharmaFECT® #1 and 4 were used as positive uptake control; and Fig. 7B illustrates a histogram showing the cellular uptake of dsODN/nanoparticles 24 hours post-transfection in several cell lines, chitosan (92-10-5, 80-40-5 or 80-10-10)/5'-6FAM labeled dsODN RecQL1 uptake in AsPC1, LS174T and A549 cell lines, DharmaFECT™ #1 was used as positive uptake control.

[0068] Fig. 8 illustrates confocal imaging of chitosan/siRNA nanoparticle uptake 24 hours post-transfection in **(A)** HepG2, **(B)** Caco-2 and **(C)** HT-29 cell

lines transfected with chitosan/dsODN-DPP-IV nanoparticles, **(D)** HepG2, **(E)** HEK293 and **(F)** RAW264.7 cell lines transfected with chitosan/dsODN-ApoB nanoparticles. Chitosan 92-10 (DDA, Mn) was labeled with rhodamine (red) and dsODN were 5' labeled with 6FAM (green). Chitosan 92-10 was complexed to siRNA at an N:P ratio of 5. Cell membranes were stained prior to imaging with CellMask™ (blue), a membrane anchoring amphipatic dye, to differentiate between internalized and membrane bound nanoparticles. Images shown represent each separate channel with dsODN in green, chitosan in red, membrane in blue, transmission DIC in grey and the merged images shown on the bottom left quadrant.

[0069] Fig. 9 illustrates confocal imaging of chitosan/siRNA nanoparticle uptake 24 hours post-transfection. LS174T cell lines transfected with chitosan/siRNA-RecQL1 nanoparticles. Images were taken 24 hours post transfection. Chitosan 92-10 (DDA, Mn) was labeled with rhodamine (red) and siRNA were 5' labeled with 6FAM (green). Chitosan 92-10 was complexed to siRNA-RecQL1 at an N:P ratio of 5. Cell membranes were stained prior to imaging with CellMask™ (blue). Images shown represent each separate channels with siRNA in green, chitosan in red, membrane in blue, transmission DIC in grey and the merge images shown on the bottom left quadrant.

[0070] Fig. 10 illustrates confocal imaging of chitosan/siRNA nanoparticle uptake 24 hours post-transfection. MCF-7 MDR cell line transfected with chitosan/siRNA-MDR1 nanoparticles. Images were taken 24 hours post transfection. Chitosan 92-10 (DDA, Mn) was labeled with rhodamine (red) and siRNA were 5' labeled Cy3 (green). Chitosan 92-10 **(A)** chitosan 80-10 **(B)** and chitosan 80-200 **(C)** were complexed to siRNA-cy3 at an N:P ratio of 5. Cell membranes were stained prior to imaging with CellMask™ (blue). Images shown represent each separate channel with siRNA in green, chitosan in red, membrane in blue, transmission DIC in grey and the merge images shown on the bottom left quadrant.

[0071] Fig. 11A illustrates histograms of real-time PCR (qPCR) analysis of the inhibition DPP-IV and ApoB gene expression in specific cell lines, HepG2

cells were transfected with: **(A)** chitosan (92-10-5, 80-80-5 and 80-10-10/siRNA-DPP-IV); **(B)** chitosan (92-10-5/siRNA-ApoB) nanoparticles, the inhibition percentage was obtained by comparing the transfected and non-transfected cells, using the ΔΔCT method; and Fig. 11B illustrates a histogram showing Real-time PCR (qPCR) analysis of the inhibition RecQL1 gene expression in specific cell lines, LS174T cells were transfected with chitosan (92-10-5, 80-40-5 and 80-10-10/siRNA-RecQL1), the inhibition percentage was obtained by comparing the transfected and non-transfected cells, using the ΔΔCT method.

[0072] Fig. 12 illustrates a histogram showing DPP-IV enzymatic activity in three different DPP-IV expressing cell lines. DPP-IV inhibition percentages were determined in comparison with siRNA-mock transfected cells. Values are expressed as mean ± s.d.; n=4 /group. *$p < 0.05$, ** $p < 0.01$.

[0073] Fig. 13 illustrates a histogram showing effects of chitosan/siRNA administration on ApoB plasma levels. Protein levels were measured by ELISA, for each treatment group. Columns and error bars represent the mean protein level relative to the untreated atherosclerotic group, Dα. The group Dμ is the normal negative control group fed a normal low fat diet.

[0074] Fig. 14 illustrates a histogram showing the therapeutic lowering of LDL/VLDL cholesterol after chitosan/siRNA administration. LDL/VLDL cholesterol levels were measured by a quantitative colorimetric ELISA kit on samples taken the day of euthanasia. Columns and error bars represent the mean cholesterol levels relative to the untreated atherosclerotic group, Dα. The group Dμ is the normal negative control group fed with a normal low fat diet.

[0075] Fig. 15 illustrates the reduction of liver cholesterol droplets in Therapeutic NanoComplex (TNC) treated animal livers. Hematoxylin-eosin stained paraffin fixed liver sections of **(A)** C1-1, **(B)** C2-1, **(C)** C3-1, **(D)** C4-1, **(E)** C5-1, **(F)** Dα-2 day, **(G)** Dα-3, **(H)** Dβ-1 and **(I)** Dμ-1 mice demonstrating the effects of chitosan/siRNA administration in cholesterol accumulation in the liver. Arrows (→) indicate cholesterol droplet accumulation. The Dα group is the

positive untreated atherosclerotic control while Dμ is the normal negative control fed with a low fat diet.

[0076] Fig. 16 illustrates resorption of inflammation in TNC treated animal liver. Safranin-O/fast-green/iron-hematoxylin stained paraffin fixed liver section of **(A)** C1-1, **(B)** C2-1, **(C)** C3-1, **(D)** C4-1, **(E)** C5-1, **(F)** Dα-2 day, **(G)** Dα-3, **(H)** Dβ-1 and **(I)** Dμ-1 mice demonstrating the resorption of the inflammatory reaction related to the chitosan/siRNA administration or atherosclerosis development. Circles (O) and arrows (→) indicate lymphoid infiltration.

[0077] Fig. 17 illustrates a histogram showing the weekly weight (g) measurements of all animal groups. All animals were weighed on the first day of each week, before each chitosan/siRNA administration. Compared to the low fat normal control Dμ, a continual weight gain over 4 weeks was observed for all animals fed with the high fat diet that was essentially unaffected by NTC treatment.

[0078] Fig. 18 illustrates a histogram showing the percentage of weight gain per week. All animals were weighed on the first day of each week, before chitosan/siRNA administration. Weight gain consists in the relative difference between the weight of the animal and its recorded weight the previous week [$(t_{n-1}-t_n)/t_{n-1}$)]. This figure show immediate weight gain or loss following the first TNC administration.

DETAILED DESCRIPTION

[0079] In accordance with the present disclosure, there is provided a novel and specific composition of a non viral vector for the efficient delivery of RNAi inducing entities such as short interfering RNAs (siRNAs), short hairpin RNAs (shRNAs), and RNAi-inducing vectors (i.e., vectors whose presence within a cell results in production of a siRNA or shRNA) to cells, tissues and organs in mammals, e.g., human. In particular, the description provides chitosan compositions with specific average molecular weight (Mn) and degree of deacetylation (DDA) ranges comprising RNAi inducing entities with specific chitosan to nucleic acid ratios.

[0080] There is thus provided compositions and methods of treating or preventing diseases or conditions associated with excessive expression or inappropriate expression of a target transcript; or inappropriate or excessive activity of a polypeptide encoded by the target transcript.

[0081] The compositions provided herein can be used in order to provide symptomatic relief, by administering RNAi inducing entities using the compositions disclosed herein to a subject at risk of, or, suffering from such a condition within an appropriate time window prior to, during, or after the onset of symptoms.

[0082] The compositions and methods may be applied for a variety of purposes, such as for example, but not limited to, studying the function of the transcript, studying the effect of different compounds of a cell or organism in the absence of, or with reduced activity of, the polypeptide encoded by the transcript. Furthermore, the composition and methods may be applied in clinical therapy for type II diabetes and its related pathologies, atherosclerosis and its related pathologies and cancer. Specifically, the compositions and methods may be applied for the inhibition of incretin degrading enzymes (DPP-IV) or any glycoregulating protein in order to treat diabetes, applied for the inhibition of ApoB gene or any atherogenic protein (i.e ApoE) in order to treat atherosclerosis, or for down-regulating the expression of RecQL1 DNA helicase or DDX5 – p68– RNA helicase respectively, but not limited to those, for treating cancer.

[0083] Particulalry, the present description relates to the use of such nucleic acids coupled with the compositions described herein as direct treatment of, for example, helicase over-expressing tumors or as radiosensitizing entities for palliative medicine. Moreover the composition and methods described herein can be used in conjunction with any other cancer treatment such as radiotherapy, surgery, hormonal treatment or conventional chemotherapy. The present description further provides compositions and methods for the enhancement of radiotherapy or used in combination with other treatment modalities.

[0084] The composition disclosed herein contains an RNAi inducing nucleic acid and a chitosan that has the following physicochemical properties: N:P ratio below 25, a chitosan with number average molecular weight (Mn) in the range of 5 kDa to 200kDa and a degree of deacetylation in the range of 80% DDA to 95% DDA. The present description demonstrate the effectiveness of composition and methods to effectively transfect different cells line and induce gene silencing comparable to commercially available lipoplexes, where transfection efficiency reached 80% at the mRNA level and cell uptake 95% in some instance, without any apparent cytotoxicity.

[0085] RNA interference (RNAi) is a process by which double-stranded RNA directs sequence specific degradation of cellular transcripts such as messenger RNA (Sharp, 2001, Genes Dev, 15:485-490; Vance and Vaucheret, 2001, Science, 292:2277-2280). This phenomenon was initially discovered in *C. elegans* (Fire et al., 1998, Nature, 391:806-811). Naturally occurring RNAi is mediated by small double stranded fragments between 21-25 nucleotide and are termed small interfering RNA. These siRNA are generated by a dsRNA-specific endonuclease, called Dicer by a process cleaving long double stranded RNA (dsRNA) into a 21 base pair small interfering RNA (siRNA) consisting of a core region of 19 base pair duplex region flanked by two nucleotide 3'over hangs (Bernstein et al., 2001, Nature, 409:363-366). siRNA are then incorporated into the RNA-induced silencing complex (RISC), and direct RISC to recognize target mRNA with complementary sequences to the siRNA leading to the cleavage of the specific transcript.

[0086] Subsequently, RNAi was quickly recognized as having great potential in clinical applications since it was discovered that RNAi can be triggered in mammalian cells by introducing synthetic 21 nucleotide RNA duplexes (siRNA) (Elbashir et al., 2001, Nature, 411:494-498), thus bypassing the requirement of Dicer mediated processing of long dsRNA.

[0087] For example, by targeting and reducing the expression of ApoB, it is possible to prevent excess formation of VLDL, thus diminishing the accumulation of these atherogenic agents in the organism (Soutschek et al.,

2004, Nature, 432:173-178). ApoB targeting at the mRNA level in non-human primate using sequence specific siRNAs demonstrated significant reductions in ApoB protein, serum cholesterol and low-density lipoprotein levels 24h post-treatment (Zimmermann et al., 2006, Nature, 441:111-114). The therapeutic effect of such treatment using lipid based nanoparticles (SNALP-siRNA) lasted for 11 days at the highest siRNA dose, thus demonstrating an immediate, potent and lasting biological effect of siRNA treatment. Unfortunately, these lipid-based vectors produced a high level of liver toxicity as indicated by elevated serum levels of aspartate aminotransferase (AST) and alanine aminotransferase (ALT) suggested hepatocyte necrosis (Zimmermann et al., 2006, Nature, 441:111-114). Thus although these reports demonstrate the importance of ApoB as a target for atherosclerotic and CVD therapies, they also highlight the current inadequacies of siRNA delivery systems to attain a safe and efficacious reduction in systemic ApoB.

[0088] Direct delivery of RNAi in the form of synthetic small interfering RNA continues to be problematic, suffering from poor cellular targeting and uptake, a short half life due to intracellular and/or extracellular nuclease degradation (i.e. RNAse) as well as limited blood stability and toxicity (Stein, 1996, Trends Biotechnol, 14:147-149; Urban-Klein et al., 2004, Gene Therapy, 1-6; Katas and Alpar, 2006, J Control Release, 115:216-225). As a consequence, the translation of RNAi into a clinical therapeutic is still pending resolution of these issues. RNAi has been shown to operate in a wide variety of different cell types when introduced into cells by means such as transfection. However, transfection efficiency depends on the delivery vehicle carrying the small interfering RNA molecule. The delivery vehicle, referred to as the vector, should be able to condense, protect and carry siRNA into target cells. Once in the vicinity of the target, non-viral vectors should promote cellular uptake, avoid lysosomal sequestration and release their content in order to achieve the desired biological effect.

[0089] Chemical modification of synthetic siRNAs has provided resistance to nuclease degradation and improved blood stability. For example, selective addition of a phosphorothioate linkage or substitution with 2'-O-methyl on the

C2 position of specific riboses increases nuclease resistance of siRNAs without compromising activity (Corey, 2007, J Clin Invest, 117:3615-3622; Whitehead et al., 2009, Nat Rev Drug Discov, 8:129-138; Judge et al., 2006, Mol Ther, 13:494-505). Nevertheless, some chemical modifications can increase cytotoxicity and off target effects and reduce mRNA hybridization (Weyermann et al., 2005, Eur J Pharm Biopharm, 59:431-438; Amarzguioui et al., 2003, Nucleic Acids Res, 31:589-595). Despite progress achieved through chemical modification to increase siRNA half life, transfection efficiency, cellular targeting and uptake remain as obstacles to effective delivery. Therefore, packaging systems which can both protect and transport chemically unmodified/modified siRNA to target cells are required. However, transfection efficiency depends on the delivery vehicle carrying the small interfering RNA molecule. The delivery vehicle, referred to as the vector, should be able to condense, protect and carry siRNA into target cells. Once in the vicinity of the target, non-viral vectors should promote cellular uptake, avoid lysosomal sequestration and release their content in order to achieve the desired biological effect. Such non-viral vectors are being tested *in vitro* and *in vivo*, demonstrating the potential translation of siRNA into a clinical reality. Nevertheless, major drawbacks are associated with such non-viral vectors. Low transfection efficiency, serum stability, aggregation and toxicity remain as major barriers to be addressed before commercialization of non-viral vectors as powerful and non-toxic tools for drug delivery in the clinic becomes a reality. The major classes of non viral vectors are discussed below:

Calcium phosphate

[0090] The major drawback of this vector is limited efficiency and its inability to protect nucleic acids from nuclease degradation. Despite the improvement of its ability to protect nucleic acids, its transfection efficiency remains low thus preventing its effective use *in vivo*.

Cationic lipids

[0091] Cationic lipids form complexes with nucleic acids via electrostatic interaction eventually forming multi lamellar lipid-nucleic acid complexes

(lipoplexes). Liposome formulations usually include a cationic lipid and a neutral lipid such as DOPE (dioleoylphosphatidylethanolamine). The neutral lipid contributes to the stability of the liposomic formulation and facilitates membrane fusion as well as contributing to the lysozomal escape by destabilizing the endosome. Lipoplexes are one of the most efficient ways of delivering nucleic acids into cultured cells. Despite their transfection efficiency, lipoplexes are toxic as observed in cultured cells and confirmed by several *in vivo* findings. The toxicity is closely associated with the charge ratio of cationic lipids to nucleic acid in the complex as well as the administered dose. More biocompatible formulations are being tested and developed in order to reduce lipoplexes associated toxicity. Reduction of toxicity is mainly achieved via grafting with other polymers or reducing the total charge of the cationic polymer.

Cationic polymers

[0092] Cationic polymers form nanoparticles of nanometric size through interactions between oppositely charged polycation and polyanion species (i.e. nucleic acids). These nanoparticles encapsulate nucleic acids, consequently preventing cargo degradation from nucleases (Romoren et al., 2003, Int J Pharm, 261:115-127). A large number of natural and synthetic cationic polymers have been used as vehicles for gene delivery or silencing. Many of these nanoparticles using cationic polymers have superior transfection efficiency and lower serum sensitivity compared to lipoplexes. Among naturally occurring polycation are proteins such as histones, cationized human serum albumin and chitosan, an aminopolysaccharide.

[0093] The group of synthetic polycations includes poly-L-Lysine (PLL), poly-L-Ornithine as well as polyamines such a polyethylenimine (PEI), polypropylenimine and polyamidoamine dendimers.

[0094] An advantage of polyplexes is that their formation does not require interaction of multiple polycations, contrary to the need of multiple lipid components of liposomes which make polyplex macroscopic properties easier to control. Another major advantage of polycation is their block structure

therefore allowing direct chemical modification to attain higher efficiency or specific cell targeting. However, despite these advantages, many cationic polymers have been found toxic because of high surface charge density since high charge density nanoparticles appear to be more toxic. Furthermore, it has been reported that the charge density in the polymer plays a more important role in cytotoxicity than the total amount of charge. Toxicity may be molecular weight dependent as well, since the cytotoxicity of PEI increases linearly with molecular weight. Moreover, accumulation of non degradable polymer such as PEI in the lysosome, a phenomenon called lysosomal sequestration, may yet be an additional contributor to toxicity.

[0095] Chitosan is a natural polymer of glucosamine and N-acetyl-glucosamine monomers linked by β-1, 4 glycosidic bonds derived from alkaline deacetylation of chitin. Chitosan molecular weight and degree of deacetylation dictate its biological and physicochemical properties. For example chitosan biodegradability is affected by the amount and distribution of acetyl groups. The absence of these groups or their random rather than block distribution results in very low rate of degradation.

[0096] Chitosan possesses a wide range of beneficial properties including biocompatibility, biodegradability, mucoadhesive properties, antimicrobial/antifungal activity and very low toxicity. Therefore, it has attracted attention of the pharmaceutical and biomedical field and became one of the most widely used non-viral vectors for nucleic acid packaging and condensation.

[0097] Several studies have addressed the effect of chitosan molecular weight and degree of deacetylation (DDA) on uptake of chitosan- plasmid DNA nanoparticle, nanoparticle trafficking and transfection efficiency on different cell lines. Huang et al. addressed this subject on A549 cells (2005, J Control Release, 106:391-406). However this study only used seven formulations (chitosan of 10,17,48,98 and 213kDa at 88% DDA; 213kDa at 61 and 46% DDA) to study the effect of average molecular weight (Mn) and DDA on transfection efficiency of pDNA without addressing the much smaller siRNA that

is typically 21bp versus thousands of base pairs in plasmids. They found that a decrease in Mn and DDA produces lower transfection efficiency for plasmids. However, the relationship between those two parameters is much more complex and demands a fine balance between chitosan Mn and DDA to achieve optimal stability. Their inability to draw a complex relationship is due to their limited number of formulations. Moreover, only one parameter at a time was varied preventing them to see a coupling effect between Mn and DDA in relation to the pH of the transfection media and to chitosan-to-DNA ratio (N:P). Another study addressing this complex relation for plasmid-chitosan polyplexes was performed by Lavertu et al. (2006, Biomaterials, 27:4815-4824). In their study, they varied the molecular weight, for several distinct DDA levels and also examined the chitosan-to-DNA ratio (N/P) and/or the pH of the transfection media. This study demonstrated that such optimization achieved high transfection efficiencies equivalent to broadly used commercial liposomes (Lipofectamine™ and Fugene™) in HEK293 cells.

[0098] The DNA binding capacity/affinity of chitosan increases when its degree of deacetylation increases to create a higher charge density along the chain to bind more tightly with pDNA to form nanoparticles (Ma et al., 2009, Biomacromolecules, 10:1490-1499). Thus chitosan with a very low DDA are unable to bind DNA efficiently and cannot form physically stable complexes to transfect cells (Koping-Hoggard et al., 2003, J Gene Med, 5:130-141). As mentioned hereinabove, DDA also exerts a dominant influence on biodegradability where high DDAs are difficult to degrade. In this light, a recent study by Koping-Hoggard et al. (2001, Gene Ther, 8:1108-1121) suggested that endosomal escape of the high Mn chitosan based complexes depends on enzymatic degradation of chitosan and would occur less readily with high DDA chitosans. The resulting degradation fragments are hypothesized to increase endosome osmolarity and lead to membrane rupture. Thus, for highly deacetylated chitosan (near 100% DDA), reduced degradability could result in reduced endosomal escape.

[0099] The influence of chitosan Mn on the ability to bind nucleic acids was evaluated in several studies. Binding affinity between oppositely charged

macromolecules is strongly dependant on the valence of each molecule, with a low valence yielding only weak binding (Danielsen et al., 2004, Biomacromolecules, 5:928-936). The reduction in chitosan valence for lower molecular weight with shorter chains has been shown to reduce its affinity to DNA (Ma et al., 2009, Biomacromolecules, 10:1490-1499). Although a high level of complex stability is desirable extracellularly for protection against enzymatic attack, MacLaughlin et al. (1998, J Control Release, 56:259-272) suggested that a high Mn chitosan can form complexes that are overly stable to transfect cells since they cannot be disassembled once inside the cell. Furthermore, Lavertu et al. (2006, Biomaterials, 27:4815-4824) showed that Mn does not appear to be a dominant factor in cellular uptake but does appear to play a role in nucleic acid binding affinity and intracellular release. These interpretations and the need for a finely balanced intermediate stability of chitosan binding to nucleic acids were further supported by direct assessment of binding affinity by isothermal titration calorimetry (Ma et al., 2009, Biomacromolecules, 10:1490-1499) and by live intracellular imaging of polyplex trafficking and disassembly (Thibault et al., 2010, Mol Ther, 18:1787-1795).

[00100] The amine to phosphate ratio has been found to play an important role in DNA binding and nanoparticle formation. For example, increasing the N:P ratio enhances chitosan binding to DNA. For the same DDA, a lower Mn chitosan requires a higher N:P ratio to completely bind plasmid DNA. Similarly at equal Mn, a lower DDA requires a higher N:P ratio to completely bind DNA (Koping-Hoggard, 2003, J Gene Med, 5:130-141; Kiang et al., 2004, Biomaterials, 25:5293-5301). pH has been shown to play an important role in transfection efficiency. Lavertu et al. (2006, Biomaterials, 27:4815-4824) showed that complexes are more stable and an increase in transfection efficiency is achieved in slightly acidic medium. This can be explained by the fact that pH reduction increases chitosan protonation and consequently the positive charge on the polyplex (zeta potential) and the binding affinity of chitosan to DNA. The combined effect of the chitosan formulation parameters (DDA, Mn, N:P and pH) was studied for plasmid DNA delivery *in vitro* by Lavertu et al. (2006, Biomaterials, 27:4815-4824). They interestingly found that

maximum transgene expression occurs for DDA: Mn values that run along a diagonal from high DDA/low Mn to low DDA/high Mn (Lavertu et al., 2006, Biomaterials, 27:4815-4824). Thus if one increases/decreases DDA, one must correspondingly decrease/increase Mn to maintain maximal transfection.

[00101] As mentioned above, pH plays an important role in transfection efficiency. Lavertu et al. (2006, Biomaterials, 27:4815-4824) showed that an increase in pH displaces the Mn for the most efficient formulation with plasmid DNA toward higher Mn because of the neutralisation of chitosan at higher pH resulting in reduced chitosan charge density. On the other hand, for a given DDA, a change in N:P ratio from 5:1 to 10:1 displaces the Mn for the most efficient formulation towards lower Mn, probably because of the stabilizing effect of increasing chitosan concentration. Thus, one can see the importance of these different formulation parameters on transfection efficiency and in the development of a more efficient and stable chitosan-DNA formulations.

[00102] The structural differences between pDNA and siRNA are believed to affect nanoparticle complexation/stability and the optimal parameters required for effective delivery. Chitosan has been used for siRNA delivery both *in vitro* and *in vivo* (de Fougerolles et al., 2007, Nat Rev Drug Discov, 6:443-453; Howard et al., 2006, Mol Ther, 14:476-484; Katas and Alpar, 2006, J Control Release, 115:216-225; Zimmermann et al., 2006, Nature, 441:111-114; and Liu et al., 2007, Biomaterials, 28:1280-1288). However, and despite attempts to identify optimal physico-chemical parameters for siRNA delivery, inconclusive results have been observed in the literature due to experimental discrepancies. For example, nanoparticle formation, stability and protection of the siRNA cargo was evaluated at pH 7.9; a pH that is unrepresentative of the physiological milieu. At this pH, chitosan is mainly deprotonated since its apparent pKa is close to 6.5, and thus unable to efficiently bind the siRNA cargo. Since complex formation was tested under these conditions, several groups have used high N:P ratios to compensate for the poor binding of chitosan to siRNA seen at pH higher than chitosan pKa. The use of these high pH values (i.e 7.9) represents an important design error and source of experimental discrepancy that led these investigators to use high N:P ratios to achieve nanoparticle complexation,

stability and cargo protection. Unfortunately, the excess chitosan may competitively affect transfection efficiency, create multiple non-specific effects and increase toxicity leading to incorrect conclusions.

[00103] For example, it was reported that intermediate DDA (80%) and high Mn (64-170 kDa) were apparently more efficient than low molecular weight chitosan (10kDa) in delivering siRNA (Katas et al., 2006, J Control Release, 115:216-225; and Liu et al., 2007, Biomaterials, 28:1280-1288). However, these high molecular weight chitosans were found to be toxic (Howard et al., 2006, Mol Ther, 14:476-484; and Richardson et al., 1999, Int J Pharm, 178:231-243). Additionally, all previous reports evaluating complex formation, other physico-chemical characteristics and transfection efficiency of chitosan/siRNA nanoparticles uniformly concluded that formulations were efficient only at very high N:P ratios (N:P >25) (Howard et al., 2006, Mol Ther, 14:476-484; Katas et al., 2006, J Control Release, 115:216-225; Liu et al., 2007, Biomaterials, 28:1280-1288). These reports did not recognize that a large portion of the excess chitosan is actually soluble and not a structural component of the nanoparticle (Ma et al., 2010, Biomacromolecules, 11:549-554). Such formulations with very high N:P ratios (N:P >25) display significant practical problems including limited dosing due to aggregation and non-specific toxic effects of large quantities of soluble chitosan.

[00104] The use here of appropriate pH conditions near chitosan pKa as well as near the physiological pH to asses nanoparticle physicochemical characteristics revealed that such high N:P were not required to form efficient nanoparticle delivery vehicles, as demonstrated in the present disclosure (Fig. 3).

[00105] Chitosan was used to deliver pharmacologically active compounds through different administrational routes including intranasal, oral, intra-peritoneal, and intramuscular routes. Chitosan/Insulin was administered through intranasal routes in rat and sheep. These formulation involved the use of a water soluble chitosan of molecular weight of 10kDa or greater, with no specification on degree of deacetylation (Illum, 1996, Danbiosyst UK Limited,

United States, vol. 5554388; 1998, Danbiosyst UK Limited, United States, vol. 5744166).

[00106] Chitosan has also been used as adjuvant for the immunization of mice through an intranasal route with soluble formulations (US patent application publication no. 2003/0039665). These formulations involved chitosan glutamate with a Mn ranging between 10-500kDa with a degree of deacetylation between 50-90%.

[00107] Chitosan has also been used to deliver nucleic acids varying from plasmid DNA to siRNA in *vitro* and *in vivo* as well. More than 40 examples of *in vivo* studies using siRNA with various delivery vehicles have been reported (de Fougerolles et al., 2007, Nat Rev Drug Discov, 6:443-453) to treat ocular (Nakamura et al., 2004, Mol Vis, 10:703-711) and pulmonary targets (Howard et al., 2006, Mol Ther, 14:476-484), or directed towards the nervous system (Kumar et al., 2006, Plos Medicine, 3:505-514), liver (Soutschek et al., 2004, Nature, 432:173-178), tumors (Grzelinski et al., 2006, Hum Gen Ther, 17:751-766) and other organs by local or systemic delivery. In one example, chitosan/siRNA nanoparticles mediated TNF-α knockdown in peritoneal macrophages for anti-inflammatory treatment in an arthritis murine model (Howard et al., 2006, Mol Ther, 14:476-484).

[00108] Several studies have examined the ability of chitosan to deliver siRNA *in vitro* and *in vivo*. Katas et al. (2006, J Control Release, 115:216-225), used two different forms of chitosan salts (CS-HCl and CS-Glutamate) with a DDA of 84% to study the influence of chitosan parameters on transfection efficiency. Four different high molecular weight chitosans were used (470kDa, 270kDa, 160kDa and 110kDa) and they found that increasing chitosan concentration from 25µg/ml (1.25:1) to 300µg/ml (15:1) increased nanoparticle size from approximately 150 nm to 450 nm (Katas et al., 2006, J Control Release, 115:216-225).

[00109] Moreover, it was shown in their study that chitosan-glutamate yielded smaller nanoparticles than chitosan-HCl. Katas et al. (2006, J Control Release,

115:216-225) found –under their experimental conditions- that complete binding of siRNA to chitosan occurred only at an N:P ratio of 100:1 and above, conditions of extreme excess of chitosan where most likely >95% of the chitosan is soluble and not complexed to siRNA (Ma et al., 2010, Biomacromolecules, 11:549-554). This large quantity of excess moderate DDA (84%) chitosan is expected to cause sustained inflammation *in vivo* and to increase adverse immunological responses (Jean et al., 2009, Gene Ther, 16:1097-1110). In their study, chitosan glutamate with a molecular weight of 470 kDa showed the highest gene silencing effect at 24 h post-transfection *in vitro* compared to its lower molecular weight or chitosan hydrochloride (Katas et al., 2006, J Control Release, 115:216-225). Ionic gelation of chitosan glutamate with an average molecular mass of 470kDa showed a higher silencing efficiency (82% mRNA knockdown) than chitosan–siRNA nanoparticles formed by simple complexation (51% mRNA knockdown) (Katas et al., 2006, J Control Release, 115:216-225).

[00110] Another group led by Howard et al. (2006, Mol Ther, 14:476-484), delivered chitosan-siRNA nanoparticles in a transgenic EGFP mouse model via the intranasal route of administration. For their study, they used chitosan at 84% DDA and 114kDa at four different N:P ratios (N:P 6, 33, 71 and 285). Higher N:P ratios resulted in smaller nanoparticles (N:P 6 = 223.6 nm vs N:P 33 = 181.6 nm) at low chitosan concentration of 250µg/ml (Howard et al., 2006, Mol Ther, 14:476-484). The same pattern was observed at higher chitosan concentration (1mg/ml) where chitosan nanoparticles with a DDA of 84%, Mn of 114 and an N:P ratio of 33 had an average diameter of 328 nm compared to 139 nm for the formulation 84-114-285 (Howard et al., 2006, Mol Ther, 14:476-484).

[00111] Their preliminary *in vitro* study showed that nanoparticle size depends on the N:P ratio and increases in the size at lower N:P ratios, suggesting high N:P ratios to be required. This finding is in contradiction to the findings presented herein, where it is demonstrated below the critical role of pH when evaluating chitosan-siRNA complexation and stability. Based on their findings, cell uptake and silencing efficiency were measured at the high N:P ratios of 36

and 57 respectively in NIH 3T3 and H1299 cell lines. Chitosan formulations at the high N:P ratio of 36 was used to study the silencing efficiency of EGFP stable cell lines. Silencing efficiency was 77.9% and 86.9% in H1299 and primary peritoneal mouse macrophage, respectively. The *in vivo* silencing efficiency of the chitosan formulation 84-114 at N:P 36 achieved 43% silencing efficiency in EGFP transgenic mouse model following a 30µg siRNA injection/day for five days compared to untreated controls (Howard et al., 2006, Mol Ther, 14:476-484).

[00112] In another *in vivo* study by Howard et al. (2009, Mol Ther, 17:162-168), a 27 base-pair siRNA targeting TNF-α mRNA was complexed to chitosan 84-114 at the N:P ratio of 63 and injected in a collagen induced arthritis (CIA) mouse model. Their formulation achieved 43% silencing as measured by TNF-α plasma levels.

[00113] Ji et al. (2009, Nanotechnology, 20:405103) suggested that 190kDa and 310kDa chitosans at DDA ranging from 75% to 85% are suitable delivery vehicles for siRNA. Similarly to the above studies, Ji et al. used chitosan formulations at a high N:P ratio of 50 for knockdown experiments of the FHL2 oncogene in Lovo cells. Their formulations achieved 69% of mRNA knockdown.

[00114] In an attempt to identify optimal parameters for chitosan delivery of siRNA, Liu et al. (2007, Biomaterials, 28:1280-1288), tested a range of chitosan with different DDA, Mn and N:P ratios and stated that N:P ratio > 25 are needed for efficient silencing. They also found that low molecular weight chitosan-siRNA (10kDa) formulations prepared at N:P 50 showed no knockdown of endogenous EGFP in H1299 human lung carcinoma cells, whereas chitosan formulations prepared with higher Mn (64.8–170 kDa) at DDA of 80% showed greater gene silencing ranging between 45% and 65%. The highest gene silencing efficiency (80%) was achieved using chitosan/siRNA nanoparticles at the extreme N:P 150 with Mn of 114 and 170 kDa respectively and DDA of 84% that correlated with their assessments of stable formation of nanoparticles with a diameter of approximately 200 nm. Additionally, Liu et al. (2007, Biomaterials, 28:1280-1288) found that a 95% DDA and 9kDa chitosan complexed to anti-EGFP

siRNA at N:P ratio of 50 had an undesirable large size of 3500 nm as measured by dynamic light scattering (DLS). Furthermore, they stated that this specific formulation did not form complexes with siRNA at N:P ratio as high as 50 according to their gel retardation assays for stability testing conducted at the basic pH of 7.9 that was shown here to produce artifactual particle disassembly. In addition, this specific formulation showed no EGFP knockdown when compared to the negative untreated control.

[00115] The above results found by others are in contrast to the novel findings presented herein where it is demonstrated that chitosan-siRNA nanoparticles can be formed at moderate to low N:P ratios (below 25 and preferably 5) using chitosan with a range of molecular weights (5 to 200kDa) at DDAs between of 80% and 95% and these nanoparticles achieve high levels of gene silencing, good stability and small size ranges compared to previously reported systems.

[00116] Chitosan coated poly(isohexyl cynoacrylate) (PIHCA) nanoparticles have also been used to deliver intravenously anti-RhoA siRNAs entities in a xenografted aggressive breast cancer model (Pille et al., 2006, Hum Gen Ther, 17:1019-1026). Administration of chitosan-coated-PIHCA-anti-RhoA siRNA nanoparticles significantly reduced cancer aggressivity *in vivo* by knockdown of over-expressed RhoA in the cancer cells. Zhang et al. studied Nanogene 042, a chitosan derived formulation, for *de novo* expression of siRNA targeting the NS1 protein in lung tissues for the prevention and treatment of Respiratory Syncitial Virus (RSV) infections in a Balb/c model (Zhang et al., 2005, Nat Med, 11:56-62). Zhang et al. used shRNA based plasmids and observed an efficient silencing of the NS1 gene and an attenuation of RSV infection coupled with a lowered viral titer load *in vivo*. Nanogene 042 showed higher transfection efficiency and induced less inflammation compared to classical high MW chitosan (Zhang et al., 2005, Nat Med, 11:56-62). However, the molecular weight of Nanogene 042 is not disclosed in the stated reference.

[00117] For the purpose of the present description, the C57BL/6 (C57BL/6NCrl) mouse model is used for enabling different embodiments. The C57BL/6 mouse model was developed by Charles River and Research Diets.

The C57BL/6 mouse model can become obese when fed a fat rich diet (D12492) with an apparent weight gain two weeks following with a fat rich diet compared to lean control. The C57BL/6 mouse model is used in multipurpose studies and hyperlipidemia research to study the level of LDL cholesterol in circulation during a high-fat diet (Soutschek et al., 2004, Nature, 432:173-178; Crooke et al., 2005, J Lipid Res, 46:872-884; Bose et al., 2008, J Nutr, 138:1677-1683). The fat rich diet (D12492) is equivalent to six times more fat than the control diet D12450B which contains only 10kcal% fat. In addition, the fat rich diet D12492 contains 300.8 (mg)/kg of cholesterol compared to 18 (mg)/kg for the control diet D12450B. Thereby, the feeding with such a high fat chow creates instability in the accumulation of LDL in arteries versus its elimination in the liver, driving the development of atherosclerosis in the C57BL/6 mouse model.

[00118] It has been found as described herein below that the compositions described herein are effective gene transfer vectors when combined with siRNA achieving *in vitro* transfection efficiencies similar to the commercial liposome DharmaFECT™. Moreover, the compositions not only achieved comparable efficiency in delivering siRNA into cells and similar silencing as DharmaFECT™, but with lower toxicity.

[00119] Uptake efficiency using chitosan/dsODN nanoparticles achieved levels comparable to or higher than the commercially used lipoplex (DharmaFECT™) with similar relative variation between cells type (Fig. 7A and 7B). Furthermore, these results are in accordance with confocal microscopy data (Fig. 8), described below, where images show a cellular distribution of chitosan and dsODN for all cell lines indicating a qualitative correlation to the FACS quantitative data. It is demonstrated herein the capability of the formulations described to transfect and efficiently deliver different siRNA into multiple cell lines (see for example Figs. 7A and 8).

[00120] Results disclosed herein clearly reveal the effectiveness of the described chitosan-based formulations to efficiently deliver siRNA and knock down specific genes at N:P ratios far below those used previously in the art. In

general, all of the low N:P ratio chitosan formulations used herein reached high level of gene silencing.

[00121] The results show nanoparticles of spherical shape (Figs. 1 and 2) with mean diameters ranging between 45-156 nm (Table 2) depending on the chitosan formulation (80-10-5, 80-40-5, 92-10-5, 92-40-5, 80-10-10, 80-80-5, 92-150-5 and 80-200-5) used and the extent of chemical modification of the siRNA. No statistical differences in nanoparticle size were observed between dsODN and un-modified siRNA-ApoB (Seq1, SEQ ID NO:5) and moderately modified siRNA-ApoB complexed to chitosan (Seq2, SEQ ID NO:6 and SEQ ID NO:7). Whereas, fully modified siRNA sequence yielded larger nanoparticles when complexed to the different chitosans.

[00122] Results obtained with specific formulations described herein are consistent with dynamic light scattering results obtained (Table 2), thereby indicating the robustness of the composition and method described herein. Furthermore, the nanoparticles formed yield reproducible sizes below 200 nm allowing for avoidance of renal clearance thus improving *in vivo* transfection efficiency and increasing circulating nanoparticles half-life.

[00123] Chitosan/siRNA stability was evaluated using the Ribogreen assay™, a fluorescence based assay, to quantitate the released siRNA following complex destabilization. The results show that chitosan/siRNA nanoparticle with an N:P ratio of 5 and 10 were stable for up to 20 hours at pH 6.5. Chitosan 80-10-5 showed the least stability when compared to other formulations. Increasing the N:P ratio for chitosan 80-10 resulted in an improvement of nanoparticle stability. Except for chitosan 80-10, increasing the N:P ratio above five did not result in an increase of nanoparticle stability (see for example Fig. 4A).

[00124] It is demonstrated that the formulations described herein can achieve levels of gene silencing comparable to the commercial liposome DharmaFECT™ without any apparent cytotoxicity. The results disclosed herein clearly reveal the effectiveness of the described chitosan-based formulations to efficiently deliver siRNA and knock down specific genes at N:P ratios (N:P=5)

far below those used previously by others (N:P > 20) (see for example Fig. 11A and 11B). In general, all of our low N:P ratio chitosan formulations reached high levels of gene silencing supporting the FACS data (see for example Fig. 7A and 7B). A tendency for the low molecular weight (10 kDa) and high DDA (92%) chitosan to be most efficient (Figs. 11 and 12) and smaller (Fig. 4B) was found suggesting a particularly optimal formulation at NP ratio 5.

[00125] It has also described that the composition described herein for the treatment of atherosclerosis reduced *in vivo* ApoB plasma levels by approximately 30% compared to the positive untreated control (called Dα below) (Fig. 13). It is also demonstrated that such a reduction resulted in ApoB serum levels similar to those of the non-atherosclerotic animal group negative control, and is thus in the therapeutic range. It is also demonstrated in the present description that the composition described herein for the treatment of atherosclerosis produced a 20% reduction in LDL-cholesterol without any apparent toxicity (Fig. 14). It is also demonstrated that chitosan based therapeutic nanocomplexes containing siRNA (TNCs) did not result in any liver toxicity as demonstrated by normal ALT/AST levels in serum.

[00126] It is further demonstrated that TNC treatment had a therapeutic effect on cholesterol accumulation in the liver three weeks post injection, where cholesterol accumulation in TNC treated animal liver was significantly reduced (Fig. 15). Similarly, chitosan based TNCs induced transient immune cell infiltration into the liver which resorbed rapidly without toxicity as demonstrated in another embodiment herein (Fig. 16). The lack of liver toxicity and the rapid resorption of immune cell infiltration indicated the possibility of increasing the injected dose to achieve yet higher ApoB and LDL-C plasma reduction.

[00127] Furthermore, it is described that naked siRNA without chitosan targeting ApoB induced an intense inflammatory response thus limiting their dosing and potential for therapeutic use in an uncomplexed form. The lack of toxicity/inflammation in TNCs treated animal at a tested dose of 1mg/kg anti-ApoB siRNA coupled with their ability to reduce ApoB plasma levels by 35% indicates their importance and potential use in a dose response study to

determine the maximal tolerated dose (MTD) and achieve higher ApoB plasma reduction.

[00128] It is demonstrated that TNC-treated animals had reduced ApoB plasma levels for at least 8 weeks following the third and last injection. Reductions in ApoB plasma levels for low N:P chitosan-based TNCs were maintained for more than seven weeks after the last injection in the C1 animal group (Figs. 13 and 16) without any apparent inflammation or liver toxicity. These results indicate a particularly promising longevity of TNC treatment and effective controlled release properties.

[00129] It is thus disclosed herein that low N:P chitosan ApoB siRNA TNCs described herein, achieved a ~35% reduction of ApoB plasma levels and a ~20% reduction in LDL/VLDL cholesterol reduction at a 1mg/kg injected dose (Figs. 13 and 14). These results suggest an effective therapeutic result has been obtained since previously claimed successful results published using liposomal delivery systems for ApoBsiRNA required higher doses to achieve similar or higher ApoB/LDL-VLDL cholesterol reduction and these doses were associated with liver toxicity and increased ALT and AST levels (Zimmermann et al., 2006, Nature, 111-114; Soutschek et al., 2004, Nature 432:173-178). For example, the use of 5mg kg^{-1} of siRNA coupled with a lipid formulation (SNALP) achieved a 73% reduction in ApoB plasma levels (Zimmermann et al., 2006, Nature, 111-114); this fivefold higher injected concentration achieved 2.5 fold higher ApoB plasma reduction compared to the results of the present invention. Furthermore, the use of siRNA targeting ApoB in Ldlr -/+, Cetp -/+ mice model using a second generation lipid LNP-OCD (LNP201) developed by Merck Inc. showed an approximately 70% reduction in LDL at 3mg kg^{-1} (Tadin-Strapps et al., 2011, J lipid Res, 52:1084-1097). Additionally, 50 mg kg^{-1} of naked cholesterol modified siRNA were required to achieve 68% and 31% reduction in ApoB plasma level depending on the siRNA sequence used (Soutschek et al., 2004, Nature, 173-178). Additionally these studies were performed in normal C57BL/6 mice fed with regular chow (lean control) on the contrary to enclosed study where C57BL/6 mice groups were fed high fat diet to simulate atherosclerosis until the completion of the study.

[00130] Furthermore, intraperitoneal administration of anti-ApoB antisense oligonucleotiode (AOS) ISIS-147764, currently in phase III clinical trial, required at least 25mg kg^{-1} administered twice weekly to C57BL/6 feed with high fat in order to achieve a 55% in ApoB plasma reduction level after six to eight week of treatment. Additionally, Crooke et al. reported a plasma cholesterol return to normal following 50 mg kg^{-1} administration twice per week for six to eight weeks (Crooke et al., 2005, J Lipid Res, 46:872-884). The effect of ISIS-147764 on cholesterol plasma reduction was observed on the fourth week of treatment (50 mg kg^{-1} twice/week).

[00131] The compositions and methods described herein demonstrate clearly the efficiency of ApoB reduction using relatively low doses (1mg kg^{-1}) when compared to prior art. Additionally, it becomes clear in the present description that increasing dose using the present disclosure and disclosed TNCs will lead to an enhanced ApoB and LDL/VLDL-C plasma reduction since ApoB reduction has been always shown to be dose-dependent (Zimmermann et al., 2006, Nature, 441:111-114; Soutschek et al., 2004, Nature, 432:173-178; Crooke et al., 2005, J Lipid Res, 46:872-884; and Crooke, 2005, Expert Opin Biol Ther, 5:907-917).

[00132] The present description provides methods for treatment of diabetes mellitus and related conditions and symptoms. Such diabetes mellitus and related conditions include insulin-dependent diabetes mellitus (type I diabetes), noninsulin-dependent diabetes mellitus (type II diabetes), insulin resistance, hyperinsulinemia, and diabetes-induced hypertension. Other diabetes-related conditions include obesity and damage to blood vessels, eyes, kidneys, nerves, autonomic nervous system, skin, connective tissue, and immune system. The composition described herein can be used either alone or in combination with insulin and/or hypoglycemic compounds.

[00133] The present description provides methods for treatment of cancer. Such cancer include breast cancer, glioma, large intestinal cancer, lung cancer, small cell lung cancer, stomach cancer, liver cancer, blood cancer, bone cancer, pancreatic cancer, skin cancer, head or neck cancer, cutaneous or intraocular

melanoma, uterine sarcoma, ovarian cancer, rectal or colorectal cancer, anal cancer, colon cancer, fallopian tube carcinoma, endometrial carcinoma, cervical cancer, vulval cancer, squamous cell carcinoma, vaginal carcinoma, Hodgkin's disease, non-Hodgkin's lymphoma, esophageal cancer, small intestine cancer, endocrine cancer, thyroid cancer, parathyroid cancer, adrenal cancer, soft tissue tumor, urethral cancer, penile cancer, prostate cancer, chronic or acute leukemia, lymphocytic lymphoma, bladder cancer, kidney cancer, ureter cancer, renal cell carcinoma, renal pelvic carcinoma, CNS tumor, glioma, astrocytoma, glioblastoma multiforme, primary CNS lymphoma, bone marrow tumor, brain stem nerve gliomas, pituitary adenoma, uveal melanoma, testicular cancer, oral cancer, pharyngeal cancer, pediatric neoplasms, leukemia, neuroblastoma, retinoblastoma, glioma, rhabdomyoblastoma and sarcoma.

[00134] One approach to circumvent MDR is the use of P-gp modulators or reversal agents compounds that inhibit the transport activity of P-gp. However, their pharmacokinetic interaction with chemotherapeutics and toxicities limit their usage in clinics. Alternatively, the expression of P-gp can be inhibited by RNA interference (RNAi). Unlike chemical regulators, this technology may provide a more specific approach to dowregulation of P-gp and resistance reversal.

[00135] Various studies using siRNA or shRNA have demonstrated the potential use of RNAi to overcome multidrug resistance phenotype. The first studies showing the proof of principle of RNAi mediated reversal of resistance by p-gp inhibition were published in 2003 (Nieth et al., 2003, FEBS letters 545(2-3):144-150) and (Wu et al., 2003, Cancer research 63(7):1515. Both studies used a transient approach with siRNA to modulate multidrug resistant phenotype in different cell models. Using 200 nM of siRNA, Hao et al. were able to suppress p-gp levels by 65% in MCF-7/ADR and A2780 Dx5, to highly resistant MDR cell lines. Furthermore, they showed that MDR1 targeted siRNA reversed resistance to p-gp transportable drugs (Doxorubicin) but did not affect the sensitivity to hydroxyurea a non P-gp substrate. These data suggest that silencing of P-gp expression mediated by siRNA is specific. However, the most pronounced transient MDR reversal of nearly 90% was achieved in the

pancreatic carcinoma derived cell line (EPP85-181RDB) and gastric carcinoma cell (EPG 85-257RDB) despite the use of smaller concentration of siRNA (100nM) (Nieth et al., 2003, FEBS letters 545(2-3):144-150. Recently, Dönmez et al. (2011, Biomedicine and Pharmacotherapy 65(2):85-89) revealed 89% in gene silencing activity of MDR1 in doxorubicin-resistant MCF-7 cell although the concentration was lower as 20 nM. These data indicate that the efficacy of RNAi may be siRNA sequence-dependent as well as cell line-dependent.

[00136] In addition to siRNA, stable antiMDR1/P-gp shRNA expression vectors were used to modulate the MDR phenotype. In one study, shRNA expression had similar efficiency compared to siRNA to down regulate MDR1/P-gp in the paclitaxel-resistant SKOV-3TR and OVCAR8TR ovarian cancer cell lines (Duan et al., 2004, Molecular cancer therapeutics 3(7):833). Furthermore, Stege et al. (2004, Cancer gene therapy 11(11):699-706) reported a complete reversal of P-gp expression by introducing a shRNA-expressing vector (psiRNA/MDR-A) into an extremely high drug-resistant human gastric carcinoma cell line EPG85-257RDB. Similarly, Yagüe et al. (2004, Gene therapy 11(14):1170-1174) observed a complete reversal of doxorubicin resistance in K562 leukaemic cells by introducing the shRNA-expressing vector pSUPER. Using the same approach, Shi et al. (2006, Cancer biology & therapy 5(1):39-47) showed also a stable downregulation of MDR1/P-gp gene expression and function induced by endogenous expression of shRNA which expressed a novel containing MDR1-siRNA expression cassette and EGFP expression gene in human epidermoid carcinoma cell lines (KBv200).

[00137] In all of the above mentioned studies, Lipofectamine 2000 (Li et al., 2006, European journal of pharmacology, 536(1):93-97) and (Dönmez, Y. and U. Gündüz, 2011, Biomedicine & Pharmacotherapy 65(2):85-89) and oligofectamine (Nieth et al., 2003, FEBS letters 545(2-3):144-150; Wu et al., 2003, Cancer research 63(7):1515; Stierle et al., 2005, Biochemical pharmacology 70(10):1424-1430; and Stierle et al., 2007, Biochimie 89(8):1033-1036), two commercially available liposomes, were used. To date, chitosan has been used for the delivery of shRNA encoding plasmids targeting the MDR1 gene. In this study, nanoparticles were formed by complex coacervation (Yang

et al., 2009, J Huazhong Univ Sci Technolog Med Sci. Apr;29(2):239-42). The maximum mRNA reduction reported in the study was 52.6% with a time dependent reversal of paclitaxel chemoresistance of up to 61.3%. No report to date has described the use of chitosan for the delivery of anti-P-gp siRNA.

[00138] The composition described herein can be used either alone or in combination with other anti-cancer compound such as Acivicin; Aclarubicin; Acodazole Hydrochloride; Acronine; Adozelesin; Aldesleukin; Altretamine; Ambomycin; Ametantrone Acetate; Aminoglutethimide; Amsacrine; Anastrozole; Anthramycin; Asparaginase; Asperlin; Azacitidine; Azetepa; Azotomycin; Batimastat; Benzodepa; Bicalutamide; Bisantrene Hydrochloride; Bisnafide Dimesylate; Bizelesin; Bleomycin Sulfate; Brequinar Sodium; Bropirimine; Busulfan; Cactinomycin; Calusterone; Caracemide; Carbetimer; Carboplatin; Carmustine; Carubicin Hydrochloride; Carzelesin; Cedefingol; Chlorambucil; Cirolemycin; Cisplatin; Cladribine; Crisnatol Mesylate; Cyclophosphamide; Cytarabine; Dacarbazine; Dactinomycin; Daunorubicin Hydrochloride; Decitabine; Dexormaplatin; Dezaguanine; Dezaguanine Mesylate; Diaziquone; Docetaxel; Doxorubicin; Doxorubicin Hydrochloride; Droloxifene; Droloxifene Citrate; Dromostanolone Propionate; Duazomycin; Edatrexate; Eflornithine Hydrochloride; Elsamitrucin; Enloplatin; Enpromate; Epipropidine; Epirubicin Hydrochloride; Erbulozole; Esorubicin Hydrochloride; Estramustine; Estramustine Phosphate Sodium; Etanidazole; Etoposide; Etoposide Phosphate; Etoprine; Fadrozole Hydrochloride; Fazarabine; Fenretinide; Floxuridine; Fludarabine Phosphate; Fluorouracil; Flurocitabine; Fosquidone; Fostriecin Sodium; Gemcitabine; Gemcitabine Hydrochloride; Hydroxyurea; Idarubicin Hydrochloride; Ifosfamide; Ilmofosine; Interferon α-2a; Interferon α-2b; Interferon α-n1; Interferon α-n3; Interferon β-Ia; Interferon γ-Ib; Iproplatin; Irinotecan Hydrochloride; Lanreotide Acetate; Letrozole; Leuprolide Acetate; Liarozole Hydrochloride; Lometrexol Sodium; Lomustine; Losoxantrone Hydrochloride; Masoprocol; Maytansine; Mechlorethamine Hydrochloride; Megestrol Acetate; Melengestrol Acetate; Melphalan; Menogaril; Mercaptopurine;. Methotrexate; Methotrexate Sodium; Metoprine;.Meturedepa; Mitindomide; Mitocarcin; Mitocromin; Mitogillin; Mitomalcin; Mitomycin; Mitosper;

Mitotane; Mitoxantrone Hydrochloride; Mycophenolic Acid; Nocodazole; Nogalamycin; Ormaplatin; Oxisuran; Paclitaxel; Pegaspargase; Peliomycin; Pentamustine; Peplomycin Sulfate; Perfosfamide; Pipobroman; Piposulfan; Piroxantrone Hydrochloride; Plicamycin; Plomestane; Porfimer Sodium; Porfiromycin; Prednimustine;. Procarbazine Hydrochloride; Puromycin; Puromycin Hydrochloride; Pyrazofurin; Riboprine; Rogletimide; Safingol; Safingol Hydrochloride; Semustine; Simtrazene; Sparfosate Sodium; Sparsomycin; Spirogermanium Hydrochloride; Spiromustine; Spiroplatin; Streptonigrin;. Streptozocin; Sulofenur; Talisomycin; Taxol; Taxotere; Tecogalan Sodium; Tegafur; Teloxantrone Hydrochloride; Temoporfin; Teniposide; Teroxirone; Testolactone; Thiamiprine; Thioguanine; Thiotepa; Tiazofurin; Tirapazamine; Topotecan Hydrochloride; Toremifene Citrate; Trestolone Acetate; Triciribine Phosphate; Trimetrexate; Trimetrexate Glucuronate; Triptorelin; Tubulozole Hydrochloride; Uracil Mustard; Uredepa; Vapreotide; Verteporfin; Vinblastine Sulfate; Vincristine Sulfate; Vindesine; Vindesine Sulfate; Vinepidine Sulfate; Vinglycinate Sulfate; Vinleurosine Sulfate; Vinorelbine Tartrate; Vinrosidine Sulfate; Vinzolidine Sulfate; Vorozole; Zeniplatin; Zinostatin; or Zorubicin Hydrochloride.

[00139] Other anti-cancer drugs include: 20-epi-1,25 dihydroxyvitamin D3; 5-ethynyluracil; abiraterone; aclarubicin; acylfulvene; adecypenol; adozelesin; aldesleukin; ALL-TK antagonists; altretamine; ambamustine; amidox; amifostine; aminolevulinic acid; amrubicin; amsacrine; anagrelide; anastrozole; andrographolide; angiogenesis inhibitors; antagonist D; antagonist G; antarelix; anti-dorsalizing morphogenetic protein-1; antiandrogen, prostatic carcinoma; antiestrogen; antineoplaston; antisense oligonucleotides; aphidicolin glycinate; apoptosis gene modulators; apoptosis regulators; apurinic acid; ara-CDP-DL-PTBA; arginine deaminase; asulacrine; atamestane; atrimustine; axinastatin 1; axinastatin 2; axinastatin 3; azasetron; azatoxin; azatyrosine; baccatin III derivatives; balanol; batimastat; BCR/ABL antagonists; benzochlorins; benzoylstaurosporine; beta lactam derivatives; beta-alethine; betaclamycin B; betulinic acid; bFGF inhibitor; bicalutamide; bisantrene; bisaziridinylspermine; bisnafide; bistratene A; bizelesin; breflate; bropirimine; budotitane; buthionine

sulfoximine; calcipotriol; calphostin C; camptothecin derivatives; canarypox IL-2; capecitabine; carboxamide-amino-triazole; carboxyamidotriazole; CaRest M3; CARN 700; cartilage derived inhibitor; carzelesin; casein kinase inhibitors (ICOS); castanospermine; cecropin B; cetrorelix; chlorins; chloroquinoxaline sulfonamide;. cicaprost; cis-porphyrin; cladribine; clomifene analogues; clotrimazole; collismycin A;. collismycin B; combretastatin A4; combretastatin analogue; conagenin; crambescidin 816; crisnatol; cryptophycin 8; cryptophycin A derivatives; curacin A; cyclopentanthraquinones; cycloplatam; cypemycin; cytarabine ocfosfate; cytolytic factor; cytostatin; dacliximab; decitabine; dehydrodidemnin B; deslorelin; dexifosfamide; dexrazoxane; dexverapamil; diaziquone; didemnin B; didox; diethylnorspermine; dihydro-5-azacytidine; dihydrotaxol, 9-; dioxamycin; diphenyl spiromustine; docosanol; dolasetron; doxifluridine; droloxifene; dronabinol; duocarmycin SA; ebselen; ecomustine; edelfosine; edrecolomab; eflornithine; elemene; emitefur; epirubicin; epristeride; estramustine analogue; estrogen agonists; estrogen antagonists; etanidazole; etoposide phosphate; exemestane; fadrozole; fazarabine; fenretinide; filgrastim; finasteride; flavopiridol; flezelastine; fluasterone; fludarabine; fluorodaunornicin hydrochloride; forfenimex; formestane; fostriecin; fotemustine; gadolinium texaphyrin; gallium nitrate; galocitabine; ganirelix; gelatinase inhibitors; gemcitabine; glutathione inhibitors;.hepsulfam; heregulin; hexamethylene bisacetamide; hypericin; ibandronic acid; idarubicin; idoxifene; idramantone; ilmofosine; ilomastat; imidazoacridones; imiquimod; immunostimulant peptides; insulin-like growth factor-1 receptor inhibitor; interferon agonists; interferons; interleukins; iobenguane; iododoxorubicin; ipomeanol, 4-; irinotecan; iroplact; irsogladine; isobengazole; isohomohalicondrin B; itasetron; jasplakinolide; kahalalide F; lamellarin-N triacetate; lanreotide; leinamycin; lenograstim; lentinan sulfate; leptolstatin; letrozole; leukemia inhibiting factor; leukocyte alpha interferon; leuprolide+estrogen+progesterone; leuprorelin; levamisole; liarozole; linear polyamine analogue; lipophilic disaccharide peptide; lipophilic platinum compounds; lissoclinamide 7; lobaplatin; lombricine; lometrexol; lonidamine; losoxantrone; lovastatin; loxoribine; lurtotecan; lutetium texaphyrin; lysofylline; lytic peptides; maitansine; mannostatin A; marimastat; masoprocol; maspin; matrilysin inhibitors; matrix metalloproteinase inhibitors; menogaril; merbarone;

meterelin; methioninase; metoclopramide; MIF inhibitor; mifepristone; miltefosine; mirimostim; mismatched double stranded RNA; mitoguazone; mitolactol; mitomycin analogues; mitonafide; mitotoxin fibroblast growth factor-saporin; mitoxantrone; mofarotene; molgramostim; monoclonal antibody, human chorionic gonadotrophin; monophosphoryl lipid A+myobacterium cell wall sk; mopidamol; multiple drug resistance gene inhibitor;. multiple tumor suppressor 1-based therapy; mustard anti cancer compound; mycaperoxide B; mycobacterial cell wall extract; myriaporone; N-acetyldinaline; N-substituted benzamides; nafarelin; nagrestip; naloxone+pentazocine; napavin; naphterpin; nartograstim; nedaplatin; nemorubicin; neridronic acid; neutral endopeptidase; nilutamide; nisamycin; nitric oxide. modulators; nitroxide antioxidant; nitrullyn; O6-benzylguanine; octreotide; okicenone; oligonucleotides; onapristone; ondansetron; ondansetron; oracin; oral cytokine inducer; ormaplatin; osaterone; oxaliplatin; oxaunomycin; paclitaxel analogues; paclitaxel derivatives; palauamine; palmitoylrhizoxin; pamidronic acid; panaxytriol; panomifene; parabactin; pazelliptine; pegaspargase; peldesine; pentosan polysulfate sodium; pentostatin; pentrozole; perflubron; perfosfamide; perillyl alcohol; phenazinomycin; phenylacetate; phosphatase inhibitors; picibanil; pilocarpine hydrochloride; pirarubicin; piritrexim; placetin A; placetin B; plasminogen activator inhibitor; platinum complex; platinum compounds; platinum-triamine complex; porfimer sodium; porfiromycin; propyl bis-acridone; prostaglandin J2; proteasome inhibitors; protein A-based immune modulator; protein kinase C inhibitor; protein kinase C inhibitors, microalgal; protein tyrosine phosphatase inhibitors; purine nucleoside phosphorylase inhibitors; purpurins; pyrazoloacridine; pyridoxylated hemoglobin polyoxyethylene conjugate; raf antagonists; raltitrexed; ramosetron; ras farnesyl protein transferase inhibitors; ras inhibitors; ras-GAP inhibitor; retelliptine demethylated; rhenium Re 186 etidronate; rhizoxin; ribozymes; RII retinamide; rogletimide; rohitukine; romurtide; roquinimex; rubiginone B1; ruboxyl; safingol; saintopin; SarCNU; sarcophytol A; sargramostim; Sdi 1 mimetics; semustine; senescence derived inhibitor 1; sense oligonucleotides; signal transduction inhibitors; signal transduction modulators; single chain antigen binding protein; sizofiran; sobuzoxane; sodium borocaptate; sodium phenylacetate; solverol;

somatomedin binding protein; sonermin; sparfosic acid; spicamycin D; spiromustine; splenopentin; spongistatin 1; squalamine; stem cell inhibitor; stem-cell division inhibitors; stipiamide; stromelysin inhibitors; sulfinosine; superactive vasoactive intestinal peptide antagonist; suradista; suramin; swainsonine; synthetic glycosaminoglycans; tallimustine; tamoxifen methiodide; tauromustine; tazarotene; tecogalan sodium; tegafur; tellurapyrylium; telomerase inhibitors; temoporfin; temozolomide; teniposide; tetrachlorodecaoxide; tetrazomine; thaliblastine; thalidomide; thiocoraline; thrombopoietin; thrombopoietin mimetic; thymalfasin; thymopoietin receptor agonist; thymotrinan; thyroid stimulating hormone; tin ethyl etiopurpurin; tirapazamine; titanocene dichloride; topotecan; topsentin; toremifene; totipotent stem cell factor; translation inhibitors; tretinoin; triacetyluridine; triciribine; trimetrexate; triptorelin; tropisetron; turosteride; tyrosine kinase inhibitors; tyrphostins; UBC inhibitors; ubenimex; urogenital sinus-derived growth inhibitory factor; urokinase receptor antagonists; vapreotide; variolin B; vector system, erythrocyte gene therapy; velaresol; veramine; verdins; verteporfin; vinorelbine; vinxaltine; vitaxin; vorozole; zanoterone; zeniplatin; zilascorb; and zinostatin stimalamer.

[00140] Anti-cancer supplementary potentiating compounds include: Tricyclic anti-depressant drugs (e.g., imipramine, desipramine, amitryptyline, clomipramine, trimipramine, doxepin, nortriptyline, protriptyline, amoxapine and maprotiline); non-tricyclic anti-depressant drugs (e.g., sertraline, trazodone and citalopram); Ca^{++} antagonists (e.g., verapamil, nifedipine, nitrendipine and caroverine); Calmodulin inhibitors (e.g., prenylamine, trifluoroperazine and clomipramine); Amphotericin B; Triparanol analogues (e.g., tamoxifen); antiarrhythmic drugs (e.g., quinidine); antihypertensive drugs (e.g., reserpine); Thiol depleters (e.g., buthionine and sulfoximine) and multiple drug resistance reducing compounds such as Cremaphor EL.

[00141] Other compounds which are useful in combination therapy for the purpose of the invention include the antiproliferation compound, Piritrexim Isethionate; the antiprostatic hypertrophy compound, Sitogluside; the benign prostatic hyperplasia therapy compound, Tamsulosin Hydrochloride; the

prostate growth inhibitor, Pentomone; radioactive compounds such as Fibrinogen I 125, Fludeoxyglucose F 18, Fluorodopa F 18, Insulin I 125, Insulin I 131, Iobenguane I 123, Iodipamide Sodium I 131, Iodoantipyrine I 131, Iodocholesterol I 131, Iodohippurate Sodium I 123, Iodohippurate Sodium I 125, Iodohippurate Sodium I 131, Iodopyracet I 125, Iodopyracet I 131, Iofetamine Hydrochloride I 123, Iomethin I 125, Iomethin I 131, Iothalamate Sodium I 125, Iothalamate Sodium I 131, Iotyrosine I 131, Liothyronine I 125, Liothyronine I 131, Merisoprol Acetate Hg 197, Merisoprol Acetate Hg 203, Merisoprol Hg 197, Selenomethionine Se 75, Technetium Tc 99m Antimony Trisulfide Colloid, Technetium Tc 99m Bicisate, Technetium Tc 99m Disofenin, Technetium Tc 99m Etidronate, Technetium Tc 99m Exametazime, Technetium Tc 99m Furifosmin, Technetium Tc 99m Gluceptate, Technetium Tc 99m Lidofenin, Technetium Tc 99m Mebrofenin, Technetium Tc 99m Medronate, Technetium Tc 99m Medronate Disodium, Technetium Tc 99m Mertiatide, Technetium Tc 99m Oxidronate, Technetium Tc 99m Pentetate, Technetium Tc 99m Pentetate Calcium Trisodium, Technetium Tc 99m Sestamibi, Technetium Tc 99m Siboroxime, Technetium Tc 99m Succimer, Technetium Tc 99m Sulfur Colloid, Technetium Tc 99m Teboroxime, Technetium Tc 99m Tetrofosmin, Technetium Tc 99m Tiatide, Thyroxine I 125, Thyroxine I 131, Tolpovidone I 131, Triolein I 125 and Triolein I 131.

[00142] As used herein, "treatment" and "treating" include preventing, inhibiting, and alleviating diabetes mellitus and related conditions and symptoms. The treatment may be carried out by administering a therapeutically effective amount of the composition described herein. In other instances, the treatment may be carried out by concurrently administering a therapeutically effective amount of a combination of insulin and the composition described herein. In still other instances, the treatment may involve concurrently administering a therapeutically effective amount of a combination of a hypoglycemic compound and the composition described herein when the diabetes mellitus and related conditions to be treated is type II diabetes, insulin resistance, hyperinsulinemia, diabetes-induced hypertension, obesity, or

damage to blood vessels, eyes, kidneys, nerves, autonomic nervous system, skin, connective tissue, or immune system.

[00143] Examples of chitosan containing chemical modification are: chitosan-based compounds having: (i) specific or non-specific cell targeting moieties that can be covalently attached to chitin and/or chitosan, or ionically or hydrophobically adhered to a chitosan-based compound complexed with a nucleic acid or an oligonucleotide, and (ii) various derivatives or modifications of chitin and chitosan which serve to alter their physical, chemical, or physiological properties. Examples of such modified chitosan are chitosan-based compounds having specific or non-specific targeting ligands, membrane permeabilization agents, sub-cellular localization components, endosomolytic (lytic) agents, nuclear localization signals, colloidal stabilization agents, agents to promote long circulation half-lives in blood, and chemical derivatives such as salts, O-acetylated and N-acetylated derivatives. Some sites for chemical modification of chitosan include: C_2(NH-CO-CH_3 or NH_2), C_3(OH), or C_6(CH_2OH).

[00144] The compositions described herein are suitable drug delivery systems with effective controlled release properties. The present compositions can be administered with any known combination therapy, such as the co-administration of a suitable delivery reagent such as, but not limited to, Mirus Transit TKO® lipophilic reagent, Lipofectin®, Lipofectamine™, Cellfectin®, polycations (e.g., polylysine) or liposomes.

[00145] Concurrent administration" and "concurrently administering" as used herein includes administering a composition as described herein and insulin and/or a hypoglycemic compound in admixture, such as, for example, in a pharmaceutical composition, or as separate formulation, such as, for example, separate pharmaceutical compositions administered consecutively, simultaneously, or at different times.

[00146] Suitable hypoglycemic compounds include, for example, metformin, acarbose, acetohexamide, glimepiride, tolazamide, glipizide, glyburide,

tolbutamide, chlorpropamide, thiazolidinediones, alpha glucosidase inhibitors, biguanindine derivatives, and troglitazone, and a mixture thereof.

[00147] Administration of the composition described herein can be a parenteral administration which includes subcutaneous, intramuscular, intradermal, intramammary, intravenous, and other administrative methods known in the art.

[00148] The present invention will be more readily understood by referring to the following examples.

EXAMPLE I
Reparation of Chitosan/ dsODN or siRNA based nanoparticles formulations

[00149] Ultrapure chitosan samples were produced using quality controlled manufacturing processes eliminate contaminants including proteins, bacterial endotoxins, toxic metals, inorganic and organic impurities. All chitosans had less than 50EU/g of bacterial endotoxins. Chitosan were selected having a 92% and 80% of degree of deacetylation (Table 1). These chitosans were produced by heterogeneous deacetylation resulting in a block rather than random distribution of acetyl groups. Chitosans were chemically degraded using nitrous acid as described previously (Lavertu et al., 2006, Biomaterials, 27:4815-4824; Lavertu et al., 2003, J Pharmaceutical and Biomedical Analysis, 32:1149-1158) to obtain specific molecular weights of 10kDa, 40kDa and 80kDa, the former at both DDAs of 92% and 80% and the latter at 80% DDA (Table 1).

Table 1

Chitosan degree of deacetylation (DDA), average molecular weight (Mn), poly-dispersity index (PDI)

	Experiment	Chitosan	DDA	Mn (kDa)	Mw	PDI
RecQL1	Confocal	Rho-92-10	92.7	10	14	1.4
RecQL1	DLS, ESEM, Protection, Stability Assay,FACS, qPCR	92-10	91.7	7.1	10.08	1.427
		80-40	82.5	38.37	53.4	1.392
		80-10	84.4	10.82	14.525	1.343

	Experiment	Chitosan	DDA	Mn (kDa)	Mw	PDI
DDP-IV	Enzymatic test	92-10	92	7.46	9.32	1.25
		80-10	80	12.40	22.41	1.80
		80-80	80.0	93.8	187.6	2.0
ApoB DDP-IV	Protection Assay,FACS, qPCR, in vivo	92-10	92.2	8.501	12.645	1.494
		80-80	80.8	71.535	118.03	1.65
		80-10	84.4	10.820	14.525	1.343
ApoB DDP-IV	Confocal	Rho-92-10	92.7	10	14	1.4
ApoB DDP-IV	Stability Assay, DLS, ESEM	92-10	91.7	7.1	10.08	1.427
		80-80	80.0	93.8	187.6	2.0
		80-10	80	12.40	22.41	1.80
		80-10	84.4	10.820	14.525	1.343
		80-40-5	82.5	38.375	53.410	1.392
		92-40-5	92.7	60.6	37.9	1.6

[00150] Small interfering RNAs targeting the DPP-IV gene were purchased from Dharmacon (Thermo scientific, Dharmacon RNAi Technologies, USA). These siRNA sense and antisense strands are synthesized with 2 nucleotides (UU) 3' overhangs. Candidates consisted in a pool of four sequences targeting the DPP-IV sequence (DPP-IV Seq1: CACUCUAACUGAUUACUUA, SEQ ID NO:1; DPP-IV Seq2: UAGCAUAUGCCCAAUUUAA, SEQ ID NO:2; DPP-IV Seq 3: CAAGUUGAGUACCUCCUUA, SEQ ID NO:3; DPP-IV Seq 4: UAUAGUAGCUAGCUUUGAU, SEQ ID NO:4). ApoB targeting siRNA sequence was custom synthesized using the 2-ACE RNA chemistry by Dharmacon (ApoB Seq1: GUCAUCACACUGAAUACCAAU, (antisense strands are synthesized with 2 nucleotides (AC) 3' overhangs), SEQ ID NO:5; ApoB Seq 2 (sense): 5' CUC UCA CAU ACA AUU GAA AdTdT 3', SEQ ID NO:7; ApoB seq 2 (antisense) 5' UUU CAA UUG UAU GUG AGA GUUoUoU 3' (oU-oU) = 2'-O-methyl-uridine overhangs, SEQ ID NO:6; ApoB Seq3 (sense): GGAAUCuuAuAuuuGAUCcA*A, SEQ ID NO:8; ApoB Seq3 (antisense): uuGGAUcAAAuAuAAGAuUCc*c*U, SEQ ID NO:9; 2'O-Methyl modified nucleotides are in lower case and phosphorothioate linkages are represented by asterisks). These sequences were published by Soutschek, et al. (2004, Nature, 432:173- 178), Zimmermann et al. (2006, Nature, 441:111-114) and Strapps et al. (2010, Nucleic Acids Research, Vol. 38, No. 14).

[00151] RecQL1 targeting siRNA sequence was custom synthesized using the 2-ACE RNA chemistry by Dharmacon (Seq1: 5′-GUUCAGACCACUUCAGCUUdTdT-3′, SEQ ID NO:10). This sequence was published by Futami et al. (2008, Cancer Sci, 99:71-80; 2008, Cancer Sci, 99:1227-1236). MDR1 targeting sequences were purchased presynthetised from Dharmacon and are available through their catalogue under the product number: M-003868-02-0010. Candidates consisted of four siRNA targeting the MDR1 sequence: Seq 1 (sense): **5'** GCUGAUCUAUGCAUCUUAUUU **3'**, SEQ ID NO:11; Seq 1 (antisense) **5'**AUAAGAUGCAUAGAUCAGCUU **3'**; SEQ ID NO:12; Seq 2 (sense): **5'**GACCAUAAAUGUAAGGUUUUU **3'**, SEQ ID NO:13; Seq 2 (Antisense): **5'** AAACCUUACAUUUAUGGUCUU **3'**, SEQ ID NO:14; Seq 3 (sense): **5'** GAAACUGCCUCAUAAAUUUUU **3'**, SEQ ID NO:15; Seq 3 (Antisense): AAAUUUAUGAGGCAGUUUCUU **3'**, SEQ ID NO:16; Seq 4 (sense): **5'**UCGAGUCACUGCCUAAUAAUU**3'**, SEQ ID NO:17; Seq 4 (Antisense): **5'**UUAUUAGGCAGUGACUCGAUU **3'**, SEQ ID NO:18.

[00152] dsODN sequences were synthesized using the phosphoramidite chemistry, (Integrated DNA Technologies, Inc) and used for , nanoparticle stability and nuclease protection assays. For flow cytometry analysis, 6-carboxyfluorescein (6FAM) 5' labeled dsODN were used (Integrated DNA technologies, USA).

[00153] The rationale of dsODN use for physico-chemical characterization of chitosan nanoparticles presented herein is their siRNA mimicking properties. These mimicking properties are due to similarities at the structural level (double stranded structure, length (21 mers) and nucleotide over hangs) between siRNA and dsODN. Additionally, charge densities are similar between siRNA and dsODN due to identical phosphate residue number/spacing on their back bone. Differences between siRNA and dsODN lie in the substitution of uracil to thymine (U → T) in the dsODN sequences, and in the deoxyribosilation of dsODN sugar back bone. The dsODN sequences were synthesized using the phosphoramidite chemistry, (Integrated DNA Technologies, Inc) and used for size and zeta potential determination, nanoparticles stability and nuclease protection assays. For confocal microscopy, and flow cytometry analysis, 6-

carboxyfluorescein (6FAM) 5' labeled dsODN were used (Integrated DNA technologies, USA).

[00154] Chitosans with specific Mn and DDA were dissolved over night on a rotary mixer at 0.5% (w/v) in hydrochloric acid using a glucosamine: HCl ratio of 1:1 at a final concentration of 5 mg/mL. Sterile filtered solutions were then diluted with deionized water to obtain the desired ratio (N:P) of amine (chitosan deacetylated groups) to phosphate (dsODNs or siRNA nucleic acids). Nanoparticles (92-10-5, 92-150-5, 80-40-5, 80-10-10, 80-10-5, 80-200-5 and 80-80-5) were then prepared by rapid mixing (pippeting) of 100 µL of diluted chitosan solution to 100 µL of dsODN or siRNA at a concentration of 0.05 µg/µL respectively; a concentration of 0.33 µg/µL dsODN was used for stability and nuclease protection assays whereas a concentration of 0.1 µg/µL was used for DLS and ESEM. Nanoparticles were incubated for 30 minutes at room temperature prior to use.

EXAMPLE II
Transfection experiments

[00155] For *in vitro* transfection, High Glucose-Dulbecco's Modified Eagle's Media (DMEM-HG) was prepared with 0.976 g/L of MES and 0.84 g/L of sodium bicarbonate ($NaHCO_3$) at pH 6.5. Transfection media without fetal bovine serum (FBS) was equilibrated overnight at 37°C in a 5% CO_2 incubator and pH adjustment to a 6.5 value at 37C was performed using sterile HCl (1N) just before transfection. For siRNA transfection performed in a 96 well plate, chitosan/siRNA nanoparticles were prepared as described above, 30 minutes before use. A 100µl siRNA solution at a concentration of 0.05µg/µl (3,704 nM) was used for siRNA complexation with chitosan at a 1:1 ratio (v/v). Following complexation, siRNA concentration becomes 0.025µg/µl (1,852 nM) and nanoparticles were incubated in a ghost plate containing DMEM-HG media, at a final concentration of 0.00135 µg/µl equivalent to 100 nM per well (10 pmol/well) of siRNA. For dsODN transfection performed in a 24 well plate, chitosan/dsODN nanoparticles were prepared as described above, 30 minutes before use. A 100µl dsODN solution at a concentration of 0.05µg/µl (3,717 nM) was used for

dsODN complexation with chitosan at a 1:1 ratio (v/v). Following complexation, siRNA concentration becomes 0.025µg/µl (1,858 nM) and nanoparticles were incubated in a ghost plate containing DMEM-HG media, at a final concentration of 0.00135 µg/µl equivalent to 600 nM per well (60 pmol/well) of dsODN. The slight difference in molecular weight between dsODN used for FACS and siRNA is due to the 6FAM labelling of dsODN. Plates containing nanoparticles were equilibrated for 10 minutes at 37°C, 5% CO_2. Medium over cells was aspirated and replenished with either 500 µl (24 well plates) or 100 µl per well (96 well plate) of the equilibrated transfection medium at pH 6.5 containing dsODN or siRNA based nanoparticles at a final concentration of 100 nM/well. FBS was added four hours following transfection, to a final concentration of 10% per well. Cells were incubated with chitosan/siRNA nanoparticles until analysis at 24 hours post-transfection. DharmaFECT™ was used as a positive control and both untreated cells and uncomplexed siRNA treated cells were used as negative controls.

[00156] The commercially available liposome, DharmaFECT™ (Dharmacon RNAi Technologies, Lafayette, CO, USA), was used as a positive control for transfection efficiency in all tested cell lines. DharmaFECT™/dsODN (flow cytometry and confocal microscopy) or DharmaFECT™/siRNA (qPCR) lipoplexes (1:2 [w/v] ratio) were prepared following the manufacturer's protocol.

[00157] The *in vitro* transfections involved HEK293, HepG2 (ApoB and DPP-IV), HT-29 (DPP-IV), Caco-2 (DPP-IV), Raw264.7 (ApoB), A549, LS174T and the AsPC1 cell lines, purchased from American Type Cell Culture (ATCC, Manassas, VA). The MCF7-MDR cell line was a gift from Dr Hamid Morjani (Paris, France). Cells were cultured in minimal essential medium (HepG2), McCoys (HT-29), Dulbecco minimum essential media high glucose (HEK293 and RAW264.7) with 1.85g/L (HEK293) or 1.5g/l (RAW264.7) of sodium bicarbonate, (LS174T), F12K (A549), RPMI-1640 (MCF-7 MDR) and RPMI-1640 (AsPC1), and supplemented with 10% FBS (Cedarlane Laboratories, Burlington, ON) at 37°C and 5% CO_2. HepG2 cells were supplemented with 8% FBS. For transfection, cells were plated in 96-well or 24-well culture plates

(Corning, NY, USA) so to obtain ~50% to ~70% of confluence the day of the transfection.

EXAMPLE III
RNA extractions and gene expression analysis

[00158] Total RNA extraction was performed using the NucleoSpin® RNA XS kit from Machery-Nagel. Cells lysis was performed by adding 100µl RA1 lysis buffer supplemented with 2µl TCEP and *Streptomyces griseus* chitosanase into each well (Alameh et al., 2010, Int J Nanomedecine, 5:473-481). DNAse treatment of sample was performed when sample were incubated with RA3 buffer before elution. RNA quantification and quality (integrity) assessment were performed using the Agilent Bioanalyzer 2100. RNA Integrity Number (RIN) equal to 7.5 was considered as an acceptance threshold for qPCR analysis.

[00159] Reverse transcription of total RNA was performed using the first strand cDNA transcriptor kit (Roche, Laval, CA). A total of 0.5-1µg of RNA/sample was used for the reverse transcription reaction using oligodT primers according to the manufacturer protocol. Gene quantification of chitosan/siRNA treated cells was performed using the ABI PRISM® 7900HT Sequence Detection System. All reactions were run in triplicate and the average values of Cts were used for quantification. Gene expression level was determined using assays with the Universal Probe Library® (UPL) from Roche™. On the other hand, gene expression level for endogenous controls (TBP, HPRT) was determined using the pre-validated TaqMan® gene expression assays. The relative quantification of target genes was determined using the △△CT method. Briefly, the Ct (threshold cycle) values of target genes were normalized to an endogenous control gene (Endogenous control) ($\triangle CT = Ct_{target} - Ct_{endoC}$) and compared with a calibrator: $\triangle\triangle CT = \triangle Ct_{Sample} - \triangle Ct_{Calibrator}$. Relative expression (RQ) was calculated using the Sequence Detection System (SDS) 2.2.2 software (Applied Biosystems) and the formula is $RQ = 2^{-\triangle\triangle CT}$.

EXAMPLE IV
Nanoparticles analysis

[00160] Size of chitosan/dsODN and chitosan/siRNA complexes was determined by dynamic light scattering at an angle of 137° at 25°C using a Malvern Zetasizer Nano ZS®. Samples were measured in triplicates using refractive index and viscosity of pure water in calculations. The zeta potential was measured in triplicates as well using laser Doppler velocimetry at 25°C using the same instrument and the dielectric constant of water for calculation. For the size determination, reported as the intensity averaged diameter, 50µl of chitosan was mixed with 50µl of dsODN or siRNA then completed to 500µl using 10mM NaCl. For zeta measurement, nanoparticles were diluted 1:2 using 500µl of 10mM NaCl. All formulations of chitosan/dsODN nanoparticles were in the range of 45-156 nm, as measured by DLS. Chitosan/siRNA nanoparticles had mean diameters in the range of 55-105 nm as measured by DLS when complexed to siRNA sequence 1 (SEQ ID NO:5) and 2 (SEQ ID NO:6 and SEQ ID NO:7) (Table 2). For siRNA sequence 3 (SEQ ID NO:8 and SEQ ID NO:9), fully modified, chitosan-siRNA nanoparticles had mean diameters in the range of 104-130 nm (Table 2). No statistical differences in nanoparticle size were observed between dsODN and un-modified siRNA-ApoB (sequence 1; SEQ ID NO:5) and moderately modified siRNA-ApoB complexed to chitosan (sequence 2; SEQ ID NO:6 and SEQ ID NO:7). However, fully modified siRNA sequence yielded larger nanoparticles when complexed to the different chitosans. Chitosan/dsODN and chitosan/siRNA nanoparticles showed higher size values with increasing Mn. No statistically significant differences were observed when comparing DDAs for these specific formulations. As expected, the excess chitosan in all formulations resulted in positively charged nanoparticles as shown by zeta potentials in Table 2, wherein DLS permitted the determination of size and zeta potential, whereas ESEM measured size only.

Table 2

Mean size – by intensity – and zeta potential, with standard deviation, of nanoparticles formed with with siRNA-RecQL1 or siRNA-MDR1 in chitosan formulations: 80-10-5, 80-10-10, 80-40-5, 80-200-5, 92-10-5, 92-150; and siRNA-DPP-IV, ODN-ApoB or siRNA-ApoB in chitosan formulations: 80-10-5, 80-10-10, 80-40-5 80-80-5, 92-10-5, 92-40-5.

Sample	Chitosan	Size (nm)	Zeta potential (mV)	ESEM (nm)
MDR1	80-10-5	70±2	12±3	62±9
	80-200-5	156±35	18±3	131±5
	92-10-5	71±15	15±2	64±8
	92-150-5	140±49	17±5	123±6
RecQL1	80-10-10	91±7	18±2	73±9
	80-40-5	86±9	18±1	97±12
	92-10-5	63±8	23±1	54±6
DPP-IV (pool of siRNA seq 1 to seq 4)	80-10-10	81±5	16±2	70-90
	80-80-5	111±12	20±2	60-100
	92-10-5	71±7	18±2	50-90
ApoB (ODN mimics siRNA ApoB seq 1) (mimics of SEQ ID NO:5)	80-10-10	64±6	19±2	67±7
	80-80-5	100±12	16±1	75±13
	92-10-5	45±4	21±2	66±5
ApoB (siRNA seq 1) (SEQ ID NO:5)	80-10-5	80±7	27±2	62±5
	80-40-5	105±6	24±5	90±7
	92-10-5	55±3	28±2	60±3
	92-40-5	69± 4	23±5	65±14
ApoB (siRNA seq 2) (SEQ ID NO:6 and SEQ ID NO:7)	80-10-5	90±4	26±4	70±8
	80-40-5	89±6	24±5	76±7
	92-10-5	57±3	26±4	54±6
	92-40-5	67±2	24±5	59±9
ApoB (siRNA seq 3) (SEQ ID NO:8 and SEQ ID NO:9)	80-10-5	139±7	19±3	89±7
	80-40-5	130±2	25±2	100±9
	92-10-5	105±3	22±5	78±5
	92-40-5	104±4	27±3	80±6

[00161] Nanoparticles formed as described above were imaged using an environmental scanning electron microscope (ESEM, Quanta 200 FEG, FEI Company Hillsboro, OR, USA). Following nanoparticle formation, TNCs were sprayed on silicon water substrate, and then sputter-coated with gold (Agar Manual Sputter Coater, Marivac Inc.) as described previously (Lavertu et al., 2003, J Pharm Biomed Anal, 32:1149-1158). Observations were performed at 20 kV in the high vacuum mode of the ESEM microscope. The average particle size (+/- standard deviation) was determined by measuring the diameter of more than 150 particles from at least 6 different fields for each fraction using the microscope XT Docu software (XT Docu, FEI Co). The robustness of size

determination was analyzed by comparison of ESEM image analysis size determination to DLS size data.

[00162] The results show nanoparticles of spherical shape (Figs. 1A, 1B, 2A and 2B) with mean diameters ranging between 45-156 nm depending on the chitosan formulation used (Table 2, ESEM). Results obtained with specific formulations described herein are consistent with dynamic light scattering results (Table 2), thereby indicating the robustness of the composition and method described herein. Furthermore, the nanoparticles formed yield reproducible sizes below 200 nm allowing for avoidance of renal clearance thus improving *in vivo* transfection efficiency and increasing circulating nanoparticles half-life.

[00163] Formation and stability of chitosan/dsODN nanoparticles and chitosan/siRNA nanoparticles were tested for up to 20 hours at pH 6.5 and 8 using different methods. Chitosan/dsODN nanoparticles were formed and were stable up to 20 hours at an N:P ratios above 2 at slightly acidic pH (pH 6.5) (Figs. 3A and 3B). At 4 hours following nanoparticle formation, no detectable dsODN were observed at N:P ratio of 1 (pH 6.5) and higher, whereas complete dsODN release was observed for the same N:P ratio at pH 8. Longer exposure time, 20h, resulted in dsODN release at N:P ratio of 2 for ApoB dsODN while higher N:P ratio (N:P 10) was able to maintain nanoparticle stability. At pH values of 8, and for the same N: P ratio of 10, partial dsODN release was observed. The specific chitosan formulations described herein assured nanoparticle stability for a minimum period of 20h at N: P ratio above 2 (N:P>2). Chitosan/siRNA stability was evaluated using the Ribogreen assay™, a fluorescence based assay, to quantitate the released siRNA following complex destabilization. The results show that chitosan/siRNA nanoparticle with an N:P ratio of 5 and 10 were stable for up to 20 hours at pH 6.5. Chitosan 80-10-5 showed the least stability when compared to other formulations. Increasing the N:P ratio for chitosan 80-10 resulted in an improvement of nanoparticle stability. Except for chitosan 80-10, increasing the N:P ratio above five did not result in an increase of nanoparticle stability as demonstrated by the data (Figs. 4A and 5). Thus, at lower N:P ratios nanoparticles were unstable and the complexation

efficiency was not optimal. At a neutral pH, nanoparticles were stable at N:P ratios between 2 and 5. At a more basic pH of 8, nanoparticles were unstable with a clear requirement to higher N:P ratios and higher molecular weight for increased stability.

[00164] The effect of chitosan parameters (DDA, MW and N:P ratio) was studied using for example anti-RecQL1 siRNA. A clear effect of the molecular weight is apparent with increased nanoparticle size when increasing chitosan MW (Figs. 4B, 4C and 4D). The DDA had a very slight effect on nanoparticle size. The N:P ratio seem to have a impact on nanoparticle size with higher nanoparticle size at increasing N:P.

[00165] The effect of siRNA concentration on nanoparticle size was studied. Our results show increased nanoparticle size with increased siRNA concentrations (Fig. 4E).

[00166] The ability of chitosan to protect dsODN sequences at low N:P ratios was assessed using a DNAse I protection assay. Nanoparticles of chitosan/dsODN (6µl) were incubated in a buffer containing (pH 6.5) 20mM MES, 1mM $MgCl_2$ and a concentration of 0, 0.5, 1, 2, 5 or 10 units of DNAse I. Samples were incubated for 30 min at 37°C. The reaction was stopped by adding 2µl of EDTA (50mM) then heated at 72°C for 15 min. Samples were then assessed by gel electrophoresis. Results demonstrate the ability of the formulations to protect siRNA mimicking double stranded oligonucleotide (Figs. 6A and 6B). All digestions were assessed using the signal intensity of the treated samples with the control (i.e. 0U DNAse I = 100% intensity). The protection is considerable and accounts for approximately 70% of complexes when using 1 unit of DNAse I/µg of DNA whereas the negative control is completely digested when 0.5 unit of DNAse I per µg of DNA is used. The protection remains efficient when increasing DNAse I concentration to 5 units per µg of DNA.

[00167] Cell uptake of RecQL1, DPP-IV and ApoB dsODN nanoparticles at different DDA, Mn and N:P ratio was evaluated using FACS analysis of

fluorescein labeled dsODN following chitosanase treatment of transfected cells thus reducing any possible bias associated with membrane bound nanoparticles as previously described (Alameh et al., 2010, Int J Nanomedicine, 5:473-481). Interestingly, results obtained with dsODN/chitosan nanoparticles indicate the cell line dependency of efficient uptake. The cell line dependency of chitosan nanoparticles uptake was associated with different endocytic pathways in previous work (Bishop, 1997, Rev Med Virol, 7:199-209; Huang et al., 2002, Pharm Res, 19:1488-1494). FACS results show that in general, cell uptake using these dsODN revealed no differences between formulations (Figs. 7A and 7B). The uptake efficiency using compositions presented herein ranged from 80% to 98% for RecQL1 (LS174T, A549 and AsPC1 cell lines), from 55% to 80% for ApoB (in HEK293, HepG2 and RAW264.7 cell lines). The uptake efficiency of the DPP-IV dsODN nanocomplexes in HepG2 cell line ranged from 73% to 99% with no statistical differences between the different formulations (92-10-5, 80-10-10 and 80-80-5). Uptake efficiency using chitosan/dsODN nanoparticles achieved levels comparable to or higher than the commercially used lipoplex (DharmaFECT™) with similar relative variation between cells type (Fig. 7A and 7B). Furthermore, these results are in accordance with confocal microscopy data (Figs. 8 to 10), described below, where images show a cellular distribution of chitosan and dsODN for all cell lines indicating a qualitative correlation to FACS quantitative data.

[00168] Confocal microscopy was used in order to assess particle uptake and internalization into the different cell lines described herein (LS174T,MCF-7 MDR, HEK293, HepG2, Caco-2 and RAW264.7). Chitosan was labeled using rhodamine whereas RecQL1-siRNA, DDP-IV-dsODN and ApoB-dsODN were labeled using fluorescein. For MCF-7 MDR nanoparticle assessment, a Cy3 labeled siRNA was used. Following the labeling process, nanoparticles were formed by mixing 1:1 volume of chitosan-rhodamine and siRNA mimicking dsODN using the procedure described above. Results suggest that formulations described in the present description were efficiently internalized into cells with a maximum release of siRNA or dsODN 24 hours post transfection. The enclosed results indicate the lack of colocalisation at 24 hrs between siRNA or dsODN

and chitosan demonstrating that complete release of the siRNA or dsODN cargo was achieved 24h post transfection. Furthermore, the diffuse staining pattern of siRNA or dsODN seen in most transfected cells is representative of complexes that have escaped endocytic vesicles (Figs. 8 to 10), consistent with previous live cell imaging work using chitosan-plasmid DNA nanoparticles (Thibault et al., 2010, Mol Ther, 18:1787-1795). Time course studies showed that particle internalization starts within an hour post transfection with a slow release dynamics to reach a maximum 24 hours post transfection.

[00169] The above described results show the capability of the formulation described in the present description to transfect and efficiently deliver different dsODN and siRNA into multiple cell lines (Figs. 8 to 11).

EXAMPLE V
Ex vivo siRNA delivery and gene expression inhibition

[00170] Chitosan specific formulations (92-10-5, 80-40-5, 80-10-10 and 80-80-5) were assessed for the siRNA delivery and subsequent inhibition of gene expression (RecQL1 mRNAs, DPP-IV, or ApoB mRNAs) in different cell lines. Results show that RecQL1, DPP-IV and ApoB coding mRNAs were down-regulated more than two fold when measured by quantitative real time PCR (Figs. 11A and 11B). These results demonstrate that the formulation described herein can achieve levels of gene silencing comparable to the commercial liposome DhamaFECT™ without any apparent cytotoxicity as observed using the alamar blue assay.

[00171] More specifically, regarding inhibiton of RecQL1 mRNAs in LS174T cells, chitosan 92-10-5 showed a high level of silencing (~80%), similar to the current gold standard commercial formulation (~80%), used in the present description as a positive control. Formulations 80-40-5 and 80-10-10 also induced significant silencing but to a lower degree than 92-10-5 and also with an increase of non-specific mock silencing, especially for formulation 80-10-10 (Fig. 11B). The results disclosed herein clearly reveal the effectiveness of the described chitosan-based formulations to efficiently deliver siRNA and knock down specific genes at N:P ratios far below (N:P=5) those used previously by

others (N:P > 20). In general, all of our low N:P ratio chitosan formulations reached high level of gene silencing supporting the FACS data (Fig. 7B).

[00172] It was found that 70% gene silencing at the messenger RNA level (mRNA) of DPP-IV or ApoB mRNAs, can be achieved using the specific formulation consisting of chitosan 92-10 with an N:P ratio of 5 (Fig. 11A). However the 70% inhibition at the messenger level is translated to a reduction of 50% of the enzymatic activity of DPP-IV (Fig. 12). This inhibition at the enzymatic level is comparable to that achieved when using the commercial lipoplex DharmaFECT™.

EXAMPLE VI

In vivo efficiency analysis of chitosan/siRNA nanoparticles

[00173] The *in vivo* efficiency of siRNA-ApoB nanoparticles was evaluated in a C57BL/6 mouse model. For each treatment modality, four animals (n= 4 except for the Dα where n=2 and the C1 group where n=3) were injected with 1 mg kg^{-1} of siRNA targeting the ApoB gene. The 1 mg kg^{-1} siRNAs targeting the ApoB gene were complexed to low molecular weight chitosan (LMW-CS) in a final volume of 0.2 ml (injected volume For example, for a 39 g mouse a 39µg siRNA – calculated for a dose of 1mgkg^{-1} – was administered following complexation of a siRNA volume of 78µl at 0.5µg/µl (37,037 nM) at a 1:1 ratio of chitosan 92-10-5. The total volume of 156 µl was then administered. The siRNA concentration following complexation becomes 0.25µg/µl (18,518 nM). Specifically, siRNA targeting the ApoB gene were complexed to chitosan formulation 92-10 (DDA, Mn) at an N:P ratio of 5 (N:P 5). In total, five groups (C1 to C5; n=4/group) were TNC treated at different times following the schedule in Table 3, wherein data for intravenous injections schedule of chitosan/siRNA-ApoB nanoparticles at a dose of 1mg kg^{-1} anti-ApoB siRNA in various C57BL/6 mice groups (n=4 animal per group) is disclosed. Each day represents the only day in the week where injections were made or euthanasia was performed. All the mice were injected once per week for three weeks with the TNC 92-10-5 (Mn-DDA-N:P), with the exception of 2 mice from the Dα group which were injected with the TNC 92-10-5 just once and euthanized 2

days later, to examine the rapidity of the therapeutic response. With the exception of these 2 mice, all other mice were euthanized within the last week of January 2011. The Dα group served as the positive untreated atherosclerotic control while Dμ was the negative control group that received the normal low fat diet. The Dβ group was the negative control group for the siRNA delivery without chitosan and was injected with uncomplexed naked siRNA. The total number of animals used for this study was 32.

Table 3

Animal study schedule

	Groups							
Day	**C1 (n=3)**	**C2 (n=4)**	**C3 (n=4)**	**C4 (n=4)**	**C5 (n=4)**	**Dα (n=4)**	**Dβ (n=4)**	**Dμ (n=4)**
23/11/10	Acclimation (All groups)							
30/11/10	Injection #1							
07/11/10	Injection #2	Injection #1						
14/12/10	Injection #3	Injection #2	Injection #1					
21/12/10		Injection #3	Injection #2	Injection #1			Injection #1	
28/12/10			Injection #3	Injection #2	Injection #1		Injection #2	
04/01/10				Injection #3	Injection #2		Injection #3	
11/01/11					Injection #3			
18/01/11						Dα-2day Injection (n=2) / Dα n=		
20/01/11						Euthanasia Dα-2day		
26/01/11	Euthanasia (C1, C2, C3)							
27/01/11				Euthanasia (C4, C5)			Euthanasia (Dα, Dβ, Dγ)	

[00174] All animals were acclimatized for two weeks before experimentation as requested by the University of Montreal Animal Ethic Committee (CDEA). Following the two week of acclimatization, high fat chow – D12492 – was fed to

all treated groups including the Dα positive group (untreated group, n=4) and the Dβ naked siRNA treated group (n=4) until the completion of the study which corresponds to the day where animals were euthanatized (Table 3). The Dμ group (n=4) was fed regular chow – D12450B – and served as the normal negative control (lean group). All treated animals were injected once a week for three weeks (Table 3). All C group animals were injected with 1 mg kg^{-1} of ApoB siRNA using the low N:P chitosan formulation 92-10-5. The last of the 3 weekly injections occurred at 7, 6, 5, 4 and 3 weeks prior to euthanizing groups C1, C2, C3, C4, C5, in order to examine the time course of treatment. Two of the 4 positive control atherosclerotic Dα animals were injected with the above formulation two days prior to euthanasia to examine the onset of treatment, with the other two remaining untreated. The D group was treated with uncomplexed naked ApoBsiRNA at 1 mg kg^{-1} while the normal low fat diet group Dμ was not treated (details in Table 3)

[00175] During the experimental schedule, phlebotomy was performed once per two weeks whereas animal weight measurement was performed once per week before TNC injection until the completion of the study. At the end of the experimental schedule and following the sacrifice of all animals (Table 3), organs such as liver and intestine were removed for analysis.

[00176] Hematological, biochemical, serological and histological analysis were performed on all animals. For instance, hematological and biochemical analysis of sera were performed by VitaTech, Montreal, Canada. The quantification of ApoB reduction in the sera was performed using an anti-ApoB ELISA whereas the quantification of LDL/VLDL cholesterol was performed using a colorimetric assay. Staining of liver sections was performed using hematoxylin-eosin staining in order to visualize fat vacuole. For the evaluation of immune cells infiltration into the liver, paraffin embedded sections were stained with Safranin-O/fast-green/iron-hematoxylin.

[00177] Hematological and biochemical analysis of all animals were performed following serum collection the day of euthanasia. Alanine aminotrasferase (ALT) and aspartate aminotrasferase (AST), two sensitive

indicator of liver damage were quantified in treated and untreated animals. A comparison of ALT and ASL plasma levels between the treated group (C5) and the positive control group (Dα) did not show any significant difference indicating an absence of liver toxicity effects of treatment with low N:P chitosan-ApoB siRNA TNCs (Table 4).

[00178] Moreover, results show that serum albumin levels were normal both in treated and untreated groups also indicating normal liver function. However, total cholesterol quantification in siRNA-ApoB treated animals showed potentially elevated serum levels similar to the positive control group (Table 4), wherein C5-2 was administered chitosan/siARN-ApoB nanoparticles, whereas Dα-3 is a positive control for atherosclerosis development respectively. Only one animal per group was used for haematological analysis because serum volumes needed are high and require the sacrifice of one animal.

Table 4

Haematologic characterization of a treated (C5-2) and untreated (Dα-3) mice.

Mice (Group-Mice)	C5-2	Dα-3
Albumin (g/L)	35	35
Bilirubin (Total) (µmol/L)	0.4	0.7
Bilirubin (Conjugated) (µmol/L)	0.1	0
ALP (IU/L)	58	55
ALT (IU/L)	120	121
AST (IU/L)	213	222
GGT (IU/L)	0	0
Cholesterol (mg/dL)	220	209
Hemolysis	1+	1+
Icterus	Normal	Normal
Lipemia	Normal	Normal

[00179] Taken together these results indicate the safety of the low N:P chitosan based siRNA nanoparticles as they do not induce any liver damage.

[00180] Apolipoprotein B plasma concentration levels in µg/ml were assessed using an anti-ApoB commercial ELISA kit (Uscn Life science Inc., China). The determination of ApoB plasma levels varied between 597µg/mL and 1,433 µg/mL depending on the groups and controls tested. The results obtained show that all treated groups had ApoB plasma levels that were ~35% reduced from

the positive atherosclerotic control group Dα to reach levels similar to those of the normal negative control (Dμ) (Fig. 13). The Dα-2day group showed a similar reduction two days following injection indicating a rapid silencing effect following TNC injection.

[00181] ApoB levels were decreased by 35% in animals receiving uncomplexed siRNA (control group; Dβ-1). Although this treatment modality (Dβ-1) was similarly effective in ApoB plasma reduction as TNCs treatment modalities (Fig. 13), it resulted in high inflammatory reactions in the liver (Fig. 16H) thus limiting its dosing to achieve effective and therapeutic silencing/ApoB plasma reduction. Additionally, results show that reductions in ApoB plasma levels for low N:P chitosan-based TNCs was maintained for more than seven weeks after the last injection in the C1 animal group (Fig. 13) without any apparent inflammation or liver toxicity. These results indicate a particularly promising the longevity of TNC treatment and effective controlled release properties.

[00182] The comparison between the Dβ-1 and the C1-C5 groups toxicity/inflammatory profiles indicate the advantage of using these specific LMW-TNCs over naked siRNA since no apparent toxicity/inflammation profile was observed (Fig. 16 and Table 4).

[00183] The LDL/VLDL cholesterol concentration was determined using a commercial quantitative colorimetric detection kit BioAssay Systems, USA). Results herein show that treated animals demonstrated a reduction in LDL/VLDL of ~20% compared to the positive control (Dα) (Fig. 14). Interestingly, group C5 demonstrated a higher concentration of VLDL/LDL compared to the untreated group despite the observed ApoB reduction (Fig. 13); a reduction comparable to other groups showing concomitant reduction of both ApoB and VLDL/LDL plasma concentration. The comparison between naked siRNA treated animals and TNCs treated animals show a similar reduction in LDL/VLDL cholesterol concentrations in accordance with previous results where ApoB reduction was similar (Figs. 13 and 14).

[00184] Histological analysis of paraffin fixed liver sections stained with hematoxylin-eosin reveal that TNC treated animals had lower cholesterol accumulation compared to the positive control Dα. Liver sections form TNC treated groups, C3 and Dβ, were found to have low levels of accumulated cholesterol similar to the normal negative control group Dμ that was fed the low fat diet. (Fig. 15). On the contrary, the group C4, C5 and Dα2 presented fatty livers similar to the positive control Dα (Fig. 15) whereas C1 and C2 present intermediate fatty livers. All together, results demonstrate that TNCs can prevent excessive cholesterol accumulation in the liver through ApoB inhibition and LDL/VLDL reduction therefore permitting the liver conversion of cholesterol into bile in C1, C2, and C3 groups. The results observed in groups C4 and C5 appear to be due to an excessive accumulation of cholesterol before TNC treatment. These results demonstrate the effectiveness of chitosan based TNCs in the treatment of atherosclerosis.

[00185] Histological analysis of paraffin fixed liver sections stained with safranin-O/fast-green/iron-hematoxylin show that chitosan based TNCs reduced the inflammatory reaction compared to naked ApoB siRNA treatment (Fig. 16). Results show that C5 group presented a higher lymphoid cell infiltration rates than the atherogenic control group thus indicating that inflammation was due to chitosan deposition in liver (Fig. 16). However, histological analysis of liver from groups C4, C3, C3 and C1 show a time dependent resorption of inflammation (Fig. 16). Furthermore, the comparison of Dα-2day and the positive untreated control Dα-3 show that chitosan effects of lymphoid cell infiltration is time dependent (Fig. 16, F and G). It is estimated that nanoparticles dependent inflammation within several weeks of treatment and is preserved during approximately three weeks until the resorption.

[00186] Comparison of Figs. 15 and 16 allows the assessment of the efficiency of the chitosan based nanoparticles to prevent cholesterol accumulation in the liver without disruption of liver integrity as demonstrated in by the ALT/ASL profiles. Furthermore, the comparison between Figs. 13 and 14 pinpoint the longevity of the treatment thus confirming our previous observations of chitosan mediated slow release.

[00187] The effect of treatment on weight gain was assessed by measuring the weight of each animal/group once per week during the present study. Results show that treatment did not affect weight gain (Fig. 17). However, it was noted that weight gain was slowed in the week following first TNC administration. For example, group C4 and C5 received their first injection on the 3rd and 4th week of investigation, respectively, which caused weight stabilization for group C4 and weight loss for group C5. This effect is also present in groups C2 and C3 on a smaller scale (Fig. 17). In fact, C5's mean weight had an accelerated weight gain (mean weight) compared to all groups from the beginning of the study until its first injection on 28-12-2010. The effect of this injection is observed on 04-01-2011 (5th week) where C5's weight increase rate slowed drastically concordantly with what is observed in Fig. 18.

[00188] While the invention has been described in connection with specific embodiments thereof, it will be understood that it is capable of further modifications and this application is intended to cover any variations, uses, or adaptations of the invention, including such departures from the present disclosure as come within known or customary practice within the art to which the invention pertains and as follows in the scope of the appended claims.

WHAT IS CLAIMED IS:

1. A composition for inhibiting a gene expression *in vivo* comprising chitosan and an RNAi-inducing nucleic acid sequence against said gene wherein the chitosan has a molecular weight (Mn) of 5 kDa to 200kDa, a degree of deacetylation (DDA) of 80% to 95%, and wherein the chitosan amine to nucleic acid phosphate ratio (N:P) is below 20.

2. The composition of claim 1, wherein the molecular weight of chitosan is 5 to 15 kDa, the DDA from 90 to 95% and the N:P ratio is from 2 to 10.

3. The composition of claim 1 or 2, wherein the molecular weight of chitosan is 10 kDa, the DDA is 92% and the N:P ratio is 5.

4. The composition of claim 1, wherein the molecular weight of chitosan is 10 kDa, 40 kDa, 80 kDa, 150 kDa or 200 kDa.

5. The composition of any one of claims 1-4, wherein the chitosan comprises block distribution of acetyl groups or a chemical modification.

6. The composition of any one of claims 1-5, wherein said chitosan has a polydispersity between 1.0 and 7.0.

7. The composition of any one of claims 1-6, wherein the RNAi-inducing nucleic acid sequence is a double stranded linear deoxyribonucleic acid or ribonucleic acid sequence between 10 to 50 nucleotides.

8. The composition of any one of claims 1-7, wherein the RNAi-inducing nucleic acid sequence is a hairpin structure of deoxyribonucleic or ribonucleic acid sequence.

9. The composition of any one of claims 1-8, wherein the RNAi-inducing nucleic acid sequence is chemically modified either on the sugar backbone, phosphate backbone and/or the nucleotide base ring.

10. The composition of any one of claims 1-9, wherein the RNAi-inducing nucleic acid sequence is a short interfering RNA, a short hairpin RNA or an RNAi-inducing vector.

11. The composition of any one of claims 1-10, wherein the RNAi-inducing nucleic acid sequence targets a gene involved in the pathogenesis of type II diabetes, atherosclerosis or cancer.

12. The composition of any one of claims 1-10, wherein the RNAi-inducing nucleic acid sequence targets a gene involved in tumor development, metastasis or the induction of chemoresistance.

13. The composition any one of claims 1-11, wherein the RNAi-inducing nucleic acid sequence targets a glycoregulating protein.

14. The composition of claim 13, wherein the glycoregulating protein is an incretin degrading enzyme.

15. The composition of claim 13, wherein the incretin degrading enzyme is dipeptydilpeptidase-IV (DPP-IV).

16. The composition any one of claims 1-11, wherein the RNAi-inducing nucleic acid sequence targets an atherogenic protein.

17. The composition of claim 16, wherein the atherogenic protein is Apolipoprotein B (ApoB), Apolipoprotein E (ApoE), Apolipoprotein B 100 (ApoB 100), Apolipoprotein B 48 (ApoB 48), Neutrophil gelatinase-associated lipocalin (NGAL), Matrix metalloproteinase-9 (MMP-9), or Cholesteryl ester transfer protein (CETP).

18. The composition of any one of claims 1-12, wherein the RNAi-inducing nucleic acid sequence targets a helicase protein, an RNA helicase, P68, DDX5, DDX32, DDX1, Akt, PKB, a member of the ABC transporters, MDR1, MRP, a member of the RAS family of proteins, SRC, HER2, EGFR, Abl, or Raf.

19. The composition of claim 18, wherein the helicase protein is a member of the RecQ family of helicases.

20. The composition of claim 18 or 19, wherein the helicase protein is RecQL1 DNA helicase.

21. The compositon of claim 18, wherein the RNAi-inducing nucleic acid sequence targets MDR1.

22. A composition as defined in any one of claims 1-21 for the treatment of diabetes mellitus and related conditions thereof, atherosclerosis and related conditions thereof, or cancer and related conditions thereof in a patient.

23. The composition of claim 22, wherein said diabetes mellitus related conditions are insulin-dependent diabetes mellitus (type I diabetes), noninsulin-dependent diabetes mellitus (type II diabetes), insulin resistance, hyperinsulinemia, diabetes-induced hypertension, obesity, damage to blood vessels, damage to eyes, damage to kidneys, damage to nerves, damage to autonomic nervous system, damage to skin, damage to connective tissue, and damage to immune system.

24. The composition of claim 22, wherein said atherosclerosis related conditions are cardiovascular diseases.

25. The composition of claims 24, wherein the cardiovascular diseases are coronary heart diseases, acute coronary syndromes or angina pectoris.

26. The composition of any one of claims 22-25, wherein said composition reduces ApoB plasma levels.

27. The composition of any one of claims 22-25, wherein said composition increases GLP-1 bioavailability.

28. The composition of any one of claims 22-27, said composition further increases the control of glucose metabolism in said patient.

29. The composition of any one of claims 22-28, said composition further reduces the blood glucose level in said patient.

30. The composition of any one of claims 22-29, said composition further reduces the cholesterol level in a patient.

31. The composition of any one of claims 22-30, said composition further reduces the low-density lipoprotein level in said patient.

32. The composition of any one of claims 22-31, wherein said composition further reduces the weight gain in said patient.

33. The composition of any one of claims 22-32, wherein said composition reduces ApoB plasma levels of at least 35% and LDL/VLDL cholesterol level of at least 20%.

34. The composition of any one of claims 22-32, further comprising insulin, a glucosidase inhibitor, a sulfonylurea, a DPP-IV inhibitor or a hypoglycemic compound.

35. The composition of any one of claims 22-34, formulated for concurrent administration with a suitable delivery reagent, insulin or a hypoglycemic compound.

36. The composition of claim 35, wherein the suitable delivery agent is Mirus Transit TKO® lipophilic reagent, lipofectin®, lipofectamine™, cellfectin®, polycations or liposomes.

37. The composition of claim 35, wherein said hypoglycemic compound is metformin, acarbose, acetohexamide, glimepiride, tolazamide, glipizide, glyburide, tolbutamide, chlorpropamide, thiazolidinediones, alpha glucosidase inhibitors, biguanindine derivatives, troglitazone, or a mixture thereof.

38. The composition of claim 34, wherein said sulfonylurea is tolbutanide, tolazamide, glisoxepide, glimipeide or glibomuride.

39. The composition of claim 34, wherein said DPP-IV inhibitor is sitagliptin, vildagliptin or saxagliptin.

40. The compositon of claim 22, wherein said cancer is breast cancer, glioma, large intestinal cancer, lung cancer, small cell lung cancer, stomach cancer, liver cancer, blood cancer, bone cancer, pancreatic cancer, skin cancer, head or neck cancer, cutaneous or intraocular melanoma, uterine sarcoma, ovarian cancer, rectal or colorectal cancer, anal cancer, colon cancer, fallopian tube carcinoma, endometrial carcinoma, cervical cancer, vulval cancer, squamous cell carcinoma, vaginal carcinoma, Hodgkin's disease, non-Hodgkin's lymphoma, esophageal cancer, small intestine cancer, endocrine cancer, thyroid cancer, parathyroid cancer, adrenal cancer, soft tissue tumor, urethral cancer, penile cancer, prostate cancer, chronic or acute leukemia, lymphocytic lymphoma, bladder cancer, kidney cancer, ureter cancer, renal cell carcinoma, renal pelvic carcinoma, CNS tumor, glioma, astrocytoma, glioblastoma multiforme, primary CNS lymphoma, bone marrow tumor, brain stem nerve gliomas, pituitary adenoma, uveal melanoma, testicular cancer, oral cancer, pharyngeal cancer, pediatric neoplasms, leukemia, neuroblastoma, retinoblastoma, glioma, rhabdomyoblastoma or sarcoma.

41. The composition of claim 22 or 40, formulated for concurrent administration with at least one of a suitable delivery reagent and an anti-cancer compound.

42. The composition of claim 41, wherein the suitable delivery agent is Mirus Transit TKO® lipophilic reagent, Lipofectin®, Lipofectamine™, Cellfectin®, polycations or liposomes.

43. The composition of any one of claims 22 and 41-42, formulated for concurrent administration during a suitable anti-cancer therapy.

44. The composition of claim 43, wherein the anti-cancer therapy is at least one of a surgical procedure, chemotherapy, hormonal therapy and localization radiation.

45. The composition of any one of claims 1-44, wherein said composition is formulated for an injection at a dose of 1mg/kg.

46. The composition of any one of claims 1-45, wherein said composition does not induce liver toxicity when administered.

47. A method for delivering a nucleic acid sequence into a cell comprising the step of contacting the composition of any one of claims 1-46 with said cell.

48. The method of claim 47, wherein said cell is a primary cell, a transformed cell or an immortalized cell.

49. A method of producing a composition for treating diabetes mellitus, atherosclerosis or cancer comprising admixing chitosan and an RNAi-inducing nucleic acid sequence in an acidic medium, wherein the chitosan has a molecular weight (Mn) of 5 kDa to 200kDa, a degree of deacetylation (DDA) of 80% to 95%, and wherein the chitosan amine to nucleic acid phosphate ratio (N:P) is below 20.

50. The method of claim 49, wherein the chitosan is dissolved in hydrochloric acid prior to admixing with the RNAi-inducing nucleic acid sequence.

51. The method of claim 50, wherein the chitosan is dissolved in a glucosamine:HCl at a ratio of 1:1.

52. The method of any one of claims 49-51, wherein the Mn of chitosan is 10 kDa, the DDA is of 80% or 92%, and wherein the chitosan amine to nucleic acid phosphate ratio (N:P) is of 5 or 10.

53. The method of any one of claims 49-52, wherein the admixing of chitosan with the RNAi-inducing nucleic acid sequence produces nanoparticles of spherical shape of sizes below 200 nm.

54. The method of claim 53, wherein the size of the nanoparticles is 45 to 156 nm.

55. A method for treating diabetes mellitus, atherosclerosis or cancer in a patient comprising administering to said patient an effective amount of a composition comprising chitosan and an RNA-inducing nucleic acid sequence, wherein the chitosan has a molecular weight (Mn) of 5 kDa to 200kDa, a degree of deacetylation (DDA) of 80% to 95%, and wherein the chitosan amine to nucleic acid phosphate ratio (N:P) is below 20.

56. The method of claim 55, wherein the molecular weight of chitosan is 5 to 15 kDa, the DDA from 90 to 95% and the N:P ratio is from 2 to 10.

57. The method of claim 55, wherein the molecular weight of chitosan is 10 kDa, the DDA is 92% and the N:P ratio is 5.

58. The method of claim 55, wherein the molecular weight of chitosan is 10 kDa, 40 kDa, 80 kDa, 150 kDa or 200 kDa.

59. The method of claim 55, wherein the chitosan comprises block distribution of acetyl groups or a chemical modification.

60. The method of claim 55, wherein said chitosan has a polydispersity between 1.0 and 7.0.

61. The method of claim 55, wherein the RNAi-inducing nucleic acid sequence is a double stranded linear deoxyribonucleic acid or ribonucleic acid sequence between 10 to 50 nucleotides.

62. The method of claim 55, wherein the RNAi-inducing nucleic acid sequence is a hairpin structure of deoxyribonucleic or ribonucleic acid sequence.

63. The method of claim 55, wherein RNAi-inducing nucleic acid sequence is chemically modified either on the sugar backbone, phosphate backbone and/or the nucleotide base ring.

64. The method of claim 55, wherein the RNAi-inducing nucleic acid sequence is a short interfering RNA, a short hairpin RNA or an RNAi-inducing vector.

65. The method of claim 55, wherein the RNAi-inducing nucleic acid sequence targets a gene involved in the pathogenesis of type II diabetes, atherosclerosis or cancer.

66. The method of claim 55, wherein the RNAi-inducing nucleic acid sequence targets a gene involved in tumor development, metastasis or the induction of chemoresistance.

67. The method of claim 55, wherein the RNAi-inducing nucleic acid sequence targets a glycoregulating protein.

68. The method of claim 67, wherein the glycoregulating protein is an incretin degrading enzyme.

69. The method of claim 68, wherein the incretin degrading enzyme is dipeptydilpeptidase-IV (DPP-IV).

70. The method of claim 55, wherein the RNAi-inducing nucleic acid sequence targets an atherogenic protein.

71. The method of claim 70, wherein the atherogenic protein is Apolipoprotein B (ApoB), Apolipoprotein E (ApoE), Apolipoprotein B 100 (ApoB 100), Apolipoprotein B 48 (ApoB 48), Neutrophil gelatinase-associated lipocalin (NGAL), Matrix metalloproteinase-9 (MMP-9), or Cholesteryl ester transfer protein (CETP).

72. The method of claim 55, wherein the RNAi-inducing nucleic acid sequence targets a helicase protein, an RNA helicase, P68, DDX5, DDX32, DDX1, Akt, PKB, a member of the ABC transporters, MDR1, MRP, a member of the RAS family of proteins, SRC, HER2, EGFR, Abl, or Raf.

73. The method of claim 72, wherein the helicase protein is a member of the RecQ family of helicases.

74. The composition of claim 72, wherein the helicase protein is RecQL1 DNA helicase.

75. The method of claim 55, wherein the RNAi-inducing nucleic acid sequence targets MDR1.

76. The method of claim 55, wherein said composition reduces ApoB plasma levels.

77. The method of claim 55, wherein said composition increases GLP-1 bioavailability.

78. The method of claim 55, said composition further increases the control of glucose metabolism in said patient.

79. The method of claim 55, said composition further reduces the blood glucose level in said patient.

80. The method of claim 55, said composition further reduces the cholesterol level in a patient.

81. The method of claim 55, said composition further reduces the low-density lipoprotein level in said patient.

82. The method of claim 55, wherein said composition further reduces the weight gain in said patient.

83. The method of claim 55, wherein said composition reduces ApoB plasma levels of at least 35% and LDL/VLDL cholesterol level of at least 20%.

84. The method of claim 55, said composition further comprising insulin, a glucosidase inhibitor, a sulfonylurea, a DPP-IV inhibitor or a hypoglycemic compound.

85. The method of claim 55, said composition administrated concurrently with a suitable delivery reagent, insulin or a hypoglycemic compound.

86. The method of claim 85, wherein the suitable delivery agent is Mirus Transit TKO® lipophilic reagent, lipofectin®, lipofectamine™, cellfectin®, polycations or liposomes.

87. The method of claim 85, wherein said hypoglycemic compound is metformin, acarbose, acetohexamide, glimepiride, tolazamide, glipizide, glyburide, tolbutamide, chlorpropamide, thiazolidinediones, alpha glucosidase inhibitors, biguanindine derivatives, troglitazone, or a mixture thereof.

88. The method of claim 84, wherein said sulfonylurea is tolbutanide, tolazamide, glisoxepide, glimipeide or glibomuride.

89. The method of claim 34, wherein said DPP-IV inhibitor is sitagliptin, vildagliptin or saxagliptin.

90. The method of claim 55, wherein said cancer is breast cancer, glioma, large intestinal cancer, lung cancer, small cell lung cancer, stomach cancer, liver cancer, blood cancer, bone cancer, pancreatic cancer, skin cancer, head or neck cancer, cutaneous or intraocular melanoma, uterine sarcoma, ovarian cancer, rectal or colorectal cancer, anal cancer, colon cancer, fallopian tube carcinoma, endometrial carcinoma, cervical cancer, vulval cancer, squamous cell carcinoma, vaginal carcinoma, Hodgkin's disease, non-Hodgkin’s lymphoma, esophageal cancer, small intestine cancer, endocrine cancer, thyroid cancer, parathyroid cancer, adrenal cancer, soft tissue tumor, urethral cancer, penile cancer, prostate cancer, chronic or acute leukemia, lymphocytic lymphoma, bladder cancer, kidney cancer, ureter cancer, renal cell carcinoma, renal pelvic carcinoma, CNS tumor, glioma, astrocytoma, glioblastoma multiforme, primary CNS lymphoma, bone marrow tumor, brain stem nerve gliomas, pituitary adenoma, uveal melanoma, testicular cancer, oral cancer,

pharyngeal cancer, pediatric neoplasms, leukemia, neuroblastoma, retinoblastoma, glioma, rhabdomyoblastoma or sarcoma.

91. The method of claim 55, sad compositon is administered with at least one of a suitable delivery reagent and an anti-cancer compound.

92. The method of claim 41, wherein the suitable delivery agent is Mirus Transit TKO® lipophilic reagent, Lipofectin®, Lipofectamine™, Cellfectin®, polycations or liposomes.

93. The method of claim 55, said compositon is administered concurrently during a suitable anti-cancer therapy.

94. The method of claim 43, wherein the anti-cancer therapy is at least one of a surgical procedure, chemotherapy, hormonal therapy and localization radiation.

95. The method of claim 55, wherein said composition is injected at a dose of 1mg/kg.

96. The method of claim 55, wherein said composition does not induce liver toxicity when administered.

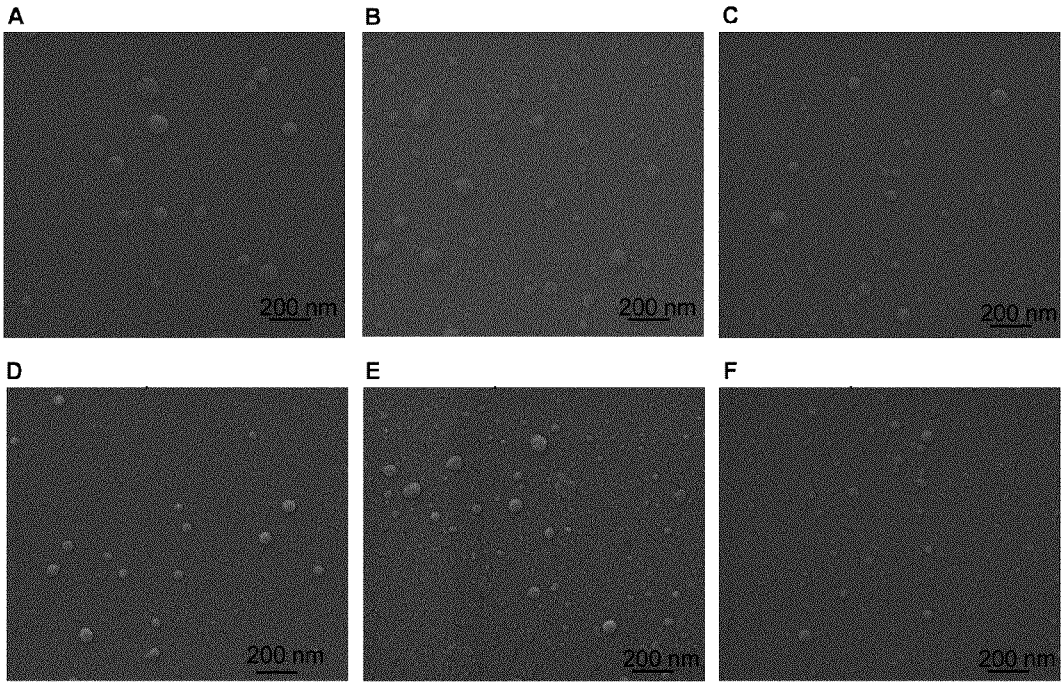
A
B
C
200 nm
200 nm
200 nm
D
E
F
200 nm
200 nm
200 nm

Fig. 1A

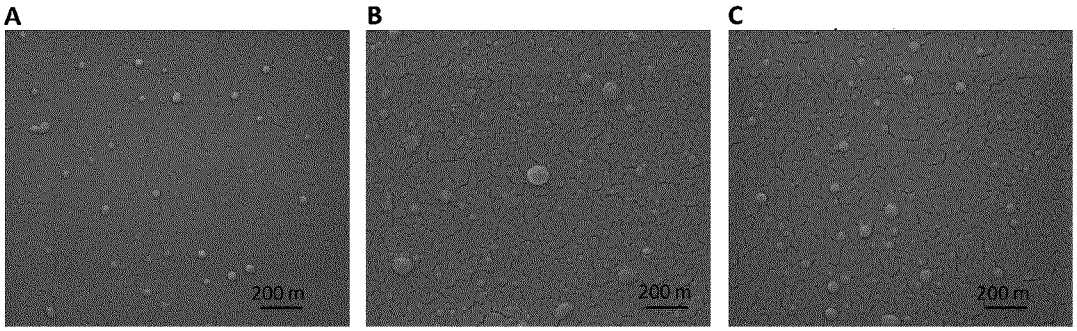
A
B
C
200 m
200 m
200 m

Fig. 1B

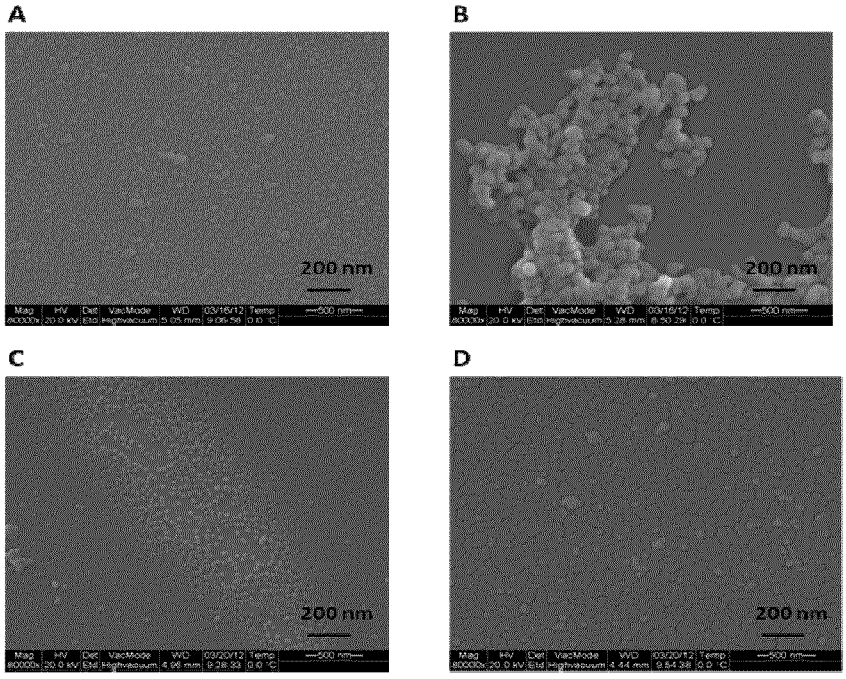

Fig. 2A

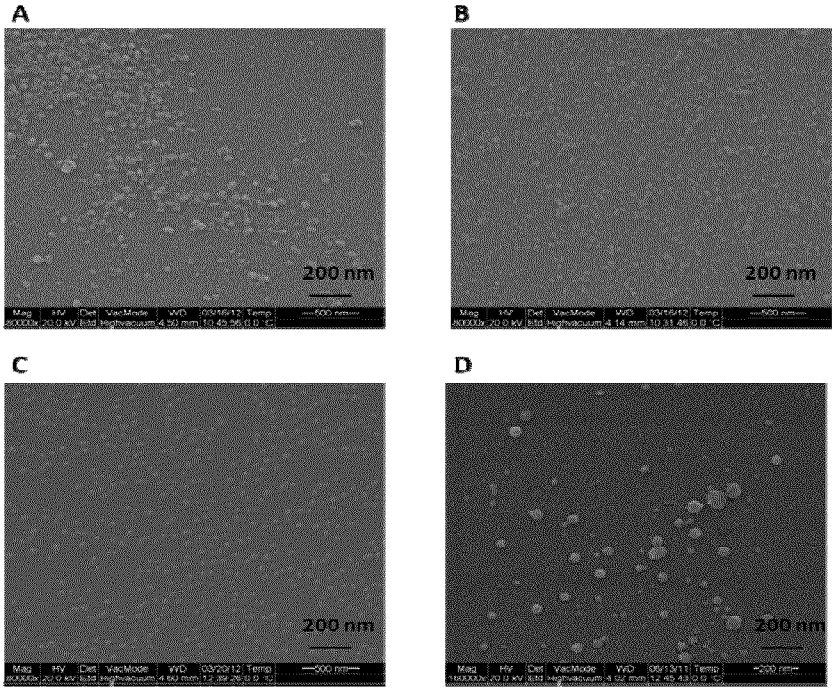

Fig. 2B

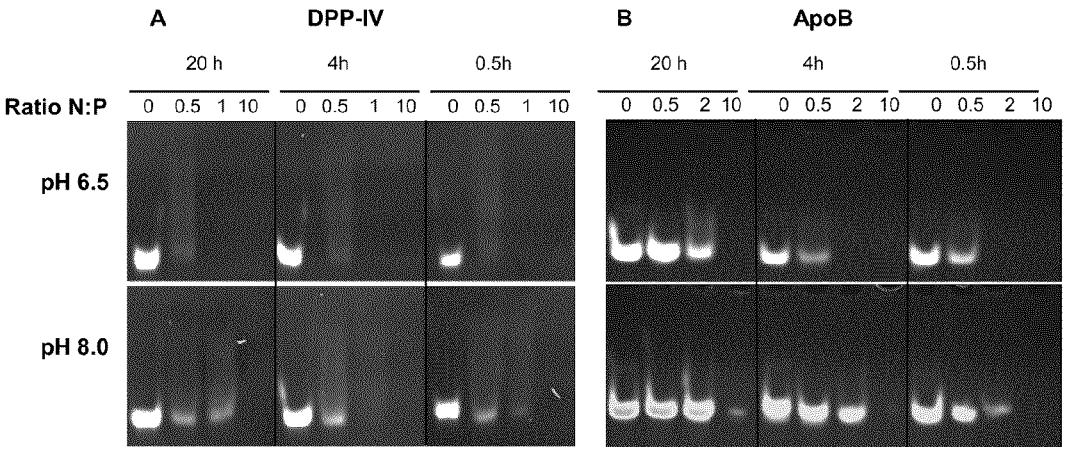
A
DPP-IV
B
ApoB
20 h
4h
0.5h
20 h
4h
0.5h
Ratio N:P
0 0.5 1 10
0 0.5 1 10
0 0.5 1 10
0 0.5 2 10
0 0.5 2 10
0 0.5 2 10
pH 6.5
pH 8.0

Fig. 3A

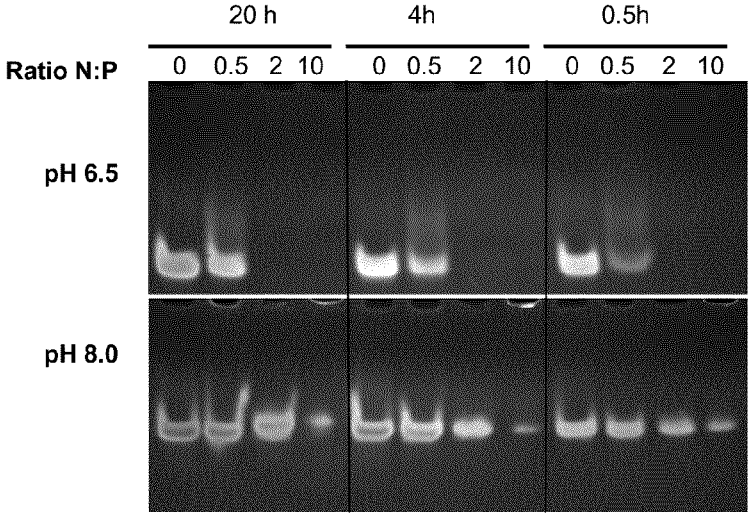
20 h
4h
0.5h
Ratio N:P
0 0.5 2 10
0 0.5 2 10
0 0.5 2 10
pH 6.5
pH 8.0

Fig. 3B

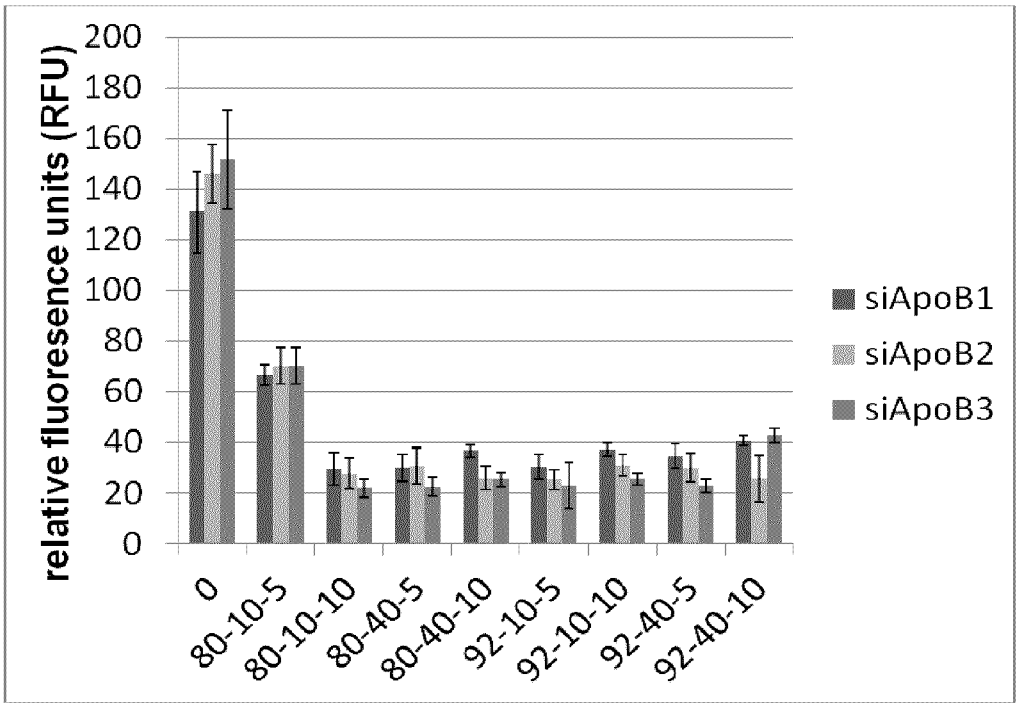
relative fluoresence units (RFU)
200
180
160
140
120
100
80
60
40
20
0
0
80-10-5
80-10-10
80-40-5
80-40-10
92-10-5
92-10-10
92-40-5
92-40-10
siApoB1
siApoB2
siApoB3

Fig. 4A

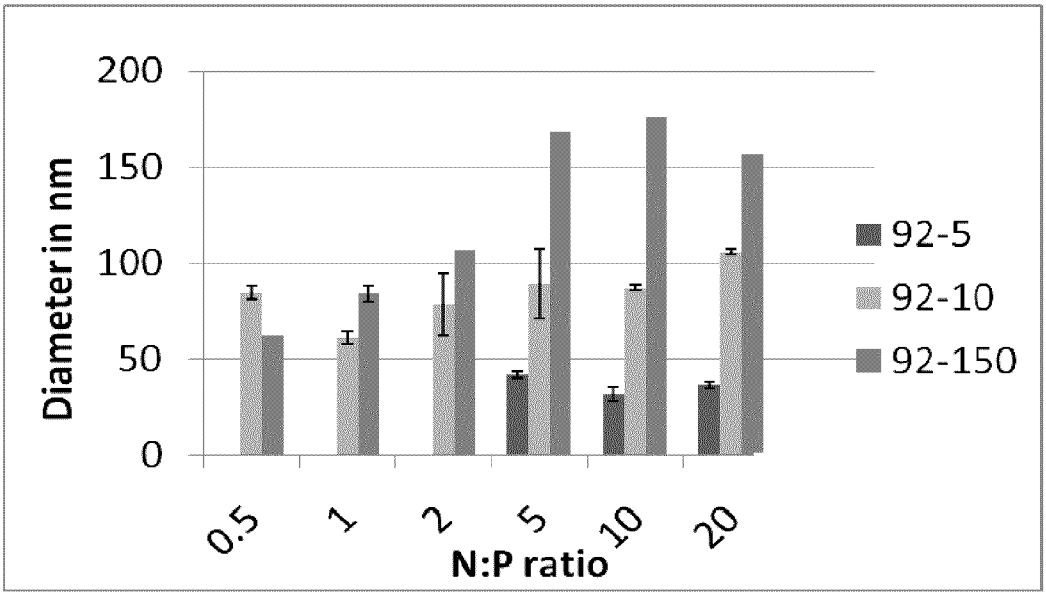
Diameter in nm
200
150
100
50
0
0.5
1
2
5
10
20
N:P ratio
92-5
92-10
92-150

Fig. 4B

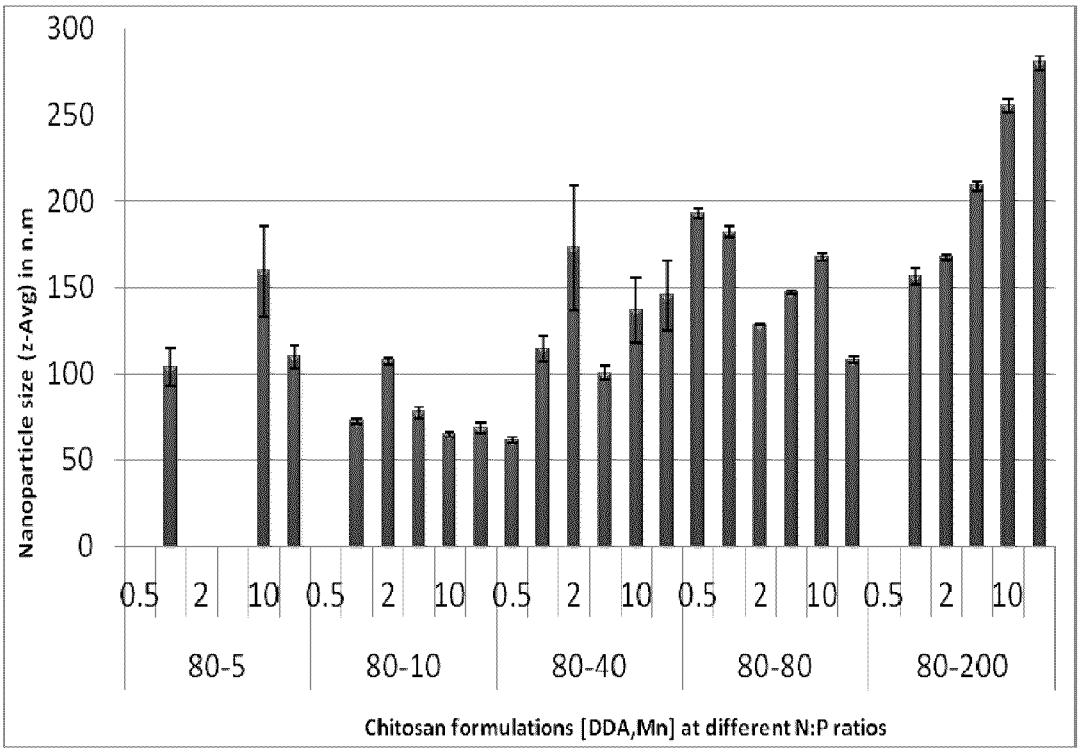
300
250
200
150
100
50
0
Nanoparticle size (z-Avg) in n.m
0.5 2 10 0.5 2 10 0.5 2 10 0.5 2 10 0.5 2 10
80-5
80-10
80-40
80-80
80-200
Chitosan formulations [DDA,Mn] at different N:P ratios

Fig. 4C

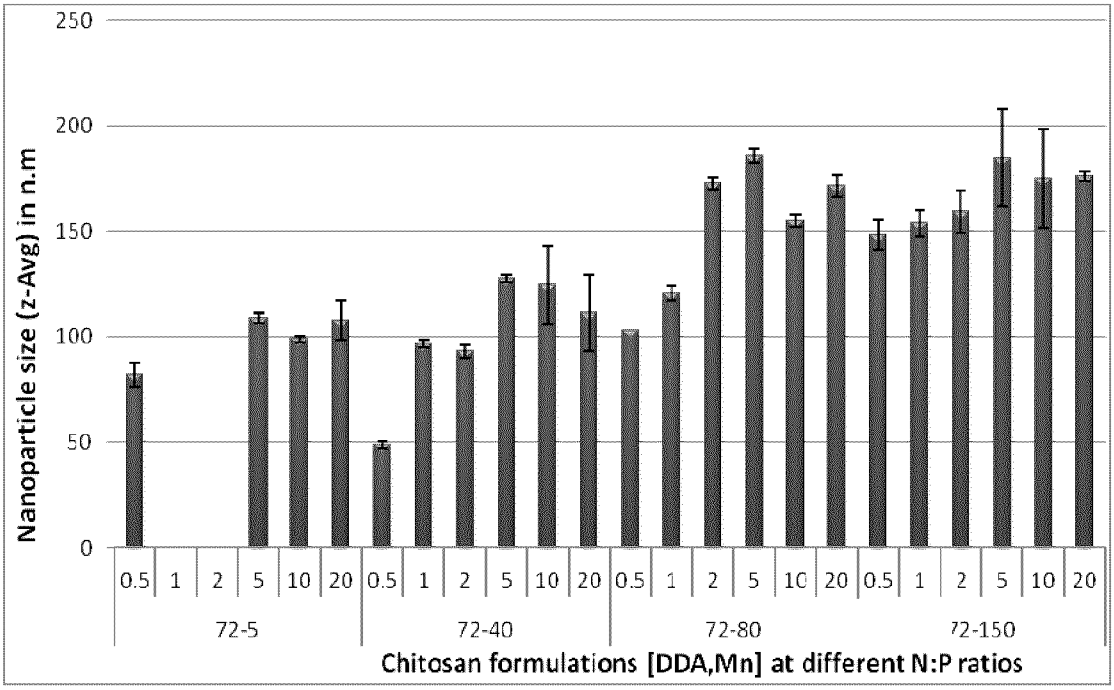
250
200
150
100
50
0
Nanoparticle size (z-Avg) in n.m
0.5 1 2 5 10 20 0.5 1 2 5 10 20 0.5 1 2 5 10 20 0.5 1 2 5 10 20
72-5
72-40
72-80
72-150
Chitosan formulations [DDA,Mn] at different N:P ratios

Fig. 4D

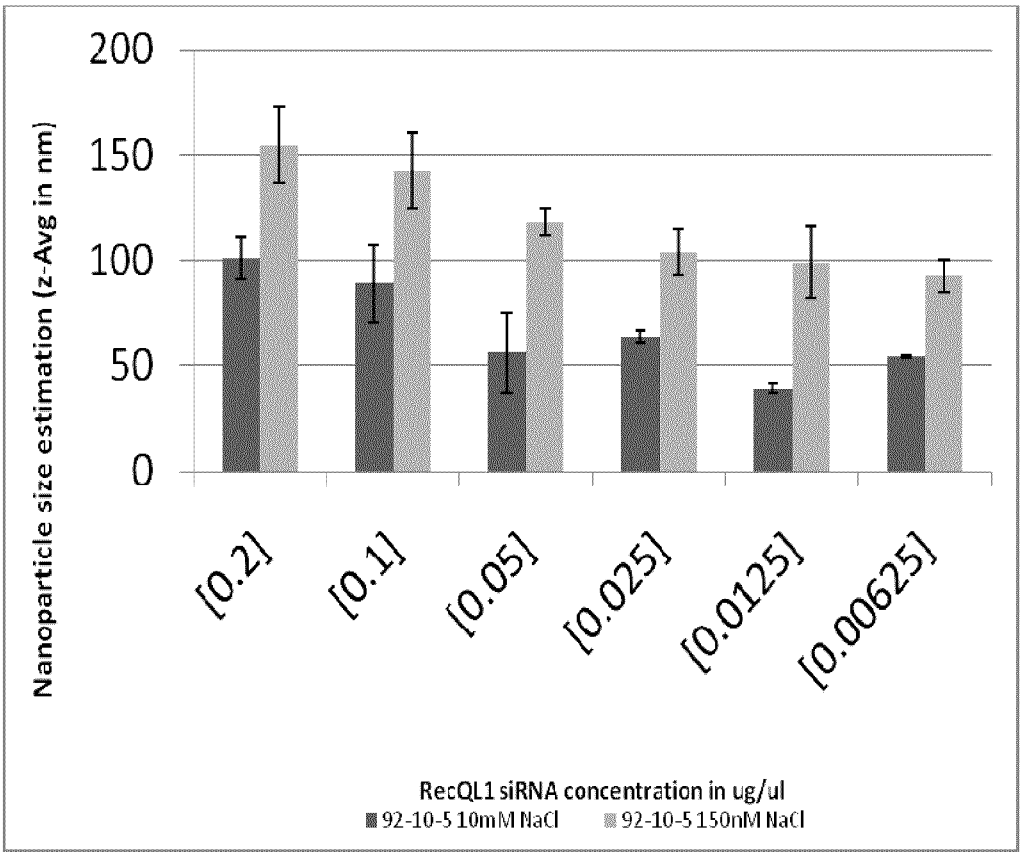
200
150
100
50
0
Nanoparticle size estimation (z-Avg in nm)
[0.2]
[0.1]
[0.05]
[0.025]
[0.0125]
[0.00625]
RecQL1 siRNA concentration in ug/ul
92-10-5 10mM NaCl
92-10-5 150nM NaCl

Fig. 4E

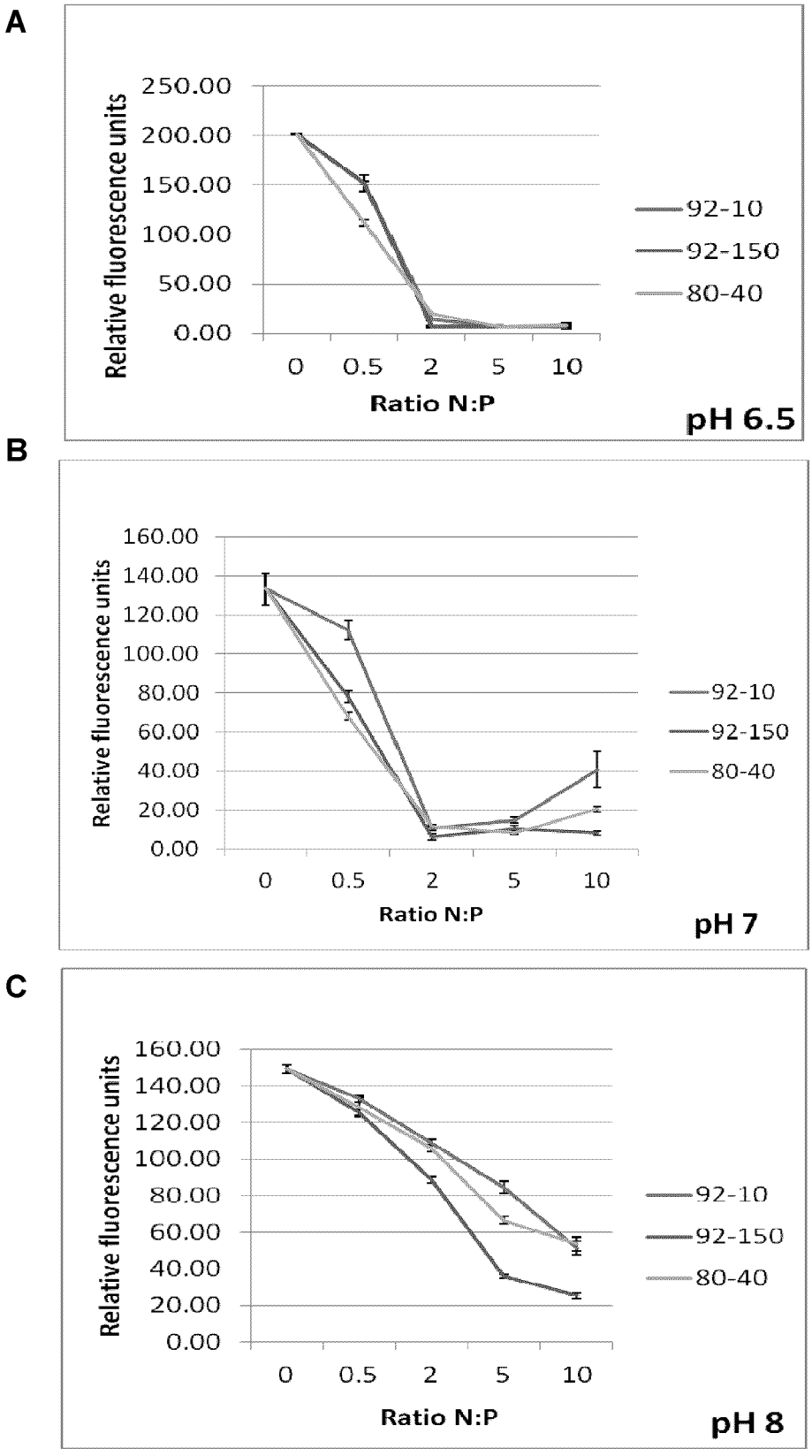
A
250.00
200.00
150.00
100.00
50.00
0.00
Relative fluorescence units
0
0.5
2
5
10
Ratio N:P
92-10
92-150
80-40
pH 6.5
B
160.00
140.00
120.00
100.00
80.00
60.00
40.00
20.00
0.00
Relative fluorescence units
0
0.5
2
5
10
Ratio N:P
92-10
92-150
80-40
pH 7
C
160.00
140.00
120.00
100.00
80.00
60.00
40.00
20.00
0.00
Relative fluorescence units
0
0.5
2
5
10
Ratio N:P
92-10
92-150
80-40
pH 8

Fig. 5

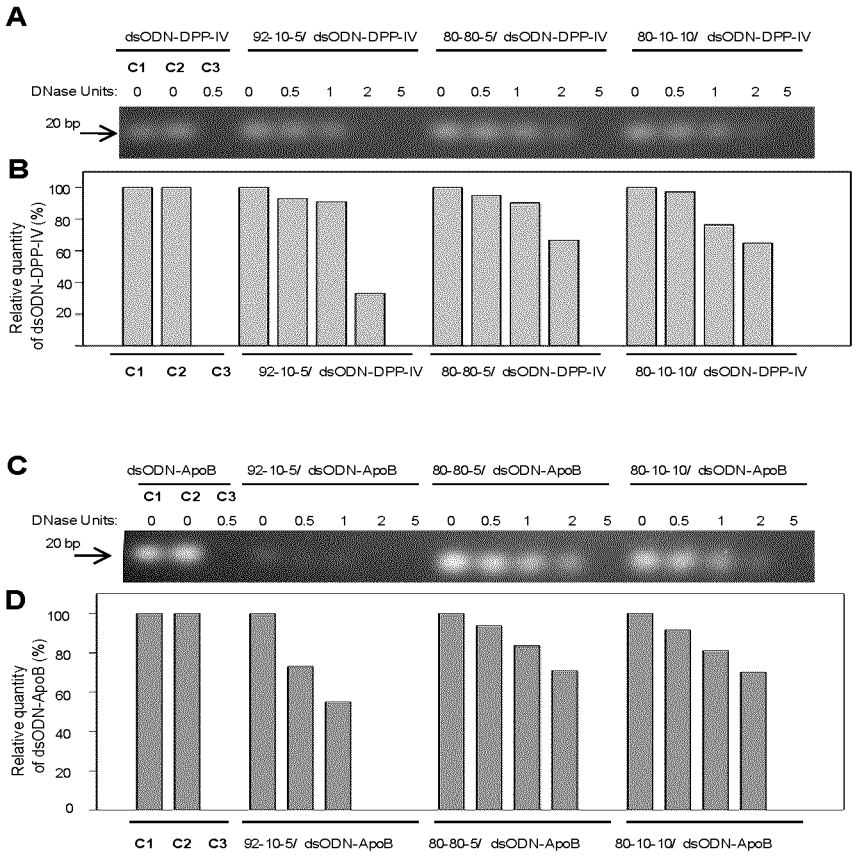
A
dsODN-DPP-IV
92-10-5/ dsODN-DPP-IV
80-80-5/ dsODN-DPP-IV
80-10-10/ dsODN-DPP-IV
C1 C2 C3
DNase Units: 0 0 0.5 0 0.5 1 2 5 0 0.5 1 2 5 0 0.5 1 2 5
20 bp
B
Relative quantity of dsODN-DPP-IV (%)
100
80
60
40
20
C1 C2 C3 92-10-5/ dsODN-DPP-IV 80-80-5/ dsODN-DPP-IV 80-10-10/ dsODN-DPP-IV
C
dsODN-ApoB
92-10-5/ dsODN-ApoB
80-80-5/ dsODN-ApoB
80-10-10/ dsODN-ApoB
C1 C2 C3
DNase Units: 0 0 0.5 0 0.5 1 2 5 0 0.5 1 2 5 0 0.5 1 2 5
20 bp
D
Relative quantity of dsODN-ApoB (%)
100
80
60
40
20
0
C1 C2 C3 92-10-5/ dsODN-ApoB 80-80-5/ dsODN-ApoB 80-10-10/ dsODN-ApoB

Fig. 6A

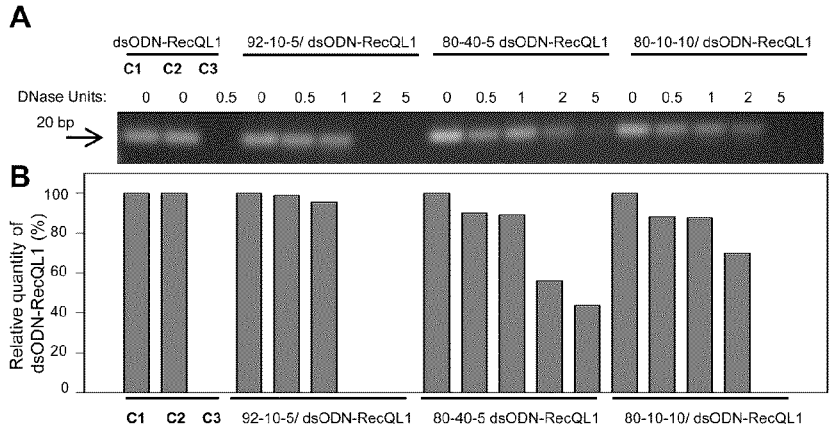
A
dsODN-RecQL1
92-10-5/ dsODN-RecQL1
80-40-5 dsODN-RecQL1
80-10-10/ dsODN-RecQL1
C1 C2 C3
DNase Units: 0 0 0.5 0 0.5 1 2 5 0 0.5 1 2 5 0 0.5 1 2 5
20 bp
B
Relative quantity of dsODN-RecQL1 (%)
100
80
60
40
20
0
C1 C2 C3 92-10-5/ dsODN-RecQL1 80-40-5 dsODN-RecQL1 80-10-10/ dsODN-RecQL1

Fig. 6B

A

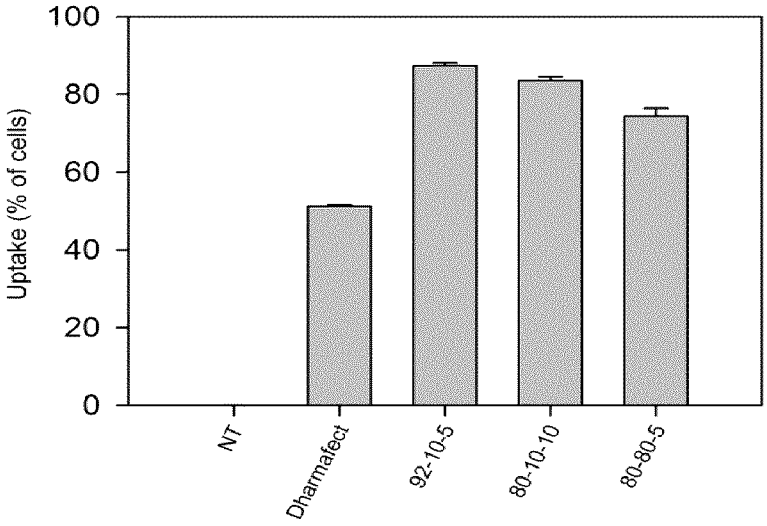
100
80
60
40
20
0
Uptake (% of cells)
NT
Dharmafect
92-10-5
80-10-10
80-80-5

B

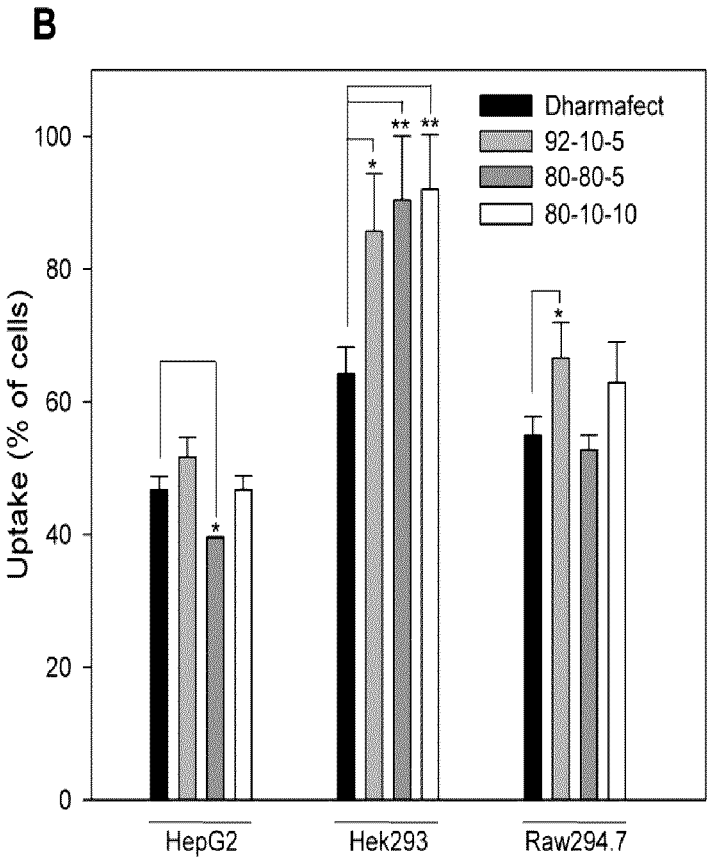
Dharmafect
92-10-5
80-80-5
80-10-10
Uptake (% of cells)
100
80
60
40
20
0
*
**
**
*
*
HepG2
Hek293
Raw294.7

Fig. 7A

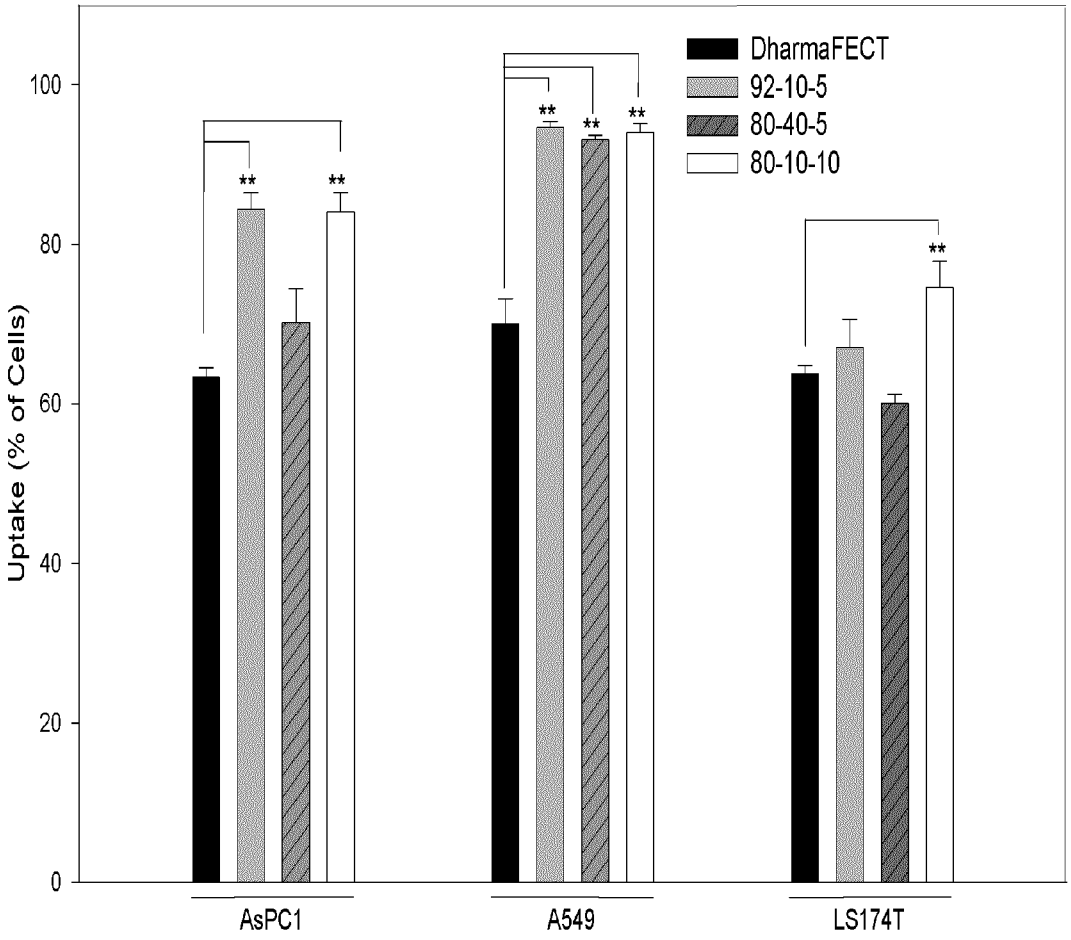
DharmaFECT
92-10-5
80-40-5
80-10-10
Uptake (% of Cells)
0
20
40
60
80
100
**
AsPC1
A549
LS174T

Fig. 7B

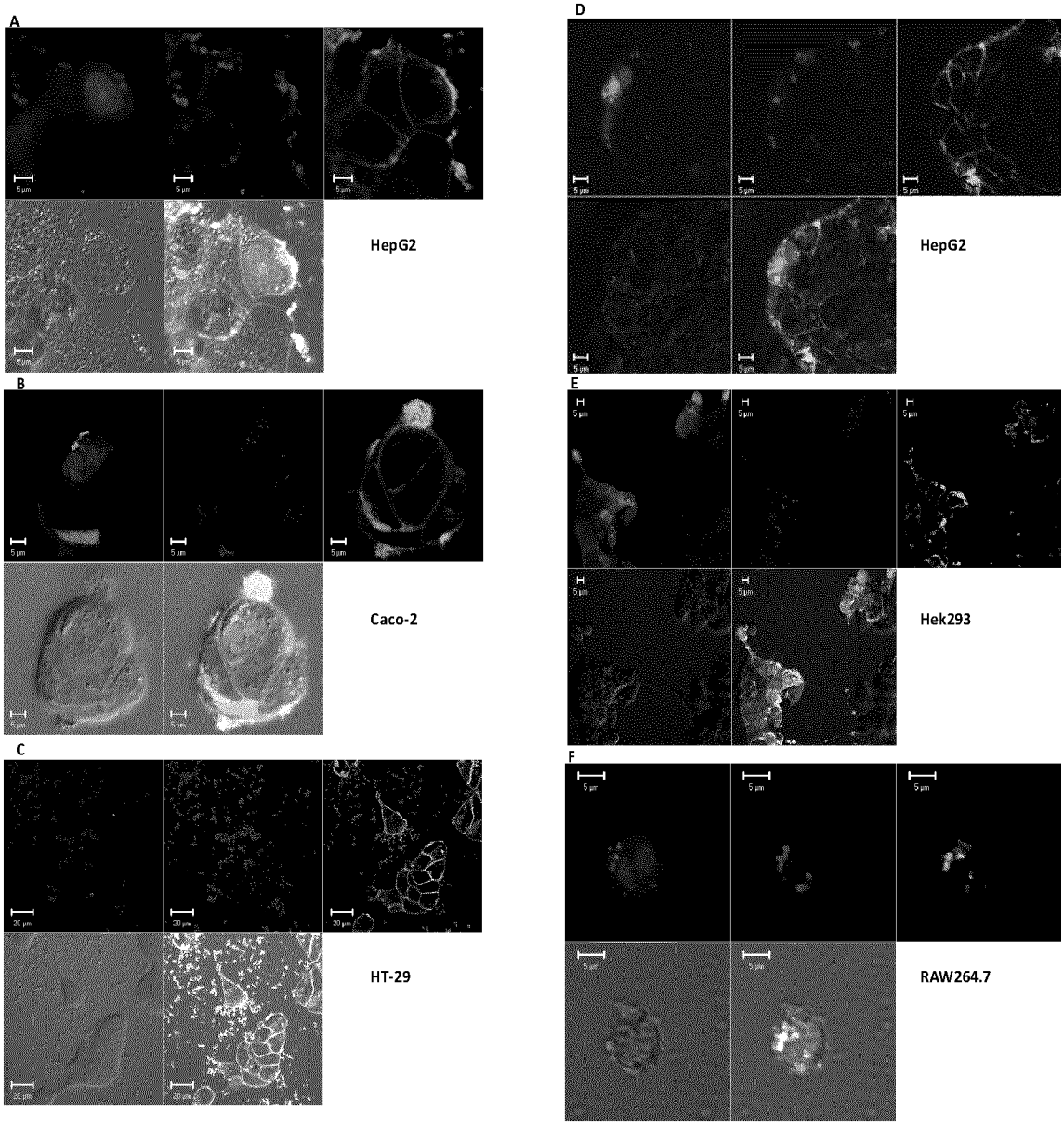

Fig. 8

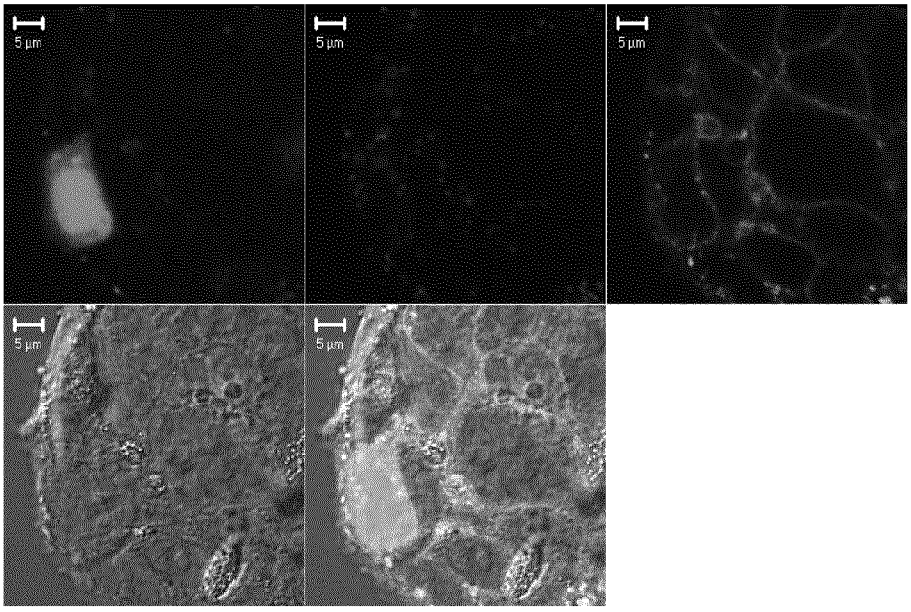

Fig. 9

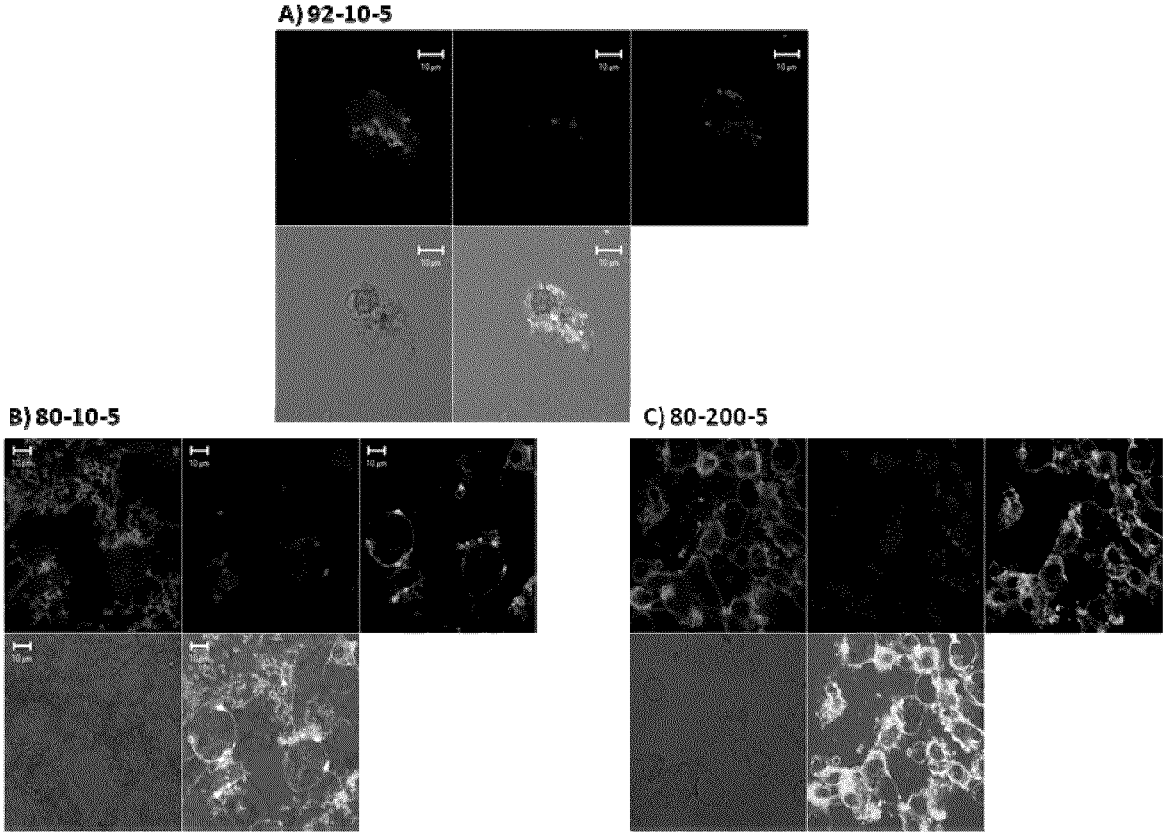

Fig. 10

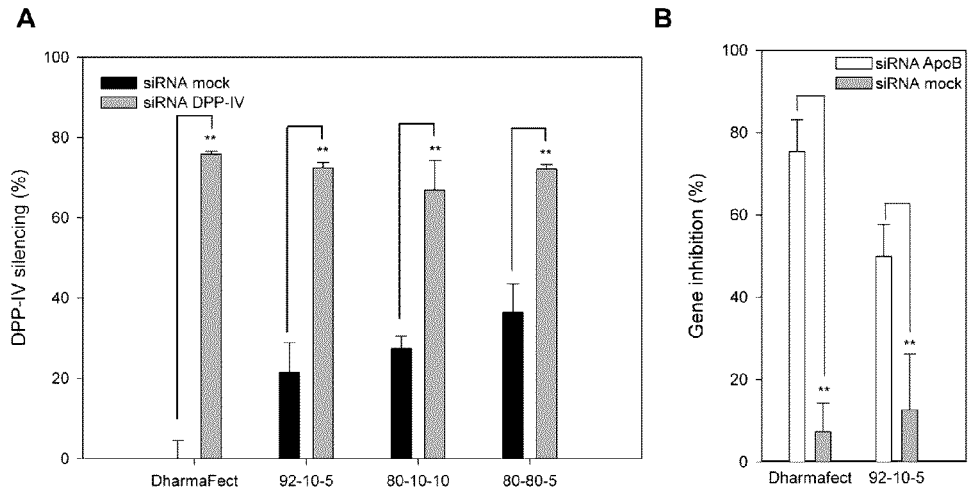

Fig. 11A

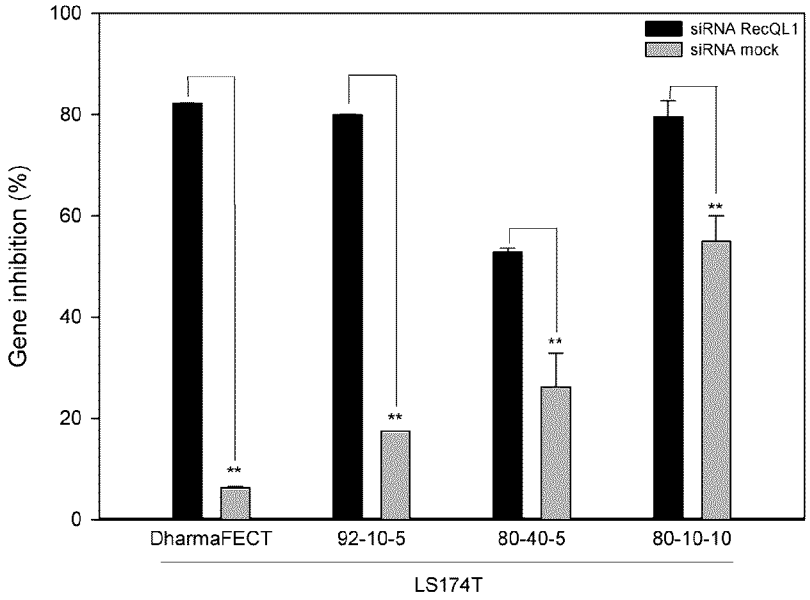

Fig. 11B

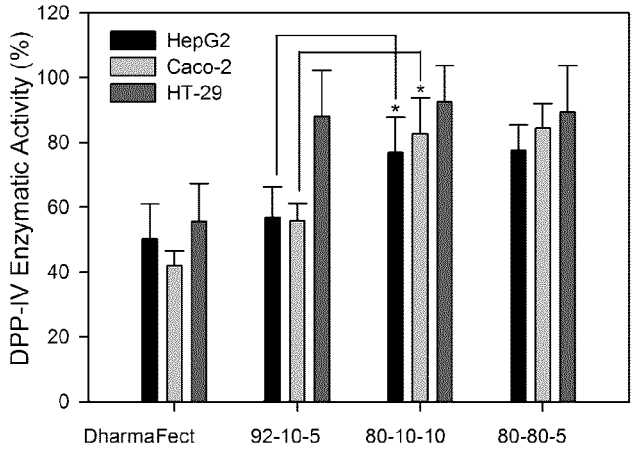

Fig. 12

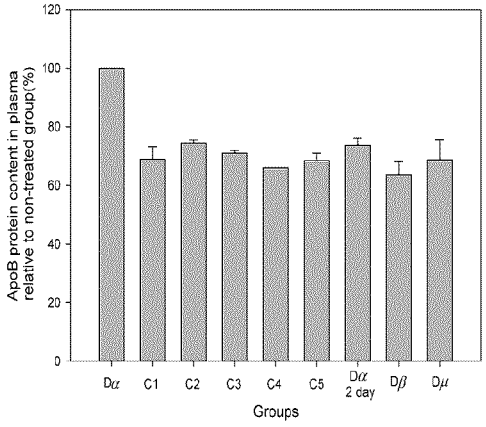

Fig. 13

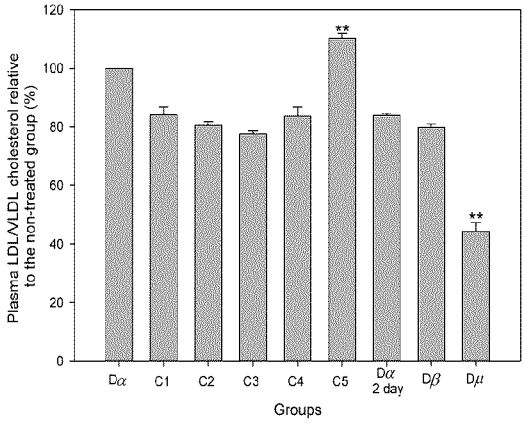

Fig. 14

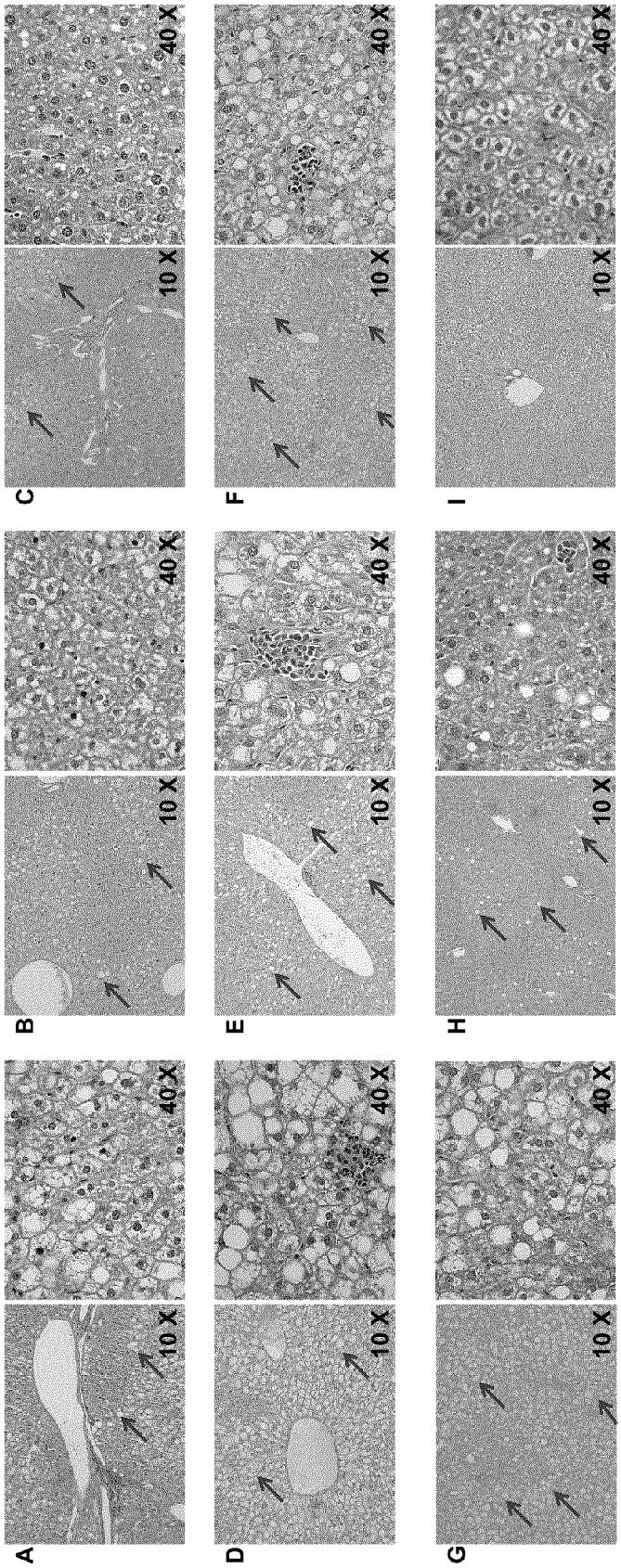
A
10 X
40 X
B
10 X
40 X
C
10 X
40 X
D
10 X
40 X
E
10 X
40 X
F
10 X
40 X
G
10 X
40 X
H
10 X
40 X
I
10 X
40 X

Fig. 15

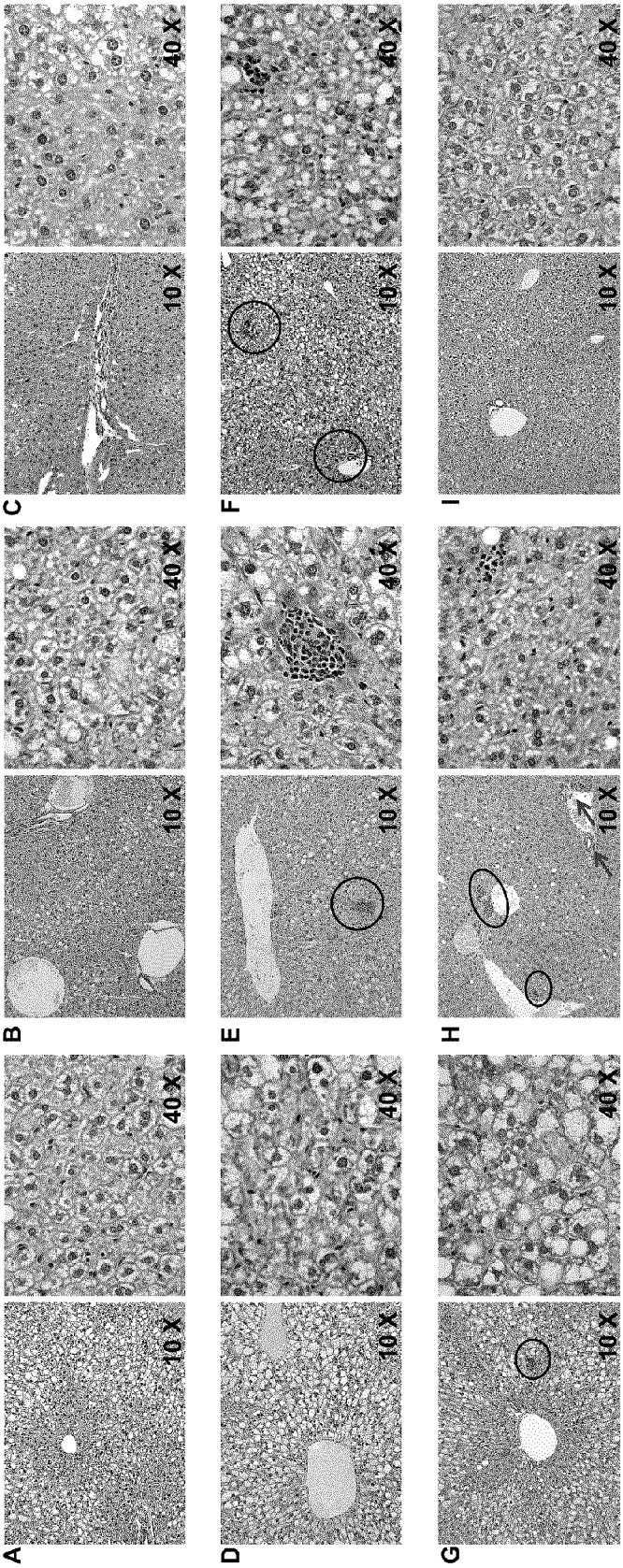
A
10 X
B
10 X
C
10 X
D
10 X
40 X
E
10 X
40 X
F
10 X
40 X
G
10 X
40 X
H
10 X
40 X
I
10 X
40 X

Fig. 16

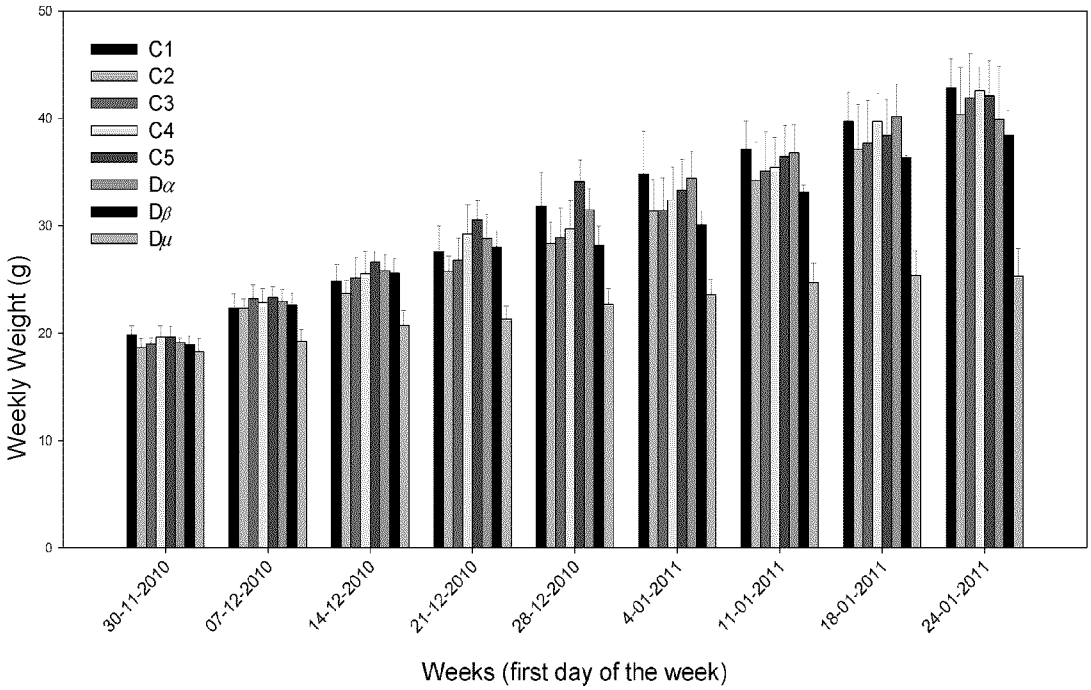
C1
C2
C3
C4
C5
Dα
Dβ
Dμ
Weekly Weight (g)
0
10
20
30
40
50
30-11-2010
07-12-2010
14-12-2010
21-12-2010
28-12-2010
4-01-2011
11-01-2011
18-01-2011
24-01-2011
Weeks (first day of the week)

Fig. 17

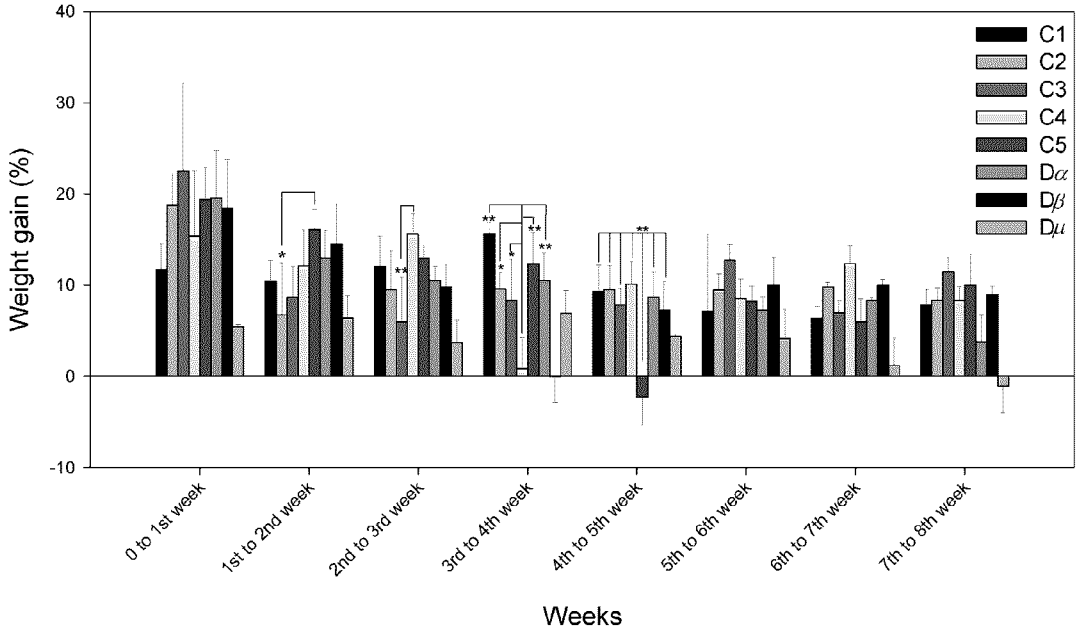
C1
C2
C3
C4
C5
Dα
Dβ
Dμ
Weight gain (%)
-10
0
10
20
30
40
0 to 1st week
1st to 2nd week
2nd to 3rd week
3rd to 4th week
4th to 5th week
5th to 6th week
6th to 7th week
7th to 8th week
Weeks

Fig. 18

INTERNATIONAL SEARCH REPORT

International application No.
PCT/CA2012/050342

A. CLASSIFICATION OF SUBJECT MATTER
IPC: ***A61K 47/36*** (2006.01) , ***A61K 31/713*** (2006.01) , ***A61P 3/10*** (2006.01) , ***A61P 35/00*** (2006.01) , ***A61P 9/10*** (2006.01)
According to International Patent Classification (IPC) or to both national classification and IPC

B. FIELDS SEARCHED

Minimum documentation searched (classification system followed by classification symbols)
IPC: ***A61K 47/36*** (2006.01) , ***A61K 31/713*** (2006.01) , ***A61P 3/10*** (2006.01) , ***A61P 35/00*** (2006.01) , ***A61P 9/10*** (2006.01)

Documentation searched other than minimum documentation to the extent that such documents are included in the fields searched

Electronic database(s) consulted during the international search (name of database(s) and, where practicable, search terms used)
Canadian patent database, Epoque, Scopus, google (sample search terms: chitosan, degree of deacetylation, DNA, RNAi, siRNA, nucleic acid, nucleoside, nucleotide and similar terms)

C. DOCUMENTS CONSIDERED TO BE RELEVANT

Category*	Citation of document, with indication, where appropriate, of the relevant passages	Relevant to claim No.
P,X	JEAN, M. et al. "Chitosan-based therapeutic nanoparticles for combination gene therapy and gene silencing of *in vitro* cell lines relevant to type 2 diabetes" *European Journal of Pharmaceutical Sciences* **2012**, *45*, 138-149. published online 9 November 2011 (9-11-2011). (see sections 2.2-2.6, 2.10.3, 3.5 3.6 and 4.)	1-11, 13-15, 22, 23, 27-29, 34-38, 45, 46 and 49-54.
X	HOWARD, K. A. et al. "RNA Interference *in Vitro* and *in Vivo* Using a Chitosan/siRNA Nanoparticle System" *Molecular Therapy* **2006**, *14(4)*, 476-484. published online 10 July 2006 (10-07-2006). (see Table 1, B and section entitled "Pulmonary RNA Interference" starting at page 479).	1-5, 6, 10-12, 22, 40-46, and 49-54.
X Y	WO 2008/020318 (HSU, E. et al.) 24 February 2011 (24-02-2011) (see in particular paragraphs [0032] - [0059], [0082][00228] [00263])	1-11 and 49-54 1-46 and 49-54
X Y	WO 2007/059605 A1 (BUSCHMANN, M. et al.) 31 May 2007 (31-05-2007) (see Tables 1 and 2, paragraphs [0047], [0066] - [0078] and claims 20 and 28)	1-11 and 49-54 1-46 and 49-54

[X] Further documents are listed in the continuation of Box C. [X] See patent family annex.

* Special categories of cited documents :
"A" document defining the general state of the art which is not considered to be of particular relevance
"E" earlier application or patent but published on or after the international filing date
"L" document which may throw doubts on priority claim(s) or which is cited to establish the publication date of another citation or other special reason (as specified)
"O" document referring to an oral disclosure, use, exhibition or other means
"P" document published prior to the international filing date but later than the priority date claimed
"T" later document published after the international filing date or priority date and not in conflict with the application but cited to understand the principle or theory underlying the invention
"X" document of particular relevance; the claimed invention cannot be considered novel or cannot be considered to involve an inventive step when the document is taken alone
"Y" document of particular relevance; the claimed invention cannot be considered to involve an inventive step when the document is combined with one or more other such documents, such combination being obvious to a person skilled in the art
"&" document member of the same patent family

Date of the actual completion of the international search	Date of mailing of the international search report
19 July 2012 (19-07-2012)	31 July 2012 (31-07-2012)

Name and mailing address of the ISA/CA	Authorized officer
Canadian Intellectual Property Office Place du Portage I, C114 - 1st Floor, Box PCT 50 Victoria Street Gatineau, Quebec K1A 0C9 Facsimile No.: 001-819-953-2476	Owen Terreau (819) 934-6370

C (Continuation). DOCUMENTS CONSIDERED TO BE RELEVANT

Category*	Citation of document, with indication, where appropriate, of the relevant passages	Relevant to claim No.
Y	CA 2 644 347 A1 (WENGEL, J. et al.) 27 September 2007 (27-09-2007) (see page 22 and claims 20 and 28)	1-12, 16-17, 22-26, 30-39, 45, 46 and 49-54.
Y	EP 1 816 194 (TAKAGI, M. et al.) 18 February 2009 (18-02-2009) (see entire document)	1-12, 18-20, 22, 23, 34-39, 45, 46 and 49-54.
Y	US 2005/0153914 A1 (MCSWIGGEN, J. et al.) 14 July 2005 (14-07-2005) (see entire document)	1-12, 21- 23, 34-39, 45, 46 and 49-54.

INTERNATIONAL SEARCH REPORT

International application No.
PCT/CA2012/050342

Box No. II Observations where certain claims were found unsearchable (Continuation of item 2 of the first sheet)

This international search report has not been established in respect of certain claims under Article 17(2)(a) for the following reasons :

1. [X] Claim Nos. : 47, 48 and 55-96

because they relate to subject matter not required to be searched by this Authority, namely :

Claims 47, 48 and 55-96 are directed to methods of treatment of the human or animal body by surgery or therapy which the International Search Authority is not required to search. However, this Authority has carried out a search based on the alleged effects or purposes/uses of the products defined in the claims.

2. [ ] Claim Nos. :

because they relate to parts of the international application that do not comply with the prescribed requirements to such an extent that no meaningful international search can be carried out, specifically :

3. [ ] Claim Nos. :

because they are dependent claims and are not drafted in accordance with the second and third sentences of Rule 6.4(a).

Box No. III Observations where unity of invention is lacking (Continuation of item 3 of first sheet)

This International Searching Authority found multiple inventions in this international application, as follows :

1. [ ] As all required additional search fees were timely paid by the applicant, this international search report covers all searchable claims.

2. [ ] As all searchable claims could be searched without effort justifying additional fees, this Authority did not invite payment of additional fees.

3. [ ] As only some of the required additional search fees were timely paid by the applicant, this international search report covers only those claims for which fees were paid, specifically claim Nos. :

4. [ ] No required additional search fees were timely paid by the applicant. Consequently, this international search report is restricted to the invention first mentioned in the claims; it is covered by claim Nos. :

Remark on Protest

[ ] The additional search fees were accompanied by the applicant's protest and, where applicable, the payment of a protest fee.

[ ] The additional search fees were accompanied by the applicant's protest but the applicable protest fee was not paid within the time limit specified in the invitation.

[ ] No protest accompanied the payment of additional search fees.

INTERNATIONAL SEARCH REPORT
Information on patent family members

International application No.
PCT/CA2012/050342

Patent document Cited in Search report	Publication Date	Patent Family Member(s)	Publication Date
WO2008020318	24-02-2011	NZ571965 A	24-02-2012
		CN102164618 A	24-08-2011
		US20110171276 A1	14-07-2011
		US20110171314 A1	14-07-2011
		EP2034954 A2	18-03-2009
		AU2007285472 A1	21-02-2008
WO2007059605 A1	31-05-2007	US2009075383 A1	19-03-2009
		EP1948810 A1	30-07-2008
		CA2628313 A1	31-05-2007
CA2644347 A1	27-09-2007	US2009182136 A1	16-07-2009
		JP2009530319 A	27-08-2009
		EP2002004 A2	17-12-2008
		EA200870366 A1	28-04-2009
		WO2007107162 A2	27-09-2007
		AU2007229161 A1	27-09-2007
EP1816194	18-02-2009	JP2012005486 A	12-01-2012
		JP4809240B2 B2	09-11-2011
		KR20070088706 A	29-08-2007
		US20090215867 A1	27-08-2009
		WO2006054625 A1	26-05-2006
US20050153914 A1	14-07-2005	- -	

(19)中华人民共和国国家知识产权局

(12)发明专利申请

(10)申请公布号 CN 103889457 A
(43)申请公布日 2014.06.25

(21)申请号 201280036662.3
(22)申请日 2012.05.24
(30)优先权数据
61/489,302 2011.05.24 US
61/489,306 2011.05.24 US
(85)PCT国际申请进入国家阶段日
2014.01.23
(86)PCT国际申请的申请数据
PCT/CA2012/050342 2012.05.24
(87)PCT国际申请的公布数据
WO2012/159215 EN 2012.11.29
(71)申请人 波利威乐赞助有限公司
地址 加拿大魁北克
(72)发明人 阿卜杜拉扎克·马尔祖基
迈克尔·D·布施曼
(74)专利代理机构 北京康信知识产权代理有限责任公司 11240
代理人 余刚 张英
(51)Int.Cl.
A61K 47/36(2006.01)
A61K 31/713(2006.01)
A61P 3/10(2006.01)
A61P 35/00(2006.01)
A61P 9/10(2006.01)

权利要求书6页 说明书35页
序列表4页 附图17页

(54)发明名称

使用特异性的基于壳聚糖的纳米复合物用于有效并安全递送 siRNA 的组合物和方法

(57)摘要

公开了通过使用壳聚糖的非病毒递送系统的特定制剂用于在体内和体外将治疗性的 RNAi 诱导性核酸有效递送至细胞的组合物和方法。具体地，组合物包含核酸和具有以下理化性质的特定的壳聚糖：数均分子量在 5kDa 至 200kDa 之间、去乙酰化程度在 80% 至 95% 之间、并且壳聚糖胺与核酸磷酸酯之比小于 20。

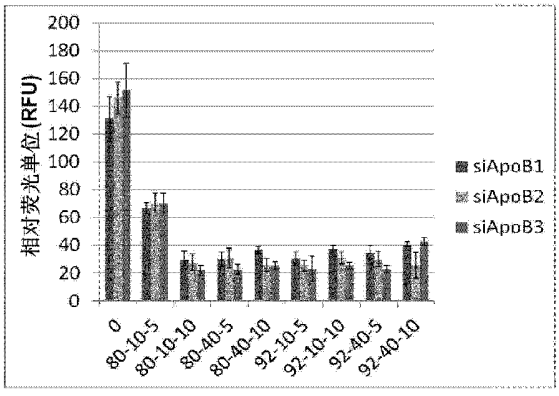

CN 103889457 A

1. 一种用于抑制体内基因表达的组合物，包含壳聚糖和抗所述基因的 RNAi 诱导性核酸序列，其中，所述壳聚糖具有 5kDa 至 200kDa 的分子量（Mn）、80% 至 95% 的去乙酰化程度（DDA），并且其中壳聚糖胺与核酸磷酸酯的比（N:P）小于 20。

2. 根据权利要求 1 所述的组合物，其中，所述壳聚糖的分子量为 5 至 15kDa、DDA 为 90 至 95% 并且 N:P 比为 2 至 10。

3. 根据权利要求 1 或 2 所述的组合物，其中，所述壳聚糖的分子量为 10kDa、DDA 为 92% 并且 N:P 比为 5。

4. 根据权利要求 1 所述的组合物，其中，所述壳聚糖的分子量为 10kDa、40kDa、80kDa、150kDa 或者 200kDa。

5. 根据权利要求 1 至 4 中任一项所述的组合物，其中所述壳聚糖包含乙酰基的嵌段分布或者化学修饰。

6. 根据权利要求 1 至 5 中任一项所述的组合物，其中，所述壳聚糖具有在 1.0 至 7.0 之间的多分散性。

7. 根据权利要求 1 至 6 中任一项所述的组合物，其中，所述 RNAi 诱导性核酸序列是 10 至 50 之间个核苷酸的双链线形脱氧核糖核酸序列或核糖核酸序列。

8. 根据权利要求 1 至 7 中任一项所述的组合物，其中，所述 RNAi 诱导性核酸序列是脱氧核糖核酸序列或核糖核酸序列的发卡结构。

9. 根据权利要求 1 至 8 中任一项所述的组合物，其中，在糖主链、磷酸酯主链和 / 或核苷酸碱基环上化学修饰所述 RNAi 诱导性核酸序列。

10. 根据权利要求 1 至 9 中任一项所述的组合物，其中，所述 RNAi 诱导性核酸序列是短干扰 RNA、短发夹 RNA 或者 RNAi 诱导载体。

11. 根据权利要求 1 至 10 中任一项所述的组合物，其中，所述 RNAi 诱导性核酸序列靶向参与 II 型糖尿病、动脉粥样硬化或癌症的发病机理的基因。

12. 根据权利要求 1 至 10 中任一项所述的组合物，其中，所述 RNAi 诱导性核酸序列靶向参与肿瘤发展、转移或诱导化疗耐药的基因。

13. 根据权利要求 1 至 11 中任一项所述的组合物，其中，所述 RNAi 诱导性核酸序列靶向糖调节蛋白。

14. 根据权利要求 13 所述的组合物，其中，所述糖调节蛋白是肠泌素降解酶。

15. 根据权利要求 13 所述的组合物，其中，所述肠泌素降解酶是二肽基肽酶 -IV（DPP-IV）。

16. 根据权利要求 1 至 11 中任一项所述的组合物，其中，所述 RNAi 诱导性核酸序列靶向致动脉粥样化蛋白。

17. 根据权利要求 16 所述的组合物，其中，所述致动脉粥样化蛋白为载脂蛋白 B（ApoB）、载脂蛋白 E（ApoE）、载脂蛋白 B100（ApoB100）、载脂蛋白 B48（ApoB48）、中性粒细胞明胶酶相关脂质运载蛋白（NGAL）、基质金属蛋白酶 -9（MMP-9）或胆固醇酯运转蛋白（CETP）。

18. 根据权利要求 1 至 12 中任一项所述的组合物，其中，所述 RNAi 诱导性核酸序列靶向解旋酶蛋白、RNA 解旋酶、P68、DDX5、DDX32、DDX1、Akt、PKB、ABC 转运子成员、MDR1、MRP、RAS 蛋白家族成员、SRC、HER2、EGFR、Abl 或 Raf。

19. 根据权利要求 18 所述的组合物，其中，所述解旋酶蛋白是解旋酶 RecQ 家族成员。

20. 根据权利要求 18 或 19 所述的组合物，其中，所述解旋酶蛋白是 RecQL1DNA 解旋酶。

21. 根据权利要求 18 所述的合成物，其中，所述 RNAi 诱导性核酸序列靶向 MDR1。

22. 一种根据权利要求 1 至 21 中任一项所限定的组合物，用于治疗患者中糖尿病及其相关病症、动脉粥样硬化及其相关病症或癌症及其相关病症。

23. 根据权利要求 22 所述的组合物，其中，所述糖尿病和相关病症是胰岛素依赖性糖尿病（I 型糖尿病）、非胰岛素依赖性糖尿病（II 型糖尿病）、胰岛素耐受、高胰岛素血症、糖尿病引起的高血压、肥胖症、血管的损伤、眼的损伤、肾的损伤、神经的损伤、自主神经系统的损伤、皮肤的损伤、结缔组织的损伤和免疫系统的损伤。

24. 根据权利要求 22 所述的组合物，其中，所述动脉粥样硬化相关病症是心血管疾病。

25. 根据权利要求 24 所述的组合物，其中所述心血管疾病是冠心病、急性冠状动脉综合征或心绞痛。

26. 根据权利要求 22 至 25 中任一项所述的组合物，其中，所述组合物降低 ApoB 血浆水平。

27. 根据权利要求 22 至 25 中任一项所述的组合物，其中，所述组合物提高 GLP-1 的生物利用度。

28. 根据权利要求 22 至 27 中任一项所述的组合物，所述组合物还提高对所述患者中的葡萄糖代谢的控制。

29. 根据权利要求 22 至 28 中任一项所述的组合物，所述组合物还降低所述患者中的血糖水平。

30. 根据权利要求 22 至 29 中任一项所述的组合物，所述组合物还降低患者中的胆固醇水平。

31. 根据权利要求 22 至 30 中任一项所述的组合物，所述组合物还降低所述患者中的低密度脂蛋白水平。

32. 根据权利要求 22 至 31 中任一项所述的组合物，其中，所述组合物还降低所述患者中的体重增加。

33. 根据权利要求 22 至 32 中任一项所述的组合物，其中，所述组合物将 ApoB 血浆水平降低至少 35%，并且将 LDL/VLDL 胆固醇水平降低至少 20%。

34. 根据权利要求 22 至 32 中任一项所述的组合物，还包含胰岛素、葡萄糖苷酶抑制剂、磺酰脲、DPP-IV 抑制剂或降血糖化合物。

35. 根据权利要求 22 至 34 中任一项所述的组合物，配制用于与适合的递送药剂、胰岛素或降血糖化合物同时给予。

36. 根据权利要求 35 所述的组合物，其中，所述适合的递送药剂是 Mirus Transit TKO® 亲脂性试剂、Lipofectin® 、Lipofectamine™、Cellfectin®、聚阳离子或脂质体。

37. 根据权利要求 35 所述的组合物，其中，所述降血糖化合物是二甲双胍、阿卡波糖、醋酸己脲、格列美脲、妥拉磺脲、格列吡嗪、格列本脲、甲苯磺丁脲、氯磺丙脲、噻唑烷二酮类、麦芽糖酶抑制剂、双胍衍生物、曲格列酮或它们的混合物。

38. 根据权利要求 34 所述的组合物，其中，所述磺酰脲是甲磺丁脲、妥拉磺脲、格列派

特、格列美脲或格列波脲。

39. 根据权利要求 34 所述的组合物，其中，所述 DPP-IV 抑制剂是西他列汀、维达列汀或沙格列汀。

40. 根据权利要求 22 所述的组合物，其中，所述癌症是乳腺癌、神经胶质瘤、大肠癌、肺癌、小细胞肺癌、胃癌、肝癌、血癌、骨癌、胰癌、皮肤癌、头颈癌、皮肤或眼内黑素瘤、子宫肉瘤、卵巢癌、直肠或结直肠癌、肛门癌、结肠癌、输卵管癌、子宫内膜癌、宫颈癌、外阴癌、鳞状细胞癌、阴道癌、霍奇金氏病、非霍奇金氏淋巴瘤、食道癌、小肠癌、内分泌癌、甲状腺癌、甲状旁腺癌、肾上腺癌、软组织肿瘤、尿道癌、阴茎癌、前列腺癌、慢性或急性白血病、淋巴细胞性淋巴瘤、膀胱癌、肾癌、输尿管癌、肾细胞癌、肾盂癌、CNS 肿瘤、神经胶质瘤、星形细胞瘤、多形性胶质母细胞瘤、原发性 CNS 淋巴瘤、骨髓瘤、脑干神经胶质瘤、垂体腺瘤、葡萄膜黑素瘤、睾丸癌、口腔癌、咽癌、小儿赘生物、白血病、成神经细胞瘤、成视网膜细胞瘤、神经胶质瘤、成横纹肌细胞瘤或肉瘤。

41. 根据权利要求 22 或 40 所述的组合物，配制用于与适合的递送药剂和抗癌化合物中的至少一种同时给予。

42. 根据权利要求 41 所述的组合物，其中，所述适合的递送药剂是 Mirus Transit TKO® 亲脂性试剂、Lipofectin® 、Lipofectamine™、Cellfectin®、聚阳离子或脂质体。

43. 根据权利要求 22 和 41 至 42 中任一项所述的组合物，配制用于在适合的抗癌疗法期间同时给予。

44. 根据权利要求 43 所述的组合物，其中，所述抗癌疗法是手术操作、化疗、激素疗法和局部辐射中的至少一种。

45. 根据权利要求 1 至 44 中任一项所述的组合物，其中，配制所述组合物用于以 1mg/kg 的剂量注射。

46. 根据权利要求 1 至 45 中任一项所述的组合物，其中，当给予时，所述组合物不引起肝脏毒性。

47. 一种用于将核酸序列递送至细胞中的方法，包括将根据权利要求 1 至 46 中任一项所述的组合物与所述细胞接触的步骤。

48. 根据权利要求 47 所述的方法，其中，所述细胞是原代细胞、转化细胞或永生化细胞。

49. 一种产生用于治疗糖尿病、动脉粥样硬化或癌症的组合物的方法，包括在酸性介质中混合壳聚糖和 RNAi 诱导性核酸序列，其中，所述壳聚糖具有 5kDa 至 200kDa 的分子量(Mn)、80% 至 95% 的去乙酰化程度(DDA)，并且其中壳聚糖胺与核酸磷酸酯的比值(N:P)低于 20。

50. 根据权利要求 49 所述的方法，其中，将所述壳聚糖在与所述 RNAi 诱导性核酸序列混合前溶解在盐酸中。

51. 根据权利要求 50 所述的方法，其中，以 1:1 的葡萄糖胺 :HCl 比值溶解所述壳聚糖。

52. 根据权利要求 49 至 51 中任一项所述的方法，其中，所述壳聚糖的 Mn 是 10kDa、DDA 是 80% 或 92%，并且其中所述壳聚糖胺与核酸磷酸酯的比值(N:P)为 5 或 10。

53. 根据权利要求 49 至 52 中任一项所述的方法，其中，混合壳聚糖与所述 RNAi 诱导性

核酸序列产生尺寸小于 200nm 的球形纳米颗粒。

54. 根据权利要求 53 所述的方法，其中，所述纳米颗粒的尺寸为 45 至 156nm。

55. 一种用于治疗患者中糖尿病、动脉粥样硬化或癌症的方法，包括向所述患者给予有效量的包含壳聚糖和 RNA 诱导性核酸序列的组合物，其中，所述壳聚糖具有 5kDa 至 200kDa 的分子量（Mn）、80% 至 95% 的去乙酰化程度（DDA），并且其中所述壳聚糖胺与核酸磷酸酯的比值（N:P）低于 20。

56. 根据权利要求 55 所述的方法，其中，所述壳聚糖的分子量为 5 至 15kDa、DDA 为 90 至 95% 并且 N:P 比为 2 至 10。

57. 根据权利要求 55 所述的方法，其中，所述壳聚糖的分子量为 10kDa、DDA 为 92% 并且 N:P 比为 5。

58. 根据权利要求 55 所述的方法，其中，所述壳聚糖的分子量为 10kDa、40kDa、80kDa、150kDa 或者 200kDa。

59. 根据权利要求 55 所述的方法，其中，所述壳聚糖包含乙酰基团的嵌段分布或者化学修饰。

60. 根据权利要求 55 所述的方法，其中，所述壳聚糖具有在 1.0 至 7.0 之间的多分散性。

61. 根据权利要求 55 所述的方法，其中，所述 RNAi 诱导性核酸序列是 10 至 50 之间个核苷酸的双链线形脱氧核糖核酸序列或核糖核酸序列。

62. 根据权利要求 55 所述的方法，其中，所述 RNAi 诱导性核酸序列是脱氧核糖核酸序列或核糖核酸序列的发卡结构。

63. 根据权利要求 55 所述的方法，其中，在所述糖主链、磷酸酯主链和 / 或核苷酸碱基环上化学修饰 RNAi 诱导性核酸序列。

64. 根据权利要求 55 所述的方法，其中，所述 RNAi 诱导性核酸序列是短干扰 RNA、短发夹 RNA 或者 RNAi 诱导载体。

65. 根据权利要求 55 所述的方法，其中，所述 RNAi 诱导性核酸序列靶向参与 II 型糖尿病、动脉粥样硬化或癌症的发病机理的基因。

66. 根据权利要求 55 所述的方法，其中，所述 RNAi 诱导性核酸序列靶向参与肿瘤发展、转移或化疗耐药诱导的基因。

67. 根据权利要求 55 所述的方法，其中，所述 RNAi 诱导性核酸序列靶向糖调节蛋白。

68. 根据权利要求 67 所述的方法，其中，所述糖调节蛋白是肠泌素降解酶。

69. 根据权利要求 68 所述的方法，其中，所述肠泌素降解酶是二肽基肽酶 -IV（DPP-IV）。

70. 根据权利要求 55 所述的方法，其中，所述 RNAi 诱导性核酸序列靶向致动脉粥样化蛋白。

71. 根据权利要求 70 所述的方法，其中所述致动脉粥样化蛋白为载脂蛋白 B（ApoB）、载脂蛋白 E（ApoE）、载脂蛋白 B100（ApoB100）、载脂蛋白 B48（ApoB48）、中性粒细胞明胶酶相关脂质运载蛋白（NGAL）、基质金属蛋白酶 -9（MMP-9）或胆固醇酯运转蛋白（CETP）。

72. 根据权利要求 55 所述的方法，其中，所述 RNAi 诱导性核酸序列靶向解旋酶蛋白、RNA 解旋酶、P68、DDX5、DDX32、DDX1、Akt、PKB、ABC 转运子成员、MDR1、MRP、RAS 蛋白家族成

员、SRC、HER2、EGFR、Abl 或 Raf。

73. 根据权利要求 72 所述的方法，其中，所述解旋酶蛋白是解旋酶 RecQ 家族成员。

74. 根据权利要求 72 所述的组合物，其中，所述解旋酶蛋白是 RecQL1DNA 解旋酶。

75. 根据权利要求 55 所述的方法，其中，所述 RNAi 诱导性核酸序列靶向 MDR1。

76. 根据权利要求 55 所述的方法，其中，所述组合物降低 ApoB 血浆水平。

77. 根据权利要求 55 所述的方法，其中，所述组合物提高 GLP-1 的生物利用度。

78. 根据权利要求 55 所述的方法，所述组合物还提高所述患者中的葡萄糖代谢的控制。

79. 根据权利要求 55 所述的方法，所述组合物还降低所述患者中的血糖水平。

80. 根据权利要求 55 所述的方法，所述组合物还降低患者中的胆固醇水平。

81. 根据权利要求 55 所述的方法，所述组合物还降低所述患者中的低密度脂蛋白水平。

82. 根据权利要求 55 所述的方法，其中，所述组合物还降低所述患者中的体重增加。

83. 根据权利要求 55 所述的方法，其中，所述组合物将 ApoB 血浆水平降低至少 35%，并且将 LDL/VLDL 胆固醇水平降低至少 20%。

84. 根据权利要求 55 所述的方法，所述组合物还包含胰岛素、葡萄糖苷酶抑制剂、磺酰脲、DPP-IV 抑制剂或降血糖化合物。

85. 根据权利要求 55 所述的方法，所述组合物与适合的递送药剂、胰岛素或降血糖化合物同时给予。

86. 根据权利要求 85 所述的方法，其中，所述适合的递送药剂是 Mirus Transit TKO® 亲脂性试剂、Lipofectin® 、Lipofectamine™、Cellfectin®、聚阳离子或脂质体。

87. 根据权利要求 85 所述的方法，其中，所述降血糖化合物是二甲双胍、阿卡波糖、醋酸己脲、格列美脲、妥拉磺脲、格列吡嗪、格列本脲、甲苯磺丁脲、氯磺丙脲、噻唑烷二酮类、麦芽糖酶抑制剂、双胍衍生物、曲格列酮或它们的混合物。

88. 根据权利要求 84 所述的方法，其中，所述磺酰脲是甲磺丁脲、妥拉磺脲、格列派特、格列美脲或格列波脲。

89. 根据权利要求 34 所述的方法，其中，所述 DPP-IV 抑制剂是西他列汀、维达列汀或沙格列汀。

90. 根据权利要求 55 所述的方法，其中，所述癌症是乳腺癌、神经胶质瘤、大肠癌、肺癌、小细胞肺癌、胃癌、肝癌、血癌、骨癌、胰癌、皮肤癌、头颈癌、皮肤或眼内黑素瘤、子宫肉瘤、卵巢癌、直肠或结直肠癌、肛门癌、结肠癌、输卵管癌、子宫内膜癌、宫颈癌、外阴癌、鳞状细胞癌、阴道癌、霍奇金氏病、非霍奇氏金淋巴瘤、食道癌、小肠癌、内分泌癌、甲状腺癌、甲状旁腺癌、肾上腺癌、软组织肿瘤、尿道癌、阴茎癌、前列腺癌、慢性或急性白血病、淋巴细胞性淋巴瘤、膀胱癌、肾癌、输尿管癌、肾细胞癌、肾盂癌、CNS 肿瘤、神经胶质瘤、星形细胞瘤、多形性胶质母细胞瘤、原发性 CNS 淋巴瘤、骨髓瘤、脑干神经胶质瘤、垂体腺瘤、葡萄膜黑素瘤、睾丸癌、口腔癌、咽癌、小儿赘生物、白血病、成神经细胞瘤、成视网膜细胞瘤、神经胶质瘤、成横纹肌细胞瘤或肉瘤。

91. 根据权利要求 55 所述的方法，所述组合物与适合的递送药剂和抗癌化合物中的至

少一种给予。

92. 根据权利要求 41 所述的方法，其中，所述适合的递送药剂是 Mirus Transit TKO® 亲脂性试剂、Lipofectin® 、Lipofectamine™、Cellfectin®、聚阳离子或脂质体。

93. 根据权利要求 55 所述的方法，所述组合物在适合的抗癌疗法期间同时给予。

94. 根据权利要求 43 所述的方法，其中，所述抗癌疗法是手术操作、化疗、激素疗法和局部辐射中的至少一种。

95. 根据权利要求 55 所述的方法，其中，所述组合物以 1mg/kg 的剂量注射。

96. 根据权利要求 55 所述的方法，其中，当给予时，所述组合物不引起肝脏毒性。

使用特异性的基于壳聚糖的纳米复合物用于有效并安全递送 siRNA 的组合物和方法

[0001] 相关申请的引用

[0002] 本专利申请要求于 2011 年 5 月 24 日提交的美国临时专利申请 US61/489306 和 2011 年 5 月 24 日提交的美国临时专利申请 US61/489302 的优先权，以上专利申请以它们的全部内容并入本文。

技术领域

[0003] 本发明涉及使用特异性的基于壳聚糖的纳米复合物用于有效递送治疗性 RNAi 诱导性核酸的组合物和方法。

背景技术

[0004] 通过 siRNA (短干扰 RNA)的基因沉默是生物学中正在发展的领域并且已逐渐成为具有治疗潜能的新型转录后基因沉默策略。基于人类基因组测序以及对疾病的分子原因的理解，根据意愿消除病原性基因的可能性是治疗多种临床病理(如糖尿病、动脉粥样硬化和癌症)的有吸引力的方法。使用 siRNA，实际上人类基因组中导致疾病的每个基因均服从调控，从而为药物发现提供了机会。然而局部给予 siRNA 已进入了临床 I 期试验，而用于成功全身递送 siRNA 的策略仍处于开发的临床前阶段。

[0005] II 型糖尿病

[0006] II 型糖尿病(T2DM)是具有不同病理表现的进行性代谢病症，并且通常与脂类代谢和糖代谢失调有关(Bell 等人，2001, Nature, 414:788-791)。II 型糖尿病的特征在于在外周组织(如肌肉、脂肪组织和肝脏)中对胰岛素作用的耐受。其特征还在于胰岛 β-细胞分泌胰岛素能力的逐渐丧失。糖尿病的长期影响是其血管并发症、微血管并发症、视网膜病、神经病和肾病的结果。大血管并发症同样与 II 型糖尿病有关，并且包括心血管和脑血管并发症。

[0007] 以下列出了目前已知的抗糖尿病药物的主要类别。双胍是通过抑制肝脏葡萄糖产生、降低肠内吸收并提高外周葡萄糖摄取来帮助控制血糖的一类药物。这类包括二甲双胍(甲福明)，它是降低葡萄糖和血液甘油三酯水平两者的药物。磺酰脲是通过刺激由胰腺 β-细胞的内源胰岛素释放来帮助控制或应对(manage)II 型糖尿病的一类药物。这类包括：甲苯磺丁脲(甲糖宁)、妥拉磺脲(甲磺氮草脲)、格列派特、格列美脲和格列波脲等。糖苷酶抑制剂刺激从胰腺细胞释放胰岛素，从而降低血糖量，并且包括瑞格列奈和那格列奈。

[0008] 不幸的是，即使当组合时，这些治疗方式通常受安全性、耐受性、体重增加、浮肿和胃肠不耐性的限制(Drucker 等人，2010, Nat Rev Drug Discov, 9:267-268；Nauck 等人，2009, Diabetes Care, 32:84-90；Ng 等人，2010, Prim Care Diabetes, 4:61-63；Truitt 等人，2010, Curr Med Res Opin, 26:1321-1331；和 Wajcberg 和 Tavaria, 2009, Expert Opin Pharmacother, 10:135-142)。另外，随着疾病的进展和 β 细胞功能衰退，当前治疗的效力减弱(Turner 等人，1999, JAMA, 281:2005-2012)。

[0009] 肠泌素作用的发现为使用能够以最小副作用来控制 T2DM 的一类治疗剂的治疗提供新的途径。主要通过高血糖素样肽 1（GLP-1）来调节的肠泌素效应（incretin effect），该高血糖素样肽 1 通过刺激胰岛素分泌来调控饭后血糖水平。GLP-1 还具有间接作用，如延缓胃排空、通过对中枢神经系统的影响促进饱腹感、促进 β 细胞生长和抑制 β 细胞凋亡，如在动物模型中所表明的（Nauck 等人，2002, J Clin Endocrinol Metab, 87:1239-1246；和 Creutzfeldt 等人，1996, Diabetes Care, 19:580-586）。然而，由于其被广泛存在的丝氨酸蛋白酶二肽基肽酶 IV（DPP-IV）快速降解，因此 GLP-1 在临床中的潜能受到阻碍。发现 DPP-IV 在 GLP-1 的 N 末端区域切割 His:Ala:Glu 序列使得能够开发 DPP-IV 耐受性 GLP-1 类似物以及开发 DPP-IV 抑制剂。

[0010] DPP-IV 抑制剂是抑制二肽基肽酶 IV 的蛋白质分解活性的新种类的药物。DPP-IV 的蛋白质分解活性降低糖调节肽（称为肠泌素）的血液水平。借此，抑制二肽基肽酶 IV 从而加强这些肠泌素的作用，特别是高血糖素样肽 1（GLP-1）。这些抑制剂包括西他列汀、维达列汀和沙格列汀，并且每天口服给予一次。

[0011] 动脉粥样硬化

[0012] 动脉粥样硬化是由动脉中动脉粥样硬化斑块的形成所引起的慢性疾病。动脉粥样硬化代表多种心血管疾病，如冠心病、急性冠状动脉综合征和心绞痛（Lloyd-Jones 等人，2010, Circulation, 121:e46-e215）。在美国，预计 2010 年动脉粥样硬化的经济成本为 5030 亿美元，主要是由于直接医学成本和间接生产率成本造成的（Lloyd-Jones 等人，2010, Circulation, 121:948-954）。尽管造成动脉粥样硬化的因素仍是未知的，但不断增加的迹象表明了血脂异常、高脂血症和炎症在该疾病的发病机理（pathogenesis）中的作用（Hanson 等人，2006, Nat Rev Immunol, 6:508-519；Montecucco 和 Mach, 2008, Clin Interv Aging, 3:341-349）。目前，由动脉粥样硬化及相关病理—心血管疾病（CVD）—所造成的发病率和致死率的降低主要是 3- 羟基 -3- 甲基戊二酰辅酶 A（HMG-CoA）还原酶抑制剂的侵入性临床应用（通常称为基于抑制素的疗法）的结果（Vermissen 等人，2008, BMJ, 337:a2423）。这些疗法减少了低密度脂蛋白胆固醇（LDL-C）。介入研究已表明当给予降低脂质的疗法时，CVD 发病率和致死率的风险降低。另外，发病率 / 致死率的降低以及 LDL-C 的降低显示出对数线性关系（Law 等人，1994, BMJ, 308:367-372）。

[0013] 降低 LDL-C 并由此降低动脉粥样硬化的替代性方法是抑制或阻断由肝脏分泌的极低密度脂蛋白（VLDL）。可以通过靶向载脂蛋白 B（ApoB）实现这种抑制，这是因为 ApoB 是 VLDL 分泌所必需的（Rutledge 等人，2010, Cell Biol, 88:251-267）。在人类中，主要由肝细胞和肠上皮细胞（entherocyte）表达 ApoB。

[0014] 在人类中，ApoB 基因位于染色体 2（2q）上并跨越 43kb。ApoB mRNA 由 28 个内含子和 29 个外显子组成并且其特征在于 16 小时的半衰期（Ludwig 等人，1987, DNA, 6:363-372；Scott, 1989, Curr Opin Cell Biol, 1:141-1147）。ApoB mRNA 的翻译产生具有 4536 个氨基酸和 517-550kDa 的表观分子量的蛋白质，并因此代表最大的单体蛋白之一。ApoB 抑制作为动脉粥样硬化及其相关 CVD 的替代性疗法的重要性在于 ApoB 通过其 β 折叠域与脂质（如磷脂、胆固醇和胆固醇酯）物理相互作用从而在肝脏中形成大脂蛋白颗粒（即 VLDL）和在肠中形成乳糜微粒的能力（在 Rutledge 等人，2010, Biochem Cell Biol, 88:251-267 中综述）。

[0015] 癌症

[0016] 经典的癌症疗法包括使用一种或几种化疗药物。由于它们的非特异性，这些治疗方式与毒性和严重的副作用有关。与化疗有关的另一个主要问题是化疗耐药随时间的发展。例如，对化疗的耐受性是与乳腺癌的控制相关的主要问题。

[0017] 癌细胞采用多种机制以获得对一种或多种化疗剂的耐受性。耐药性的主要机制包括(1)可溶性药物的降低的胞内摄取，(2)改变药物造成所需细胞损伤的能力的细胞遗传和表型变化，和(3)通过细胞表面转运体的提高的药物排出，导致多种药物耐受性(MDR)。在所有这些情况下，对单一化疗实体的耐受性总是与抗其他化疗剂的广泛耐药性类型有关。

[0018] 最常见的和研究的耐受性机制之一是通过在药物到达作用位点之前将其泵出细胞的转运蛋白使胞内药物浓度降低，从而所述细胞适应低药物浓度而不会经历药物诱导的细胞死亡。这些转运体中的大多数在 ATP- 结合盒跨膜蛋白超家族中。

[0019] 在人类中，到目前为止已识别出 48 个 ABC 基因(ATP- 结合盒家族中的基因)。在乳腺癌中，实际上到目前为止所报道的所有 MDR 耐受性均与下列之一密切相关 :p- 糖蛋白(P-gp)、多药耐受性相关蛋白(MRP)和乳腺癌耐药蛋白(BCRP)。

[0020] 在多种癌组织中，P-gp 是参与药物的 ATP 依赖性流出的最常见的蛋白。一段时间内，相信过表达 P-gp 是能够在哺乳动物肿瘤细胞中赋予 MDR 的唯一蛋白。在乳腺癌中，52% 的化疗患者的 P-gp 由于疗法而上调。编码 P-gp 的基因称为 ABCB1 (mdr1)并且位于染色体 7 的位置 q21.12 处。ABCB1 由 28 个外显子组成，其产物产生 1.2kb 的 mRNA。P-gp 的蛋白质序列分析显示存在两个胞外域，每个域含有 6 个推定跨膜区段和 ATP 结合共有基序。

[0021] 此外，参与维持基因组完整性和稳定性的一类感兴趣的酶是 DNA 解旋酶。这些蛋白质通过 ATP 依赖性机制在 DNA 复制、修复、重组和转录中起到重要作用，所述机制将双螺旋基因组链解开，从而使得修复机构能够接近受损或错配的 DNA。

[0022] 例如，解旋酶的 RecQ 家族已显示在重组、修复和 Holliday 接合点形成中起到重要作用。最近，这些解旋酶已涉及转录后基因沉默过程(Cogoni 和 Macino, 1999, Science, 286:2342-2344)。在该过程中，在可以起始任何杂交和沉默机制前，需要解旋酶来分离双链 DNA。对该家族蛋白已提出了其他作用。例如，据信 RecQL.1 在核蛋白输送中起作用，这是因为它与起核定位信号作用的 QIP1 和 QIP2 蛋白两者相互作用，如在两种杂交筛选中所显示的(Seki 等人, 1997, 234:48-53)。

[0023] RecQ 家族由 5 个成员组成，并且根据它们是否含有另外的羧基末端基团或氨基末端基团可以将其分为两组。这些基因中的突变导致癌症发病率提高以及其他生理异常(Karow 等人, 2000, Curr Opin Genet Dev, 10:32-38 ;Kawabe 等人, 2000, Oncogene, 19:4767-4772)。这些异常包括布卢姆氏综合征(BLM)、韦耳纳氏综合征(WRN)和 Rothmund-Thompson 综合征(RecQ4)。人 RecQL.1 基因是该家族中第一个识别的人成员，并且显示与大肠杆菌(E.coli)DNA 解旋酶 RecQ 具有广泛的同源性，并且位于染色体 12p11 上(Puranam 和 Blackshear, 1994, J Biol Chem, 269:29838-29845 ;Puranam 等人, 1995, Genomics, 26:595-598)。

[0024] 据信在癌性细胞系(如 AsPC1、A549 和 LS174T 等)中促使 RecQL.1 过表达以补偿这些癌性细胞中的高重组率，从而防止细胞凋亡(Futami 等人, 2008, Cancer Sci, 99:71-80)。在这些细胞系中或者在鼠异种移植模型中，使用特异性 siRNA 使

RecQL.1 基因沉默导致癌性细胞死亡的增加和肿瘤块的减小(Futami 等人,2008,Cancer Sci,99:71-80)。

[0025] 参与维持体内平衡稳定性和功能完整性的另一类酶是 RNA 解旋酶。这些酶的特征在于存在中央定位的“解旋酶域”,其由 8 个保守基序组成。基于这些基序,将 RNA 解旋酶分为不同家族。需要这些保守基序来进行 NTP 水解和 RNA 解旋(RNA unwinding)功能(Linder 等人,2001,Trends Biochem Sci.,26:339-341;Tanner 和 Linder,2001,Mol Cell,8:251-262)。与 RNA 解旋酶有关的另一个功能是破坏 RNA- 蛋白质相互作用(Jankowsky 等人,2001,Science,291:121-125)。这些酶是可以调节它们的 NTP 酶和解旋酶活性的分子复合物的成员(Silverman 等人,2003,Gene,312:1-16)。在转录后事件中这些解旋酶的固有特征起到重要作用,因为调节 RNA 二级结构调控了如剪接(Balvay 等人,1993,Bioessays,15:165-169)和翻译(van der Velden 和 Thomas,1999,Int J Biochem Cell Biol,31:87-106)等步骤。

[0026] RNA 加工分子(如 RNA 解旋酶)的调节异常已涉及人类病理和癌症发展。涉及人类病理的这些解旋酶的实例包括 DDX1/5/6/9/10 和 DHX32 等(Abdelhaleem,2004,Anticancer Res,2004,24:3951-3953;Abdelhaleem,2004,Biocim Biophys Acta,1704:37-46)。这些解旋酶含有特征性 DEAD 盒结构域并且在大多数癌症中上调(Abdelhaleem,2004,Anticancer Res,2004,24:3951-3953;Abdelhaleem,2004,Biocim Biophys Acta,1704:37-46)。

[0027] 目前,仍需要提供通过保持 siRNA 体内递送的替代性疗法。具体地,非常期望提供用于治疗 II 型糖尿病、动脉粥样硬化和癌症的替代性方法。

发明内容

[0028] 本发明的一个目标是提供包含壳聚糖和 RNA 诱导性核酸序列的组合物,其中所述壳聚糖具有 5kDa 至 200kDa 的分子量(Mn),80% 至 95% 去乙酰化程度(DDA),并且其中壳聚糖胺与核酸磷酸酯(nucleic acid phosphate)的比值(N:P)低于 20。

[0029] 本发明的另一个目标是提供如本文所述用于治疗患者中糖尿病、动脉粥样硬化或癌症和 / 或相关病症的组合物。

[0030] 根据本发明,提供了产生用于治疗糖尿病、动脉粥样硬化或癌症和 / 或相关病症的组合物的方法,其包括在酸性介质中混合壳聚糖和 RNA 诱导性核酸序列,其中壳聚糖具有 5kDa 至 200kDa 的分子量(Mn),80% 至 95% 的去乙酰化程度(DDA),并且其中壳聚糖胺与核酸磷酸酯的比值(N:P)低于 20。

[0031] 根据本发明,还提供了如本文所限定的组合物用于治疗患者中糖尿病、动脉粥样硬化或癌症和 / 或相关病症的应用;或者在制造用于治疗患者中糖尿病、动脉粥样硬化或癌症和 / 或相关病症的药物中的应用。

[0032] 本发明的一个目标是提供如本文所描述用于治疗患者中的癌症或逆转化疗耐药(chemoresistance)或两者的组合的组合物。根据本发明,提供了产生用于治疗癌症或者使化疗耐药癌症对经典化疗敏感或两者均有的组合物的方法。

[0033] 本发明的另一个目标是提供治疗患者中糖尿病、动脉粥样硬化或癌症和 / 或相关病症的方法,其包括向患者给予有效量的如本文所限定的组合物,更具体地是包含壳聚糖和 RNA 诱导性核酸序列的组合物,其中所述壳聚糖具有 5kDa 至 200kDa 的分子量(Mn)、80%

至 95% 的去乙酰化程度(DDA),并且其中壳聚糖胺与核酸磷酸酯的比值(N:P)低于 20。

[0034] 还提供了用于将核酸序列递送到细胞中的方法,包括使本文所描述的组合物与细胞接触的步骤。

[0035] 在一个实施方式中,壳聚糖的分子量为 5 至 15kDa,DDA 为 90 至 95%,并且 N:P 比为 2 至 10 ;优选地,壳聚糖的分子量为 10kDa,DDA 为 92% 并且 N:P 比为 5。

[0036] 在其他实施方式中,壳聚糖的分子量为 10kDa、40kDa、80kDa、150kDa 或者 200kDa。

[0037] 在另一个实施方式中,壳聚糖包含嵌段分布的乙酰基基团或者化学修饰。

[0038] 在其他实施方式中,壳聚糖具有在 1.0 至 7.0 之间的多分散性。

[0039] 在其他实施方式中,RNA 诱导性核酸序列为 10 至 50 之间个核苷酸的双链线形脱氧核糖核酸序列 ;RNA 诱导性核酸序列为 10 至 50 之间个核苷酸的双链线形核糖核酸序列 ;RNA 诱导性核酸序列为脱氧核糖核酸序列或核糖核酸序列的发卡结构 ;和 / 或 RNA 诱导性核酸序列为短干扰 RNA、短发夹 RNA 或 RNAi 诱导载体。

[0040] 在另一个实施方式中,在糖主链、磷酸酯主链和 / 或核苷酸碱基环上化学修饰 RNAi 诱导性核酸序列。

[0041] 优选地,RNA 诱导性核酸序列靶向参与 II 型糖尿病、动脉粥样硬化或者癌症发病机理的基因 ;如,例如,参与肿瘤发展、转移或者化疗耐药的诱导或获得的基因,糖调控蛋白或致动脉粥样化蛋白 ;如,例如,肠泌素降解酶 ;如,例如,二肽基肽酶 -IV (DPP-IV);如,例如,载脂蛋白 B (ApoB)、载脂蛋白 E (ApoE)、载脂蛋白 B100 (ApoB100)、载脂蛋白 B48 (ApoB48)、中性粒细胞明胶酶相关脂质运载蛋白(NGAL)、基质金属蛋白酶 -9 (MMP-9)或胆固醇酯运转蛋白(CETP)。

[0042] 在另一个实施方式中,RNAi 诱导性核酸序列靶向解旋酶蛋白、RNA 解旋酶、P68、DDX5、DDX32、DDX1、Akt、PKB、ABC 转运子成员、MDR1、MRP、RAS 蛋白家族成员、SRC、HER2、EGFR、Abl 或 Raf。

[0043] 在另一个实施方式中,解旋酶蛋白是解旋酶 RecQ 家族成员,如,例如,RecQL.1DNA 解旋酶。另外,RNAi 诱导性核酸序列靶向 MDR1。

[0044] 在另一个实施方式中,糖尿病相关病症为胰岛素依赖性糖尿病(I 型糖尿病)、非胰岛素依赖性糖尿病(II 型糖尿病)、胰岛素耐受、高胰岛素血症、糖尿病诱导的高血压、肥胖症、血管损伤、眼损伤、肾损伤、神经损伤、自律神经系统损伤、皮肤损伤、结缔组织损伤和免疫系统损伤。

[0045] 在其他实施方式中,动脉粥样硬化相关病症为心血管疾病,如,例如,冠心病、急性冠状动脉综合征或心绞痛。

[0046] 在另一个实施方式中,组合物降低 ApoB 血浆水平 ;提高 GLP-1 的生物利用度 ;提高对患者中葡萄糖代谢的控制 ;降低患者中的血糖水平 ;降低患者中的胆固醇水平 ;降低患者中的低密度脂蛋白水平 ;和 / 或降低患者中的体重增加。

[0047] 在其他实施方式中,组合物使 ApoB 血浆水平降低至少 35% 并且使 LDL/VLDL 胆固醇水平降低至少 20%。

[0048] 在另一个实施方式中,配制组合物用于皮下给予、肌内给予、静脉内给予、皮内给予、乳房内给予、腹膜内给予、口服给予或胃肠给予。

[0049] 在具体的实施方式中,配制组合物用于以 1mg/kg 的剂量注射。

[0050] 在另一个实施方式中，本文所描述的组合物可以包含胰岛素、葡萄糖苷酶抑制剂、磺酰脲、DPP-IV 抑制剂或降血糖化合物。

[0051] 还可以配制本文所描述的组合物用于与适合的递送药剂、胰岛素或降血糖化合物同时给予；如，递送药剂为 Mirus Transit TKO® 亲脂性试剂、lipofectin®、lipofectamine™、cellfectin®、聚阳离子或脂质体；或者这类降血糖化合物为二甲双胍、阿卡波糖、醋酸己脲、格列美脲、妥拉磺脲、格列吡嗪、格列本脲、甲苯磺丁脲、氯磺丙脲、噻唑烷二酮、麦芽糖酶抑制剂、双胍衍生物、曲格列酮或其混合物；这类磺酰脲为甲磺丁脲、妥拉磺脲、格列派特、格列美脲或格列波脲；这类 DPP-IV 抑制剂为西他列汀、维达列汀或沙格列汀。

[0052] 在一个实施方式中，癌症为乳腺癌、神经胶质瘤、大肠癌、肺癌、小细胞肺癌、胃癌、肝癌、血癌、骨癌、胰癌、皮肤癌、头颈癌、皮肤或眼内黑素瘤、子宫肉瘤、卵巢癌、直肠或结直肠癌、肛门癌、结肠癌、输卵管癌、子宫内膜癌、宫颈癌、外阴癌、鳞状细胞癌、阴道癌、霍奇金氏病、非霍奇金氏淋巴瘤、食道癌、小肠癌、内分泌癌、甲状腺癌、甲状旁腺癌、肾上腺癌、软组织肿瘤、尿道癌、阴茎癌、前列腺癌、慢性或急性白血病、淋巴细胞性淋巴瘤、膀胱癌、肾癌、输尿管癌、肾细胞癌、肾盂癌、CNS 肿瘤、神经胶质瘤、星形细胞瘤、多形性胶质母细胞瘤、原发性 CNS 淋巴瘤、骨髓肿瘤、脑干神经胶质瘤、垂体腺瘤、葡萄膜黑素瘤、睾丸癌、口腔癌、咽癌、小儿肿瘤、白血病、成神经细胞瘤、成视网膜细胞瘤、神经胶质瘤、成横纹肌细胞瘤或肉瘤。

[0053] 在另一个实施方式中，配制组合物用于与适合的递送药剂和抗癌化合物中的至少一种同时给予。

[0054] 适合的递送药剂可以是 Mirus Transit TKO® 亲脂性试剂、Lipofectin®、Lipofectamine™、Cellfectin®、聚阳离子或脂质体。

[0055] 还描述了配制化合物用于在适合的抗癌治疗期间同时给予，如抗癌疗法是手术操作、化疗、激素疗法和局部辐射中的至少一种。

[0056] 在优选的实施方式中，给予时所述组合物不引起肝毒性和炎症。

[0057] 本文所述的组合物还可以包含 pH 在 5 至 7.1 之间的转染媒介；本文所述的组合物可以配制为干燥粉末；和 / 或本文所述的组合物是水性媒介中的颗粒悬液。

[0058] 在另一个实施方式中，在与 RNA 诱导性核酸序列混合之前，将壳聚糖溶解在盐酸中。

[0059] 优选地，壳聚糖以 1:1 的比值溶解在葡萄糖胺 :HCl 中。

[0060] 在另一个实施方式中，使壳聚糖与 RNA 诱导性核酸序列混合产生尺寸小于 200nm，优选地尺寸为 45 至 156nm 的球形纳米颗粒。

[0061] 在一个实施方式中，细胞为原代细胞、转化细胞或永生化细胞。

[0062] 在另一个实施方式中，在与 RNAi 诱导性核酸序列混合之前，将壳聚糖溶解在盐酸中。

[0063] 在另一个实施方式中，壳聚糖的 Mn 为 10kDa，DDA 为 80% 或 92%，并且其中壳聚糖胺与核酸磷酸酯的比值（N:P）为 5 或 10。

附图说明

[0064] 现将对附图进行说明。

[0065] 图 1A 显示球形壳聚糖 /dsODN 纳米颗粒的环境扫描电子显微镜(ESEM)图像以及(A)92-10-5 壳聚糖 /dsODN-DPP-IV 纳米颗粒、(B)80-80-5 壳聚糖 /dsODN-DPP-IV 纳米颗粒、(C)80-10-10 壳聚糖 /dsODN-DPP-IV 纳米颗粒、(D)92-10-5 壳聚糖 /dsODN-ApoB 纳米颗粒、(E)80-80-5 壳聚糖 /dsODN-ApoB 纳米颗粒和(F)80-10-10 壳聚糖 /dsODN-ApoB 纳米颗粒的总体尺寸分布 ;并且图 1B 显示球形壳聚糖 /dsODN 纳米颗粒的环境扫描电子显微镜(ESEM)图像以及(A)92-10-5 壳聚糖 /dsODN-RecQL1 纳米颗粒、(B)80-40-5 壳聚糖 /dsODN-RecQL1 纳米颗粒和(C)80-10-10 壳聚糖 /dsODN-RecQL1 纳米颗粒的总体尺寸分布。

[0066] 图 2A 显示球形壳聚糖 /siRNA 纳米颗粒的环境扫描电子显微镜(ESEM)图像以及(A)80-10-5 壳聚糖 /siRNA-ApoB 纳米颗粒、(B)80-40-5 壳聚糖 /siRNA-ApoB 纳米颗粒、(C)92-10-5 壳聚糖 /siRNA-ApoB 纳米颗粒和(D)92-40-5 壳聚糖 /siRNA-ApoB 纳米颗粒的总体尺寸分布 ;并且图 2B 显示球形壳聚糖 /siRNA 纳米颗粒的环境扫描电子显微镜(ESEM)图像以及(A)80-10-5 壳聚糖 /siRNA-MDR1 纳米颗粒、(B)80-200-5 壳聚糖 /siRNA-MDR1 纳米颗粒、(C)92-10-5 壳聚糖 /siRNA-MDR1 纳米颗粒和(D)92-150-5 壳聚糖 /siRNA-MDR1 纳米颗粒的总体尺寸分布。

[0067] 图 3A 显示以不同 pH 值和经过不同时间段孵育的具有多种 N:P 比的壳聚糖 /dsODN 纳米颗粒的聚丙烯酰胺凝胶电泳相片图。显示与(A) dsODN-DPP-IV 和(B) dsODN-ApoB 复合并且在 pH6.5 (MES)和 pH8 (TAE)下孵育 0.5h、4h 和 20h 的壳聚糖 92-10 ;并且图 3B 显示在不同 pH 值和不同时间段孵育的具有多种 N:P 比的壳聚糖 /dsODN 纳米颗粒的聚丙烯酰胺凝胶电泳。与 dsODN-RecQL1 复合并且在 pH6.5 (MES)和 pH8 (TAE)下孵育 0.5h、4h 和 20h 的壳聚糖 92-10。如果纳米颗粒在上述条件下不稳定,则释放模拟 siRNA 的 dsODN 并在凝胶中迁移。

[0068] 图 4A 显示在 pH6.5 下壳聚糖 /siRNA 纳米颗粒稳定性的柱状图,不同的 DDA 和 MW 的壳聚糖制剂与三种不同的抗 -ApoB siRNA 序列(siApoB1、siApoB2 和 siApoB3)以 N:P 比 5 和 10 复合并孵育 20 小时,并且在纳米颗粒形成后,将用于核酸定量的 RNA 嵌入性染料 Ribogreen™ 加入到每个样品中以测量未复合的 RNA 分数,从而高荧光值表示颗粒分解和不稳定性 ;图 4B 显示表示 MW 对纳米颗粒尺寸的影响的柱状图,将 DDA 为 92% 并且 MW 不同的壳聚糖以不同的 N:P 比复合至抗 RecQL1siRNA ;图 4C 显示表示 MW 对纳米颗粒尺寸的影响的柱状图,将 DDA 为 80% 并且 MW 不同的壳聚糖以不同的 N:P 比复合至抗 RecQL1siRNA ;图 4D 显示了表示 MW 对纳米颗粒尺寸的影响的柱状图。将 DDA 为 72% 并且 MW 不同的壳聚糖以不同的 N:P 比复合至抗 RecQL1siRNA ;并且图 4E 显示表示通过动态光散射所测量的 RecQL.1siRNA 浓度对纳米颗粒尺寸影响和盐对纳米颗粒尺寸的影响的柱状图,将具有 92% 的 DDA 和 10 的分子量的壳聚糖以 5 的 N:P 比复合以提高抗 RecQL1siRNA 的浓度。

[0069] 图 5 显示在不同的 pH 下,DDA、MW 和 N:P 比对纳米颗粒稳定性的影响,其中低荧光表示颗粒稳定。将具有不同 DDA、MW 的壳聚糖以不同的 N:P 比复合至抗 MDR1siRNA 以形成纳米颗粒。将后者在不同的 pH 下孵育并使用 Ribogreen™ 测定测量 siRNA 释放。

[0070] 图 6A 显示壳聚糖 /dsODN 纳米颗粒的核酸酶保护测定的结果,(A)与 dsODN-DPP-IV 复合的壳聚糖(92-10-5 或者 80-10-10)、(B) DNA 酶 I 消化后剩余的 dsODN-DPP-IV、

(C) 与 dsODN-ApoB 复合的壳聚糖(92-10-5 或者 80-10-10)、(D) DNA 酶 I 消化后剩余的 dsODN-ApoB,使用处理样品与对照的信号强度评估所有消化(即 0U DNA 酶 I=100% 强度);并且图 6B 显示壳聚糖 /dsODN 纳米颗粒的核酸酶保护测定结果 :(A)与 dsODN-RecQL1 复合的壳聚糖(92-10-5、80-40-5 或 80-10-10)、(B)DNA 酶 I 消化后剩余的 dsODN-RecQL1,使用处理样品与对照的信号强度评价所有消化(即 0U DNA 酶 I=100% 强度)。

[0071] 图 7A 显示几个细胞系中转染后 24h dsODN/ 纳米颗粒的细胞摄取的柱状示意图 :(A) HepG2 细胞系中壳聚糖(92-10-5、80-80-5 或 80-10-10) /5′ -6FAM 标记的 dsODN DPP-IV 摄取 ; 和(B) HepG2、HEK293 和 RAW264.7 细胞中壳聚糖(92-10-5、80-80-5 或 80-10-10) /5′ -6FAM 标记的 dsODN-ApoB 摄取,DharmaFECT™#1 和 4 用作阳性摄取对照 ; 并且图 7B 显示了几个细胞系中转染后 24h dsODN/ 纳米颗粒的细胞摄取的柱状图,AsPC1、LS174T 和 A549 细胞系中壳聚糖(92-10-5、80-40-5 或 80-10-10)/5′ -6FAM 标记的 dsODN RecQL.1 摄取,DharmaFECT™#1 用作阳性摄取对照。

[0072] 图 8 显示用壳聚糖 /dsODN-DPP-IV 纳米颗粒转染的(A) HepG2、(B) Caco-2 和(C) HT-29 细胞系和用壳聚糖 /dsODN-ApoB 纳米颗粒转染的(D) HepG2、(E) HEK293 和(F) RAW264.7 细胞系中转染后 24 小时的壳聚糖 /siRNA 纳米颗粒摄取的共聚焦成像图。用罗丹明(红色)标记壳聚糖 92-10 (DDA,Mn)并且用 6FAM (绿色)5′ 标记 dsODN。将壳聚糖 92-10 以 N:P 比 5 复合至 siRNA。在成像前,用 CellMask™ (蓝色,膜锚定两亲染料)对细胞膜染色以区分内化和膜结合纳米颗粒。所显示的图像表示每个单独的通道,其中 dsODN 为绿色、壳聚糖为红色、膜为蓝色、传输 DIC 为灰色,并且在左下方四分之一处显示了合并的图像。

[0073] 图 9 显示转染后 24 小时壳聚糖 /siRNA 纳米颗粒摄取的共聚焦图像。用壳聚糖 /siRNA-RecQL1 纳米颗粒转染 LS174T 细胞系。转染后 24 小时拍摄图像。用罗丹明(红色)标记壳聚糖 92-10 (DDA, Mn) 并且用 6FAM (绿色) 5′ 标记 siRNA。将壳聚糖 92-10 以 N:P 比 5 复合至 siRNA-RecQL1。在成像前,用 CellMask™ (蓝色)对细胞膜染色。所显示的图像表示每个单独的通道,其中 siRNA 为绿色,壳聚糖为红色,膜为蓝色,传输 DIC 为灰色,并且在左下方四分之一处显示了合并的图像。

[0074] 图 10 显示转染后 24 小时壳聚糖 /siRNA 纳米颗粒摄取的共聚焦图像。用壳聚糖 /siRNA-MDR1 纳米颗粒转染 MCF-7MDR 细胞系。转染后 24 小时拍摄图像。用罗丹明(红色)标记壳聚糖 92-10 (DDA,Mn)并且用 Cy3 (绿色)5′ 标记 siRNA。将壳聚糖 92-10 (A)、壳聚糖 80-10 (B)和壳聚糖 80-200 (C)以 N:P 比 5 复合至 siRNA-cy3。在成像前,用 CellMask™ (蓝色)对细胞膜染色。所显示的图像表示每个单独的通道,其中 siRNA 为绿色,壳聚糖为红色,膜为蓝色,传输 DIC 为灰色,并且在左下方四分之一处显示了合并的图像。

[0075] 图 11A 显示特异性细胞系中 DPP-IV 和 ApoB 基因表达抑制的实时 PCR (qPCR) 分析的柱状图,用(A) 壳聚糖(92-10-5、80-80-5 和 80-10-10/siRNA-DPP-IV) ;(B) 壳聚糖(92-10-5/siRNA-ApoB) 纳米颗粒转染 HepG2 细胞,通过使用 AACT 法比较转染和非转染细胞获得了抑制百分比 ;并且图 11B 显示特异性细胞系中 RecQL.1 基因表达抑制的实时 PCR (qPCR) 分析的柱状图,用壳聚糖(92-10-5、80-40-5 和 80-10-10/siRNA-RecQL1) 转染 LS174T 细胞,通过使用 AACT 法比较转染和非转染细胞获得抑制百分比。

[0076] 图 12 显示三种不同的 DPP-IV 表达细胞系中 DPP-IV 酶活力的柱状图。与 siRNA- 模拟转染的细胞相比确定 DPP-IV 抑制百分比。值表示为平均值 ± 标准偏差 ;n=4/ 组。

*p<0.05，**p<0.01。

[0077] 图 13 显示壳聚糖 /siRNA 给予对 ApoB 血浆水平影响的柱状图。对于每个处理组，用 ELISA 测量蛋白水平。柱和误差线代表相对于未处理的动脉粥样硬化组 Dα 的平均蛋白水平。组 Dμ 是饲喂正常低脂饲料的正常阴性对照组。

[0078] 图 14 显示壳聚糖 /siRNA 给予后，治疗性降低的 LDL/VLDL 胆固醇的柱状图。通过对安乐死当天所采集的样品的定量比色 ELISA 试剂盒测量 LDL/VLDL 胆固醇含量。柱和误差线代表相对于未处理的动脉粥样硬化组 Dα 的平均胆固醇水平。组 Dμ 是饲喂正常低脂饲料的标准阴性对照组。

[0079] 图 15 显示治疗剂 NanoComplex（TNC）处理的动物肝脏中肝胆固醇微滴的减小。(A)C1-1、(B)C2-1、(C)C3-1、(D)C4-1、(E)C5-1、(F)Dα-2 天、(G)Dα-3、(H)Dβ-1 和 (I)Dμ-1 小鼠的苏木精 - 伊红染色石蜡固定的肝切片显示壳聚糖 /siRNA 给予在肝脏中胆固醇积累中的作用。箭头(→)表明胆固醇微滴积累。Dα 组是阳性未处理动脉粥样硬化对照，而 Dμ 是饲喂低脂饲料的标准阴性对照。

[0080] 图 16 显示 TNC 处理动物肝脏中炎症的再吸收。(A)C1-1、(B)C2-1、(C)C3-1、(D)C4-1、(E)C5-1、(F)Dα-2 天、(G)Dα-3、(H)Dβ-1 和 (I)Dμ-1 小鼠的番红精 -O/ 固绿 / 铁苏木精染色石蜡固定的肝脏切片显示与壳聚糖 /siRNA 给予或动脉粥样硬化发展有关的炎症反应的再吸收。圆圈(O)和箭头(→)指示了淋巴浸润。

[0081] 图 17 显示所有动物组每周体重(g)测量的柱状图。在每次给予壳聚糖 /siRNA 前，在每周的第一天称重所有动物。与低脂正常对照 Dμ 相比，对所有饲喂高脂饲料的动物观察到了 4 周的体重持续增加，这基本上不受 NTC 处理的影响。

[0082] 图 18 显示每周体重增加百分比的柱状图。在每次给予壳聚糖 /siRNA 前，在每周的第一天称重所有动物。体重增加是动物体重与其上周所记录的体重之间的相对差 $[(t_{n-1}-t_n)/t_{n-1})]$。该图显示第一次 TNC 给予后紧接的体重增加或降低。

具体实施方式

[0083] 根据本发明，提供了用于将 RNAi 诱导实体如短干扰 RNA（siRNA）、短发夹 RNA（shRNA）和 RNAi 诱导载体(即在细胞内存在导致 siRNA 或 shRNA 产生的载体)有效递送至哺乳动物(例如人)中细胞、组织和器官的非病毒载体的新的并且特异性的组合物。具体地，本说明提供了具有特定平均分子量(Mn)和去乙酰化程度(DDA)范围的壳聚糖组合物，其包含具有特定壳聚糖与核酸比值的 RNAi 诱导性实体。

[0084] 因此，提供了治疗或预防与靶标转录本的过度表达或不当表达有关的；或者与由靶标转录本所编码的多肽的不当活性或过度活性有关的疾病或病症的组合物和方法。

[0085] 可以在症状发生之前、期间或之后的适当时间窗口内通过使用本文所公开的组合物向具有罹患该病症风险或患有该病症的受试者给予 RNAi 诱导性实体来使用本文提供的组合物以提供症状缓解。

[0086] 所述组合物和方法可以应用于多种目的，如，例如，但不限于：研究转录本的功能、研究在不存在转录本编码的多肽或者所述多肽的活性降低的情况下细胞或生物的不同化合物的影响。此外，所述组合物和方法可以在临床疗法中应用于 II 型糖尿病及其相关病理、动脉粥样硬化及其相关病理和癌症。具体地，组合物和方法可以应用于抑制肠泌

素降解酶(DPP-IV)或任何糖调节蛋白以治疗糖尿病,应用于抑制ApoB基因或任何致动脉粥样化蛋白(即ApoE)以治疗动脉粥样硬化,或者分别应用于使RecQL.1DNA解旋酶或DDX5-p68-RNA解旋酶的表达下调(但不限于那些)以用于治疗癌症。

[0087] 具体地,本说明涉及本文所述的组合物结合的这些核酸结合作为(例如)解旋酶过表达性肿瘤或作为辐射致敏实体的直接治疗的减轻药剂的应用。此外,本文所述的组合物和方法可以结合任何其他癌症治疗使用,如放射疗法、手术、激素治疗或常规化疗。本说明还提供用于以提高放射疗法或结合其他治疗方式使用的组合物和方法。

[0088] 本文所公开的组合物含有RNAi诱导性核酸和具有以下物理化学性质的壳聚糖:N:P比小于25、壳聚糖具有在5kDa至200kDa范围的数均分子量(Mn)内和在80%DDA至95%DDA范围内的去乙酰化程度。本说明表明组合物和方法与可商购的脂质-核酸复合物可比的有效转染不同细胞系并诱导基因沉默的有效性,其中转染效率在mRNA水平达到80%,并且在一些情况下达到95%的细胞摄取,而无任何明显的细胞毒性。

[0089] RNA干扰(RNAi)是双链RNA通过其来指导细胞转录本(如信使RNA)序列特异性降解的方法(Sharp,2001,Genes Dev,15:485-490;Vance和Vaucheret,2001,Science,292:2277-2280)。最早在秀丽线虫(C.elegans)中发现该现象(Fire等人,1998,Nature,391:806-811)。天然发生的RNAi是通过21-25之间个核苷酸的小双链片段(并被称为小干扰RNA)介导的。这些siRNA是通过dsRNA特异性核酸内切酶(称为Dicer)通过将长双链RNA(dsRNA)切割成21个碱基对的小干扰RNA(siRNA)的过程产生的,所述小干扰RNA由侧接有两个核苷酸3′突出的19个碱基对的双螺旋区的核心区组成(Bernstein等人,2001,Nature,409:363-366)。然后,将siRNA并入RNA诱导的沉默复合物(RISC)中,并指导RISC以识别对siRNA具有互补序列的靶标mRNA,从而导致特定转录本的切割。

[0090] 随后,由于发现可以通过引入合成的21个核苷酸的RNA双螺旋(siRNA)来引发哺乳动物细胞中的RNAi(Elbashir等人,2001,Nature,411:494-498),并因此避开了Dicer介导的对长dsRNA加工的需要,因而RNAi很快被认为在临床应用中具有巨大潜能。

[0091] 例如,通过靶向并降低ApoB的表达,有可能防止过量形成VLDL,从而减少生物中这些致动脉粥样化剂的积累(Soutschek等人,2004,Nature,432:173-178)。使用序列特异性siRNA,在非人灵长类中在mRNA水平上ApoB靶向表明在处理后24h,ApoB蛋白、血清胆固醇和低密度脂蛋白水平的显著降低(Zimmermann等人,2006,Nature,441:111-114)。以最高的siRNA剂量,使用基于脂肪的纳米颗粒(SNALP-siRNA)的这种治疗的治疗效果持续了11天,因此表明了siRNA治疗的快速、有效和持久的生物学效应。不幸地,这些基于脂肪的载体产生了高水平的肝脏毒性,如通过天冬氨酸转氨酶(AST)和丙氨酸转氨酶(ALT)的血清水平升高所指示的提示肝细胞的坏死(Zimmermann等人,2006,Nature,441:111-114)。因此,尽管这些报道表明ApoB作为动脉粥样硬化的和CVD疗法的靶标的重要性,但是它们还突出了当前siRNA递送系统达到全身性ApoB的安全和有效减少的不足。

[0092] 以合成小干扰RNA形式的直接递送RNAi仍是有问题的,其具有较差的细胞靶向和摄取,以及由于胞内和/或胞外核酸酶的降解(即RNA酶)和有限的血液稳定性和毒性而造成的短半衰期(Stein,1996,Trends Biotechnol,14:147-149;Urban-Klein等人,2004,Gene Therapy,1-6;Katas和Alpar,2006,J Control Release,115:216-225)。因

此，RNAi 向临床治疗剂的翻译仍是这些问题未解决的方法。当通过如转染的方式引入细胞时，RNAi 已显示在多种不同的细胞类型中操作。然而，转染效率取决于携带小干扰 RNA 分子的递送载体。被称为载体的所述递送载体应能够凝聚、保护并将 siRNA 携带到靶细胞中。一旦邻近靶标，非病毒载体应促进细胞摄取，避免溶酶体封存并释放它们的内容物以实现所需的生物学效应。

[0093] 合成的 siRNA 的化学修饰提供对核酸酶降解的抵抗并改善血液稳定性。例如，选择性添加硫代磷酯键或用 2′ -O- 甲基在特定核糖的 C2 位置上的取代提高 siRNA 的核酸酶耐受性而不会损伤活性（Corey，2007，J Clin Invest，117：3615-3622；Whitehead 等人，2009，Nat Rev Drug Discov，8：129-138；Judge 等人，2006，Mol Ther，13：494-505）。然而，一些化学修饰可以提高细胞毒性和脱靶效应并降低 mRNA 杂交（Weyermann 等人，2005，Eur J Pharm Biopharm，59：431-438；Amarzguioui 等人，2003，Nucleic Acids Res，31：589-595）。尽管通过化学修饰提高 siRNA 半衰期、转染效率从而实现了进展，但是细胞靶标和摄取仍是有效递送的障碍。因此，需要可以保护并将化学未修饰 / 修饰的 siRNA 递送至靶细胞的包装系统。然而，转染效率取决于携带小干扰 RNA 分子的递送载体。被称为载体的递送载体应能够凝聚、保护并将 siRNA 携带到靶细胞中。一旦邻近靶标，非病毒载体应促进细胞摄取，避免溶酶体封存并释放它们的内容物以实现所需的生物学效应。这些非病毒载体正在进行体外和体内测试，证明 siRNA 向临床现实的可能转化。尽管如此，主要缺点与这些非病毒载体有关。低转染效率、血清稳定性、聚集和毒性仍是非病毒载体在临床中作为强大并且无毒的药物递送工具的商业化前需要解决的主要障碍。以下讨论了非病毒载体的主要类别：

[0094] 磷酸钙

[0095] 该载体的主要缺点是有限的效率以及它不能保护核酸不受核酸酶降解。尽管其保护核酸的能力得到改善，但是其转染效率仍很低，从而防止它有效的体内应用。

[0096] 阳离子脂质

[0097] 阳离子脂质通过静电相互作用与核酸形成复合物，并最终形成多片层脂质 - 核酸复合物（lipoplexes）。脂质体制剂通常包括阳离子脂质和中性脂质如 DOPE（二油酰磷脂酰乙醇胺）。中性脂质有助于脂质体制剂的稳定性，并且有利于膜融合并通过使内涵体不稳定来促进溶酶体逃逸。脂质 - 核酸复合物是将核酸递送至培养细胞的最有效的方法之一。不管它们的转染效率，如在培养细胞中所观察到的和通过几项体内发现所确认的，脂质 - 核酸复合物是有毒的。这种毒性与复合物中阳离子脂质与核酸的电荷比以及所给予的剂量密切相关。正在测试和开发生物相容性更好的制剂以降低与脂质 - 核酸复合物相关的毒性。主要是通过接枝其他聚合物或降低阳离子聚合物的总电荷实现毒性的降低。

[0098] 阳离子聚合物

[0099] 阳离子聚合物通过带有相反电荷的聚阳离子和聚阴离子物质（即核酸）之间的相互作用形成纳米尺寸的纳米颗粒。这些纳米颗粒封装核酸，从而防止所递送的载物（cargo）被核酸酶降解（Romoren 等人，2003，Int J Pharm，261：115-127）。已经将多种天然和合成阳离子聚合物用作基因递送或沉默的载体。与脂质 - 核酸复合物相比，使用阳离子聚合物的这些纳米颗粒中的多种具有优异的转染效率和低血清敏感度。天然存在的聚阳离子是蛋白质如组蛋白、阳离子化人血清白蛋白和壳聚糖（氨基多糖）。

[0100] 合成聚阳离子的组包括聚 -L- 赖氨酸(PLL)、聚 -L- 鸟氨酸以及聚胺,如聚亚乙基亚胺(PEI)、聚丙烯亚胺和聚酰胺 - 胺树枝状聚合物。

[0101] polyplexe 的优势在于它们的形成不需要多个聚阳离子的相互作用,这与脂质体需要多个脂质组分相反,从而使得 polyplex 的宏观性质易于控制。聚阳离子的另一个主要优点是它们的嵌段结构,因此允许直接化学修饰以达到更高的效率或特异性细胞靶向。然而,除了这些优势之外,已发现多种阳离子聚合物由于高表面电荷密度而是有毒的,这是因为高电荷密度的纳米颗粒似乎毒性更强。此外,已报道在聚合物中电荷密度在细胞毒性中起到比总电荷量更重要的作用。毒性也可以是分子量依赖性的,这是因为 PEI 的细胞毒性随分子量线性提高。此外,不可降解的聚合物(如 PEI)在溶酶体中的积累可能是造成毒性的另外原因,这种现象称为溶酶体封存。

[0102] 壳聚糖是通过 β -1,4 糖苷键连接的葡萄糖胺和 N- 乙酰葡萄糖胺单体的天然聚合物,其来源于几丁质的碱性去乙酰化作用。壳聚糖的分子量和去乙酰化程度决定了它的生物学和物理化学性质。例如,壳聚糖的生物降解能力受乙酰基的量和分布的影响。这些基团的缺少或它们的随机性而非嵌段分布导致了极低的降解率。

[0103] 壳聚糖具有广泛的有益性质,其包括生物相容性、生物降解能力、粘膜粘附性、抗菌 / 抗真菌活性以及极低的毒性。因此,它已引起了制药学和生物医学领域的注意并成为用于核酸包装和凝聚的最广泛使用的非病毒载体之一。

[0104] 几项研究已解决了壳聚糖分子量和去乙酰化程度(DDA)对不同细胞系的壳聚糖 - 质粒 DNA 纳米颗粒的摄取、纳米颗粒运输以及转染效率的影响。Huang 等人对 A549 细胞进行了该主题的研究(2005,J Control Release,106:391-406)。然而,该研究仅使用了 7 种制剂(88%DDA 的 10、17、48、98 和 213kDa 的壳聚糖 ;61 和 46%DDA 的 213kDa 的壳聚糖)来研究平均分子量(Mn)和 DDA 对 pDNA 的转染效率的影响,而未针对相对于质粒中数千个碱基对要小很多的 siRNA (其通常为 21bp)。它们发现 Mn 和 DDA 的减小对于质粒产生了较低的转染效率。然而,这两个参数之间的关系要复杂得多并且在壳聚糖 Mn 和 DDA 之间需要精细的平衡以实现最佳的稳定性。它们不能得出复杂的关系,这是由于它们有限的制剂个数。此外,相对于转染培养基的 pH 和壳聚糖 -DNA 比(N:P),每次仅改变一个参数阻止他们观察 Mn 和 DDA 之间的偶联作用。Lavertu 等人进行了针对质粒 - 壳聚糖 polyplexe 的这种复杂关系的另一项研究(2006,Biomaterials,27:4815-4824)。在它们的研究中,他们对于几个不同的 DDA 水平改变了分子量,并且还检验了壳聚糖 -DNA 比(N/P)和 / 或转染培养基的 pH。该研究表明在 HEK293 细胞中这种优化实现了与广泛使用的商品化脂质体(Lipofectamine™ 和 Fugene™)相当的高转染效率。

[0105] 当去乙酰化程度提高时,沿着链产生更高的电荷密度以更紧密地与 pDNA 结合以形成纳米颗粒,从而壳聚糖的 DNA 结合能力 / 亲合力提高(Ma 等人,2009,Biomacromolecules,10:1490-1499)。因此,具有极低 DDA 的壳聚糖不能有效结合 DNA 并且不能形成物理学稳定的复合物以转染细胞(Koping-Hoggard 等人,2003,J Gene Med,5:130-141)。如上文所提及的,在高 DDA 难以降解的情况下,DDA 还对生物降解能力的产生主要影响。就此而言,Koping-Hoggard 等人最近的研究(2001,Gene Ther,8:1108-1121)表明基于高 Mn 壳聚糖的复合物的红细胞浆质逃逸取决于壳聚糖的酶促降解并且对于高 DDA 壳聚糖将不易发生。假设所得的降解片段会提高内涵体渗透性并导致膜破裂。因此,对于高度去乙酰化的壳聚糖

(近 100%DDA),降低的可降解性可以导致降低的红细胞浆质逃逸。

[0106] 在几项研究中评价了壳聚糖 Mn 对结合核酸的能力的影响。带相反电荷的大分子之间的结合亲合力强烈取决于每个分子的化合价,其中低化合价仅获得弱结合(Danielsen 等人 ,2004,Biomacromolecules,5:928-936)。对于具有短链的低分子量的壳聚糖,其化合价的降低已表明会降低其对 DNA 的亲合力(Ma 等人 ,2009,Biomacromolecules,10:1490-1499)。尽管在胞外期望高水平的复合物稳定性以保护不受酶促进攻,但 MacLaughlin 等人(1998,J Control Release,56:259-272)暗示高 Mn 壳聚糖可以形成对于转染细胞过度稳定的复合物,这是因为一旦进入细胞内部,它们不能分解。此外,Lavertu 等人(2006,Biomaterials,27:4815-4824)表明 Mn 似乎不是细胞摄取的主要因素,但是似乎的确在核酸结合亲合力和胞内释放方面起作用。通过由等温滴定量热法(Ma 等人 ,2009,Biomacromolecules,10:1490-1499)和通过 polyplex 运输和分解的活细胞内成像(Thibault 等人 ,2010,Mol Ther,18:1787-1795)直接评估结合亲合力从而进一步支持了这些解释以及对结合至核酸的壳聚糖的精细平衡的中间产物稳定性的需要。

[0107] 已发现胺与磷酸酯的比值在 DNA 结合和纳米颗粒形成中起重要作用。例如,提高 N:P 比会提高壳聚糖对 DNA 的结合。对于相同的 DDA,低 Mn 壳聚糖需要高 N:P 比以完全结合质粒 DNA。类似地,Mn 相同时,较低的 DDA 需要较高的 N:P 比以完全结合 DNA (Koping-Hoggard,2003,J Gene Med,5:130-141 ;Kiang 等人 ,2004,Biomaterials,25:5293-5301)。已表明 pH 在转染效率中起重要作用。Lavertu 等人(2006,Biomaterials,27:4815-4824)示出在微酸性的介质中,复合物更稳定并且实现了转染效率的提高。这可以由以下事实解释 :pH 的降低会提高壳聚糖的质子化,并因此提高 polyplex 上的正电荷(ζ 电位)和壳聚糖对 DNA 的结合亲合力。Lavertu 等人研究了壳聚糖制剂参数(DDA、Mn、N:P 和 pH)对于质粒 DNA 体外递送的综合影响(2006,Biomaterials,27:4815-4824)。他们有趣地发现对于 DDA:Mn 值沿着对角线从高 DDA/ 低 Mn 向低 DDA/ 高 Mn 移动时,发生了最大转基因表达(Lavertu 等人 ,2006,Biomaterials,27:4815-4824)。因此,如果提高 / 降低 DDA,则必须相应地降低 / 提高 Mn 以维持最大转染。

[0108] 如上所述,pH 在转染效率方面起重要作用。Lavertu 等人(2006,Biomaterials,27:4815-4824)表明对于质粒 DNA 趋向较高 Mn 的最有效制剂,pH 的提高替代了 Mn,这是因为在较高 pH 时,壳聚糖的中和导致壳聚糖电荷密度降低。另一方面,对于给定的 DDA,对于趋向于较小 Mn 的最有效制剂,N:P 比从 5:1 至 10:1 的变化替代了 Mn,这可能是由于提高壳聚糖浓度的稳定作用。因此,可以看出这些不同制剂参数对转染效率以及在开发更有效并且更稳定的壳聚糖 -DNA 制剂中的重要性。

[0109] 据信 pDNA 和 siRNA 之间的结构差异影响纳米颗粒复合作用 / 稳定性以及有效递送所需的最佳参数。壳聚糖已用于体外和体内的 siRNA 递送(de Fougerolles 等人 ,2007,Nat Rev Drug Discov,6:443-453 ;Howard 等人 ,2006,Mol Ther,14:476-484 ;Katas 和 Alpar,2006,J Control Release,115:216-225 ;Zimmermann 等人 ,2006,Nature,441:111-114 ;和 Liu 等人 ,2007,Biomaterials,28:1280-1288)。然而,尽管尝试去鉴别 siRNA 递送的最佳物理化学参数,但是由于实验差异,在文献中观察到非确定的结果。例如,在 pH7.9 下评价了 siRNA 载物的纳米颗粒形成、稳定性和保护 ;这个 pH 不是典型的生理学环境。在该 pH 下,壳聚糖主要是去质子化的,这是因为其表观 pKa 接近

6.5，并且因此不能有效地结合 siRNA 载物。由于在这些条件下测试复合物形成，因此几个研究小组已使用高 N:P 比来补偿在 pH 高于壳聚糖 pKa 条件下所观察到的壳聚糖与 siRNA 之间较差的结合。这些高 pH 值的使用（即 7.9）代表了导致这些研究人员使用高 N:P 比来实现纳米颗粒复合、稳定性和载物保护的重要设计错误和实验差异来源。不幸地，过量的壳聚糖可以竞争性影响转染效率，产生多种非特异性影响并提高毒性，从而导致了错误结论。

[0110] 例如，据报道在递送 siRNA 时，中等 DDA（80%）和高 Mn（64-170kDa）比低分子量壳聚糖（10kDa）明显更有效（Katas 等人，2006, J Control Release, 115:216-225；和 Liu 等人，2007, Biomaterials, 28:1280-1288）。然而，发现这些高分子量壳聚糖有毒（Howard 等人，2006, Mol Ther, 14:476-484；和 Richardson 等人，1999, Int J Pharm, 178:231-243）。另外，先前所有评价壳聚糖 /siRNA 纳米颗粒的复合物形成、其他物理化学特性和转染效率的报道均得到以下结论：制剂仅在极高 N:P 比（N:P>25）时是有效的（Howard 等人，2006, Mol Ther, 14:476-484；Katas 等人，2006, J Control Release, 115:216-225；Liu 等人，2007, Biomaterials, 28:1280-1288）。这些报道未认识到大部分的过量的壳聚糖实际是可溶的并且不是纳米颗粒的结构组分（Ma 等人，2010, Biomacromolecules, 11:549-554）。由于大量可溶性壳聚糖的聚集和非特异性毒性影响，这些具有极高 N:P 比（N:P>25）的制剂显示出显著的实际问题，包括有限的剂量。

[0111] 在本文中，使用接近壳聚糖 pka 以及接近生理学 pH 的适当 pH 条件来评估纳米颗粒的物理化学特性，显示了不需要这种高 N:P 以形成有效的纳米颗粒递送载体，如在本发明中所证明的（图 3）。

[0112] 通过不同的给予途径（包括鼻内、口服、腹膜内和肌内途径），壳聚糖被用于递送药理学活性化合物。在大鼠和绵羊中通过鼻内途径给予壳聚糖 / 胰岛素。这些制剂涉及使用 10kDa 或以上分子量的水溶性壳聚糖，对去乙酰化程度没有说明（Ilium, 1996, Danbiosyst UK Limited, United States, vol. 5554388；1998, Danbiosyst UK Limited, United States, vol. 5744166）。

[0113] 通过用可溶性制剂的鼻内途径壳聚糖还被用作用于免疫小鼠的佐剂（美国专利申请公开号 US2003/0039665）。这些制剂涉及具有 10-500kDa 之间的 Mn 范围以及 50-90% 之间的去乙酰化程度的壳聚糖谷氨酸盐。

[0114] 壳聚糖还被用于体外以及体内递送从质粒 DNA 到 siRNA 的核酸。已报道了通过局部或全身递送，用具有多种递送载体的 siRNA 的体内研究的超过 40 个实例（de Fougerolles 等人，2007, Nat Rev Drug Discov, 6:443-453）以治疗眼（Nakamura 等人，2004, Mol Vis, 10:703-711）和肺靶标（Howard 等人，2006, Mol Ther, 14:476-484），或针对神经系统（Kumar 等人，2006, Plos Medicine, 3:505-514）、肝（Soutschek 等人，2004, Nature, 432:173-178）、肿瘤（Grzelinski 等人，2006, Hum Gen Ther, 17:751-766）和其他器官。在一个实例中，在关节炎鼠模型中，壳聚糖 /siRNA 纳米颗粒介导腹膜巨噬细胞中 TNF-α 的敲低以用于抗炎治疗（Howard 等人，2006, Mol Ther, 14:476-484）。

[0115] 几项研究已检验了壳聚糖体外和体内递送 siRNA 的能力。Katas 等人（2006, J Control Release, 115:216-225），使用具有 84%DDA 的两种不同形式的壳聚糖盐（CS-HCl 和 CS- 谷氨酸盐）来研究壳聚糖参数对转染效率的影响。使用了四种不同的高分子量壳聚糖

(470kDa、270kDa、160kDa 和 110kDa)并且他们发现将壳聚糖浓度从 25μg/ml (1.25:1)提高至 300μg/ml (15:1)会使纳米颗粒尺寸从约 150nm 增大至 450nm (Katas 等人,2006,J Control Release,115:216-225)。

[0116] 此外,在他们的研究中表明壳聚糖 - 谷氨酸盐产生比壳聚糖 -HCl 更小的纳米颗粒。Katas 等人(2006,J Control Release,115:216-225)发现在他们的实验条件下,siRNA 与壳聚糖的完全结合仅在 N:P 比为 100:1 或以上发生,这是壳聚糖极端过量的情况,并且其中很可能 >95% 的壳聚糖是可溶性的并且未复合至 siRNA(Ma 等人,2010,Biomacromolecules,11:549-554)。预期这种中等 DDA (84%)壳聚糖的大量过量会导致体内持续炎症并增加不利的免疫学相应(Jean 等人,2009,Gene Ther,16:1097-1110)。在它们的研究中,与低分子量壳聚糖谷氨酸盐或壳聚糖盐酸盐相比,470kDa 分子量的壳聚糖谷氨酸盐在体外转染后 24h 显示出最高的基因沉默(Katas 等人,2006,J Control Release,115:216-225)。具有 470kDa 的平均分子量的壳聚糖谷氨酸盐的离子凝胶化显示出比通过简单复合所形成的壳聚糖 -siRNA 纳米颗粒(51%mRNA 抑制)更高的沉默效率(82%mRNA 抑制)(Katas 等人,2006,J Control Release,115:216-225)。

[0117] Howard 等人领导的另一个小组(2006,Mol Ther,14:476-484)通过鼻内给予途径在转基因 EGFP 小鼠模型中递送壳聚糖 -siRNA 纳米颗粒。对于他们的研究,他们以四个不同的 N:P 比(N:P6、33、71 和 285)使用 84%DDA 和 114kDa 的壳聚糖。在 250μg/ml 的低壳聚糖浓度下,较高的 N:P 比产生较小的纳米颗粒(N:P6=223.6nm 相对于 N:P33=181.6nm)(Howard 等人,2006,Mol Ther,14:476-484)。在较高壳聚糖浓度(1mg/ml)下观察到了相同的模式,其中与制剂 84-114-285 的 139nm 相比,具有 84% 的 DDA、114 的 Mn 和 33 的 N:P 比的壳聚糖纳米颗粒具有 328nm 的平均直径(Howard 等人,2006,Mol Ther,14:476-484)。

[0118] 他们初步的体外研究显示纳米颗粒尺寸取决于 N:P 比,并且在较低 N:P 比下尺寸增加,这表明需要高 N:P 比。该发现与本发明的发现相矛盾,其中当评价壳聚糖 -siRNA 复合作用和稳定性时显示出低于 pH 的关键作用。基于他们的发现,分别在 NIH3T3 和 H1299 细胞系中测量了在 36 和 57 的高 N:P 比时的细胞摄取和沉默效率。在 36 的高 N:P 比时的壳聚糖制剂被用于研究 EGFP 稳定细胞系的沉默效率。在 H1299 和原代腹膜小鼠巨噬细胞中沉默效率分别为 77.9% 和 86.9%。在 EGFP 转基因小鼠模型中,每天注射 30μg siRNA,注射 5 天后,与未处理对照相比,N:P36 时壳聚糖制剂 84-114 的体内沉默效率达到 43% 沉默效率(Howard 等人,2006,Mol Ther,14:476-484)。

[0119] 在 Howard 等人的另一项体内研究中(2009,Mol Ther,17:162-168),靶向 TNF-α mRNA 的 27 个碱基对的 siRNA 被以 63 的 N:P 比复合至壳聚糖 84-114,并在胶原诱导的关节炎(CIA)小鼠模型中注射。如通过 TNF-α 血浆水平所测量的,他们的制剂实现了 43% 的沉默。

[0120] Ji 等人(2009,Nanotechnology,20:405103)暗示 DDA 范围在 75% 至 85% 的 190kDa 和 310kDa 壳聚糖是适合 siRNA 的递送载体。与上述研究类似,Ji 等人使用高 N:P 比 50 的壳聚糖制剂在 Lovo 细胞中进行 FHL2 致癌基因的抑制实验。他们的制剂实现了 69% 的 mRNA 敲低。

[0121] 为了确定壳聚糖递送 siRNA 的最佳参数,Liu 等人(2007,Biomaterials,28:1280-1288)测试了一系列具有不同 DDA、Mn 和 N:P 比的壳聚糖,并且表明 N:P 比 >25 是有效沉默所需的。他

们还发现以 N:P50 制备的低分子量壳聚糖 -siRNA（10kDa）制剂在 H1299 人肺癌细胞中未显示出内源 EGFP 的敲低，而在 80%DDA 以较高 Mn（64.8-170kDa）制备的壳聚糖制剂显示出 45% 至 65% 范围之间的较高的基因沉默。以极端 N:P150 其中分别使用 114kDa 和 170kDa 的 Mn 以及 84% 的 DDA，使用壳聚糖 /siRNA 纳米颗粒实现了最高的基因沉默效率（80%），这些参数与具有约 200nm 直径的纳米颗粒的稳定形成的评估有关。另外，通过动态光散射（DLS）所测量的，Liu 等人（2007, Biomaterials, 28:1280-1288）发现以 50 的 N:P 比复合至抗 EGFP siRNA 的 95%DDA 和 9kDa 壳聚糖具有不期望的 3500nm 的大尺寸。此外，他们表明根据用于在 7.9 的碱性 pH 下（该 pH 在本文中显示产生了人为颗粒分解）进行的稳定性测试的凝胶阻滞测定，该具体制剂不会与 siRNA 以高达 50 的 N:P 比形成复合物。另外，与阴性未处理对照相比，该具体制剂未显示出 EGFP 敲低。

[0122] 其他人所发现的上述结果与本文所提供的新的发现相反，其中证实使用一系列分子量（5 至 200kDa）的、DDA 在 80% 至 95% 之间的壳聚糖可以在中等至低 N:P 比（低于 25 并且优选地 5）下形成壳聚糖 -siRNA 纳米颗粒，并且与先前报道的系统相比，这些纳米颗粒实现了高水平的基因沉默、优良的稳定性和小尺寸范围。

[0123] 壳聚糖涂覆的聚（异己基氰丙烯酸酯）（PIHCA）纳米颗粒还用于在异种移植侵袭性乳腺癌模型中静脉内递送抗 RhoA siRNA 实体（Pille 等人，2006, Hum Gen Ther, 17:1019-1026）。给予壳聚糖涂覆的 PIHCA- 抗 RhoA siRNA 纳米颗粒通过敲低癌细胞中过表达的 RhoA 显著降低癌症的体内侵袭性。Zhang 等人研究了壳聚糖衍生制剂 Nanogene042 用于靶向肺组织中 NS1 蛋白的 siRNA 的从头表达，从而用于在 Balb/c 模型中预防和治疗呼吸道合胞病毒（RSV）感染（Zhang 等人，2005, Nat Med, 11:56-62）。Zhang 等人使用基于 shRNA 的质粒并观察到 NS1 基因的有效沉默和 RSV 感染的降低，并伴随着降低的体内病毒滴度载量。与典型的高 MW 壳聚糖相比，Nanogene042 显示出较高的转染效率并引起较少的炎症（Zhang 等人，2005, Nat Med, 11:56-62）。然而，在声明的参考文献中未公开 Nanogene042 的分子量。

[0124] 出于本发明的目的，将 C57BL/6（C57BL/6NCrl）小鼠模型用于进行不同的实施方式。Charles River 和 Research Diets 开发了 C57BL/6 小鼠模型。当饲喂高脂肪饲料（D12492）时，C57BL/6 小鼠模型可以变的肥胖，与瘦对照相比，用高脂肪饲料后两周，体重增加显著。在多种目的的研究中以及在研究高脂肪饲料期间循环系统中 LDL 胆固醇水平的高脂血症研究中使用了 C57BL/6 小鼠模型（Soutschek 等人，2004, Nature, 432:173-178；Crooke 等人，2005, J Lipid Res, 46:872-884；Bose 等人，2008, J Nutr, 138:1677-1683）。高脂肪饲料（D12492）相当于仅含有 10kcal% 脂肪的对照饲料 D12450B 中的脂肪的 6 倍。另外，与对照饲料 D12450B 的 18(mg)/kg 相比，高脂肪饲料 D12492 含有 300.8(mg)/kg 的胆固醇。借此，相对于肝脏中的消除，饲喂这种高脂肪饲料在动脉中 LDL 的积累中产生了不稳定性，从而驱使 C57BL/6 小鼠模型中动脉粥样硬化的发展。

[0125] 如下文中所述，已发现当与 siRNA 结合时本文所述的组合物是有效的基因转移载体，从而实现了与商品化脂质体 DharmaFECT™ 类似的体外转染效率。此外，所述组合物不仅在将 siRNA 递送到细胞中实现了与 DharmaFECT™ 相当的效率和类似的沉默，而且毒性更低。

[0126] 使用壳聚糖 /dsODN 纳米颗粒的摄取效率达到了与商业化使用的脂质 - 核酸复合物（DharmaFECT™）相当或更高的水平，并且在细胞类型之间具有类似的相对变化（图 7A 和

7B)。此外,这些结果与如下所描述的共聚焦显微镜数据(图 8)一致,其中图像显示对于所有细胞系的壳聚糖和 dsODN 的细胞分布,表明了与 FACS 定量数据的定性关系。在本文中,已表明制剂转染并将不同 siRNA 有效递送至多个细胞系的能力(参见例如,图 7A 和图 8)。

[0127] 本文所公开的结果清楚地显示所描述的基于壳聚糖的制剂有效递送 siRNA 并以远低于本领域先前使用的那些的 N:P 比敲低特定基因的有效性。一般说来,本文所使用的所有低 N:P 比壳聚糖制剂达到了高水平的基因沉默。

[0128] 结果显示基于所使用的壳聚糖制剂(80-10-5、80-40-5、92-10-5、92-40-5、80-10-10、80-80-5、92-150-5 和 80-200-5)和 siRNA 化学修饰程度,球形纳米颗粒(图 1 和 2)具有在 45-156nm 的范围内的平均直径(表 2)。在 dsODN 和未修饰的 siRNA-ApoB(Seq1, SEQ ID NO:5)和复合至壳聚糖的适度修饰的 siRNA-ApoB (Seq2, SEQ ID NO:6 和 SEQ ID NO:7)之间在纳米颗粒尺寸方面未观察到统计学差异。然而,当复合至不同的壳聚糖时,完全修饰的 siRNA 序列获得了较大的纳米颗粒。

[0129] 使用本文所描述的具体制剂获得的结果与所获得的动态光散射结果一致(表 2),从而表明本文所描述的组合物和方法的稳健性。此外,所形成的纳米颗粒获得了可重复的小于 200nm 的尺寸,从而使得能够避免肾清除,从而改善体内转染效率并提高循环纳米颗粒的半衰期。

[0130] 使用荧光类测定 Ribogreen 测定™ 评价壳聚糖 /siRNA 的稳定性以在复合物非稳定化后定量所释放的 siRNA。结果表明具有 5 和 10 的 N:P 比的壳聚糖 /siRNA 纳米颗粒在 pH6.5 下稳定持续长达至 20 小时。当与其他制剂相比时,壳聚糖 80-10-5 显示了最低的稳定性。提高壳聚糖 80-10 的 N:P 比产生纳米颗粒稳定性的改善。除壳聚糖 80-10 外,将 N:P 比提高至 5 以上不会产生纳米颗粒稳定性的提高(参见,例如,图 4A)。

[0131] 据证实本文所描述的制剂可以达到与商品化脂质体 DharmaFECT™ 可比的基因沉默水平而无任何显著的细胞毒性。本文所公开的结果清楚地显示所描述的基于壳聚糖的制剂以远低于他人先前所使用的那些(N:P>20)的 N:P 比(N:P=5)有效递送 siRNA 并敲低特异性基因的有效性(参见例如,图 11A 和图 11B)。一般来说,申请人的所有低 N:P 比壳聚糖制剂达到了高水平的基因沉默,这支持了 FACS 数据(参见,例如,图 7A 和图 7B)。发现低分子量(10kDa)和高 DDA (92%)壳聚糖趋向于最有效(图 11 和 12)并且更小(图 4B),提示了 NP 比为 5 时特别优化的制剂。

[0132] 还描述了与阳性未处理对照(以下称为 Dα)相比,用于治疗动脉粥样硬化的本文所描述的组合物体内地将 ApoB 血浆水平降低了约 30%。还表明这种降低产生与非动脉粥样硬化动物组阴性对照的那些类似的 ApoB 血清水平,并因此处于治疗范围内。本发明还证明用于动脉粥样硬化治疗的本文所描述的组合物对 LDL-胆固醇产生了 20% 的降低,而无任何显著毒性(图 14)。还表明含有 siRNA 的基于壳聚糖的治疗性纳米复合物(TNC)不会导致任何肝脏毒性,如通过血清中正常 ALT/AST 水平所证明的。

[0133] 还证明在注射后三周,TNC 治疗对于肝脏中胆固醇的积累具有治疗效果,其中在 TNC 治疗的动物肝脏中胆固醇的积累显著降低(图 15)。类似地,基于壳聚糖的 TNC 引起免疫细胞对肝脏的短暂侵润,肝脏快速吸收而无毒性,如在本文的另一个实施方式中所表明的(图 16)。没有肝脏毒性以及免疫细胞侵润的快速再吸收表明提高注射剂量以实现较高 ApoB 和 LDL-C 血浆降低的可能性。

[0134] 此外，描述了靶向 ApoB 的无壳聚糖的裸露 siRNA 诱导了强烈的炎性相应，从而限制了它们的剂量和以未复合形式用于治疗性使用的可能。以 1mg/kg 抗 ApoB siRNA 的测试剂量在 TNC 治疗的动物中没有毒性 / 炎症并且它们将 ApoB 血浆水平降低 35% 的能力表明了它们的重要性以及在确定最大耐药量（MTD）和实现更高 ApoB 血浆降低的剂量反应研究中的潜在应用。

[0135] 证明了在第三次和最后一次注射后，TNC 治疗动物的 ApoB 血浆水平降低持续至少 8 周。在 C1 动物组中，在最后一次注射后，基于低 N:P 壳聚糖的 TNC 的 ApoB 血浆水平降低维持 7 周以上（图 13 和图 16），而无任何明显的炎症或肝脏毒性。这些结果表明 TNC 治疗特别有前途的耐久性和有效的控制释放性质。

[0136] 因此，本文公开了本文所描述的低 N:P 壳聚糖 ApoB siRNA TNC 以 1mg/kg 注射剂量实现了 ApoB 血浆水平的 35% 的降低以及 LDL/VLDL 胆固醇的 20% 的降低（图 13 和 14）。这些结果表明已经获得了有效的治疗结果，这是因为发表的先前主张的成功结果使用用于 ApoBsiRNA 的脂质体递送系统需要较高的剂量以实现类似或更高的 ApoB/LDL-VLDL 胆固醇降低，并且这些剂量与肝脏毒性以及 ALT 和 AST 水平的提高有关（Zimmermann 等人，2006, Nature, 111-114 ; Soutschek 等人，2004, Nature432:173-178）。例如，使用 5mg kg^{-1} 的 siRNA 与脂质结合的制剂（SNALP）实现在 ApoB 血浆水平方面 73% 的降低（Zimmermann 等人，2006, Nature, 111-114）；与本发明的结果相比，这种高 5 倍的注射浓度实现了高 2.5 倍的 ApoB 血浆降低。此外，在使用由 Merck Inc. 开发的第二代脂质 LNP-OCD（LNP201）的 Ldlr-/+、Cetp-/+ 小鼠模型中，以 3mg kg^{-1} 使用靶向 ApoB 的 siRNA 显示出约 70% 的 LDL 减少（Tadin-Strapps 等人，2011, J lipid Res, 52:1084-1097）。另外，取决于所使用的 siRNA 序列，需要 50mg kg^{-1} 的裸露胆固醇修饰的 siRNA 以实现 ApoB 血浆水平 68% 和 31% 的减少（Soutschek 等人，2004, Nature, 173-178）。另外，与随附的研究相反，在所述研究中 C57BL/6 小鼠组饲喂高脂肪饲料以模拟动脉粥样硬化直至研究结束，在饲喂常规饲料（瘦对照）的正常 C57BL/6 小鼠中进行这些研究。

[0137] 此外，目前处于临床 III 期试验的抗 ApoB 反义寡核苷酸（AOS）ISIS-147764 的腹膜内给予需要向用高脂肪饲喂的 C57BL/6 给予至少 25mg kg^{-1}、每周两次，从而在 6 至 8 周的治疗后实现 55% 的 ApoB 血浆降低水平。另外，Crooke 等人报道在给予 50mg kg^{-1} 每周两次持续 6 至 8 周后，血浆胆固醇恢复正常（Crooke 等人，2005, J Lipid Res, 46:872-884）。在治疗的第四周（50mg kg^{-1}，两次 / 周）观察到 ISIS-147764 对胆固醇血浆降低的影响。

[0138] 本文所描述的组合物和方法清楚地表明当与现有技术相比时，使用相对低剂量（1mg kg^{-1}）时 ApoB 降低的效率。另外，本发明中变得清楚的是使用本发明披露并公开的 TNC，提高剂量将导致增强的 ApoB 和 LDL/VLDL-C 血浆降低，这是因为 ApoB 降低总是表现为剂量依赖性的（Zimmermann 等人，2006, Nature, 441:111-114 ; Soutschek 等人，2004, Nature, 432:173-178 ; Crooke 等人，2005, J Lipid Res, 46:872-884 ; 和 Crooke, 2005, Expert Opin Biol Ther, 5:907-917）。

[0139] 本发明提供了用于治疗糖尿病以及相关病症和症状的方法。这些糖尿病和相关病症包括胰岛素依赖性糖尿病（I 型糖尿病）、非胰岛素依赖性糖尿病（II 型糖尿病）、胰岛素耐受、高胰岛素血症和糖尿病引起的高血压。其他糖尿病相关病症包括肥胖症以及血管、眼、肾、神经、自主神经系统、皮肤、结缔组织和免疫系统的损伤。本文所描述的组合物可以

单独使用或者与胰岛素和 / 或降血糖化合物结合使用。

[0140] 本发明提供了用于治疗癌症的方法。这些癌症包括乳腺癌、神经胶质瘤、大肠癌、肺癌、小细胞肺癌、胃癌、肝癌、血癌、骨癌、胰癌、皮肤癌、头颈癌、皮肤或眼内黑素瘤、子宫肉瘤、卵巢癌、直肠或结直肠癌、肛门癌、结肠癌、输卵管癌、子宫内膜癌、宫颈癌、外阴癌、鳞状细胞癌、阴道癌、霍奇金氏病、非霍奇金氏淋巴瘤、食道癌、小肠癌、内分泌癌、甲状腺癌、甲状旁腺癌、肾上腺癌、软组织肿瘤、尿道癌、阴茎癌、前列腺癌、慢性或急性白血病、淋巴细胞性淋巴瘤、膀胱癌、肾癌、输尿管癌、肾细胞癌、肾盂癌、CNS 肿瘤、神经胶质瘤、星形细胞瘤、多形性胶质母细胞瘤、原发性 CNS 淋巴瘤、骨髓瘤、脑干神经胶质瘤、垂体腺瘤、葡萄膜黑素瘤、睾丸癌、口腔癌、咽癌、小儿肿瘤、白血病、成神经细胞瘤、成视网膜细胞瘤、神经胶质瘤、成横纹肌细胞瘤和肉瘤。

[0141] 克服 MDR 的一个方法是使用抑制 P-gp 输送活性的 P-gp 调节剂或逆转剂化合物。然而，它们与化疗剂的药代动力学相互作用以及毒性限制了它们的临床应用。作为另外一种选择，可以通过 RNA 干扰（RNAi）抑制 P-gp 的表达。与化学调节剂不同，该技术可以为 P-gp 的下调以及耐受性逆转提供更特异的方法。

[0142] 使用 siRNA 或 shRNA 的多种研究证明 RNAi 克服多种药物耐受性表型的潜在应用。2003 年发表了示出 RNAi 通过 p-gp 抑制介导耐受性逆转的原理性证据的首次研究（Nieth 等人，2003，FEBS letters545(2-3):144-150 和 Wu 等人，2003，Cancer research63(7):1515）。两项研究均使用了用 siRNA 的瞬时方法来调节不同细胞模型中多种药物耐受性表型。使用 200nM 的 siRNA，Hao 等人能够在 MCF-7/ADR 和 A2780Dx5 中将高度耐受性 MDR 细胞系的 p-gp 水平抑制 65%。此外，他们显示靶向 MDR1 的 siRNA 逆转了对 p-gp 可输送药物（多柔比星）的耐受性，但是它不影响对非 p-gp 底物的羟基脲的敏感性。这些数据表明由 siRNA 介导的 P-gp 表达的沉默是特异性的。然而，尽管使用了较低的 siRNA 浓度（100nM），但是在源自胰腺癌的细胞系（EPP85-181RDB）和胃癌细胞（EPG85-257RDB）中实现了几乎 90% 的最显著的瞬时 MDR 逆转（Nieth 等人，2003，FEBS letters545(2-3):144-150）。最近，Donmez 等人（2011，Biomedicine and Pharmacotherapy65(2):85-89）显示尽管浓度低至 20nM，但是在多柔比星耐受性 MCF-7 细胞中实现了 89% 的 MDR1 的基因沉默活性。这些数据表明 RNAi 的效力可以是 siRNA 序列依赖性的和细胞系依赖性的。

[0143] 除 siRNA 之外，将稳定的抗 MDR1/P-gp shRNA 表达载体用于调节 MDR 表型。在一项研究中，与 siRNA 相比，在紫杉醇耐受性 SKOV-3TR 和 OVCAR8TR 卵巢癌细胞系中 shRNA 表达对 MDR1/P-gp 的下调具有相似的效率（Duan 等人，2004，Molecular cancer therapeutics3(7):833）。此外，Stege 等人（2004，Cancer gene therapy11(11):699-706）报道了通过将 shRNA- 表达载体（psiRNA/MDR-A）引入到极高药物耐受性的人胃癌细胞系 EPG85-257RDB 中完全逆转了 P-gp 表达。类似地，Yague 等人（2004，Gene therapy11(14):1170-1174）观察到了通过引入 shRNA 表达载体 pSUPER，在 K562 白血病细胞中完全逆转多柔比星耐受性。使用相同方法，Shi 等人（2006，Cancer biology&therapy5(1):39-47）还显示通过 shRNA 的内源表达引起了 MDR1/P-gp 基因表达和功能的稳定下调，其表达了含有 MDR1-siRNA 的新型表达盒和人表皮样癌细胞系（KBv200）中的 EGFP 表达基因。

[0144] 在所有上述研究中，使用了两种可商购的脂质体 Lipofectamine2000（Li 等人，2006, European journal of pharmacology, 536(1):93-97 和 Donmez, Y. 和 U. Gunduz, 2011, Biomedicine&Pharmacotherapy65(2):85-89）以及 oligofectamine（Nieth 等人，2003, FEBS letters545(2-3):144-150；Wu 等人，2003, Cancer research63(7):1515；Stierle 等人，2005, Biochemical pharmacology70(10):1424-1430；和 Stierle 等人，2007, Biochimie89(8):1033-1036）。到目前为止，壳聚糖已用于递送靶向 MDR1 基因的 shRNA 编码质粒。在该研究中，通过复合凝聚形成纳米颗粒（Yang 等人，2009, J Huazhong Univ Sci Technolog Med Sci. Apr;29(2):239-42）。在该研究中报道的最大 mRNA 降低为 52.6%，其中紫杉醇化疗耐药的时间依赖性逆转为多达至 61.3%。到目前为止，尚未报道过壳聚糖用于递送抗 P-gp siRNA 的应用。

[0145] 本文所描述的组合物可以单独使用或者其他抗癌化合物结合使用，抗癌化合物如：阿西维辛；阿柔比星；盐酸阿考达唑；山油柑碱；阿多来新；阿地白介素；六甲密胺；丙氨肽霉素；醋酸双氢胺蒽醌；氨鲁米特；胺苯吖啶；阿那曲唑；氨茴霉素；门冬酰胺酶；曲林菌素；氮杂胞苷；氮替派；阿佐霉素；巴马司他；苄替哌；比卡鲁胺；盐酸必桑郡；二甲磺酸双奈法德；比折来新；硫酸博来霉素；布喹那钠；溴匹利明；白消安；放线菌素 C；卡普睾酮；卡拉酰胺；卡贝替姆；碳铂；卡氮芥；盐酸卡柔比星；卡折来新；西地芬戈；苯丁酸氮芥；西罗里霉素；顺铂；克拉屈滨；甲磺酸克雷斯托；环磷酰胺；阿糖胞苷；达卡巴嗪；更生霉素；盐酸柔红霉素；脱氧氮杂胞苷；右奥马铂；地扎呱宁；甲磺酸地扎呱宁；地吖醌；多西他赛；阿霉素；盐酸阿霉素；着洛西芬；柠檬酸着洛西芬；丙酸屈他雄酮；偶氮霉素；依达曲沙；盐酸依洛尼塞；依沙芦星；恩络铂；苯环丙炔酯；依匹哌啶；盐酸表柔比星；厄布洛唑；盐酸依索比星；雌莫司汀；磷酸雌莫司汀钠；依他硝唑；依托泊苷；磷酸依托泊苷；氯苯乙嘧胺；盐酸法曲唑；法扎拉滨；维甲酰酚胺；氟尿苷；磷酸氟达拉滨；氟尿嘧啶；氟环胞苷；磷喹酮；福司曲星钠；吉西他滨；盐酸吉西他滨；羟基脲；盐酸伊达比星；异环磷酰胺；依莫佛新；干扰素 α-2a；干扰素 α-2b；干扰素 α-n1；干扰素 α-n3；干扰素 β-1a；干扰素 γ-1b；异丙铂；盐酸依立替康；醋酸兰瑞肽；来曲唑；醋酸亮丙瑞林；盐酸利阿唑；洛美曲索钠；罗氮芥；盐酸洛索蒽醌；马丙考；美登素；盐酸氮芥；醋酸甲地孕酮；醋酸美仑孕酮；苯丙氨酸氮芥；美洛格瑞；巯嘌呤；甲氨喋呤；甲氨喋呤钠；四甲尿烷亚胺；美妥替哌；米汀多酰胺；米托卡星；丝裂红素；丝林霉素；丝裂马菌素；丝裂霉素；丝裂帕菌素；米托坦；盐酸米托蒽醌；麦考酚酸；洛可达唑；诺加拉霉素；奥马铂；亚磺酰吡啶；紫杉醇；天门冬酰胺酶；佩利霉素；戊氮芥；硫酸培来霉素；哌磷酰胺；哌泊溴烷；哌泊舒凡；盐酸必散特隆；普卡霉素；普洛美坦；卟吩姆钠；泊非霉素；松龙苯芥；盐酸甲基苄肼；嘌呤霉素；盐酸嘌呤霉素；吡唑霉素；利波腺苷；洛太米特；沙芬戈；盐酸沙芬戈；甲环亚硝脲；双曲秦；磷乙酰天冬氨酸钠；稀疏霉素；盐酸螺旋锗；螺旋氮芥；顺螺铂；链黑霉素；链脲霉素；磺氯苯脲；他利霉素；紫杉醇；泰素帝；替可加兰钠；喃氟啶；盐酸替洛蒽醌；替莫泊芬；替尼泊苷；台罗西隆；睾内酯；硫咪嘌呤；硫鸟嘌呤；噻替哌；噻唑呋林；替拉扎明；盐酸拓扑替康；柠檬酸托瑞米芬；甲基诺龙；磷酸曲西瑞宾；曲美沙特；三甲曲沙葡萄醛酯；曲普瑞林；盐酸妥布氯唑；尿嘧啶氮芥；乌瑞替哌；伐普肽；维替泊芬；维替泊芬；硫酸长春碱；硫酸长春新碱；长春花碱酰胺；长春地辛；硫酸长春地辛；硫酸长春匹定；硫酸长春苷酯；硫酸环氧长春碱；酒石酸长春烯碱；硫酸异长春碱；硫酸长春氮芥；伏罗唑；折尼拉汀；新制癌菌素；或盐酸佐柔比

星。

[0146] 其他抗癌药物包括：20- 表 -1,2,5- 二羟基维生素 D3；5- 乙炔基尿嘧啶；阿比特龙；阿柔比星；酰基富烯；腺环戊醇(adecypenol)；阿多来新；阿地白介素；ALL-TK 拮抗剂；六甲密胺；氨莫司汀；阿米达克斯(磺胺异氧唑，amidox)；阿米斯丁；氨基乙酰丙酸；氨柔比星；胺苯吖啶；阿那格雷；阿那曲唑；穿心莲内酯；血管生成抑制剂；拮抗剂 D；拮抗剂 G；安雷利克斯；抗背部化形态发生蛋白 -1；抗雄激素物质，前列腺癌；雌激素对抗剂；抗瘤酮；反义寡核苷酸；甘氨酸艾菲地可宁；细胞凋亡基因调节剂；细胞凋亡调节剂；脱嘌呤核酸；ara-CDP-DL-PTBA；精氨酸脱氨基酶；阿苏拉尼(asulacrine)；阿他美坦；阿曲氮芥；海洋环肽 1；海洋环肽 2；海洋环肽 3；阿扎司琼；阿扎毒素；重氮酪氨酸；浆果赤霉素 III 衍生物；巴览醇(balanol)；巴马司他；BCR/ABL 拮抗剂；苯并氯辛(benzochlorins)；苯甲酰星形孢菌素；β- 内酰胺衍生物；β-alethine；β- 克拉霉素 B（β-clamycin B)；桦木酸；bFGF 抑制剂；比卡鲁胺；必桑郡；双氮丙啶基精胺(bisaziridinylspermin)；双奈法德；比斯他西 A（bistratene A)；比折来新；布瑞福特(breflate)；溴匹利明；布朵替坦；丁硫氨酸亚砜胺；卡泊三醇；卡弗他丁 C；喜树碱衍生物；金丝雀痘 IL-2；卡培他滨；氨甲酰 - 氨基 - 三唑；羧基氨基三唑；CaRestM3；CARN700；软骨源抑制剂；卡折来新；酪蛋白激酶抑制剂(ICOS)；澳粟精胺；天蚕抗菌肽 B；西曲瑞克；氯仑(chlorlns)；氯喹噁啉磺酰胺(chloroquinoxaline sulfonamide)；西卡前列素；顺叶啉；克拉屈滨；氯米芬类似物；克霉唑；克里斯霉素 A；克里斯霉素 B；考布他汀 A4；考布他汀类似物；科纳基尼(conagenin)；克拉贝司丁(crambescidin)816；克雷斯托(克利钠托，crisnatol)；克利特非辛 8；克利特非辛 A 衍生物；库拉辛 A（curacin A)；环戊烷蒽醌；环普拉坦(cycloplatam)；西匹霄素(cypemycin)；阿糖胞苷十八烷基磷酸盐(cytarabine ocfosfate)；溶细胞因子；磷酸己烷雌酚；达昔单抗；地西他滨(decitabin)；脱氢代代宁 B(dehydrodidemnin B)；地洛瑞林；右异环磷酰胺；右丙亚胺；右维拉帕米；地吖醌；代代宁 B；地丹诺辛(didox)；二乙基去甲精胺(diethylnorspermine)；二氢 -5- 氮杂胞苷；二氢紫杉酚；9- 多喜霉素(9-dioxamycin)；二苯基螺莫司汀；二十二烷醇；多拉司琼；脱氧氟尿苷；屈洛西芬；屈大麻酚；多卡霉素 SA(duocarmycin SA)；依布硒啉(ebselen)；依考莫司汀；依地福新；依决可单抗；依氟鸟氨酸；榄香烯；乙嘧替氟；表柔比星；依立雄胺；雌莫司汀类似物；雌激素激动剂；雌激素拮抗剂；依他硝唑；磷酸依托泊苷；依西美坦；法曲唑；法扎拉滨；维甲酰酚胺；非格司亭；非那雄胺；黄酮吡醇(flavopiridol)；氟卓斯汀；夫阿斯通(fluasterone)；氟达拉滨；盐酸氟柔红霉素(fluorodaunorunicin)；福芬美克(forfenimex)；福美司坦；福司曲星(fostriecin)；福莫司汀(fotemustine)；钆特沙弗林(gadolinium texaphyrin)；硝酸镓；加洛他滨；加尼瑞克；明胶酶抑制剂；吉西他滨；谷胱甘肽抑制剂；西磺非(hepsulfam)；神经生长因子(heregulin)；六亚甲基二乙酰胺；金丝桃素；伊班膦酸；伊达比星；碘昔芬；伊决孟酮；依莫佛新；伊洛马司他；咪唑并吖啶酮；咪喹莫特；免疫促进肽；胰岛素样生长因子受体 -1 抑制剂；干扰素激动剂；干扰素；白细胞介素；碘苄胍；碘阿霉素；4- 甘薯黑苦醇；伊立替康；伊罗普拉；伊索格拉定；异苯嘎唑(isobengazole)；软海绵素 B（isohomohelicondrin B)；伊他司琼；叶克立得(海绵生物肽，jasplakinolide)；环缩肽 KF（kahalalide F)；片螺素 N- 三乙酸盐；生长妥林(兰瑞肽，lanreotide)；雷拉霉素(leinamycin)；来格司亭；硫酸蘑菇多糖；乐普他丁(leptolstatin)；来曲唑；白血病抑制因子；白细胞 α 干扰素；亮丙立

得 + 雌激素 + 黄体酮 ;亮丙瑞林 ;左旋咪唑 ;利阿唑 ;直链多胺类似物 ;亲脂二糖肽 ;亲脂铂化合物 ;利索里胺 7 (lissoclinamide7);洛巴铂 ;蚯蚓磷脂 ;洛美曲索 ;氯尼达明 ;洛索蒽醌 ;洛伐他汀 ;罗唑利宾 ;勒托替康 ;镥特萨卟啉(lutetium texaphyrin);利索茶碱(lysofylline);溶菌肽 ;美坦新 ;曼诺他丁 A (mannostatin A);马立马司他(marimastat);马索罗酚(masoprocol);脉丝平(maspin);基质溶解因子抑制剂 ;基质金属蛋白酶抑制剂 ;美洛格瑞 ;美巴龙(merbarone);美替瑞林 ;甲硫氨酸酶 ;甲氧氯普胺 ;MIF 抑制剂 ;米非司酮 ;米替福星 ;米立司亭 ;错配双链 RNA ;米托胍腙 ;二溴卫矛醇 ;丝裂霉素类似物 ;米托萘胺(mitonafide);米托托新(mitotoxin) 成纤维细胞生长因子 - 肥皂草毒蛋白 ;米托蒽醌 ;莫法罗汀 ;莫格拉司亭 ;单克隆抗体 ;人绒毛膜促性腺激素 ;单磷酰脂质 A+ 分枝杆菌(myobacterium) 细胞壁 sk ;莫哌达醇(mopidamol);多药物抗性基因抑制剂 ;基于多瘤抑制剂 -1 的疗法 ;芥子(mustard) 抗癌化合物 ;印度洋海绵 B (mycaperoxide B);分枝杆菌细胞壁提取物 ;美拉普龙(myriaporone);N- 乙酰地那林 ;N- 取代苯酰胺类 ;奈法瑞林 ;纳格替普(nagrestip);纳洛酮 + 喷他佐辛 ;纳帕维(napavin);萘萜二醇(naphterpin);那托司亭(nartograstim);奈达铂 ;奈莫柔比星 ;奈立膦酸 ;中性肽链内切酶 ;尼鲁米特 ;尼萨霉素(nisamycin);氧化氮调节剂 ;一氧化二氮抗氧化剂 ;尼图仑(nitrullyn);O6- 苯甲基鸟嘌呤 ;奥曲肽 ;奥克西农(okicenone);寡核苷酸 ;奥那斯酮 ;昂丹司琼 ;奥拉辛(oracin);口服细胞因子诱导物 ;奥马铂 ;奥沙特隆 ;奥沙利铂 ;奥沙霉素(oxaunomycin);紫杉醇类似物 ;紫杉醇衍生物 ;帕洛胺(palauamine);帕米托左新(palmitoylrhizoxin);帕米膦酸 ;人参炔三醇 ;巴洛米芬 ;帕拉沙星(parabactin);泊泽尼普定 ;培加帕酶(pegaspargase);培得星 ;木聚硫钠 ;喷托他丁 ;喷曲唑(pentrozole);潘氟隆 ;哌磷酰胺 ;紫苏子醇 ;苯阿诺霉素(phenazinomycin);乙酸苯酯 ;磷酸酶抑制剂 ;溶血链球菌 Su ;盐酸匹罗卡品 ;吡喃阿霉素 ;吡曲克辛 ;普司亭 A (placetin A);普司亭 B (placetin B);纤溶酶原激活物抑制剂 ;铂复合物 ;铂化合物 ;铂 - 三胺复合物 ;卟吩姆钠 ;泊非霉素 ;丙基双吖啶酮 ;前列腺素 J2 ;蛋白酶体抑制剂 ;基于蛋白 A 的免疫调节剂 ;蛋白激酶 C 抑制剂,微藻(microalgal);蛋白酪氨酸磷酸酶抑制剂 ;嘌呤核苷磷酸化酶抑制剂 ;红紫素 ;吡唑啉吖啶 ;吡醇羟乙酯化的血红蛋白聚氧乙烯缀合物 ;raf 拮抗剂 ;雷替曲塞 ;雷莫司琼 ;ras 法呢基蛋白转移酶抑制剂 ;ras 抑制剂 ;ras-GAP 抑制剂 ;去甲基化雷替尼卜定 ;铼 Re186 依替膦酸盐 ;根霉素 ;核酶 ;RII 维甲酰胺 ;洛太米特 ;罗希吐碱 ;罗莫肽(romurtide);罗喹美克 ;如格吉农 B1 (rubiginone B1);如波西(ruboxyl);沙芬戈 ;萨托平(saintopin);SarCNU ;沙克非托 A (sarcophytol A);沙格司亭 ;Sdi1 模拟物 ;司莫司汀 ;老化细胞衍生的抑制因子 1 ;正义寡核苷酸 ;信号转导抑制剂 ;信号转导调节剂 ;单链抗原结合蛋白 ;西佐非兰 ;索布佐生 ;硼卡钠 ;苯乙酸钠 ;索喔醇(solverol);生长调节素结合蛋白 ;索纳明 ;膦乙天门冬氨酸 ;斯皮卡霉素 D (spicamycinD);螺莫司汀 ;斯耐潘定 ;海绵抑制素 1 (spongistatin1);角鲨胺 ;干细胞抑制剂 ;干细胞分裂抑制剂 ;斯皮酰胺(stipiamide);溶基质蛋白酶抑制剂 ;苏非诺辛(sulfinosine);强效血管活性肠肽拮抗剂 ;苏他地他(suradista);苏拉明 ;苦马豆素 ;合成的糖胺聚糖 ;他莫司汀 ;甲硫氨酸他莫昔芬 ;塔罗氮芥 ;他佐罗汀 ;替可加兰钠 ;喃氟啶 ;特鲁拉吡喃鎓盐(tellurapyrylium);端粒酶抑制剂 ;替莫泊芬(temoporfin);替莫唑胺 ;替尼泊苷 ;四氯癸烷氧化物(tetrachlorodecaoxide);四唑胺(tetrazomine);噻布拉亭(thaliblastine);萨力多胺 ;噻可拉林 ;血小板生成素 ;血小板生成素模拟物 ;胸腺法新 ;

胸腺生成素受体激动剂；胸腺曲南；促甲状腺激素；锡本紫红素乙酯；替拉扎明；二氯环戊二烯钛；拓扑替康；陶普森亭（topsentin）；托瑞米芬；全能干细胞因子；翻译抑制因子；维甲酸；三乙酰基尿苷；曲西瑞宾；曲美沙特；曲普瑞林；托烷司琼；妥罗雄脲；酪氨酸激酶抑制剂；酪氨酸磷酸化抑制剂（tyrphostins）；UBC 抑制剂；乌苯美司；尿生殖管源的生长抑制因子；尿激酶受体拮抗剂；伐普肽；伐若啉 B（variolin B）；载体系统，红细胞基因治疗；维拉雷琐；藜芦明；维丁（verdins）；维替泊芬；长春瑞滨；维克萨汀（vinxaltine）；维他辛（vitaxin）；伏罗唑；扎诺特隆；折尼拉汀；亚苄维 C；净司他丁替马拉美。

[0147] 抗癌补充加强化合物包括：三环抗抑郁药物（例如，丙米嗪、地昔帕明、阿米替林、氯米帕明、曲米帕明、多塞平、去甲替林、普罗替林、阿莫沙平和马普替林）；非三环抗抑郁药物（例如，舍曲林、曲唑酮和西酞普兰）；Ca++ 拮抗剂（例如，维拉帕米、硝苯地平、尼群地平和卡罗维林）；调钙蛋白抑制剂（例如，普尼拉明、三氟拉嗪和氯米帕明）；两性霉素 B；曲帕拉醇类似物（例如，他莫昔芬）；抗节律不齐药物（例如，奎尼丁）；抗高血压药（例如，利舍平）；降硫醇药（例如，丁硫氨酸和磺基肟）以及多个降低耐药性的化合物，如 Cremaphor EL。

[0148] 出于本发明的目的，在组合疗法中有用的其他化合物包括抗增殖化合物，吡曲克辛羟乙基磺酸盐；抗前列腺增生化合物，西托糖苷；良性前列腺肥大疗法化合物，坦洛新盐酸盐；前列腺生长抑制剂，喷托孟；放射性化合物，如纤维蛋白原 I125、脱氧葡萄糖 F18、氟多巴 F18、胰岛素 I125、胰岛素 I131、碘苄胍 I123、胆影钠 I131、碘安替比林 I131、碘胆甾醇 I131、碘马尿酸钠 I123、碘马尿酸钠 I125、碘马尿酸钠 I131、碘奥酮 I125、碘奥酮 I131、盐酸碘非他胺 I123、碘双胺喹 I125、碘双胺喹 I131、碘酞钠 I125、碘酞钠 I131、碘酪氨酸 I131、碘塞罗宁 I125、碘塞罗宁 I131、醋酸汞丙醇 197、醋酸汞丙醇 203、汞丙醇 197、硒蛋氨酸 Se75、三硫化二锑锝 Tc99m、比西酸锝 Tc99m、地索苯宁锝 Tc99m、依替膦酸锝 Tc99m、依沙美肟锝 Tc99m、锝 Tc99m 呋膦、葡庚糖酸锝 Tc99m、利多苯宁碘 Tc99m、甲溴苯宁锝 Tc99mm、亚甲膦酸锝 Tc99m、亚甲膦酸二钠锝 Tc99m、锝 Tc99m 巯替肽、奥昔膦酸锝 Tc99m、喷替酸锝 Tc99m、喷替酸钙三钠锝 Tc99m、司他比锝 Tc99m、西硼肟锝 Tc99m、二巯丁二酸锝 Tc99m、锝 Tc99m 胶体硫、替肟锝 Tc99m、替曲膦锝 Tc99m、甲状腺素 I125、甲状腺素 I131、碘托泊酮 I131、三油精 I125 和三油精 I131。

[0149] 如本文所使用的，“治疗”包括预防、抑制和减轻糖尿病及相关病症和症状。可以通过给予治疗有效量的本文所述的组合物来进行治疗。在其他情况下，可以通过同时给予治疗有效量的胰岛素和本文所述的组合物的组合来进行治疗。在其他情况下，当待治疗的糖尿病和相关病症是 II 型糖尿病、胰岛素抵抗、高胰岛素血症、糖尿病引起的高血压、肥胖症或者对血管、眼、肾、神经、自主神经系统、皮肤、结缔组织或免疫系统的损伤时，治疗可以包括同时给予治疗有效量的降血糖化合物和本文所述的组合物的组合。

[0150] 含有化学修饰的壳聚糖的实例为：基于壳聚糖的化合物，其具有（i）可以共价连接到几丁质和 / 或壳聚糖上，或者通过离子或疏水作用附着到与核酸或寡核苷酸复合的壳聚糖类化合物上的特异性或非特异性细胞靶向部分，和（ii）用于改变它们的物理、化学或生理学性质的几丁质和壳聚糖的多种衍生物或修饰。这些修饰的壳聚糖的实例为具有特异性或非特异性靶向配体的壳聚糖类化合物、膜渗透剂、亚细胞定位组分、内涵体溶解（细胞溶解）剂、核定位信号、胶体稳定剂、促进血液中长循环半衰期的试剂、以及化学衍生物，如盐类、O- 乙酰化衍生物和 N- 乙酰化衍生物。壳聚糖的用于化学修饰的一些位点包括：

C_2(NH-CO-CH_3 或 NH_2)、C_3(OH) 或 C_6(CH_2OH)。

[0151] 本文所描述的组合物是具有有效控制释放性质的适合的药物递送系统。本发明的组合物可以与任何已知组合疗法一起给予，如共给予适合递送药剂，如(但不限于)Mirus Transit TKO®亲脂性试剂、Lipofectin®、Lipofectamine™、Cellfectin®、聚阳离子(例如，聚赖氨酸)或脂质体。

[0152] 如本文所使用的“同时给予”包括如以混合物给予本文所描述的组合物和胰岛素和/或降血糖化合物，如，例如，在药物组合物中，或作为单独的制剂，如，例如，顺序、同时或以不同时间给予的单独的药物组合物。

[0153] 适合的降血糖化合物包括，例如，二甲双胍、阿卡波糖、醋酸己脲、格列美脲、妥拉磺脲、格列吡嗪、格列本脲、甲苯磺丁脲、氯磺丙脲、噻唑烷二酮类、α 麦芽糖酶抑制剂、双胍衍生物和曲格列酮，以及它们的混合物。

[0154] 本文所述的组合物的给予可以是肠胃外给予，其包括皮下、肌内、皮内、乳房内、静脉内和本领域中已知的其他给予方法。

[0155] 通过参考以下实施例，将更容易理解本发明。

[0156] 实施例 I

[0157] 制备基于壳聚糖/dsODN 或 siRNA 的纳米颗粒制剂

[0158] 使用质量控制的生产方法生产超纯壳聚糖样品，其中消除了污染物，包括蛋白质、细菌内毒素、有毒金属、无机和有机杂质。所有壳聚糖具有小于 50EU/g 的细菌内毒素。选择具有 92% 和 80% 的去乙酰化程度的壳聚糖(表 1)。这些壳聚糖是通过非均匀去乙酰化(heterogeneous deacetylation)产生的，从而使得乙酰基嵌段而不是随机分布。使用如上所述的亚硝酸将壳聚糖化学降解(Lavertu 等人，2006,Biomaterials,27:4815-4824；Lavertu 等人，2003,J Pharmaceutical and Biomedical Analysis,32:1149-1158)以获得 10kDa、40kDa 和 80kDa 的特定分子量，前者的 DDA 为 92% 和 80% 两者，后者为 80%DDA(表 1)。

[0159] 表 1

[0160] 壳聚糖的去乙酰化程度(DDA)、平均分子量(MN)、多分散指数(PDI)

[0161]

	实验	壳聚糖	DDA	Mn（kDa）	Mw	PDI
RecQL1	共聚焦	Rho-92-10	92.7	10	14	1.4
RecQL1	DLS，ESEM，保护，稳定性分析，FACS，qPCR	92-10	91.7	7.1	10.08	1.427
		80-40	82.5	38.37	53.4	1.392
		80-10	84.4	10.82	14.525	1.343
DDP-IV	酶学测试	92-10	92	7.46	9.32	1.25
		80-10	80	12.40	22.41	1.80
		80-80	80.0	93.8	187.6	2.0
ApoB DDP-IV	蛋白质分析，FACS，qPCR，在体内	92-10	92.2	8.501	12.645	1.494
		80-80	80.8	71.535	118.03	1.65
		80-10	84.4	10.820	14.525	1.343
ApoB DDP-IV	共聚焦	Rho-92-10	92.7	10	14	1.4
ApoB DDP-IV	稳定性分析，DLS，ESEM	92-10	91.7	7.1	10.08	1.427
		80-80	80.0	93.8	187.6	2.0
		80-10	80	12.40	22.41	1.80
		80-10	84.4	10.820	14.525	1.343
		80-40-5	82.5	38.375	53.410	1.392
		92-40-5	92.7	60.6	37.9	1.6

[0162] 靶向DPP-IV基因的小干扰RNA购自Dharmacon（Thermo scientific,Dharmacon RNAi Technologies,USA）。这些siRNA正义和反义链是合成的具有2个核苷酸(UU)3′突出。候选序列由靶向DPP-IV序列的四条序列的池组成(DPP-IV Seq1：CACUCUAACUGAUUACUUA,SEQ ID NO:1;DPP-IV Seq2:UAGCAUAUGCCCAAUUUAA,SEQ ID NO:2;DPP-IV Seq3:CAAGUUGAGUACCUCCUUA,SEQ ID NO:3;DPP-IV Seq4：UAUAGUAGCUAGCUUUGAU,SEQ ID NO:4)。靶向ApoB的siRNA序列是使用Dharmacon的2-ACE RNA化学定制合成的(ApoB Seq1:GUCAUCACACUGAAUACCAAU,(反义链是与2个核苷酸(AC)3′突出合成的),SEQ I D NO:5;ApoB Seq2（正义）:5′ CUC UCA CAU ACA AUU GAA AdTdT3′，SEQ ID NO:7;ApoB seq2（反义）:5′ UUU CAA UUG UAU GUG AGA GUUoUoU3′ (oU-oU)=2′ -O-甲基-脲苷突出，SEQ ID NO:6；ApoB Seq3（正义）:GGAAUCuuAuAuuuGAUCcA*A,SEQ ID NO:8;ApoB Seq3（反义）：uuGGAUcAAAuAuAAGAuUCc*c*U,SEQ I D NO:9;2′ O-甲基修饰的核苷酸用下标表示，硫代磷酸键用星号表示)。这些序列是由Soutschek等人(2004,Nature,432:173-178)，Zimmermann等人(2006,Nature,441:111-114)和Strapps等人(2010,Nucleic Acids Research,Vol.38,No.14)等人发表的。

[0163] 靶向RecQL.1的siRNA序列是使用Dharmacon的2-ACE RNA化学定制合成的(Seq1:5′ -GUUCAGACCACUUCAGCUUdTdT-3′,SEQ ID NO:10)。该序列是由Futami等人发表

的(2008,Cancer Sci,99:71-80;2008,Cancer Sci,99:1227-1236)。靶向MDR1的序列以预先合成的形式购自Dharmacon,并且通过它们的目录以产品号:M-003868-02-0010可得。候选由4条靶向MDR1的siRNA序列组成:Seq1(正义):5′ GCUGAUCUAUGCAUCUUAUUU3′,SEQ ID NO:11;Seq1(反 义):5 ′ AUAAGAUGCAUAGAUCAGCUU3 ′;SEQ ID NO:12;Seq2(正 义):5 ′ GACCAUAAAUGUAAGGUUUUU3 ′,SEQ ID NO:13;Seq2(反 义):5 ′ AAACCUUACAUUUAUGGUCUU3 ′,SEQ ID NO:14;Seq3(正 义):5 ′ GAAACUGCCUCAUAAAUUUUU3 ′,SEQ ID NO:15;Seq3(反 义):AAAUUUAUGAGGCAGUUUCUU3 ′,SEQ ID NO:16;Seq4(正义):5 ′ UCGAGUCACUGCCUAAUAAUU3 ′,SEQ ID NO:17;Seq4(反 义):5′ UUAUUAGGCAGUGACUCGAUU3′,SEQ ID NO:18。

[0164] 使用亚磷酰胺化学法(Integrated DNA Technologies,Inc)合成dsODN序列,并将其用于纳米颗粒稳定性和核酸酶保护测定。对于流式细胞术分析,使用6-羧基荧光素(6FAM)5′标记的dsODN(Integrated DNA technologies,USA)。

[0165] 用于本文所提供的壳聚糖纳米颗粒的物理化学鉴定的dsODN的基本原理是它们的siRNA模拟性质。这些模拟性质是由于siRNA和dsODN之间在结构水平(双链结构,长度(21聚体)和核苷酸突出)上的相似性所造成的。另外,siRNA和dsODN之间的电荷密度类似,这是由于它们主链上相同的磷酸酯残基个数/间隔所造成的。siRNA和dsODN之间的差异在于dsODN序列中用胸腺嘧啶替代尿嘧啶(U → T),并且在于dsODN糖主链的脱氧核糖基化。使用亚磷酰胺化学法(Integrated DNA Technologies,Inc)合成dsODN序列,并将其用于尺寸和 ζ 电位确定、纳米颗粒稳定性和核酸酶保护测定。对于共聚焦显微术和流式细胞术分析,使用6-羧基荧光素(6FAM)5′标记的dsODN(Integrated DNA technologies,USA)。

[0166] 使用1:1的葡萄糖胺:HCl之比、以5mg/mL的最终浓度在旋转搅拌器中以0.5%(w/v)将具有特定Mn和DDA的壳聚糖在盐酸中溶解过夜。然后,用去离子水稀释无菌滤过的溶液以获得所需的胺(壳聚糖去乙酰化基团)与磷酸盐(dsODN或siRNA核酸)的比值(N:P)。然后,通过将100μL稀释的壳聚糖溶液分别与浓度为0.05μg/μL的100μL dsODN或siRNA快速混合(吸放,pippeting)制备纳米颗粒(92-10-5、92-150-5、80-40-5、80-10-10、80-10-5、80-200-5和80-80-5);将浓度0.33μg/μL的dsODN用于稳定性分析和核酸酶保护分析,而将浓度0.1μg/μL的用于DLS和ESEM。使用前,将纳米颗粒在室温下孵育30分钟。

[0167] 实施例II

[0168] 转染实验

[0169] 对于体外转染,用0.976g/L的MES和0.84g/L的碳酸氢钠($NaHCO_3$)在pH6.5下制备高葡萄糖-达尔伯克氏改良的伊格尔氏培养基(DMEM-HG)。将不含胎牛血清(FBS)的转染培养基在37℃下在5%CO_2孵育箱中平衡过夜,并且在即将转染前使用无菌HCl(1N)在37℃下将pH调节至6.5。对于在96孔板中进行的siRNA转染,在使用前30分钟,如上所描述制备壳聚糖/siRNA纳米颗粒。将浓度0.05μg/μl(3,704nM)的100μl siRNA溶液用于siRNA与壳聚糖1:1(v/v)复合。复合后,siRNA的浓度为0.025μg/μl(1852nM),并且以0.00135μg/μl的终浓度(相当于100nM siRNA每孔(10pmol/孔))将纳米颗粒在含有DMEM-HG培养基的微量板中孵育。对于在24孔板中进行的dsODN转染,在使用前30分

钟，如上所描述制备壳聚糖 /dsODN 纳米颗粒。将浓度 0.05μg/μl（3,717nM）的 100μl dsODN 溶液用于 dsODN 与壳聚糖 1:1（v/v）复合。复合后，siRNA 的浓度为 0.025μg/μl（1858nM），并且以 0.00135μg/μl 的终浓度（相当于 600nM dsODN 每孔（60pmol/ 孔））将纳米颗粒在含有 DMEM-HG 培养基的微量板中孵育。用于 FACS 的 dsODN 和 siRNA 之间分子量的细微差异是由于 dsODN 的 6FAM 标记所造成的。将含有纳米颗粒的板在 37℃，5%CO_2 下平衡 10 分钟。将细胞上方的培养基吸出并补充 500μl（24 孔板）或 100μl 每孔（96 孔板）的含有最终浓度为 100nM/ 孔的基于 dsODN 或 siRNA 的纳米颗粒的平衡的转染培养基（pH6.5）。转染后 4 小时加入 FBS 至 10% 每孔的终浓度。将细胞与壳聚糖 /siRNA 纳米颗粒孵育直至转染后 24 小时进行分析。将 DharmaFECT™ 用作阳性对照，并将未处理的细胞和未复合的 siRNA 处理的细胞用作阴性对照。

[0170] 在所有测试细胞系中，将可商购的脂质体 DharmaFECT™（Dharmacon RNAi Technologies, Lafayette, CO, USA）用作转染效率的阳性对照。按照生产商的规程，制备 DharmaFECT™/dsODN（流式细胞术和共聚焦显微镜术）或 DharmaFECT™/siRNA（qPCR）的脂质 - 核酸复合物（1:2[w/v] 比）。

[0171] 参与体外转染的 HEK293、HepG2（ApoB 和 DPP-IV）、HT-29（DPP-IV）、Caco-2（DPP-IV）、Raw264.7（ApoB）、A549、LS174T 和 AsPC1 细胞系均购自美国典型细胞培养中心（ATCC, Manassas, VA）。MCF7-MDR 细胞系是 Hamid Morjani 博士（Paris, France）赠送的。细胞在最低必需培养基（HepG2）、McCoys（HT-29）、添加了 1.85g/L（HEK293）或 1.5g/l（RAW264.7）碳酸氢钠的高葡萄糖达尔伯克最低必须培养液（HEK293 和 RAW264.7）、（LS174T）、F12K（A549）、RPMI-1640（MCF-7MDR）和补充有 10%FBS（Cedarlane Laboratories, Burlington, ON）的 RPMI-1640（AsPC1）中在 37℃和 5%CO_2 条件下培养。HepG2 细胞补充有 8%FBS。对于转染，将细胞在 96 孔或 24 孔培养板（Corning, NY, USA）中铺板，从而在转染当天获得约 50% 至约 70% 的汇合度。

[0172] 实施例 III

[0173] RNA 提取和基因表达分析

[0174] 使用得自 Machery-Nagel 的 NucleoSpin® RNA XS 试剂盒进行总 RNA 提取。通过向每个孔中加入添加有 2μl TCEP 和灰色链霉菌（Streptomyces griseus）壳聚糖酶的 100μl RA1 溶胞缓冲液进行细胞溶解（Alameh 等人，2010, Int J Nanomedecine, 5:473-481）。当洗脱前，将样品与 RA3 缓冲液孵育来进行样品的 DNA 酶处理。使用 Agilent Bioanalyzer2100 进行 RNA 定量和性质（完整性）评价。RNA 完整指数（RIN）等于 7.5，这被认为是 qPCR 分析可接受的阈值。

[0175] 使用第一链 cDNA 转录试剂盒（the first strand cDNA transcriptor kit）（Roche, Laval, CA）进行总 RNA 的反转录。根据生产商的规程，使用 oligodT 引物，将总计 0.5-1μg 的 RNA/ 样品用于反转录反应。使用 ABI PRISM® 7900HT 序列检测系统进行壳聚糖 /siRNA 处理的细胞的基因定量。所有反应重复三次，并将 Ct 的平均值用于定量。使用得自 Roche™ 的 Universal Probe Library®（UPL）进行测定，确定基因表达水平。另一方面，使用预证的 TaqMan® 基因表达测定确定内源对照（TBP、HPRT）的基因表达水平。使用 ΔΔCT 法确定靶标基因的相对定量。简要地，将靶标基因的 Ct（循环阈值）值归一化至

内源对照基因(内源对照)($\Delta CT=Ct_{靶标}-Ct_{内源对照}$),并且与校准物进行比较:$\Delta\Delta CT=\Delta Ct_{样品}-\Delta Ct_{校准物}$。使用序列检测系统(SDS)2.2.2 软件(Applied Biosystems)计算相对表达(RQ),公式为 $RQ=2^{-\Delta\Delta CT}$。

[0176] 实施例 IV

[0177] 纳米颗粒分析

[0178] 在 25℃下以 137° 角,使用 Malvern Zetasizer Nano ZS®通过动态光散射确定壳聚糖 /dsODN 和壳聚糖 /siRNA 复合物的尺寸。在计算中使用折射率和纯水的粘度,重复测量样品三次。使用相同仪器在 25℃下同样使用多普勒激光测速法重复测量 ζ 电位三次以及水的介电常数用于计算。对于报告为强度平均直径的尺寸测定,将 50μl 的壳聚糖与 50μl 的 dsODN 或 siRNA 混合,然后使用 10mM NaCl 最终达到 500μl。对于 ζ 测量,使用 500μl 的 10mM NaCl 将纳米颗粒 1:2 稀释。如通过 DLS 所测量的,所有壳聚糖 /dsODN 纳米颗粒制剂在 45-156nm 范围内。当复合至 siRNA 序列 1(SEQ ID NO:5)和 2(SEQ ID NO:6 和 SEQ ID NO:7)时,如通过 DLS 所测量的,壳聚糖 /siRNA 纳米颗粒的平均直径在 55-105nm 的范围内(表 2)。对于完全修饰的 siRNA 序列 3(SEQ ID NO:8 和 SEQ ID NO:9),壳聚糖 -siRNA 纳米颗粒具有在 104-130nm 的范围内的平均直径(表 2)。在 dsODN 和未修饰的 siRNA-ApoB(序列 1 ;SEQ ID NO:5)和复合至壳聚糖的中度修饰的 siRNA-ApoB(序列 2 ;SEQ ID NO:6 和 SEQ ID NO:7)之间在纳米颗粒尺寸方面未观察到统计学差异。然而,当复合至不同的壳聚糖时,完全修饰的 siRNA 序列获得了较大的纳米颗粒。随着 Mn 的提高,壳聚糖 /dsODN 和壳聚糖 /siRNA 纳米颗粒表现出较高的尺寸值。当对于这些特定制剂比较 DDA 时,未观察到统计学显著差异。如所期望的,所有制剂中过量的壳聚糖导致产生带正电荷的纳米颗粒,如通过表 2 中 ζ 电位所示,其中 DLS 允许确定尺寸和 ζ 电位,而 ESEM 仅测量尺寸。

[0179] 表 2

[0180] 在壳聚糖制剂:80-10-5、80-10-10、80-40-5、80-200-5、92-10-5、92-150 中用 siRNA-RecQL1 或 siRNA-MDR1 形成的纳米颗粒 ;和在壳聚糖制剂 80-10-5、80-10-10、80-40-5、80-80-5、92-10-5、92-40-5 中用 siRNA-DPP-IV、ODN-ApoB 或 siRNA-ApoB 形成的纳米颗粒的具有标准偏差的平均直径—通过强度—和 ζ 电位

[0181]

样品	壳聚糖	尺寸(nm)	ζ电位(mV)	ESEM
MDR1	80-10-5	70±2	12±3	62±9
	80-200-5	156±35	18±3	131±5
	92-10-5	71±15	15±2	64±8
	92-150-5	140±49	17±5	123±6
RecQL1	80-10-10	91±7	18±2	73±9
	80-40-5	86±9	18±1	97±12
	92-10-5	63±8	23±1	54±6
DPP-IV(siRNA seq1 至 seq4 的池)	80-10-10	81±5	16±2	70-90
	80-80-5	111±12	20±2	60-100
	92-10-5	71±7	18±2	50-90
ApoB(ODN 模拟 siRNA ApoB seq1) (SEQ ID NO:5 的模拟)	80-10-10	64±6	19±2	67±7
	80-80-5	100±12	16±1	75±13
	92-10-5	45±4	21±2	66±5
ApoB(siRNA seq1) (SEQ ID NO:5)	80-10-5	80±7	27±2	62±5
	80-40-5	105±6	24±5	90±7
	92-10-5	55±3	28±2	60±3
	92-40-5	69±4	23±5	65±14
ApoB(siRNA seq2) (SEQ ID NO:6 和 SEQ ID NO:7)	80-10-5	90±4	26±4	70±8
	80-40-5	89±6	24±5	76±7
	92-10-5	57±3	26±4	54±6
	92-40-5	67±2	24±5	59±9
ApoB(siRNA seq3) (SEQ ID NO:8 和 SEQ ID NO:9)	80-10-5	139±7	19±3	89±7
	80-40-5	130±2	25±2	100±9
	92-10-5	105±3	22±5	78±5
	92-40-5	104±4	27±3	80±6

[0182] 使用环境扫描电子显微镜(ESEM,Quanta200FEG,FEI Company Hillsboro,OR,USA)成像如上所描述的形成的纳米颗粒。纳米颗粒形成后,将TNC喷涂在硅片基底上,然后溅射喷金(Agar Manual Sputter Coater,Marivac Inc.)。以20kV,在ESEM显微镜的高真空模式下进行观察。使用显微镜XT Docu软件(XT Docu,FEI Co),通过对每个部分测量来自至少6个不同区域的超过150个颗粒的直径来确定平均颗粒尺寸(+/-标准偏差)。通过将ESEM图像分析尺寸确定值与DLS尺寸数据进行比较来分析尺寸确定值的稳健性。

[0183] 结果显示取决于所使用的壳聚糖制剂,球形纳米颗粒(图1A、1B、2A和2B)的平均直径范围在45-156nm之间(表2,ESEM)。使用本文所描述的具体制剂获得的结果与动态光

散射结果一致(表 2),借此表明了本文所述的组合物和方法的稳健性。此外,所形成的纳米颗粒获得了可重复的小于 200nm 的尺寸,从而使得能够避免肾清除,从而改善体内转染效率并提高循环纳米颗粒的半衰期。

[0184] 使用不同的方法,在 pH6.5 和 8 下测试壳聚糖 /dsODN 纳米颗粒和壳聚糖 /siRNA 纳米颗粒的形成和稳定性持续多达至 20 小时。在微酸性 pH (pH6.5)下,在 N:P 比大于 2 时,形成了壳聚糖 /dsODN 纳米颗粒并且其稳定长达至 20 小时(图 3A 和图 3B)。在纳米颗粒形成后 4 小时,在 1 (pH6.5)和以上的 N:P 比时,未观察到可检测的 dsODN,然而在 pH8 下,对于相同的 N:P 比观察到完全的 dsODN 释放。更长的暴露时间(20h)导致在 N:P 比为 2 时用于 ApoB dsODN 的 dsODN 释放,然而较高的 N:P 比(N:P10)能够维持纳米颗粒的稳定性。在 pH 值为 8 时,并且对于相同的 10 的 N:P 比,观察到了部分 dsODN 释放。本文所描述的特定的壳聚糖制剂确保在 N:P 比大于 2(N:P>2)时,20h 的最短周期的纳米颗粒稳定性。使用基于荧光的测定的 Ribogreen 测定评价了壳聚糖 /siRNA 的稳定性,以在复合物不稳定后定量所释放的 siRNA。结果表明具有 5 和 10 的 N:P 比壳的聚糖 /siRNA 纳米颗粒在 pH6.5 下稳定长达 20 小时。当与其他制剂相比时,壳聚糖 80-10-5 显示出最低的稳定性。提高壳聚糖 80-10 的 N:P 比获得纳米颗粒稳定性的改善。除了壳聚糖 80-10,将 N:P 比提高至 5 以上不会获得纳米颗粒稳定性的提高,如数据所示(图 4A 和 5)。因此,在低 N:P 比下,纳米颗粒是不稳定的并且复合效率不是最优的。在中性 pH 下、N:P 比在 2 至 5 之间时,纳米颗粒是稳定的。在更碱性的 pH8 时,纳米颗粒是不稳定的,并且明确要求更高的 N:P 比和更高的分子量以提高稳定性。

[0185] 使用例如抗 -RecQL1siRNA 研究壳聚糖参数(DDA、MW 和 N:P 比)的影响。当提高壳聚糖 MW 时,随着纳米颗粒尺寸的提高,分子量清楚的影响是显著的(图 4B、4C 和 4D)。DDA 对纳米颗粒尺寸的影响极小。在高 N:P 时,对于较高的纳米颗粒尺寸,N:P 比似乎对纳米颗粒尺寸有影响。

[0186] 研究了 siRNA 浓度对纳米颗粒尺寸的影响。申请人的结果显示随着 siRNA 浓度的提高,纳米颗粒尺寸增大(图 4E)。

[0187] 使用 DNA 酶 I 保护分析评估低 N:P 比时壳聚糖保护 dsODN 序列的能力。在含有 20mM MES、1mM MgCl2 和浓度为 0、0.5、1、2、5 或 10 单位 DNA 酶 I 的缓冲液(pH6.5)中孵育壳聚糖 /dsODN 的纳米颗粒(6μl)。样品在 37℃下孵育 30 分钟。通过加入 2μl 的 EDTA (50mM)终止反应,然后在 72℃下加热 15 分钟。然后,通过凝胶电泳评估样品。结果表明制剂保护模拟双链寡核苷酸的 siRNA 的能力(图 6A 和 6B)。使用处理样品与对照的信号强度评估所有消化(即 0U DNA 酶 I=100% 强度)。当使用 1 单位 DNA 酶 /μg DNA 时,保护是显著的并且占约 70% 的复合物,然而当使用 0.5 单位 DNA 酶 I/μg DNA 时,阴性对照完全消化。当将 DNA 酶 I 浓度提高至 5 单位 /μg DNA 时,保护仍有效。

[0188] 在用壳聚糖酶处理转染细胞并因此降低与如前所描述的膜结合纳米颗粒有关的任何可能偏差后,使用荧光素标记的 dsODN 的 FACS 分析评价不同 DDA、Mn 和 N:P 比时 RecQL.1、DPP-IV 和 ApoB dsODN 纳米颗粒的细胞摄取(Alameh 等人,2010,Int J Nanomedicine,5:473-481)。有趣地,用 dsODN/ 壳聚糖纳米颗粒获得的结果表明有效摄取的细胞系依赖性。壳聚糖纳米颗粒摄取的细胞系依赖性与上述工作中不同的内吞途径有关(Bishop,1997,Rev Med Virol,7:199-209 ;Huang 等人,2002,Pharm Res,19:1488-1494)。

FACS 结果表明一般地，使用这些 dsODN 的细胞摄取显示在制剂之间无差异(图 7A 和图 7B)。使用本文出现的组合物的摄取效率对于 RecQL.1 (LS174T、A549 和 AsPC1 细胞系)在 80% 至 98% 的范围内，对于 ApoB (在 HEK293、HepG2 和 RAW264.7 细胞系中) 在 55% 至 80% 的范围内。DPP-IV dsODN 纳米复合物在 HepG2 细胞系中的摄取效率在 73% 至 99% 的范围内，并且在不同制剂(92-10-5、80-10-10 和 80-80-5)之间无统计学差异。使用壳聚糖 /dsODN 纳米颗粒的摄取效率达到了与商业化使用的脂质 - 核酸复合物(DharmaFECT™)相当或更高的水平，并且在细胞类型之间的相对变化类似(图 7A 和图 7B)。此外，这些结果与如下所述的共聚焦显微镜数据(图 8 至图 10)一致，其中图像显示所有细胞系的壳聚糖和 dsODN 的细胞分布，表明与 FACS 定量数据的定性关系。

[0189] 使用共聚焦显微术来评估颗粒摄取和内化进入本文所描述的不同细胞系(LS174T、MCF-7MDR、HEK293、HepG2、Caco-2 和 RAW264.7)。使用罗丹明标记壳聚糖，而使用荧光素标记 RecQL1-siRNA、DDP-IV-dsODN 和 ApoB-dsODN。对于 MCF-7MDR 纳米颗粒评估，使用 Cy3 标记的 siRNA。在标记处理后，通过使用如上所描述的步骤使壳聚糖 - 罗丹明和模拟 dsODN 的 siRNA 按 1:1 的体积混合形成纳米颗粒。结果表明在本发明中所描述的制剂能够有效地内化进入细胞，并在转染后 24 小时具有 siRNA 或 dsODN 的最大的释放。所包括的结果表明在 24 小时，siRNA 或 dsODN 和壳聚糖之间缺少共定位，证明在转染后 24 小时实现 siRNA 或 dsODN 载物的完全释放。此外，在大多数转染细胞中观察到的 siRNA 或 dsODN 的弥散染色类型表明复合物已逃逸出胞吞囊泡(endocytic vesicles) (图 8 至图 10)，这与使用壳聚糖 - 质粒 DNA 纳米颗粒的上述活细胞成像工作一致(Thibault 等人，2010, Mol Ther, 18:1787-1795)。时间过程研究显示颗粒内化是在转染后 1 小时内开始的，这时具有缓慢释放动力学，并且在转染后 24 小时达到最大。

[0190] 上文所描述的结果显示在本发明中所描述的制剂转染并将不同的 dsODN 和 siRNA 有效递送至多个细胞系的能力(图 8 至图 11)。

[0191] 实施例 V

[0192] 离体 siRNA 递送和基因表达抑制

[0193] 在不同的细胞系中评估壳聚糖特定制剂(92-10-5、80-40-5、80-10-10 和 80-80-5)的 siRNA 递送和后续基因表达(RecQL.1mRNA、DPP-IV 或 ApoB mRNA)抑制。结果显示当通过定量实时 PCR 测量时，编码 RecQL.1、DPP-IV 和 ApoB 的 mRNA 下调了 2 倍以上(图 11A 和 11B)。这些结果表明本文所述的制剂可以达到与商品化脂质体 DhamaFECT™ 相当的基因沉默水平而无任何显著细胞毒性，如使用阿尔玛(alamar)蓝测定所观察到的。

[0194] 更具体地，对于 LS174T 细胞中 RecQL.1mRNA 的抑制，壳聚糖 92-10-5 显示出高沉默水平(约 80%)，这与在本发明中作用阳性对照的当前金标准商品化制剂(约 80%)类似。制剂 80-40-5 和 80-10-10 也引起了显著的沉默，但是比 92-10-5 的程度低，并且还表现出非特异性模拟沉默的提高，特别是对于制剂 80-10-10 (图 11B)。本文所公开的结果清楚地显示所描述的壳聚糖基制剂以远低于他人先前所使用的那些(N:P>20)的 N:P 比(N:P=5)有效递送 siRNA 并敲低特异性基因的有效性。一般来说，申请人所有的低 N:P 比壳聚糖制剂达到了高水平的基因沉默，这支持了 FACS 数据(图 7B)。

[0195] 发现在 DPP-IV 或 ApoB mRNA 的信使 RNA 水平(mRNA)，使用由 N:P 比为 5 的壳聚糖 92-10 组成的特定制剂可以实现 70% 的基因沉默(图 11A)。然而，信使水平 70% 抑制翻译为

DPP-IV 的酶活力的 50% 的降低(图 12)。在酶水平上的这种抑制与使用商品化的脂质 - 核酸复合物 DharmaFECT™ 时所达到的水平相当。

[0196] 实施例 VI

[0197] 壳聚糖 /siRNA 纳米颗粒的体内有效性分析

[0198] 在 C57BL/6 小鼠模型中评价 siRNA-ApoB 纳米颗粒的体内效率。对于每种处理方式,用 1mg kg^{-1} 的靶向 ApoB 基因的 siRNA 注射 4 只动物(n=4,除了 Dα 中 n=2,C1 组中 n=3)。在 0.2ml 的最终体积(注射体积)中,将 1mg kg^{-1} 靶向 ApoB 基因的 siRNA 复合至低分子量壳聚糖(LMW-CS)。例如,对于 39g 小鼠,在以 0.5μg/μl(37,037nM)、78μl 的体积 siRNA 以壳聚糖 92-10-5 的 1:1 的比值复合后,给予 39μg siRNA—对于 1mg kg^{-1} 的剂量计算出的量。那么,给予 156μl 的总体积。复合后,siRNA 的浓度为 0.25μg/μl (18,518nM)。具体地,将靶向 ApoB 基因的 siRNA 以 5 的 N:P 比(N:P5)复合至壳聚糖制剂 92-10 (DDA,Mn)。总体上,按照表 3 中的时间表,在不同时间对 5 个组(C1 至 C5 ;n=4/ 组)进行 TNC 处理,其中公开了多个 C57BL/6 小鼠组(n=4 只动物每组)中以 1mg kg^{-1} 抗 ApoB siRNA 的剂量的壳聚糖 /siRNA-ApoB 纳米颗粒的静脉注射时间表的数据。每天表示该周中进行注射或安乐死的那天。除了 Dα 组中 2 只小鼠仅注射 TNC92-10-5 一次并在 2 天后安乐死以检验治疗剂反应速度外,用 TNC92-10-5(Mn-DDA-N:P)对所有小鼠每周注射一次持续注射三周。除了那 2 只小鼠外,将所有其他小鼠在 2011 年 1 月的最后一周内安乐死。Dα 组用作阳性未处理的动脉粥样硬化对照,而 Dμ 为接受正常低脂饲料的阴性对照组。Dβ 组是无壳聚糖的 siRNA 递送、并注射了未复合的裸露的 siRNA 的阴性对照组。用于该研究的动物总数为 32。

[0199] 表 3

[0200] 动物研究日程表

[0201] 组

[0202]

日期	C1 (n=3)	C2 (n=4)	C3 (n=4)	C4 (n=4)	C5 (n=4)	Dα (n=4)	Dβ (n=4)	Dμ (n=4)
23/11/10					顺应（所有组）			
30/11/10	注射 #1							
07/11/10	注射 #2	注射 #1						
14/12/10	注射 #3	注射 #2	注射 #1					
21/12/10		注射 #3	注射 #2	注射 n#1			注射 #1	
28/12/10			注射 #3	注射 n#2	注射 n#1		注射 #2	
04/01/11				注射 n#3	注射 n#2		注射 #3	
11/01/11					注射 n#3			
18/01/11						Dα-2 天 注射(n=2) Dα n=		
20/01/11						安乐死 Dα-2 天		
26/01/11	安乐死(C1, C2, C3)							
27/01/11				安乐死(C4, C5)			安乐死(Dα, Dβ，Dμ)	

[0203] 根据蒙特利尔大学动物伦理委员会（CDEA）的要求，在实验前对所有动物顺应 2 周。在顺应 2 周后，将高脂饲料—D12492—饲喂给包括 Dα 阳性组（未处理组，n=4）和 Dβ 裸露 siRNA 处理组（n=4）在内的所有处理组，直至研究结束，即将动物安乐死的那天（表 3）。Dμ 组（n=4）饲喂常规饲料—D12450B—并将其用作标准阴性对照（瘦组）。所有处理动物每周注射一次持续三周（表 3）。使用低 N:P 壳聚糖制剂 92-10-5，用 1mg kg^{-1} 的 ApoB siRNA 注射所有 C 组动物。持续的三次每周注射发生在将 C1、C2、C3、C4、C5 组安乐死前的 7、6、5、4 和 3 周，以检查处理的时间进程。在安乐死前 2 天对 4 只阳性对照动脉粥样硬化 Dα 动物中的 2 只注射上述制剂以检查治疗的发生，而其余 2 只保持未处理。用 1mg kg^{-1} 未复合的裸露 ApoB siRNA 处理 D 组，而不处理正常低脂饲料组 Dμ （详见表 3）。

[0204] 在实验日程期间，每两周进行一次放血，并且每周在 TNC 注射前进行一次动物体重测量，直至研究结束。在实验日程结束并处死所有动物后（表 3），除去器官（如肝脏和肠）进行分析。

[0205] 对所有动物进行血液学、生物化学、血清学和组织学分析。例如，通过 VitaTech, Montreal, Canada 进行血清的血液学和生物化学分析。使用抗 ApoB ELISA 对血清中 ApoB 的减少进行定量，而使用比色测定进行 LDL/VLDL 胆固醇定量。使用苏木精 - 伊红染液对肝脏切片进行染色，以使脂肪空泡可视化。对于免疫细胞侵润肝脏的评价，用番红精 -O/ 固绿 / 铁苏木精染色石蜡包埋的切片。

[0206] 在安乐死当天采集血清后，对所有动物进行血液学和生物化学分析。在处理和未处理动物中对两个作为肝脏损伤的灵敏指示的丙氨酸氨基转移酶（ALT）和天冬氨酸氨基转移酶（AST）进行定量。处理组（C5）和阳性对照组（Dα）之间 ALT 和 ASL 血浆水平的比较未显示出任何显著差异，这表明用低 N:P 壳聚糖 -ApoB siRNA TNC 处理没有肝脏毒性作用（表 4）。

[0207] 此外，结果显示在处理和未处理组中血清白蛋白水平均为正常，这也表明了正常的肝功能。然而，siRNA-ApoB 处理的动物中总胆固醇的定量显示了与阳性对照组中类似的血清水平的可能升高(表 4)，其中 C5-2 给予了壳聚糖 /siRNA-ApoB 纳米颗粒，而 Dα -3 是动脉粥样硬化发展的阳性对照。每组仅有 1 只动物用于血液学分析，这是因为所需的血清体积较大并且需要处死 1 只动物。

[0208] 表 4

[0209] 处理的(C5-2)和未处理的(Dα -3)小鼠的血液学鉴定

[0210]

小鼠(组-小鼠)	C5-2	Dα-3
白蛋白(g/L)	35	35
胆红素 (总) (μmol/L)	0.4	0.7
胆红素 (结合的) (μmol/L)	0.1	0
ALP (IU/L)	58	55
ALT (IU/L)	120	121
AST (IU/L)	213	222
GGT (IU/L)	0	0
胆固醇 (mg/dL)	220	209
溶血	1+	1+
黄疸	正常	正常
脂血	正常	正常

[0211] 综合起来，这些结果表明由于不引起任何肝损伤，基于低 N:P 壳聚糖的 siRNA 纳米颗粒是安全的。

[0212] 使用抗 ApoB 商品化 ELISA 试剂盒(Uscn Life science Inc.,China)以 μg/ml 为单位评估载脂蛋白 B 的血浆浓度水平。取决于所测试的组和对照，ApoB 血浆水平的确定值在 597μg/mL 至 1,433μg/mL 之间变化。所获得的结果显示所有处理组的 ApoB 血浆水平比阳性动脉粥样硬化对照组 Dα 降低了约 35%，并达到了与标准阴性对照(Dμ)类似的水平(图 13)。Dα -2 天组在注射后 2 天显示出类似的降低，表明 TNC 注射后的快速沉默作用。

[0213] 在接受未复合 siRNA 的动物(对照组 ;Dβ -1)中 ApoB 水平降低 35%。虽然这种处理方式(Dβ -1)与 TNC 处理方式在 ApoB 血浆降低方面的有效性类似(图 13)，但是它在肝脏中导致高炎症反应(图 16H)从而限制其实现有效的并且治疗性沉默 /ApoB 血浆降低的剂量。另外，结果显示在 C1 动物组中在最后一次注射后，在基于低 N:P 壳聚糖的 TNC 的 ApoB 血浆水平方面降低维持 7 周以上(图 13)而无任何明显的炎症或肝脏毒性。这些结果表明 TNC 治疗特别有前途的耐久性和有效的控制释放性质。

[0214] Dβ -1 和 C1-C5 组之间毒性 / 炎症谱的比较表明了相比于裸露 siRNA，使用这些特定 LMW-TNC 的优势，因为未观察到明显的毒性 / 炎症谱(图 16 和表 4)。

[0215] 使用商品化定量比色检测试剂盒(BioAssay Systems,USA)测定 LDL/VLDL 胆固醇浓度。本文的结果显示与阳性对照(Dα)相比，处理动物证明 LDL/VLDL 降低约 20%(图 14)。有趣地，尽管观察到了 ApoB 降低，但与未处理组相比，C5 组显示出更高的 VLDL/LDL 浓度(图 13);与其他组相当的降低显示出 ApoB 和 VLDL/LDL 血浆浓度伴随降低。根据 ApoB 降低类似的上述结果，裸露 siRNA 处理的动物和 TNC 处理的动物之间的比较显示出 LDL/VLDL 胆固醇浓度类似的降低(图 13 和图 14)。

[0216] 用苏木精 - 伊红染色的石蜡固定肝脏切片的组织学分析显示，与阳性对照 Dα 相比，TNC 处理动物的胆固醇积累更低。发现 TNC 处理组、C3 和 Dβ 的肝脏切片具有低水平的

胆固醇积累，这与饲喂低脂饲料的标准阴性对照组 Dμ 类似(图 15)。相反，C4、C5 和 Dα2 组出现与阳性对照 Dα 类似的脂肪肝(图 15)，而 C1 和 C2 出现中度脂肪肝。综合地，结果表明在 C1、C2 和 C3 组中，TNC 可以通过 ApoB 抑制和 LDL/VLDL 降低防止肝脏中过多的胆固醇积累，并因此使得胆固醇能够肝转化为胆汁。在 C4 和 C5 组中观察到的结果似乎是由于 TNC 处理前过度的胆固醇积累所造成的。这些结果表明基于壳聚糖的 TNC 在动脉粥样硬化治疗中的有效性。

[0217] 用番红精 -O/ 固绿 / 铁苏木精染色的石蜡固定肝脏切片的组织学分析显示与裸露 ApoB siRNA 处理相比，基于壳聚糖的 TNC 减少炎症反应(图 16)。结果表明 C5 组表现出比致动脉粥样化对照组更高的淋巴样细胞侵润率，并因此表明炎症是由于肝脏中壳聚糖的沉积所造成的(图 16)。然而，C4、C3、C3 和 C1 组中肝脏的组织学分析显示了炎症的时间依赖性再吸收(图 16)。此外，Dα-2 天和阳性未处理对照 Dα-3 之间的比较显示壳聚糖对淋巴样细胞浸润的影响是时间依赖性的(图 16F 和图 16G)。据估计，治疗几周内的纳米颗粒依赖性炎症将保持约 3 周直至再吸收。

[0218] 图 15 和 16 的比较使得能够评估基于壳聚糖的纳米颗粒防止肝脏中胆固醇积累而不破坏肝脏完整性的效率，如通过 ALT/ASL 谱所显示的。此外，图 13 和 14 之间的比较查明了治疗的耐久性，从而确认了申请人先前对壳聚糖介导的缓慢释放的观察。

[0219] 通过在本研究期间每周对每组中每只动物的体重测量一次来评估处理对体重增加的作用。结果显示处理不影响体重增加(图 17)。然而，注意到在第一次 TNC 给予后的一周中，体重增加减缓。例如，C4 和 C5 组分别在研究的第 3 周和第 4 周接受了它们的第一次注射，这使得 C4 组体重稳定和 C5 组体重减轻。该作用在 C2 和 C3 组中也以较小量级存在(图 17)。事实上，与所有组相比，从研究开始直至其在 2010 年 12 月 28 日进行第一次注射，C5 组的平均体重具有加快的体重增加(平均体重)。在 2011 年 1 月 4 日(第 5 周)观察了该注射的影响，其中 C5 组的体重增加率显著减缓，这与图 18 中所观察到的相协调。

[0220] 尽管已结合具体实施方式说明了本发明，但是应理解能够进一步进行修改，并且本专利申请旨在覆盖本发明的任何变化、用途或改进，包括在本发明所属领域内的已知或习惯实践范围内和在随附权利要求范围内对本发明的这些偏离。

[0001]

PW16699_序列表

序列表

<110> MERZOUKI, Abderrazzak
BUSCHMANN, Michael D.

<120> 使用特异性的基于壳聚糖的纳米复合物用于有效并安全递送siRNA的组合物和方法

<130> 05015490-58PCT

<150> 61/489,306
<151> 2011-05-24

<150> 61/489,302
<151> 2011-05-24

<160> 18

<170> FastSEQ for Windows Version 4.0

<210> 1
<211> 19
<212> RNA
<213> 人工序列

<220>
<223> DPP-IV 序列 Seq1

<400> 1
cacucuaacu gauuacuua 19

<210> 2
<211> 19
<212> RNA
<213> 人工序列

<220>
<223> DPP-IV 序列 Seq2

<400> 2
uagcauaugc ccaauuuaa 19

<210> 3
<211> 19
<212> RNA
<213> 人工序列

<220>
<223> DPP-IV 序列 Seq3

<400> 3
caaguugagu accuccuua 19

<210> 4
<211> 19
<212> RNA
<213> 人工序列

<220>
<223> DPP-IV 序列 Seq4

<400> 4
uauaguagcu agcuuugau 19

<210> 5
<211> 21
<212> RNA
<213> 人工序列

<220>
<223> ApoB 序列 Seq1

<400> 5
gucaucacac ugaauaccaa u 21

[0002]

<210> 6
<211> 23
<212> RNA
<213> 人工序列

<220>
<223> ApoB seq 2 (反义)

<220>
<221> 修饰的碱基
<222> (21)...(22)
<223> um

<400> 6
uuucaauugu augugagagu uuu 23

<210> 7
<211> 21
<212> RNA
<213> 人工序列

<220>
<223> ApoB seq 2 (正义)

<220>
<221> 修饰的碱基
<222> (20)...(21)
<223> n = 胸腺嘧啶脱氧核苷

<400> 7
cucucacaua caauugaaan n 21

<210> 8
<211> 21
<212> RNA
<213> 人工序列

<220>
<223> ApoB Seq3 (正义)

<220>
<221> 修饰的碱基
<222> 19
<223> cm

<220>
<221> 修饰的碱基
<222> 7, 8, 10, 12, 13, 14
<223> um

<220>
<223> 位置 18 和 19 之间的硫代磷酸酯键

<400> 8
ggaaucuuau auuugaucca a 21

<210> 9
<211> 23
<212> RNA
<213> 人工序列

<220>
<223> ApoB Seq3 (反义):

<220>
<221> 修饰的碱基
<222> 1, 2, 11, 13, 18
<223> um

<220>
<221> 修饰的碱基
<222> 7, 21, 22
<223> cm

[0003]

<220>
<223> 位置 21 和 23 之间的硫代磷酸酯键

<400> 9
uuggaucaaa uauaagauuc ccu 23

<210> 10
<211> 21
<212> RNA
<213> 人工序列

<220>
<223> 靶向RecQL1的siRNA 序列 (Seq1)

<220>
<221> 修饰的碱基
<222> (20)...(21)
<223> n = 胸腺嘧啶脱氧核苷

<400> 10
guucagacca cuucagcuun n 21

<210> 11
<211> 21
<212> RNA
<213> 人工序列

<220>
<223> MDR1 Seq 1 (正义)

<400> 11
gcugaucuau gcaucuuauu u 21

<210> 12
<211> 21
<212> RNA
<213> 人工序列

<220>
<223> MDR1 Seq 1 (反义)

<400> 12
auaagaugca uagaucagcu u 21

<210> 13
<211> 21
<212> RNA
<213> 人工序列

<220>
<223> MDR1 Seq 2 (正义)

<400> 13
gaccauaaau guaagguuuu u 21

<210> 14
<211> 21
<212> RNA
<213> 人工序列

<220>
<223> MDR1 Seq 2 (反义)

<400> 14
aaaccuuaca uuuauggucu u 21

<210> 15
<211> 21
<212> RNA
<213> 人工序列

<220>
<223> MDR1 Seq 3 (正义)

<400> 15

[0004]

gaaacugccu cauaaauuuu u 21

<210> 16
<211> 21
<212> RNA
<213> 人工序列

<220>
<223> MDR1 Seq 3 (反义)

<400> 16
aaauuuauga ggcaguuucu u 21

<210> 17
<211> 21
<212> RNA
<213> 人工序列

<220>
<223> MDR1 Seq 4 (正义)

<400> 17
ucgagucacu gccuaauaau u 21

<210> 18
<211> 21
<212> RNA
<213> 人工序列

<220>
<223> MDR1 Seq 4 (反义)

<400> 18
uuauuaggca gugacucgau u 21

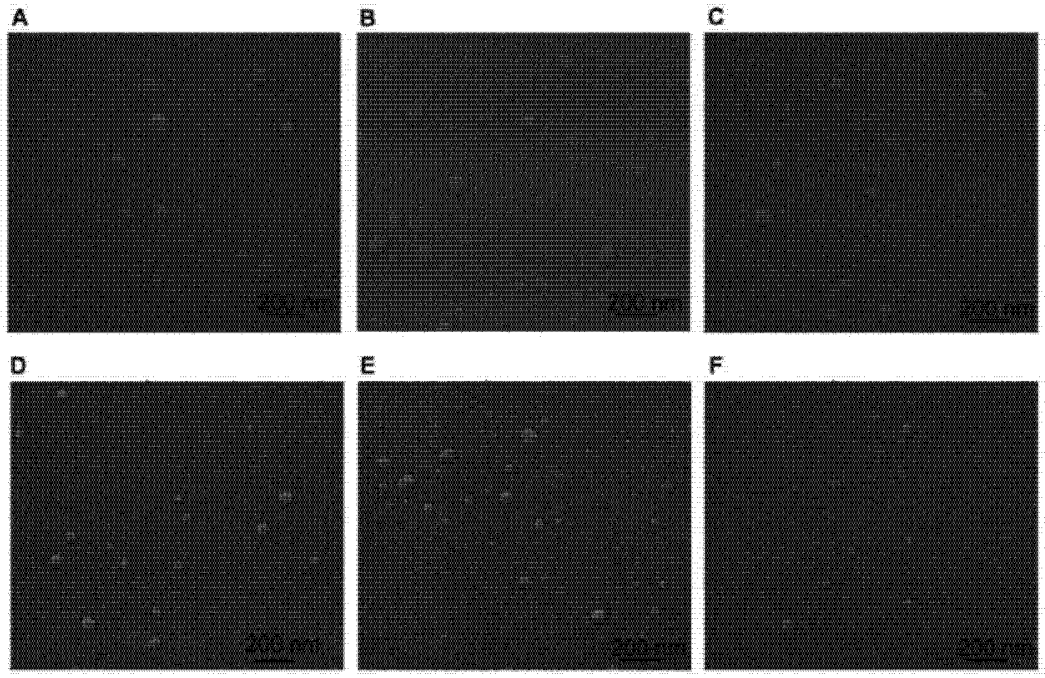

图 1A

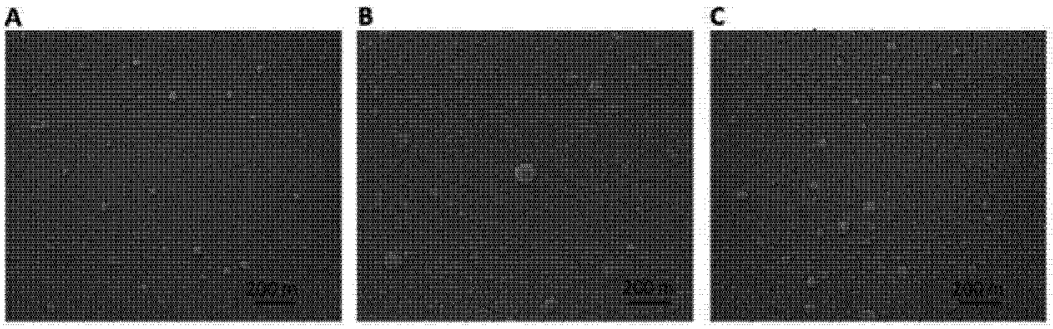

图 1B

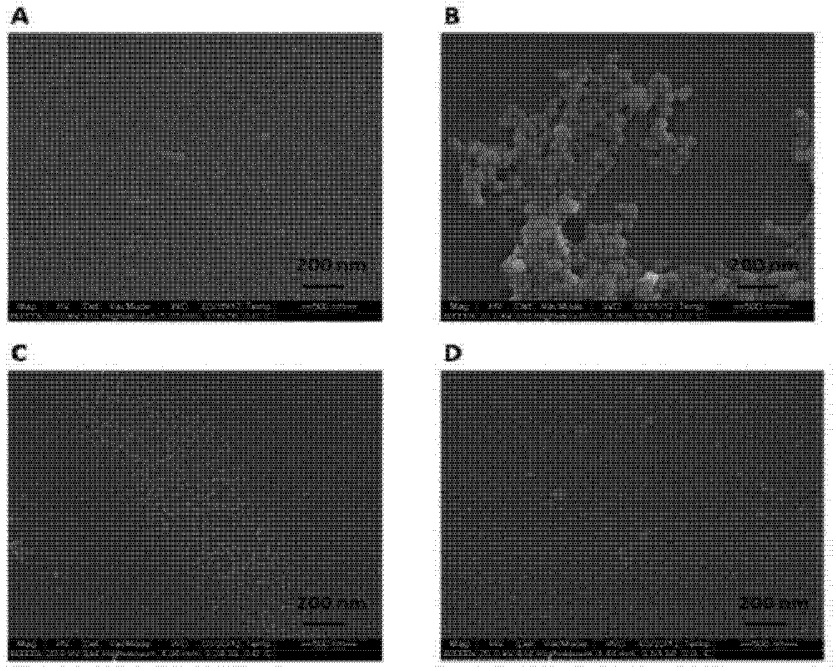

图 2A

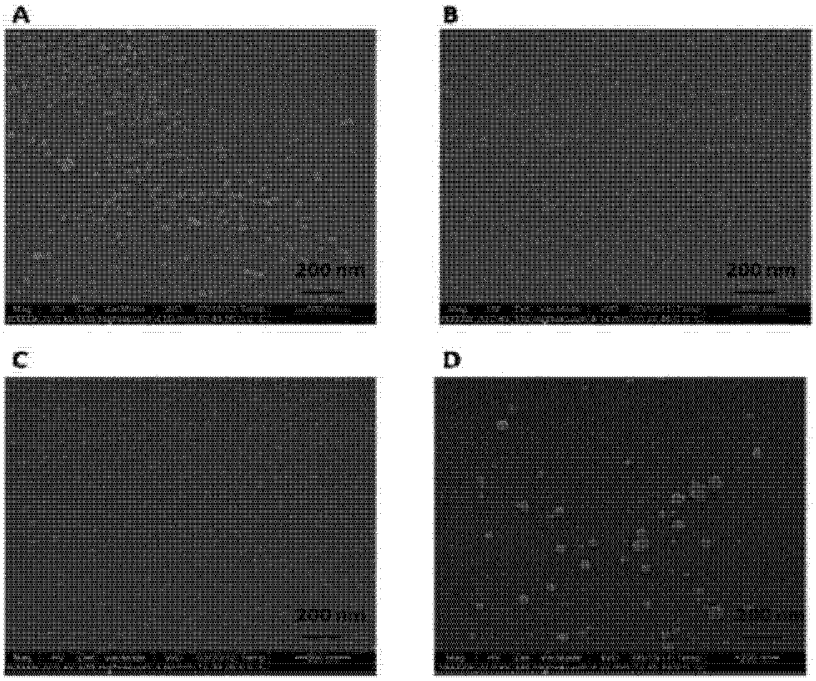

图 2B

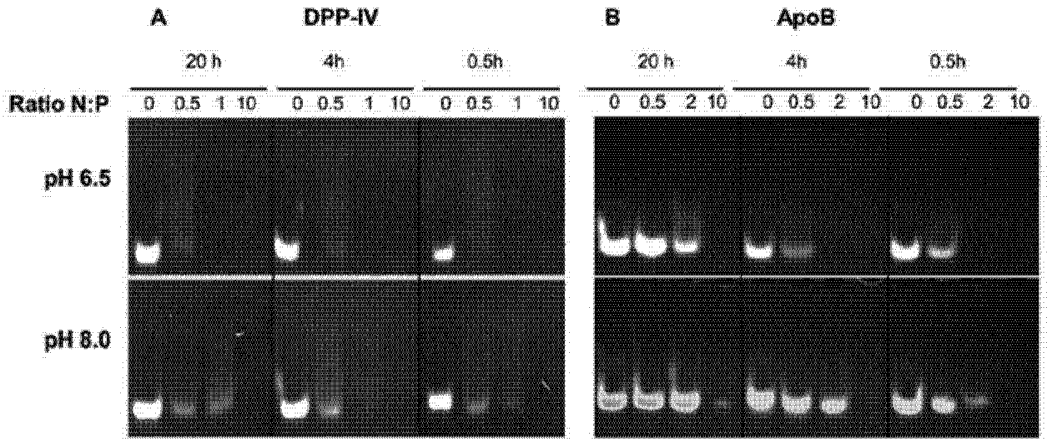
A
DPP-IV
B
ApoB
20 h
4h
0.5h
20 h
4h
0.5h
Ratio N:P
0 0.5 1 10
0 0.5 1 10
0 0.5 1 10
0 0.5 2 10
0 0.5 2 10
0 0.5 2 10
pH 6.5
pH 8.0

图 3A

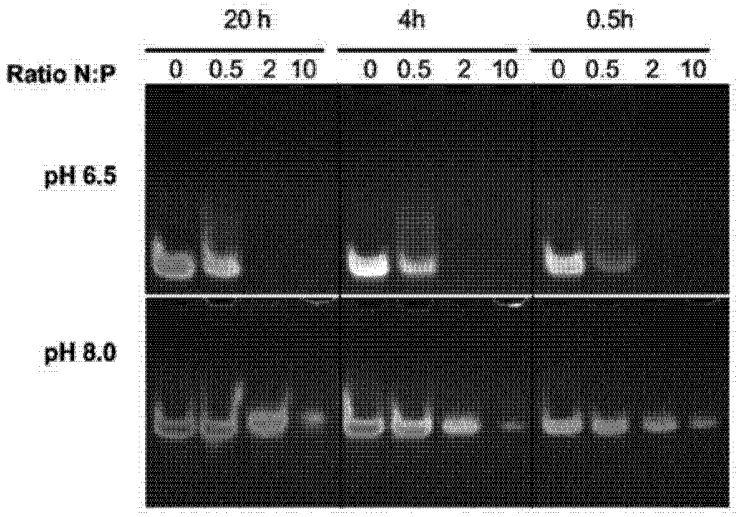
20 h
4h
0.5h
Ratio N:P
0 0.5 2 10
0 0.5 2 10
0 0.5 2 10
pH 6.5
pH 8.0

图 3B

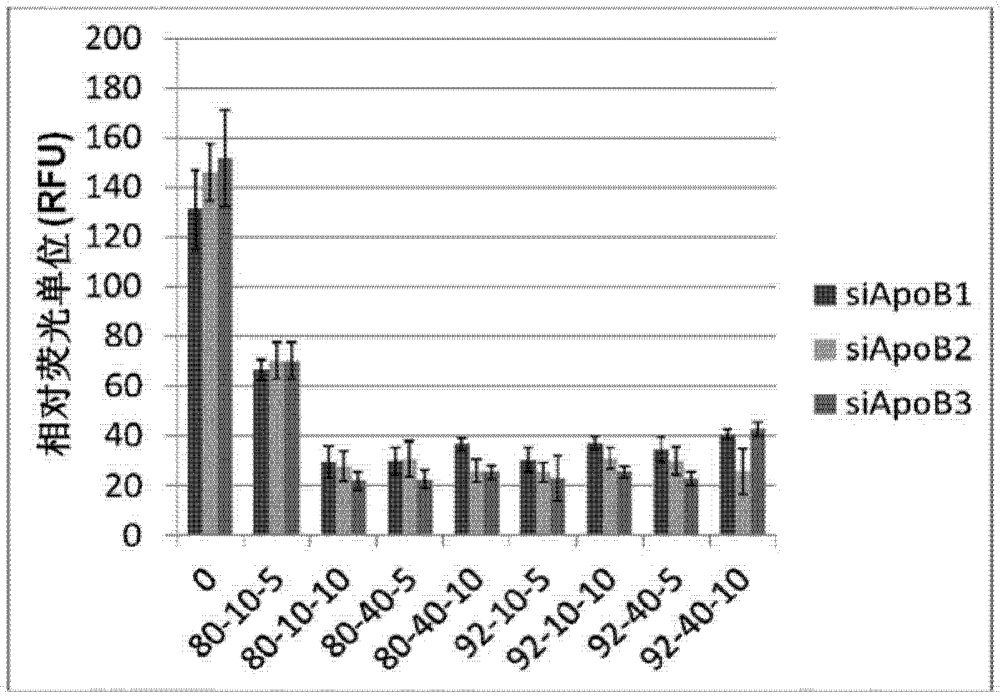
200
180
160
140
120
100
80
60
40
20
0
相对荧光单位(RFU)
siApoB1
siApoB2
siApoB3
0
80-10-5
80-10-10
80-40-5
80-40-10
92-10-5
92-10-10
92-40-5
92-40-10

图 4A

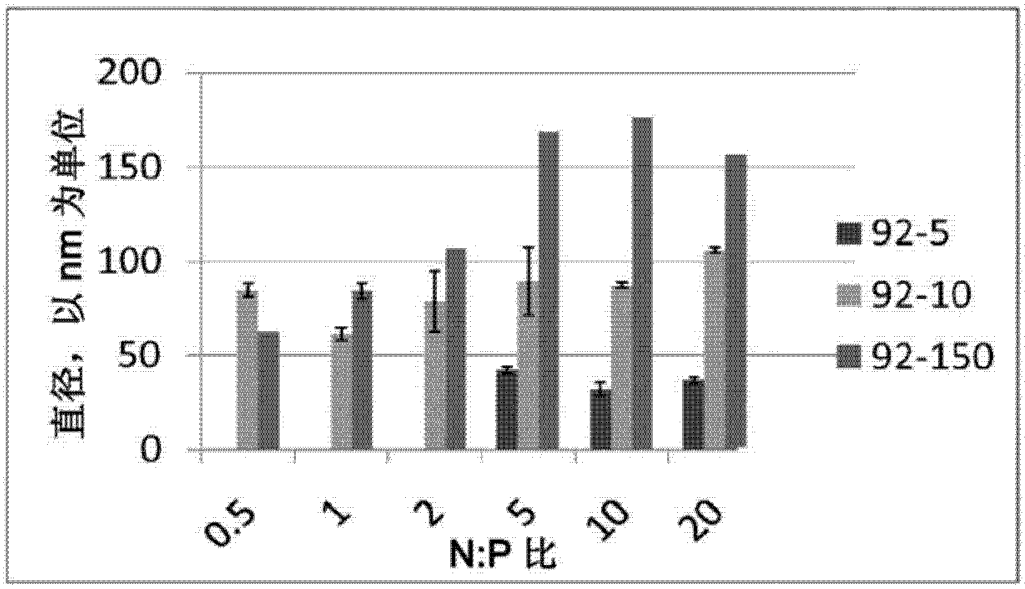
200
150
100
50
0
直径，以 nm 为单位
92-5
92-10
92-150
0.5
1
2
5
10
20
N:P 比

图 4B

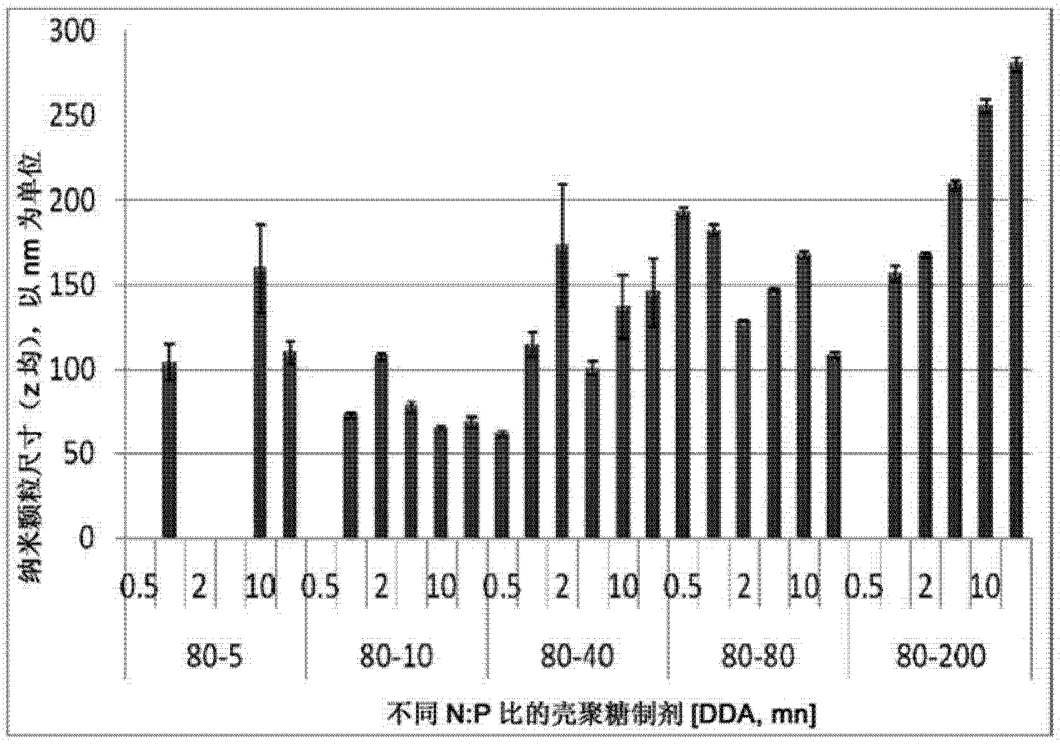
300
250
200
150
100
50
0
纳米颗粒尺寸（z均），以 nm 为单位
0.5 2 10 0.5 2 10 0.5 2 10 0.5 2 10 0.5 2 10
80-5
80-10
80-40
80-80
80-200
不同 N:P 比的壳聚糖制剂 [DDA, mn]

图 4C

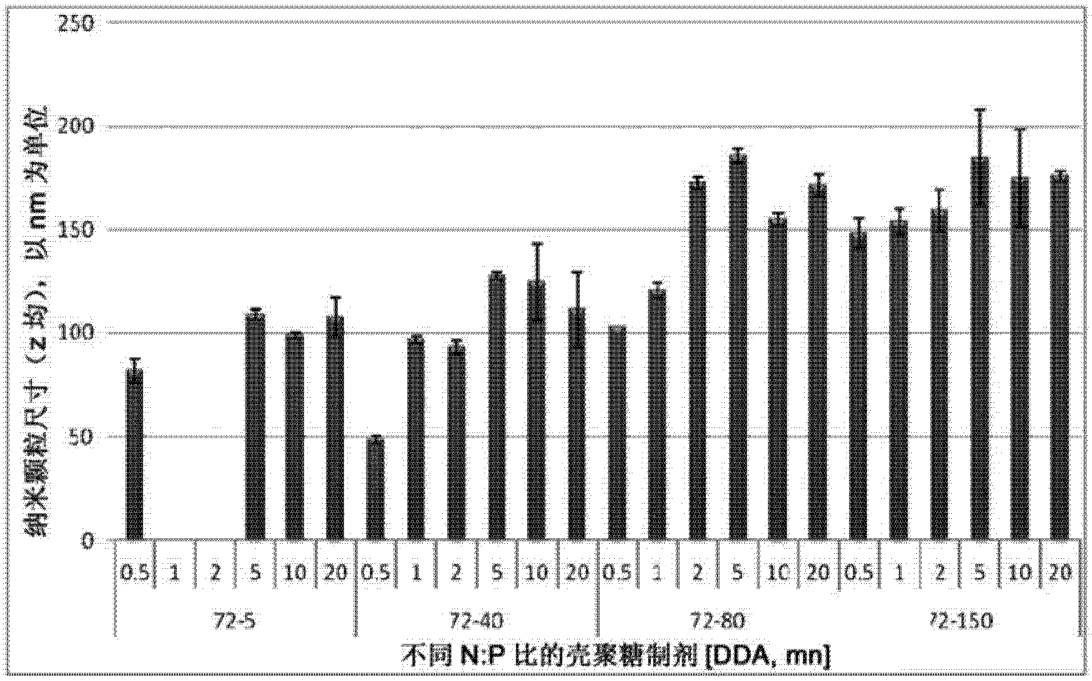
250
200
150
100
50
0
纳米颗粒尺寸（z均），以 nm 为单位
0.5 1 2 5 10 20 0.5 1 2 5 10 20 0.5 1 2 5 10 20 0.5 1 2 5 10 20
72-5
72-40
72-80
72-150
不同 N:P 比的壳聚糖制剂 [DDA, mn]

图 4D

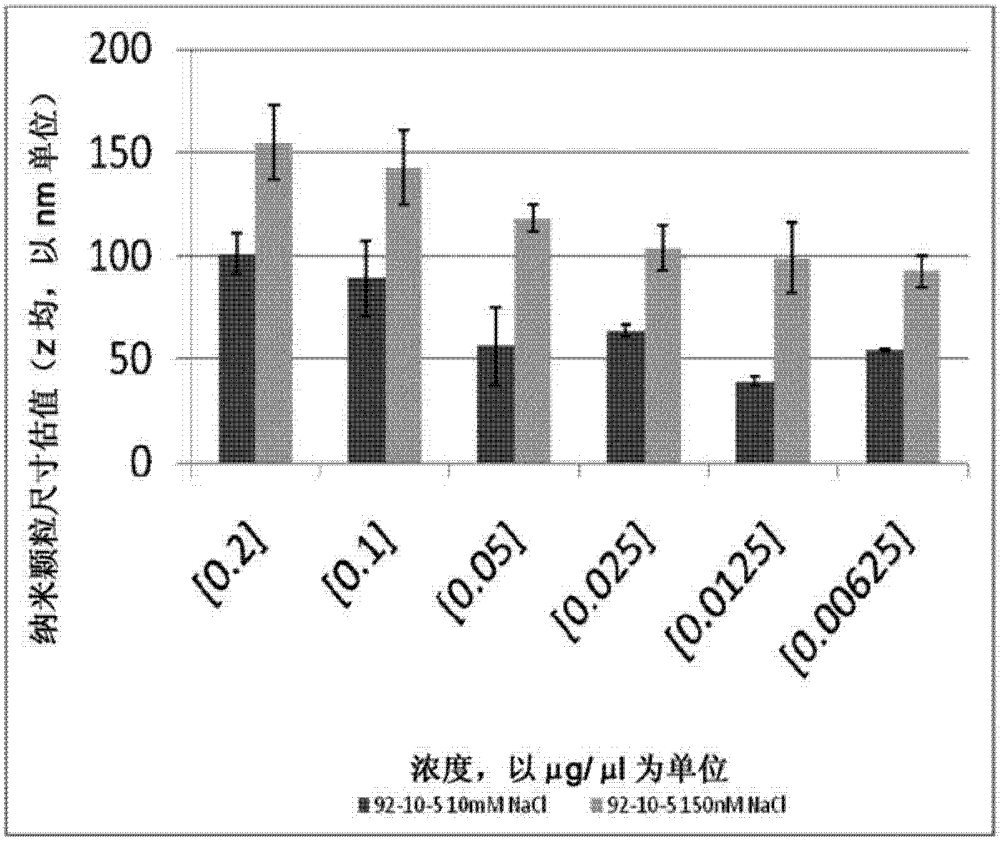
200
150
100
50
0
纳米颗粒尺寸估值（z 均，以 nm 单位）
[0.2]
[0.1]
[0.05]
[0.025]
[0.0125]
[0.00625]
浓度，以 μg/μl 为单位
92-10-5 10mM NaCl
92-10-5 150nM NaCl

图 4E

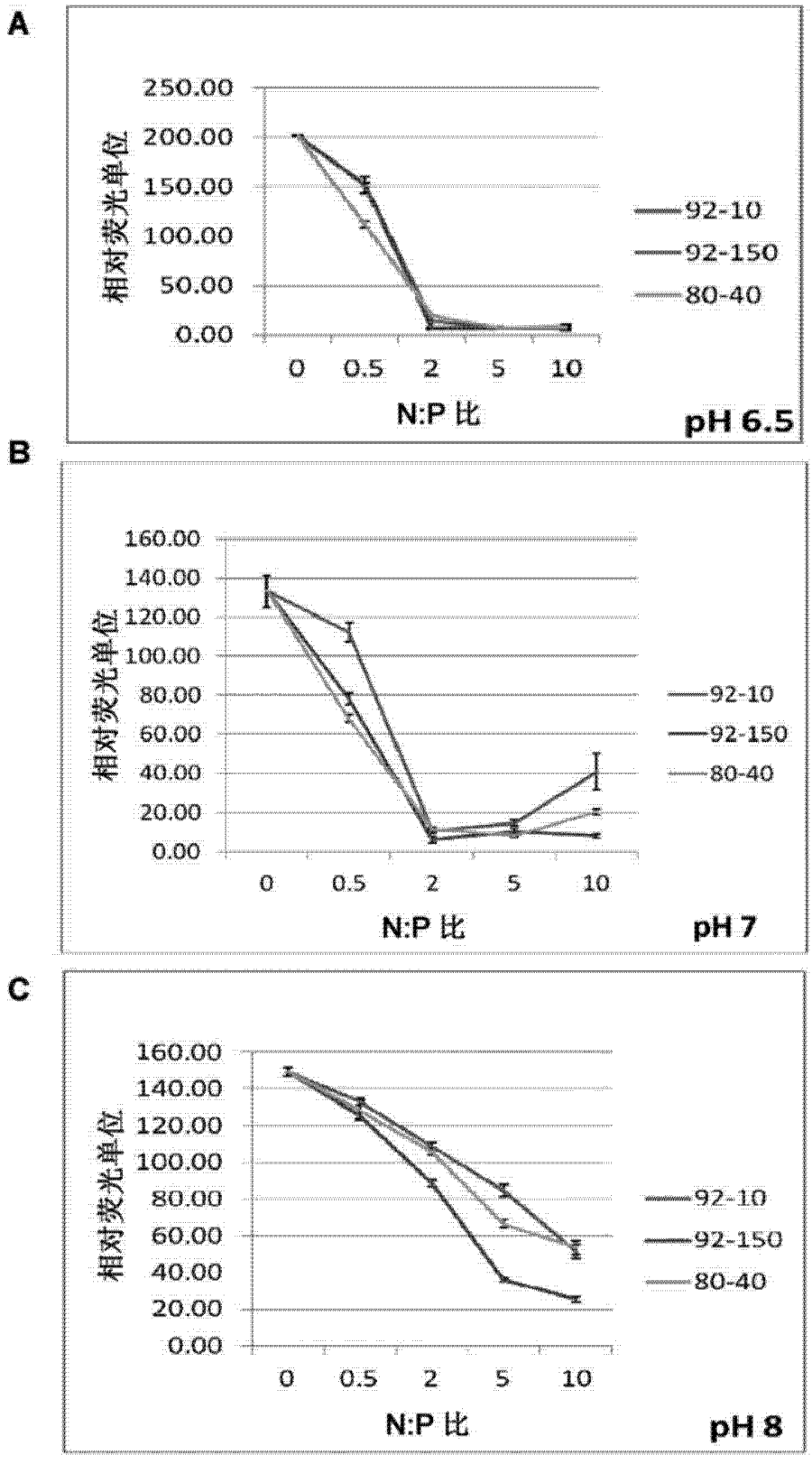
A
250.00
200.00
150.00
100.00
50.00
0.00
相对荧光单位
0
0.5
2
5
10
N:P 比
92-10
92-150
80-40
pH 6.5
B
160.00
140.00
120.00
100.00
80.00
60.00
40.00
20.00
0.00
相对荧光单位
0
0.5
2
5
10
N:P 比
92-10
92-150
80-40
pH 7
C
160.00
140.00
120.00
100.00
80.00
60.00
40.00
20.00
0.00
相对荧光单位
0
0.5
2
5
10
N:P 比
92-10
92-150
80-40
pH 8

图 5

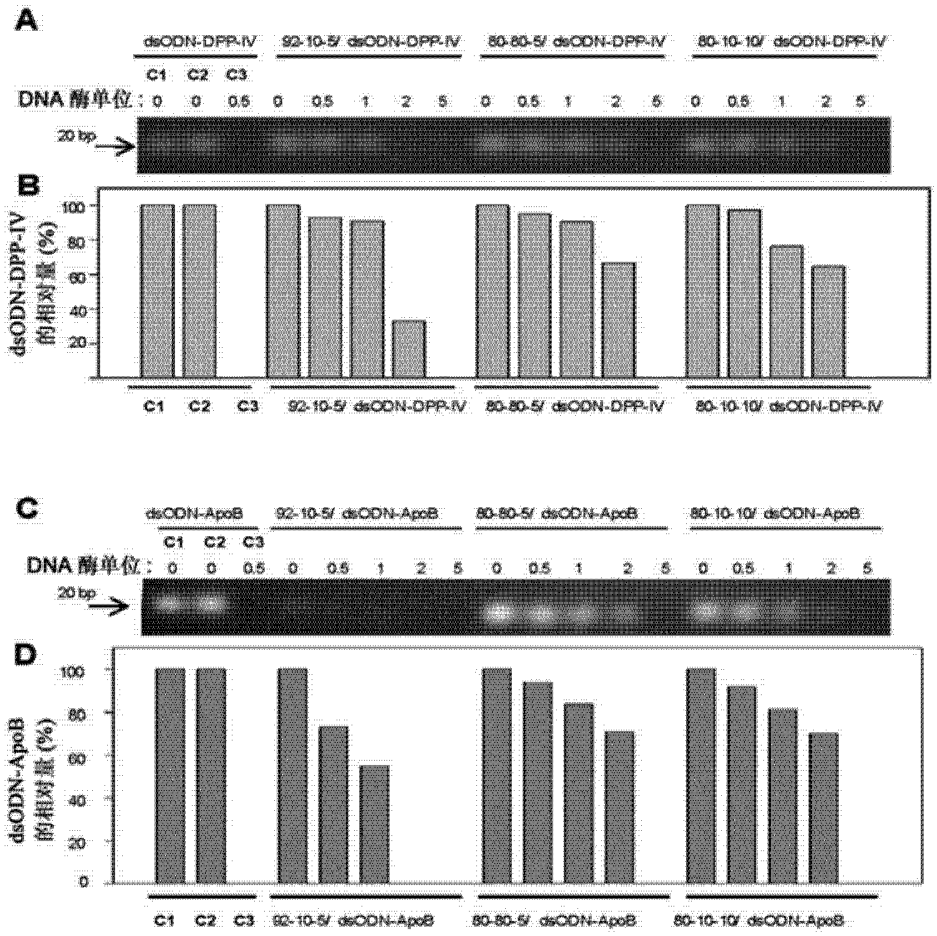
A
dsODN-DPP-IV
92-10-5/ dsODN-DPP-IV
80-80-5/ dsODN-DPP-IV
80-10-10/ dsODN-DPP-IV
C1 C2 C3
DNA 酶单位：0 0 0.5 0 0.5 1 2 5 0 0.5 1 2 5 0 0.5 1 2 5
20 bp
B
dsODN-DPP-IV 的相对量 (%)
100
80
60
40
20
C1 C2 C3 92-10-5/ dsODN-DPP-IV 80-80-5/ dsODN-DPP-IV 80-10-10/ dsODN-DPP-IV
C
dsODN-ApoB
92-10-5/ dsODN-ApoB
80-80-5/ dsODN-ApoB
80-10-10/ dsODN-ApoB
C1 C2 C3
DNA 酶单位：0 0 0.5 0 0.5 1 2 5 0 0.5 1 2 5 0 0.5 1 2 5
20 bp
D
dsODN-ApoB 的相对量 (%)
100
80
60
40
20
0
C1 C2 C3 92-10-5/ dsODN-ApoB 80-80-5/ dsODN-ApoB 80-10-10/ dsODN-ApoB

图 6A

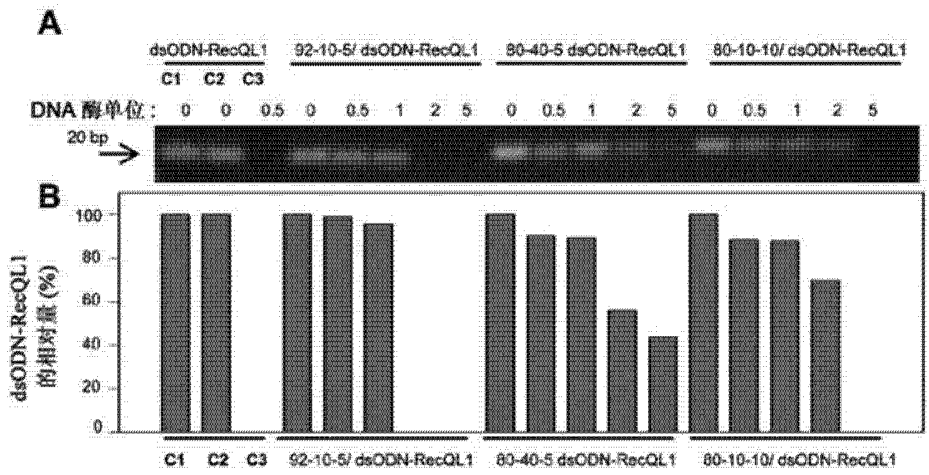
A
dsODN-RecQL1
92-10-5/ dsODN-RecQL1
80-40-5 dsODN-RecQL1
80-10-10/ dsODN-RecQL1
C1 C2 C3
DNA 酶单位：0 0 0.5 0 0.5 1 2 5 0 0.5 1 2 5 0 0.5 1 2 5
20 bp
B
dsODN-RecQL1 的相对量 (%)
100
80
60
40
20
0
C1 C2 C3 92-10-5/ dsODN-RecQL1 80-40-5 dsODN-RecQL1 80-10-10/ dsODN-RecQL1

图 6B

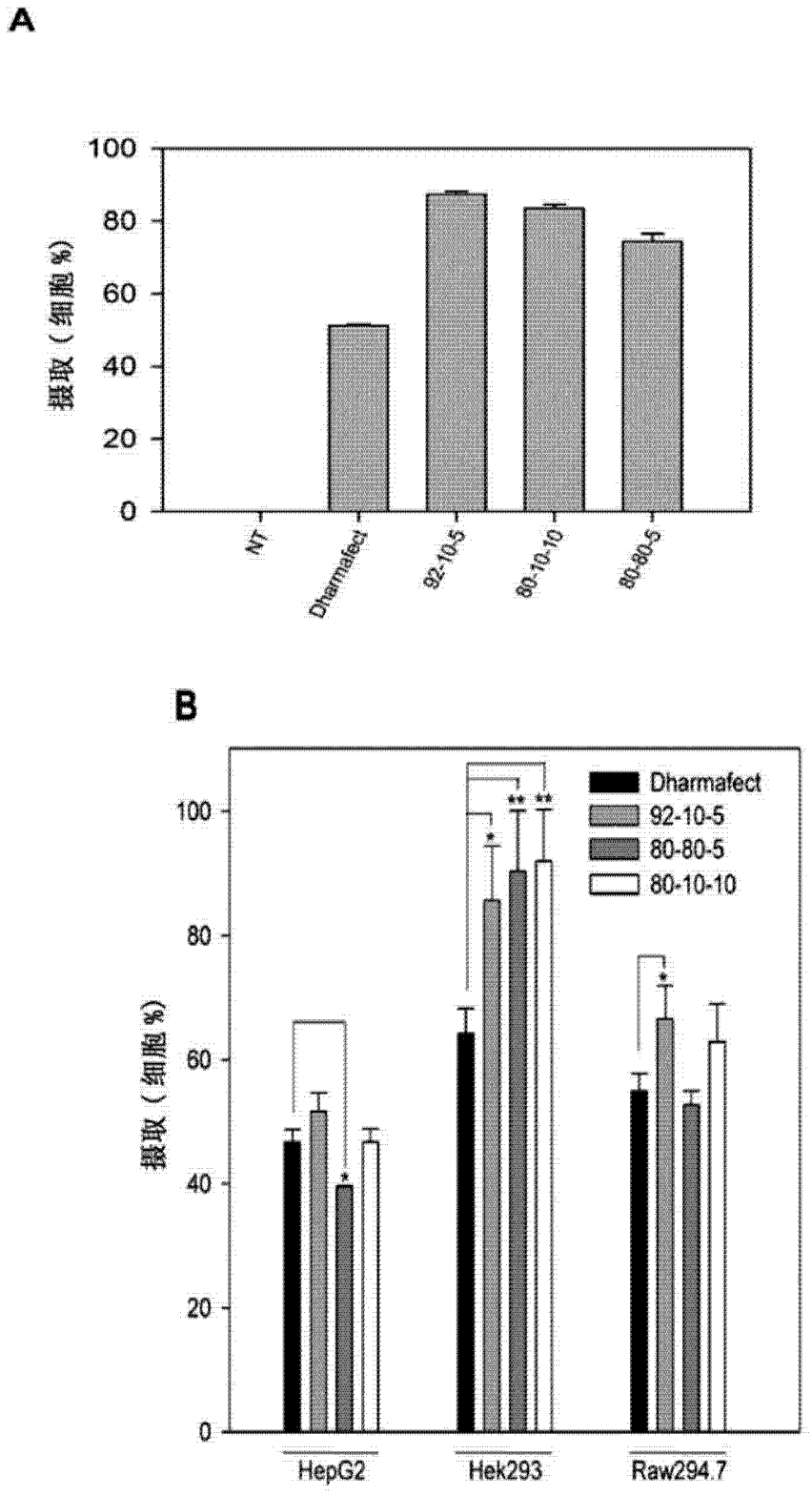
A
100
80
60
40
20
0
摄取（细胞%）
NT
Dharmafect
92-10-5
80-10-10
80-80-5
B
Dharmafect
92-10-5
80-80-5
80-10-10
100
80
60
40
20
0
摄取（细胞%）
HepG2
Hek293
Raw294.7

图 7A

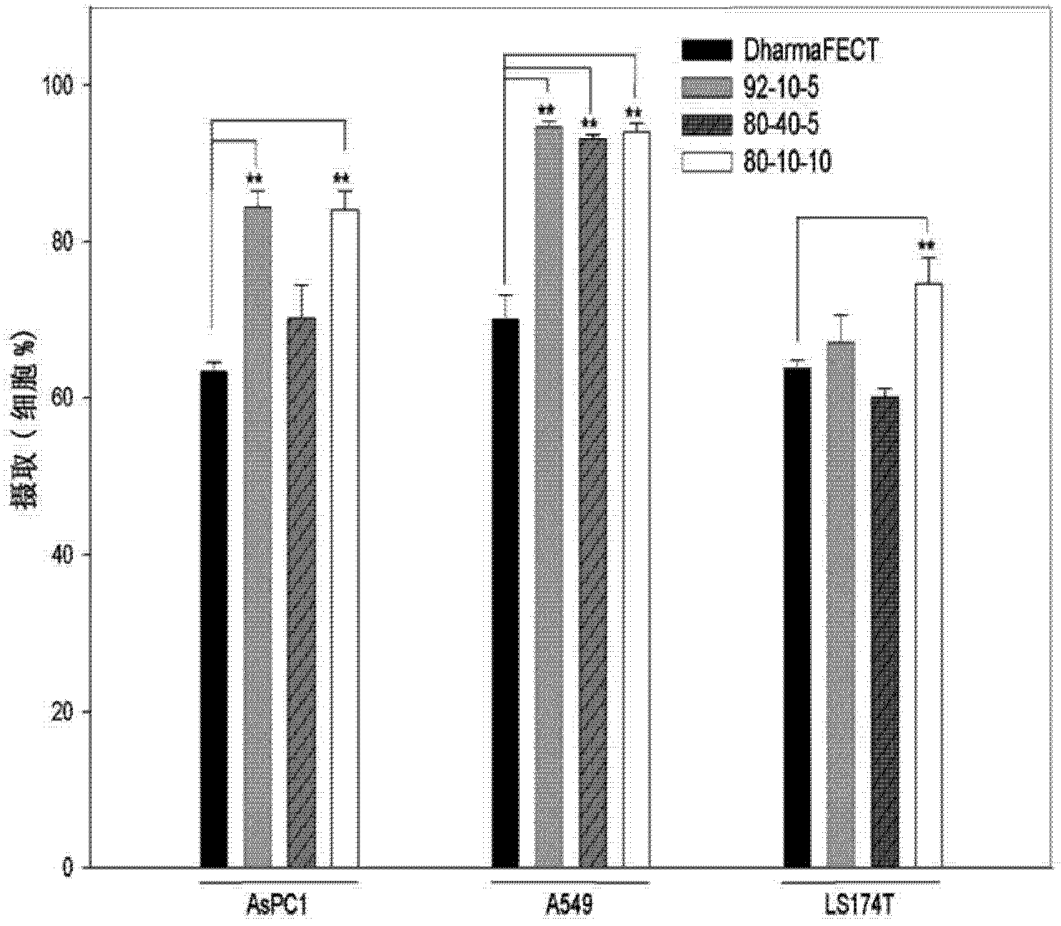
DharmaFECT
92-10-5
80-40-5
80-10-10
摄取（细胞%）
100
80
60
40
20
0
**
AsPC1
A549
LS174T

图 7B

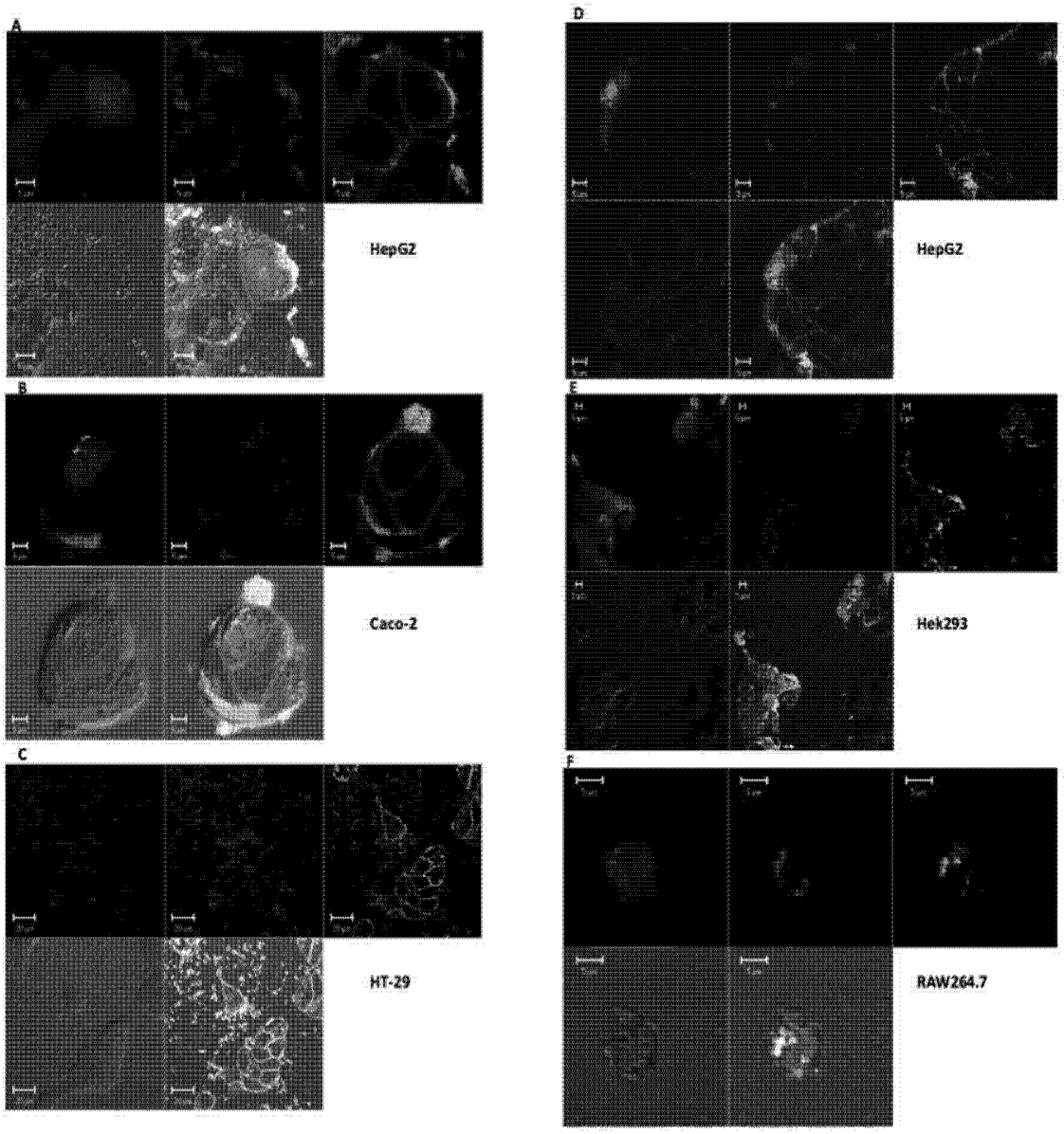

图 8

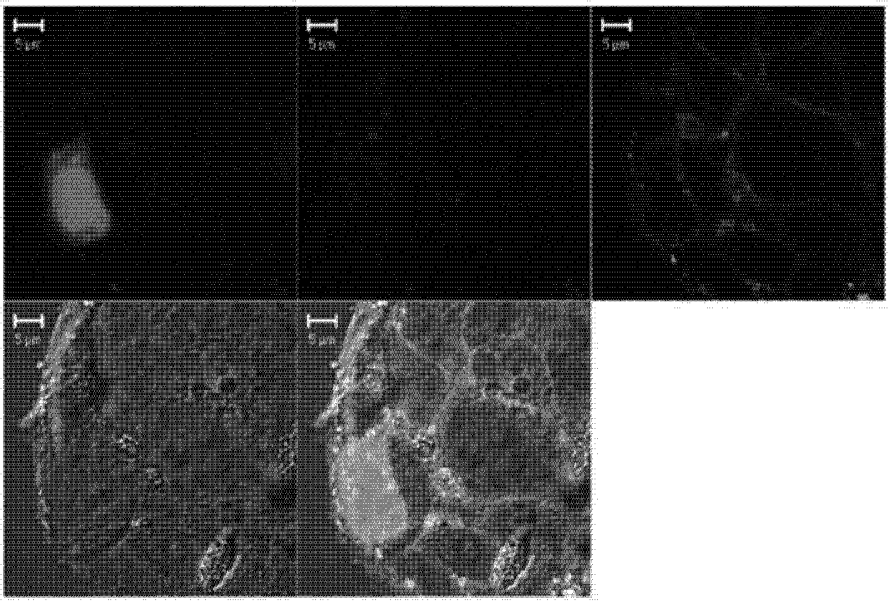

图 9

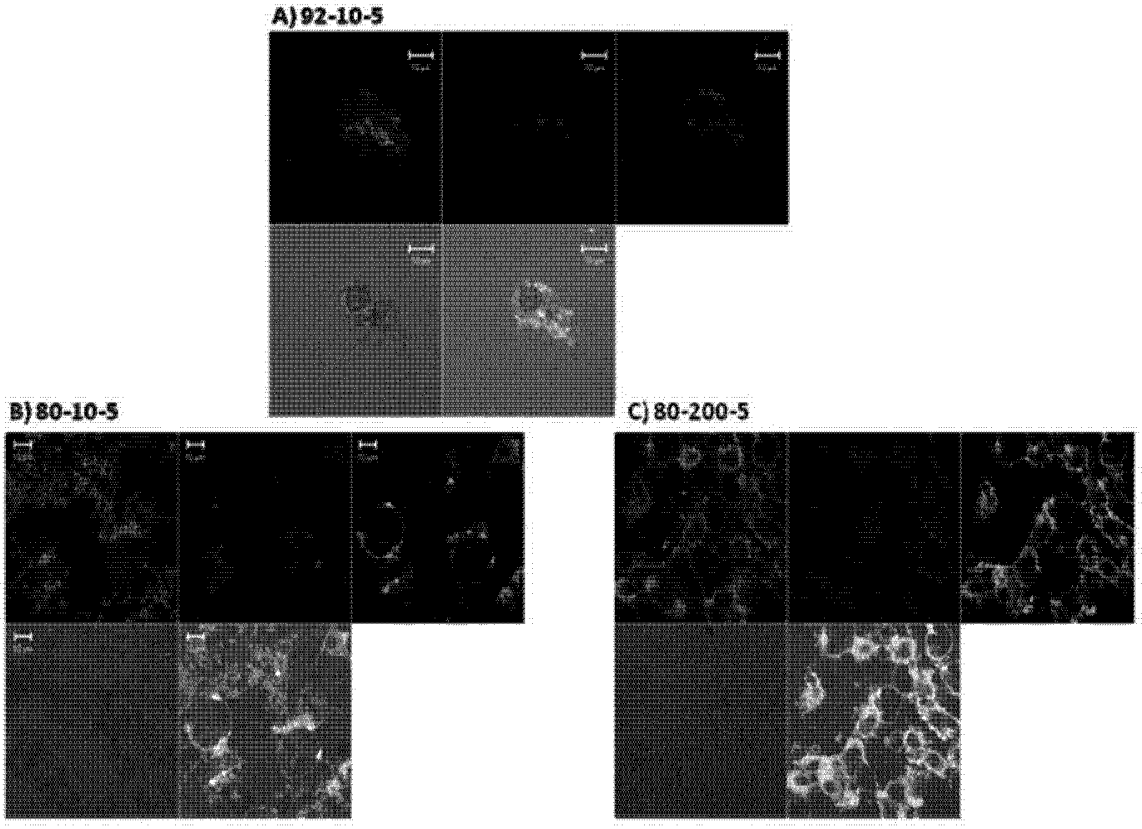

图 10

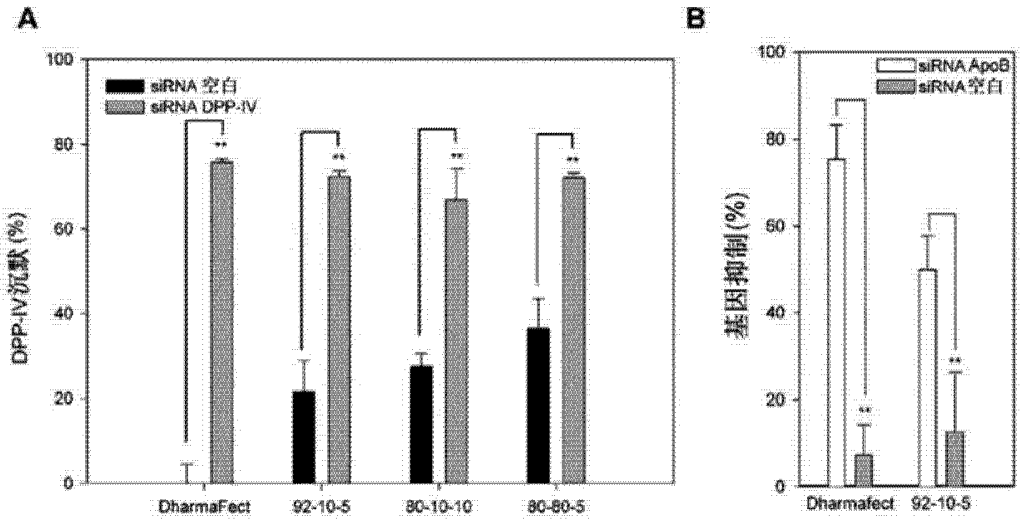
A
B
siRNA 空白
siRNA DPP-IV
DPP-IV沉默(%)
DharmaFect
92-10-5
80-10-10
80-80-5
siRNA ApoB
siRNA空白
基因抑制(%)
Dharmafect
92-10-5

图 11A

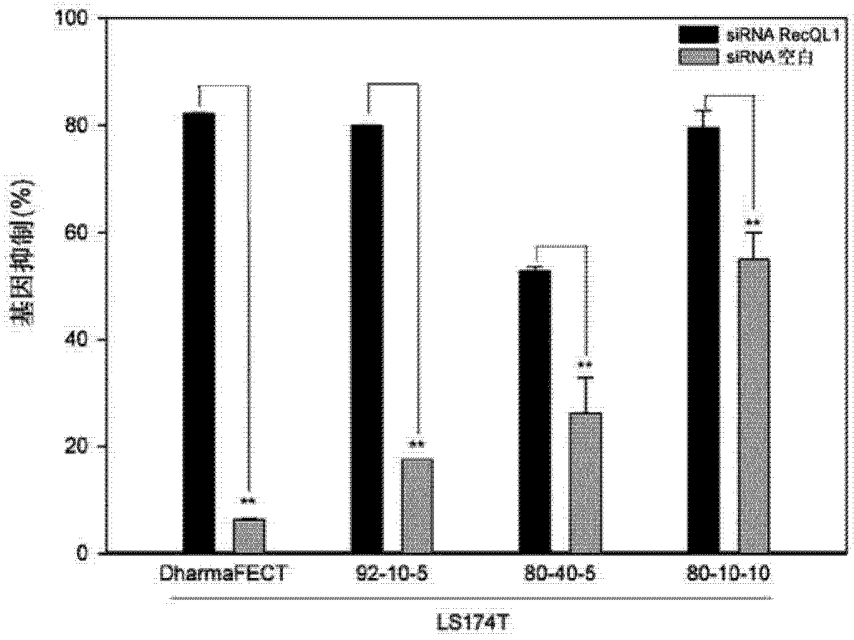
siRNA RecQL1
siRNA 空白
基因抑制(%)
DharmaFECT
92-10-5
80-40-5
80-10-10
LS174T

图 11B

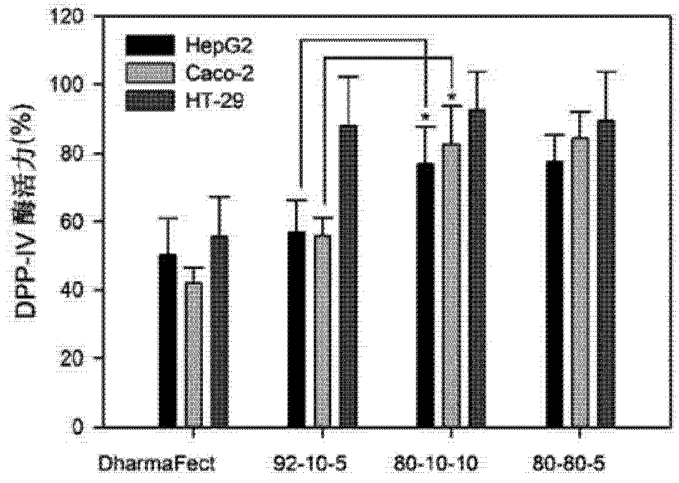
DPP-IV 酶活力(%)
HepG2
Caco-2
HT-29
DharmaFect
92-10-5
80-10-10
80-80-5

图 12

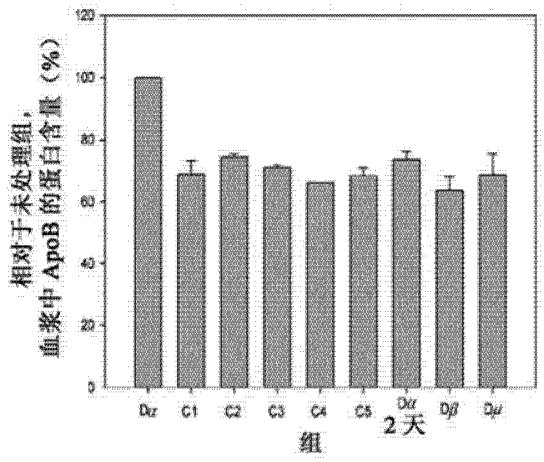
相对于未处理组，血浆中 ApoB 的蛋白含量（%）
组
2 天

图 13

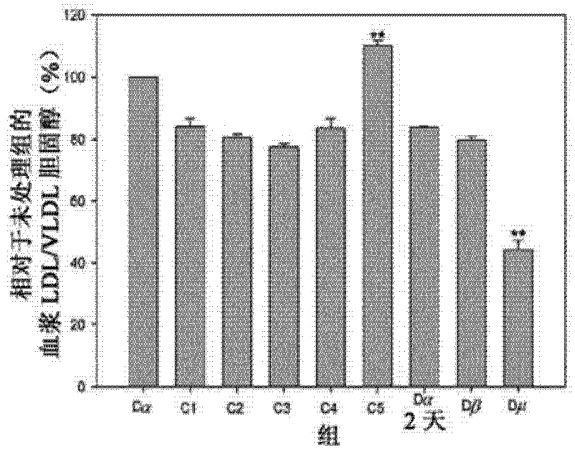
相对于未处理组的血浆 LDL/VLDL 胆固醇（%）
组
2 天

图 14

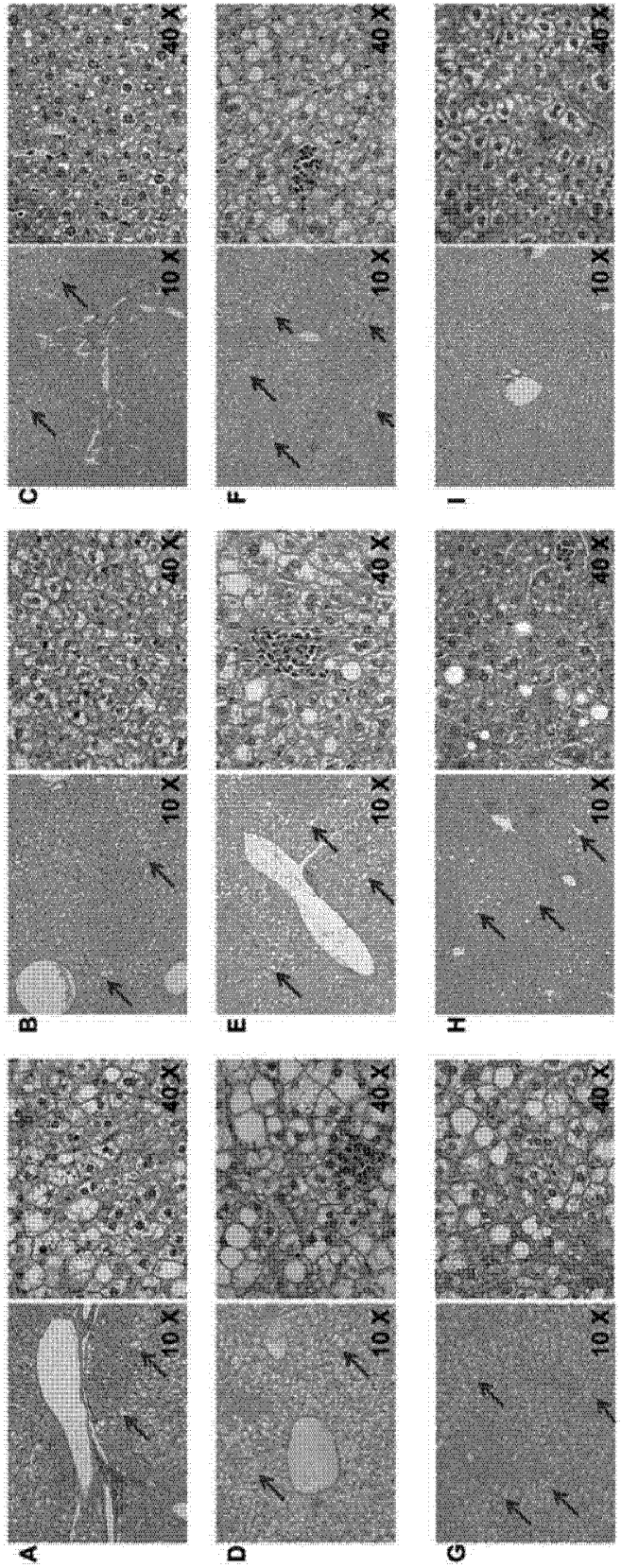

图 15

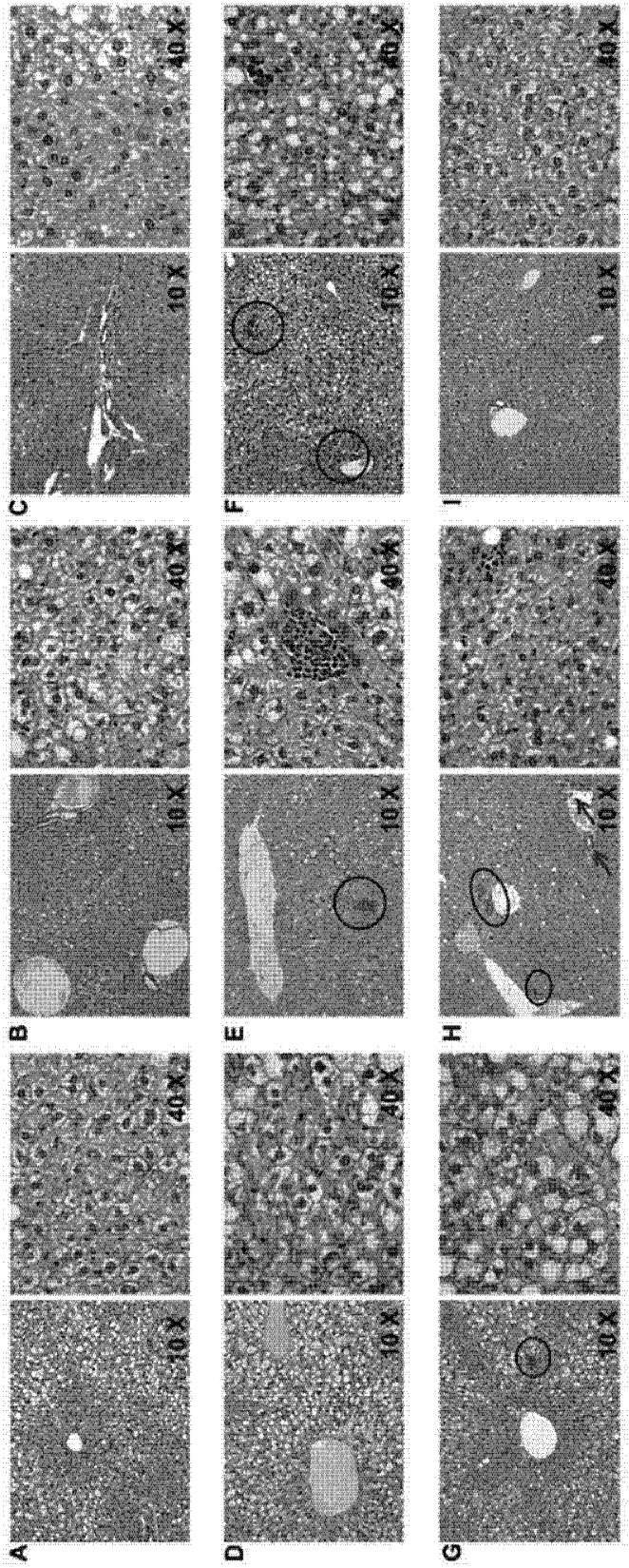

图 16

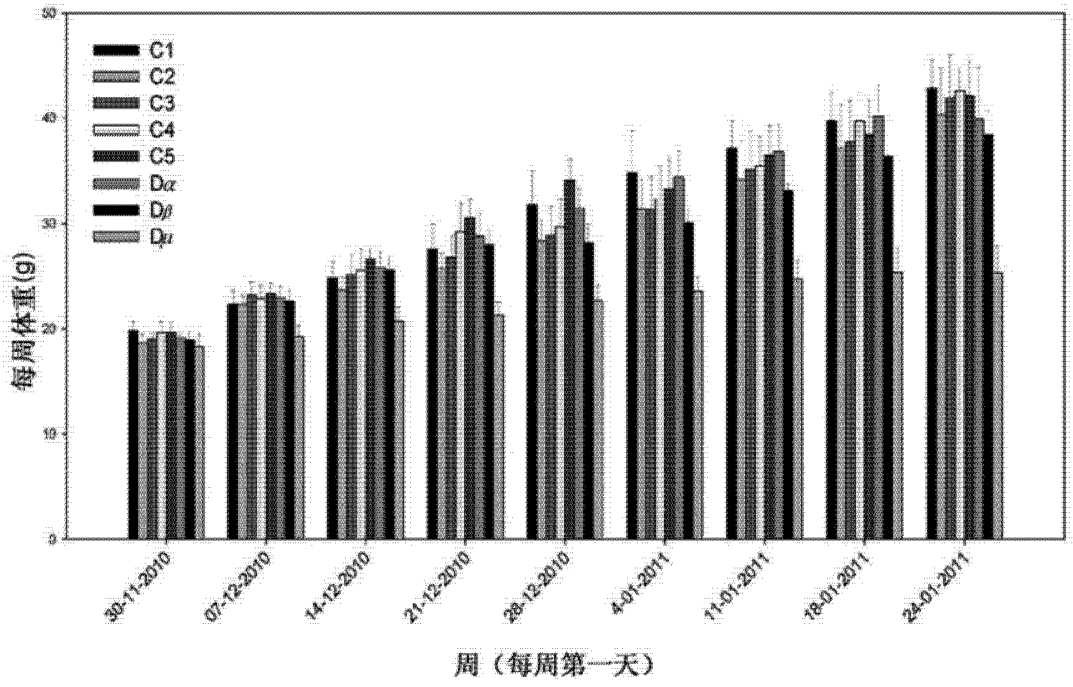
C1
C2
C3
C4
C5
Dα
Dβ
Dμ
每周体重(g)
30-11-2010
07-12-2010
14-12-2010
21-12-2010
28-12-2010
4-01-2011
11-01-2011
18-01-2011
24-01-2011
周（每周第一天）

图 17

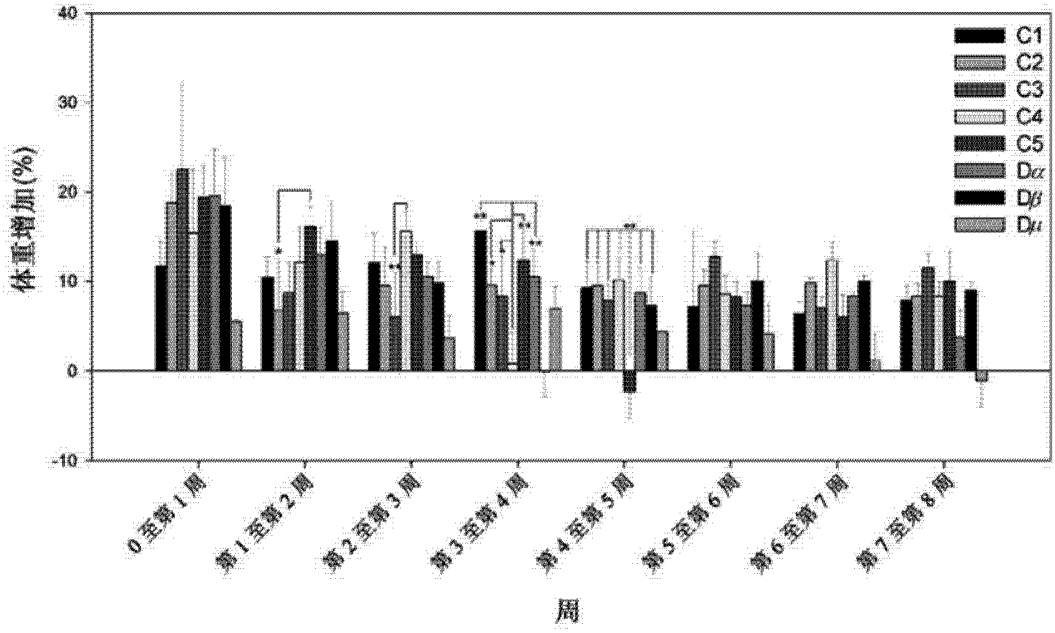
C1
C2
C3
C4
C5
Dα
Dβ
Dμ
体重增加(%)
0 至第 1 周
第 1 至第 2 周
第 2 至第 3 周
第 3 至第 4 周
第 4 至第 5 周
第 5 至第 6 周
第 6 至第 7 周
第 7 至第 8 周
周

图 18